

1-1-2013

Deterioration Caused By Sulfide-Bearing Aggregates: Performance Test Development

Bradley Maguire
Ryerson University

Follow this and additional works at: <http://digitalcommons.ryerson.ca/dissertations>



Part of the [Civil Engineering Commons](#)

Recommended Citation

Maguire, Bradley, "Deterioration Caused By Sulfide-Bearing Aggregates: Performance Test Development" (2013). *Theses and dissertations*. Paper 2091.

**DETERIORATION CAUSED BY SULFIDE-BEARING AGGREGATES:
PERFORMANCE TEST DEVELOPMENT**

by

Bradley Maguire, B.Eng
Ryerson University
2006-2011

A thesis

presented to Ryerson University

in partial fulfillment of the
requirements for the degree of
Master of Applied Science
in the Program of
Civil Engineering

Toronto, Ontario, Canada, 2013

©Bradley Maguire 2013

Declaration of Authorship

I hereby declare that I am the sole author of this thesis. This is a true copy of the thesis, including any required final revisions, as accepted by my examiners.

I authorize Ryerson University to lend this thesis to other institutions or individuals for the purpose of scholarly research

I further authorize Ryerson University to reproduce this thesis by photocopying or by other means, in total or in part, at the request of other institutions or individuals for the purpose of scholarly research.

I understand that my thesis may be made electronically available to the public.

Author's Signature

A handwritten signature in black ink, appearing to read 'M. McGuire', written over a horizontal line.

Date

Sept 11th, 2013

Abstract

DETERIORATION CAUSED BY SULFIDE-BEARING AGGREGATES: PERFORMANCE TEST DEVELOPMENT

Master of Applied Science, 2013

Bradley Maguire

Department of Civil Engineering

Ryerson University

Recently in Quebec Canada, concrete structures suffered very rapid deterioration within 3 to 5 years of construction. The deterioration was caused by an iron sulfide, namely pyrrhotite, in the coarse aggregate that suffered oxidation inside concrete and promoted sulfate attack; indicated by the presence of ferric oxyhydroxides (“rust”), gypsum, ettringite, and thaumasite. The goal of the current work was to reproduce this reaction under accelerated laboratory conditions, in progression of a performance test. Conditions to promote pyrrhotite oxidation and internal sulfate attack were provided; exposure cycles were tested with heating and cooling, and saturation in oxidizing agents or lime solution. Oxidation was induced in concrete samples, however, other mechanisms contributed to deterioration. The bleach was found to promote NaCl and Friedel’s salt formation, furthermore, it seemed to mitigate expansion from sulfate attack. Sulfoaluminate decomposition was also found to cause secondary ettringite formation. More optimization to the test methods was recommended.

Acknowledgments

I would like to express my genuine gratitude to my supervisor for this project, Dr. Medhat Shehata, for providing me with the opportunity to complete this research. His dedication and enthusiasm for his work and his students are unsurpassed and very inspiring. His guidance, comments, motivation, and stimulating engagement provided excellent opportunities for my education, and encouraged my development on both the professional and personal levels.

I would like to thank my parents and my siblings for their endless love and support. They provided me with the opportunity to pursue this degree, and it would not have been possible without their guidance, advice, encouragement, and reassurance.

A special appreciation is extended to my fellow members of Dr. Shehata's research team, stimulating conversations, research advice and discussion, help, and companionship through seemingly endless hours in the lab were all very well received.

Table of Contents

DETERIORATION CAUSED BY SULFIDE-BEARING AGGREGATES: PERFORMANCE TEST DEVELOPMENT	i
Declaration of Authorship.....	ii
Abstract.....	iii
Acknowledgments	iv
Table of Contents	v
List of Tables	ix
List of Figures.....	x
1 Introduction.....	1
1.1 Analysis of Distressed Concrete	2
1.2 Possible Reaction Series	3
1.3 Objectives and Research Significance	3
2 Literature Review	5
2.1 Iron Sulfide Oxidation	5
2.1.1 Pyrrhotite.....	5
2.2 Sulfate Attack.....	6
2.2.1 Ettringite	6
2.2.1.1 Calcium Sulfate.....	7
2.2.1.2 Sodium Sulfate.....	8
2.2.1.3 Sulfuric Acid.....	9
2.2.1.4 Delayed Ettringite Formation	9
2.2.1.5 Secondary Ettringite Formation.....	10
2.2.2 Thaumasite.....	10
2.3 Physical Salt Attack	11
2.3.1 Sodium Chloride (NaCl).....	11
2.4 Chlorides in Concrete	12
2.4.1 Friedel’s Salt.....	12
2.5 Wetting and Drying Cycles.....	13
2.6 Mix Design Parameters.....	14
2.6.1 Water-to-Cement Ratio (w/c)	14
2.6.2 Cement Content	14

2.6.3	Silica Fume	15
2.6.4	Air-Entraining Admixture.....	15
3	Experimental Procedures.....	16
3.1	Scope of Work	16
3.1.1	Test Development	16
3.1.2	Sample Preparation	16
3.2	Materials	17
3.2.1	Aggregates	17
3.2.1.1	Sulfide.....	17
3.2.1.2	Dolostone	18
3.2.1.3	Fine Aggregate.....	18
3.2.2	Cementing Materials.....	19
3.2.2.1	General Use Portland Cement.....	19
3.2.2.2	High Silica Fume Cement (HSF).....	19
3.2.3	Solutions	19
3.2.3.1	Bleach	20
3.2.3.2	Hydrogen Peroxide	20
3.2.3.3	Hydrogen Peroxide Bleach (HPB).....	20
3.2.3.4	Lime Solution.....	20
3.2.4	Air-Entraining Admixture.....	21
3.3	Methodologies.....	21
3.3.1	Mix Design.....	21
3.3.1.1	Phase I.....	21
3.3.1.2	Phase II.....	22
3.3.2	Moisture Conditions.....	23
3.3.2.1	Absorption and Drying	23
3.3.2.2	Relative Humidity.....	24
3.3.3	Phase I.....	25
3.3.4	Phase II.....	28
3.3.4.1	Series 1	29
3.3.4.2	Series 2.....	31
3.3.4.3	Series 3.....	32
3.3.4.4	Series 4.....	33

3.3.5	Phase III	33
3.3.6	Phase IV	34
3.3.7	Scanning Electron Microscopy (SEM)	35
3.3.8	Other Testing Procedures.....	35
4	Results and Analysis	36
4.1	Moisture Conditions.....	36
4.1.1	Absorption and Drying	36
4.1.2	Relative Humidity (RH).....	40
4.2	Phase I.....	42
4.2.1	Heating to 150°C	42
4.2.1.1	150°C / Dry.....	42
4.2.1.2	150°C / 23°C Soaking.....	47
4.2.1.3	150°C / 5°C Soaking.....	50
4.2.2	Heating to 60°C	53
4.2.2.1	60°C/Dry.....	53
4.2.2.2	60°C /23°C Soaking.....	54
	Scanning Electron Microscopy on I-S60/23	56
	EDS Mapping: I-S60/23	62
	Iron Sulfide Oxidation	64
	Scanning Electron Microscopy on I-D60/23	69
	EDS Mapping: I-D60/23.....	73
4.2.2.3	60°C/5°C Soaking.....	75
4.3	Phase II.....	78
4.3.1	Series 1.....	78
4.3.2	Series 2.....	79
4.3.2.1	Bleach Soaking	80
	Scanning Electron Microscopy	83
	II-S60A	83
	II-S60B.....	102
	II-D60A.....	112
	II-D60B.....	118
	Comparison.....	122
4.3.2.2	Lime Soaking.....	123

4.3.3	Series 3.....	125
4.3.4	Series 4.....	126
4.4	Phase III	127
4.5	Phase IV	128
4.6	Additional Testing	129
4.6.1	Phase III Cylinders.....	129
4.6.2	Raw Aggregates	130
5	Discussion.....	135
5.1	Analysis of Reaction Mechanisms.....	135
5.1.1	Phase I.....	135
5.1.2	Phase II.....	137
5.2	Performance Test Development.....	140
5.2.1	Testing Without Oxidizing Agent.....	140
5.2.2	Testing With Oxidizing Agent.....	141
6	Conclusions.....	143
7	Recommendations for Future Research	145
	Appendices.....	147
	Appendix A.....	147
	Appendix B	149
	List of References.....	150

List of Tables

Table 3.2.1: Aggregate properties.....	18
Table 3.2.2: Chemical analysis of GU cement used in samples	19
Table 3.3.1: Phase II concrete proportions for 0.65 w/c mix.....	23
Table 3.3.2: Phase II concrete proportions for 0.45 w/c mix.....	23
Table 3.3.3: Phase I testing program	26
Table 3.3.4: Phase II Series 1 testing program; all soaking was after stabilization at 23°C, and all samples had 0.65 w/c	30
Table 3.3.5: Phase II Series 2 testing program; cycles included drying at 60°C with soaking at 23°C for 2-hours, twice a week; humidity was uncontrolled (low) during heating/drying	31
Table 3.3.6: Phase II Series 2 testing program with alternate cement; cycles included drying at 60°C with soaking at 23°C for 2-hours, twice a week; humidity was uncontrolled (low) during heating/drying	31
Table 3.3.7: Phase II Series 4 testing program with humidity maintained at 100%; cycles included heating to 60°C above water in containers, with bleach soaking at 23°C for 2-hours, twice a week.....	33
Table 3.3.8: Phase III testing program; cycles included soaking at 23°C for 24-hours twice a week; humidity was uncontrolled (low) during 24-hours of heating/drying twice a week	34
Table 3.3.9: Phase IV testing program; cycles included soaking at 23°C for 24-hours once a week; humidity was uncontrolled (low) during 5-days of heating/drying at 60°C each week.....	34
Table 4.3.1: Phase II SEM samples I.D. and related information	83
Table 4.3.2: Phase I and Phase II comparison of lime soaked samples.....	124
Table 4.6.1: Strength results for Phase III cylinder testing; all samples have w/c=0.65, were tested with 24-hour soaking at 23°C twice a week, and 24-hours heating/drying to 60°C twice a week	130
Table B.1: Phase I concrete mix proportions with w/c of 0.62 and Sulfide coarse aggregate ...	149
Table B.2: Phase I concrete mix proportions with w/c of 0.45 and Sulfide coarse aggregate ...	149
Table B.3: Phase II concrete mix proportions with w/c of 0.65 and Sulfide coarse aggregate ..	149
Table B.4: Phase II concrete mix proportions with w/c of 0.45 and Sulfide coarse aggregate ..	149

List of Figures

Figure 1.1.1: Pictures of damaged concrete foundations in Quebec, Canada.....	1
Figure 3.3.1: Heat cycle schematics for different testing regimes over 14-days – Samples were soaked in solution (lime or bleach) while at temperatures of 5°C or 23°C, except A) Phase I 60°C/Dry.....	27
Figure 4.1.1: Absorption of 76x76x256mm prisms with water over 24-hours	37
Figure 4.1.2: Drying of 76x76x256mm prisms over 72-hours	37
Figure 4.1.3: Absorption of 76x76x256mm prisms with water over 7-days.....	38
Figure 4.1.4: Drying of 76x76x256mm prisms over 7-days.....	39
Figure 4.1.5: Relative humidity values for drying at 60°C over 72-hours	40
Figure 4.1.6: Equilibrium relative humidity values after 28-days of testing, all drying was at 60°C; RH measurements were taken adjacent to respective testing measurement, at the time of dry readings after stabilization for 24-hours	41
Figure 4.2.1: Phase I results from 1 heating/cooling cycle per week to 150°C/23°C and no wetting cycles; samples were measured after 24-hours stabilization at 23°C	43
Figure 4.2.2: Image of Phase I Sulfide-0.45 sample tested under dry conditions with hot/cold cycles of 150°C/23°C.....	44
Figure 4.2.3: Image of Phase I Dolostone-0.62 specimen tested under dry conditions with hot/cold cycles of 150°C/23°C	45
Figure 4.2.4: Image of fractured Phase I Dolostone-0.62 specimen tested under dry conditions with hot/cold cycles of 150°C/23°	46
Figure 4.2.5: Image of severely cracked Phase I Dolostone-0.45 sample tested under dry conditions with hot/cold cycles of 150°C/23°C.....	47
Figure 4.2.6: Phase I results from heating/drying to 150°C for 7-days and soaking cycles at 23°C for 7-days; thus 2 wet/dry cycles per 28-days were experienced	48
Figure 4.2.7: Image of Phase I samples with w/c of 0.45 tested with 7-days heating/drying at 150°C and soaking at 23°C, the Dolostone sample with staining is shown on top, and the Sulfide sample is below.....	49
Figure 4.2.8: Images of fractured specimen from Phase I Dolostone-0.45 sample tested with 7-day heating/drying at 150°C and 7-day soaking at 23°C; fractured concrete sample shown in A) and C), removed aggregate particle causing fracture shown in B)	50

Figure 4.2.9: Phase I results from 7-days heating/drying to 150°C and 7-days soaking cycles at 5°C, thus 2 wet/dry cycles per 28-days was experienced	51
Figure 4.2.10: Images of fractured specimen from Phase I Dolostone-0.45 sample tested with 7-days heating/drying at 150°C with 7-days soaking at 5°C; fractured concrete sample shown in A) and C), removed aggregate particle causing fracture shown in B)	52
Figure 4.2.11: Phase I results from heating/cooling cycles to 60°C/23°C and no wetting cycles	53
Figure 4.2.12: Phase I results from heating/drying to 60°C for 7-days and soaking cycles at 23°C for 7-days; thus 2 wet/dry cycles per 28-days were experienced	54
Figure 4.2.13: SEM image of Phase I Sulfide-0.45 sample showing ettringite in paste at 57-weeks of testing; made with Sulfide aggregate, 0.65 w/c, and tested with 7-days drying at 60°C and 7-days soaking at 23°C	57
Figure 4.2.14: SEM image and EDS analysis of Phase I Sulfide-0.45 sample showing condensed ettringite at 57-weeks of testing; made with Sulfide aggregate, 0.65 w/c, and tested with 7-days drying at 60°C and 7-days soaking at 23°C	58
Figure 4.2.15: SEM image and EDS analysis of Phase I Sulfide-0.45 sample showing ettringite crystals in an air void at 57-weeks of testing; made with Sulfide aggregate, 0.65 w/c, and tested with 7-days drying at 60°C and 7-days soaking at 23°C	59
Figure 4.2.16: SEM image of Phase I Sulfide-0.45 sample showing ettringite crystals in an air void at 57-weeks of testing; made with Sulfide aggregate, 0.65 w/c, and tested with 7-days drying at 60°C and 7-days soaking at 23°C	60
Figure 4.2.17: SEM image and EDS analysis of I-S60/23 showing condensed ettringite within the cement matrix; made with Sulfide aggregate, 0.65 w/c, and tested with 7-days drying at 60°C and 7-days soaking at 23°C	61
Figure 4.2.18: I-S60/23 EDS mapping analysis results A)SEM Image of area B)Sulfur C)Iron D)Aluminium E)Calcium F)Silicon; made with Sulfide aggregate, 0.65 w/c, and tested with 7-days drying at 60°C and 7-days soaking at 23°C.....	63
Figure 4.2.19: SEM image of I-S60/23 showing iron interaction with paste; made with Sulfide aggregate, 0.65 w/c, and tested with 7-days drying at 60°C and 7-days soaking at 23°C.....	65
Figure 4.2.20: SEM image and EDS analysis of I-S60/23 showing a pyrrhotite inclusion with very little oxidation; made with Sulfide aggregate, 0.65 w/c, and tested with 7-days drying at 60°C and 7-days soaking at 23°C	66
Figure 4.2.21: SEM image of I-S60/23 showing a partially oxidized pyrrhotite inclusion that was examined via a line scan in Figure 4.2.22; made with Sulfide aggregate, 0.65 w/c, and tested with 7-days drying at 60°C and 7-days soaking at 23°C	67

Figure 4.2.22: Line scan of I-S60/23 showing A) a partially oxidized pyrrhotite inclusion, and the relative amounts of the analysis results for B) Sulfur C) Oxygen and D) Iron; made with Sulfide aggregate, 0.65 w/c, and tested with 7-days drying at 60°C and 7-days soaking at 23°C 68

Figure 4.2.23: SEM image and EDS analysis of I-D60/23 showing condensed ettringite in large concentrations in cement matrix; made with Dolostone aggregate, 0.65 w/c, and tested with 7-days drying at 60°C and 7-days soaking at 23°C..... 70

Figure 4.2.24: SEM image and EDS analysis of I-D60/23 showing condensed ettringite in cement matrix; made with Dolostone aggregate, 0.65 w/c, and tested with 7-days drying at 60°C and 7-days soaking at 23°C 71

Figure 4.2.25: SEM image and EDS analysis of I-D60/23 showing ettringite crystals in an air void; made with Dolostone aggregate, 0.65 w/c, and tested with 7-days drying at 60°C and 7-days soaking at 23°C..... 72

Figure 4.2.26: I-D60/23 SEM image of mapping area; made with Dolostone aggregate, 0.65 w/c, and tested with 7-days drying at 60°C and 7-days soaking at 23°C 73

Figure 4.2.27: I-D60/23 mapping analysis results A) SEM image of area B) Sulfur C) Magnesium D) Aluminium E) Calcium F) Silicon; made with Dolostone aggregate, 0.65 w/c, and tested with 7-days drying at 60°C and 7-days soaking at 23°C 74

Figure 4.2.28: Phase I results from heating/drying to 60°C for 7-days and soaking cycles at 5°C for 7-days; thus 2 wet/dry cycles per 28-days were experienced 75

Figure 4.2.29: Side-by-side comparison of Phase I testing with 7-days soaking at 23°C from Figure 4.2.12 and 7-days soaking at 23°C from Figure 4.2.28; tested with 7-days drying at 60°C 76

Figure 4.3.1: Phase II Series 1 results for sulphide aggregate with w/c of 0.65; all soaking was at 23°C after 24-hours stabilization 79

Figure 4.3.2: Phase II Series 2 results; all samples have w/c of 0.65 and were tested with 2-hours soaking in bleach at 23°C twice a week 80

Figure 4.3.3: Phase II Series 2 Results; all samples tested with drying at 60°C and 2-hours soaking in bleach at 23°C twice a week 81

Figure 4.3.4: Phase II Series 2 Results; all samples made with HSF cement and tested with drying at 60°C and 2-hours soaking in bleach at 23°C twice a week..... 82

Figure 4.3.5: SEM image and EDS analysis for II-S60A showing oxidation; made with Sulfide coarse aggregate, w/c of 0.65, and tested with drying at 60°C and 2-hours soaking in bleach at 23°C twice a week 85

Figure 4.3.7: SEM image and EDS analysis for II-S60A showing gypsum crystals; made with Sulfide coarse aggregate, w/c of 0.65, and tested with drying at 60°C and 2-hours soaking in bleach at 23°C twice a week	87
Figure 4.3.8: SEM image for II-S60A showing gypsum crystals; made with Sulfide coarse aggregate, w/c of 0.65, and tested with drying at 60°C and 2-hours soaking in bleach at 23°C twice a week.....	88
Figure 4.3.9: SEM image for II-S60A showing large analysis area; made with Sulfide coarse aggregate, w/c of 0.65, and tested with drying at 60°C and 2-hours soaking in bleach at 23°C twice a week.....	89
Figure 4.3.10: SEM image and EDS analysis for II-S60A showing gypsum and large area; made with Sulfide coarse aggregate, w/c of 0.65, and tested with drying at 60°C and 2-hours soaking in bleach at 23°C twice a week	91
Figure 4.3.11: SEM image and EDS analysis for II-S60A showing oxidized pyrrhotite; made with Sulfide coarse aggregate, w/c of 0.65, and tested with drying at 60°C and 2-hours soaking in bleach at 23°C twice a week	92
Figure 4.3.12: SEM image and EDS analysis for II-S60A showing oxidized pyrrhotite; made with Sulfide coarse aggregate, w/c of 0.65, and tested with drying at 60°C and 2-hours soaking in bleach at 23°C twice a week	93
Figure 4.3.13: SEM image and EDS analysis for II-S60A showing gypsum; made with Sulfide coarse aggregate, w/c of 0.65, and tested with drying at 60°C and 2-hours soaking in bleach at 23°C twice a week	94
Figure 4.3.14: Secondary electron image of gypsum crystals in cement paste in II-S60A; made with Sulfide coarse aggregate, w/c of 0.65, and tested with drying at 60°C and 2-hours soaking in bleach at 23°C twice a week	95
Figure 4.3.15: SEM image and EDS analysis for II-S60A showing presence of sulfur; made with Sulfide coarse aggregate, w/c of 0.65, and tested with drying at 60°C and 2-hours soaking in bleach at 23°C twice a week	96
Figure 4.3.16: SEM image and EDS analysis for II-S60A showing gypsum and Friedel's salt; made with Sulfide coarse aggregate, w/c of 0.65, and tested with drying at 60°C and 2-hours soaking in bleach at 23°C twice a week	97
Figure 4.3.17: SEM image and EDS analysis for II-S60A showing Friedel's salt; made with Sulfide coarse aggregate, w/c of 0.65, and tested with drying at 60°C and 2-hours soaking in bleach at 23°C twice a week	99
Figure 4.3.18 SEM image and EDS analysis for II-S60A showing Friedel's salt; made with Sulfide coarse aggregate, w/c of 0.65, and tested with drying at 60°C and 2-hours soaking in bleach at 23°C twice a week	100

Figure 4.3.19: SEM image and EDS analysis for II-S60A showing Friedel's	101
Figure 4.3.20: SEM image and EDS analysis for II-S60B showing NaCl salts in crack; made with Sulfide coarse aggregate, w/c of 0.65, and tested with drying at 60°C and 2-hours soaking in bleach at 23°C twice a week	104
Figure 4.3.21: SEM image and EDS analysis for II-S60B showing NaCl salts in crack; made with Sulfide coarse aggregate, w/c of 0.65, and tested with drying at 60°C and 2-hours soaking in bleach at 23°C twice a week	105
Figure 4.3.22: SEM image and EDS analysis for II-S60B showing gypsum in ITZ; made with Sulfide coarse aggregate, w/c of 0.65, and tested with drying at 60°C and 2-hours soaking in bleach at 23°C twice a week	106
Figure 4.3.23: SEM image for II-S60B showing NaCl salts in crack; made with Sulfide coarse aggregate, w/c of 0.65, and tested with drying at 60°C and 2-hours soaking in bleach at 23°C twice a week	107
Figure 4.3.24: SEM image and EDS analysis for II-S60B showing Friedel's salt; made with Sulfide coarse aggregate, w/c of 0.65, and tested with drying at 60°C and 2-hours soaking in bleach at 23°C twice a week	108
Figure 4.3.25: SEM image and EDS analysis for II-S60B showing a mixture of important elements and possible crystal formations; made with Sulfide coarse aggregate, w/c of 0.65, and tested with drying at 60°C and 2-hours soaking in bleach at 23°C twice a week	109
Figure 4.3.26: SEM image and EDS analysis for II-S60B showing NaCl salt; made with Sulfide coarse aggregate, w/c of 0.65, and tested with drying at 60°C and 2-hours soaking in bleach at 23°C twice a week	110
Figure 4.3.27: SEM image of II-S60B showing severe cracking in an aggregate particle; made with Sulfide coarse aggregate, w/c of 0.65, and tested with drying at 60°C and 2-hours soaking in bleach at 23°C twice a week	111
Figure 4.3.28 SEM image and EDS analysis for II-D60A showing NaCl salt in coarse aggregate; made with Dolostone coarse aggregate, w/c of 0.65, and tested with drying at 60°C and 2-hours soaking in bleach at 23°C twice a week	113
Figure 4.3.29: SEM image and EDS analysis for II-D60A showing NaCl salt in coarse aggregate; made with Dolostone coarse aggregate, w/c of 0.65, and tested with drying at 60°C and 2-hours soaking in bleach at 23°C twice a week	114
Figure 4.3.30: SEM image and EDS analysis for II-D60A showing cubic NaCl salt crystal in air void; made with Dolostone coarse aggregate, w/c of 0.65, and tested with drying at 60°C and 2-hours soaking in bleach at 23°C twice a week	115

Figure 4.3.31: SEM image and EDS analysis for II-D60A showing Friedel’s salt; made with Dolostone coarse aggregate, w/c of 0.65, and tested with drying at 60°C and 2-hours soaking in bleach at 23°C twice a week	116
Figure 4.3.32: SEM image of II-D60A showing severe cracking; made with Dolostone coarse aggregate, w/c of 0.65, and tested with drying at 60°C and 2-hours soaking in bleach at 23°C twice a week.....	117
Figure 4.3.33: SEM image and EDS for II-D60B showing NaCl salt; made with Dolostone coarse aggregate, w/c of 0.65, and tested with drying at 60°C and 2-hours soaking in bleach at 23°C twice a week	119
Figure 4.3.34: SEM image of II-D60B showing large cracks filled with NaCl salt; made with Dolostone coarse aggregate, w/c of 0.65, and tested with drying at 60°C and 2-hours soaking in bleach at 23°C twice a week	120
Figure 4.3.35: SEM image of II-D60B showing large crack in ITZ filled with NaCl salt; made with Dolostone coarse aggregate, w/c of 0.65, and tested with drying at 60°C and 2-hours soaking in bleach at 23°C twice a week	121
Figure 4.3.36: SEM image of II-D60B showing large cracks filled with NaCl salt; made with Dolostone coarse aggregate, w/c of 0.65, and tested with drying at 60°C and 2-hours soaking in bleach at 23°C twice a week.....	122
Figure 4.3.37: Phase II Series 2 Results; all samples were soaked in lime solution for 2-hours at 23°C twice a week, with drying at 60°C.....	124
Figure 4.3.38: Phase II Series 3 results; after Series 2 exposure, samples soaked in lime solution at 5°C for 7-days, with hot/cold cycles to 23°C/5°C	125
Figure 4.3.39: Phase II Series 4 results; all samples tested with humidity maintained at 100% at all times, all samples had w/c of 0.65, heating to 60°C with 2-hour bleach soaking at 23°C twice a week	126
Figure 4.4.1: Phase 3 results; all samples have w/c=0.65, were tested with 24-hour soaking at 23°C twice a week, and 24-hours heating/drying to 60°C twice a week.....	127
Figure 4.5.1: Phase IV results; all samples have w/c=0.65, were tested with 24-hour soaking at 23°C once a week, and 5-days heating/drying to 60°C	128
Figure 4.6.1: Cylinders tested under Phase III conditions, bleach soaked on left, lime solution soaked on the right; all samples have w/c=0.65, were tested with 24-hour soaking at 23°C twice a week, and 24-hours heating/drying to 60°C twice a week.....	129
Figure 4.6.2: SEM image and EDS analysis for Sulfide aggregate showing pyrrhotite; exposed only to environmental conditions.....	132

Figure 4.6.3: SEM image and EDS analysis for Sulfide aggregate showing oxidized pyrrhotite; exposed only to environmental conditions	133
Figure 4.6.4: SEM image and EDS analysis for Sulfide aggregate showing potentially oxidized pyrrhotite; exposed only to environmental conditions.....	134
Figure 5.1.1: Proposed reaction series for Phase II Series 2 Sulfide sample; made with w/c of 0.65, and tested with drying at 60°C and 2-hours soaking in bleach at 23°C twice a week.....	139
Figure A.5.2.1: Typical month of Phase I dry testing.....	147
Figure A.5.2.2: Typical month of Phase I wet/dry testing.....	147
Figure A.5.2.3: Typical month of Phase II Series 2 testing.....	148
Figure A.5.2.4: Transition from Phase II Series 2 to Series 3 testing.....	148

1 Introduction

In recent years, a rapid concrete deterioration has been observed in a few housing developments in the Trios-Rivières area in Quebec, Canada. Detrimental cracking was seen after just 3 to 5 years of construction and crack widths up to 5mm wide were observed in the interior of the foundation walls, as seen in Figure 1.1.1-B).

A)



Map cracking in foundation

B)



Interior crack in foundation

C)



Pop-out with yellowish staining

D)



Cracked masonry caused by foundation expansion

Figure 1.1.1: Pictures of damaged concrete foundations in Quebec, Canada

This problem has affected more than 900 residential owners, who face serious issues related to deterioration of their concrete foundations and slabs. In some cases the deterioration warranted

immediate remedial actions. This distressed concrete is the point of reference for all testing in this study, and will be referred to as “the foundations” from here forward. Yellowish staining, map cracking, and pop-outs were observed on the surface of the foundation walls, shown in Figure 1.1.1. Sealer was used to fill the cracks in A). Also, some exposed coarse aggregate particles showed rust (iron oxyhydroxides) on their surface, seen in Figure 1.1.1-C). A crack is seen in the masonry in Figure 1.1.1-D) that was thought to be caused by expansion of the foundation. Concrete removed from the foundations was examined using petrographic techniques, the results of which are discussed by Duchesne and Fournier. Also, concrete taken from the foundations was examined further by Rodrigues et al.. A summary of the results of these 2 papers is discussed in the following section. Damage and expansion caused by oxidation of iron sulfide minerals has been observed in other cases, but it occurred at a much slower rate and was not detrimental to the structure. Since the case in Quebec occurred over such a short period of time this problem is now of great importance to the concrete industry in Canada. There is currently very little information available on the exact reaction mechanism causing this severe damage.

1.1 Analysis of Distressed Concrete

During the first study, concrete removed from the foundations was examined and coarse aggregate particles were found to include a significant amount of iron sulfides; pyrite and large grains of pyrrhotite. The pyrite was found to be intact, while evidence of oxidation and iron oxyhydroxides was found, associated with degrading pyrrhotite. Cracking was found extended through the paste and aggregate particles. Scanning electron microscopy (SEM) was used to confirm the presence of iron oxyhydroxides, gypsum, and ettringite in proximity with pyrrhotite (Duchesne & Fournier, 2011). In the subsequent study, concrete cores were often highly damaged, with an important amount of cracking observed around and through coarse aggregate particles. Oxidation of pyrrhotite, followed by internal sulfate attack was determined to cause the formation of gypsum, ettringite, and thaumasite. White halos were often observed around oxidized coarse aggregate particles that contained iron sulfides. Thaumasite sulfate attack (TSA) was suspected of being the major contributor to the damage observed in this study (Rodrigues et al., 2012).

1.2 Possible Reaction Series

Concrete is known to be an aggressive environment for some minerals since the pore solution is very alkaline, and the pH is often above 13. The deterioration observed in the foundations, was derived from the oxidation of pyrrhotite present in the coarse aggregate particles; exposure to oxygen and humidity can cause this reaction, even inside of concrete. This oxidation reaction is known to be associated with a volume increase, and the release of sulfuric acid. The sulfuric acid is then thought to cause internal sulfate attack on the concrete, where the sulfate in the sulfuric acid reacts with calcium hydroxide of the cement, promoting gypsum formation. The gypsum may then proceed to continue reacting with the cement to first produce ettringite, followed by thaumasite (Brown, 2002; Kohler, Heinz, & Urbonas, 2006). These reactions are discussed in detail in the following sections. Expansion is expected from 2 contributors in the previous reaction series; the oxidation reaction, and the sulfate attack. Sulfate attack is thought to be far more expansive, and thus be the major contributor to the concrete deterioration, especially when thaumasite is involved (Duchesne & Fournier, 2011; Rodrigues et al., 2012).

1.3 Objectives and Research Significance

Since the presence of iron sulfides in aggregates has recently become recognized as a concrete durability problem in Canada, there is currently a great need for more information on the subject. Several objectives were maintained throughout testing during the current work. The primary goal was to better understand the mechanism responsible for concrete deterioration. There is currently no similar reaction mechanisms understood that experience this type of deterioration. This degradation needed to be reproduced in the lab, and an accelerated version of the reaction was desired. There is very little information available regarding the promotion of this specific series of reactions inside of concrete. The ultimate goal of the current work was to provide information towards the development of a performance test. There is currently no such test to predict the performance of concrete when coarse aggregates with this type of composition are used. While pyrrhotite is known to be a mineral found in aggregates across Canada, the relative amount and grain sizes observed in Quebec have not yet been seen elsewhere. Thus, it is important to determine the relative amount of pyrrhotite that can be considered acceptable for use in concrete. Once a test has been established, the information yielded from it could also provide insight into

mitigation techniques. Recent attempts to reproduce this degradation in the lab have proven unsuccessful (Duchesne & Fournier, 2011; Rodrigues et al., 2012). This work attempts to provide more information on reproducing this reaction under laboratory condition, with methods tailored for performance test development.

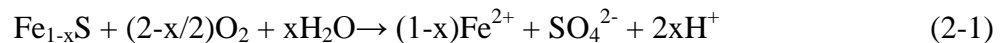
2 Literature Review

2.1 Iron Sulfide Oxidation

Iron sulfides are known to be unstable in the presence of moisture and oxygen; they undergo an oxidation reaction commonly referred to as “rusting”. During this reaction, iron oxides are formed on the surface of the pyrrhotite, and sulfuric acid is released (Belzile, Chen, Cai, & Li, 2004). When this occurs inside of concrete, the sulfuric acid is expected to react with the calcium hydroxide in the cement to form gypsum, ettringite, and/or thaumasite, as discussed in Sections 1.2 and 2.2. Since the iron sulfide oxidation and sulfate attack reactions are both associated with a volume increase, it would follow that this series of reactions has the potential to cause severe damage in concrete, if the appropriate conditions are provided. Of the 2 iron sulfide minerals present in this study, pyrrhotite (FeS) and pyrite (FeS₂), pyrite dissolves only in the presence of an oxidant, while pyrrhotite is known to do so with or without an oxidative process (Chinchon-Paya, Aguado, & Chinchon, 2012). Also, the solubility of FeS was found to be 4 times higher than that of FeS₂ (Schmidt, Leemann, Gallucci, & Scrivener, 2011).

2.1.1 Pyrrhotite

Pyrrhotite, generally written as FeS, is known to be unstable and highly reactive; it is considered as one of the most reactive sulfide minerals (Rodrigues et al., 2012). The general formula for pyrrhotite is Fe_{1-x}S, with x varying from 0 (FeS) to 0.125 (Fe₇S₈) (Rodrigues et al., 2012). The mechanisms of the different pyrrhotite oxidation processes are understood and reviewed elsewhere (Belzile et al., 2004). A basic review of the general iron oxidation reaction is presented here. The oxidation reaction of pyrrhotite in the presence of water and oxygen is shown in Equation (2-1), ferrous iron (Fe²⁺) and sulfuric acid (SO₄²⁻) are seen as the reaction products.



In Equation (2-2), the ferrous iron goes on to react further with oxygen to produce ferric ions (Fe³⁺). The reaction comes to completion upon the formation of ferric oxyhydroxides, principally

ferrihydrite ($\text{Fe}_2\text{O}_3 \cdot 0.5(\text{H}_2\text{O})$) and goethite (FeOOH) (Rodrigues et al., 2012), shown in Equation (2-3) as $\text{Fe}(\text{OH})_3$.



This reaction is well understood as a similar process is responsible for the damage of concrete caused by reinforcement corrosion. Researchers have examined 40-year old dam concrete and found that only 30-40% of the pyrrhotite present in the coarse aggregates was reacted (Schmidt et al., 2011).

2.2 Sulfate Attack

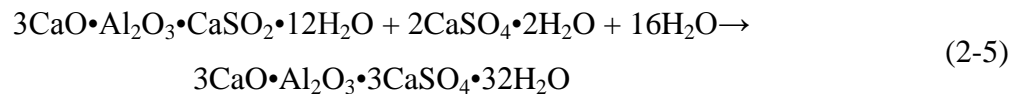
Sulfate attack is a term used to describe a general type of concrete deterioration. The definition of sulfate attack is deterioration of concrete that involves a sulfate (Collepari, 2003; Neville, 2011). There are many different types of sulfate attack, depending on the source of the sulfate and the type of reaction that occurs. Sulfate attack can be divided into several categories depending on the mechanism responsible for the damage. Sulfates may crystallize as salt and cause damage in a purely physical manner, which is referred to as physical salt attack, discussed in a later section (2.3). Sulfates may also undergo a chemical reaction with the concrete, known as chemical sulfate attack. In this section we will look at the main types of chemical sulfate attack mechanisms. It should be noted here that there are 2 general sources of sulfates in concrete; internal sulfate attack (ISA) occurs when sulfates are supplied by the concrete mixture itself, while external sulfate attack (ESA) occurs when the sulfates are supplied by the environment and enter the concrete after hardening (Collepari, 2003). The main reaction products that lead to concrete deterioration during sulfate attack are known as gypsum, ettringite, thaumasite, and magnesium hydroxide; the first 3 will be discussed in detail in the following sections, while the latter is outside of the scope of the current work.

2.2.1 Ettringite

Ettringite ($3\text{CaO} \cdot \text{Al}_2\text{O}_3 \cdot 3\text{CaSO}_4 \cdot 32\text{H}_2\text{O}$) is formed in concrete as a product of the reaction between gypsum ($\text{CaSO}_4 \cdot 2\text{H}_2\text{O}$) and calcium aluminate phases (C_3A) (Shi, Wang, & Behnood, 2012). It can form directly from the reaction between gypsum and calcium aluminate according to the reaction:



Equation (2-4) shows a 131% volume increase, from the reactants to the ettringite. This percentage is calculated based on stoichiometry and compound densities (Clifton & Pommersheim, 1994). Ettringite can also form via the formation of monosulfate (monosulfoaluminate) ($3\text{CaO} \cdot \text{Al}_2\text{O}_3 \cdot \text{CaSO}_2 \cdot 12\text{H}_2\text{O}$), when gypsum (CaSO_4) is present, according to the following equation:



Equation (2-5) shows a volume increase of 55% (Clifton & Pommersheim, 1994). Ettringite may form while the concrete is still plastic (before hardening) which is known as primary ettringite formation (PEF), or early ettringite formation. PEF does not cause distress to concrete, it is encouraged, and is useful in retarding concrete setting time, this is the reason for adding gypsum to the cement (Colleparidi, 2003). Secondary ettringite formation (SEF) occurs once the concrete has hardened. It is SEF that causes the deterioration in concrete that is referred to as classic sulfate attack. This typically occurs from ESA processes, as discussed below, but can also occur from ISA, which will be discussed in detail in Section 2.2.1.5. When ettringite forms after concrete hardening, it will put pressure on the concrete that can cause expansion and cracking (Colleparidi, 2003). Ettringite causes damage to concrete because of the volume increase experienced upon formation, associated with a large amount of hydration. The exact amount of physical volume increase is not generally agreed upon, it has been reported to be anywhere from 2 to 7 times larger in volume than its constituent reactants (Monteny et al., 2000).

2.2.1.1 Calcium Sulfate

Calcium sulfate (CaSO_4), also known as gypsum, may be present in the concrete from either internal or external sources. Gypsum can cause ISA from 2 sources; if the cement contains too much gypsum, or if the aggregates are contaminated with gypsum (Colleparidi, 2003). Gypsum can also cause ESA as calcium sulfate solution can enter concrete from an environmental source. Gypsum is involved with most other chemical sulfate attack mechanisms, as it is formed as an intermediate product in deterioration development. The formation of gypsum itself is generally

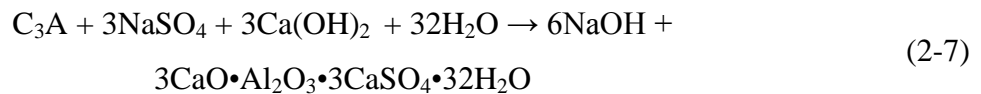
associated with a volume increase by a factor of 1.2, but whether it causes damage or not is still a topic of debate (Monteny et al., 2000). Some researchers believe it can be the leading cause of cracking, while others believe it exists in a through-solution form that does not cause expansion (Neville, 2004). Gypsum has a modulus of elasticity less than that of concrete, so it is thought to exert pressure on the concrete, but not likely cause much expansion (Collepari, 2003). Although, it has been postulated that gypsum will soften the cement gel, lower concrete strength and elastic modulus, and make it more susceptible to damage by ettringite (Clifton & Pommersheim, 1994). What is generally agreed upon is that gypsum will react with C₃A to form ettringite and cause damage to the concrete.

2.2.1.2 Sodium Sulfate

Sodium sulfate (NaSO₄) is typically considered ESA; it can enter concrete in solution from an environmental source. Sodium sulfate attack is the predominant type of sulfate attack that occurs in California (Neville, 2004). Sodium sulfate present in concrete can react with calcium hydroxide (Ca(OH)₂) to form gypsum according to the following equation:



The reaction described in equation (2-6) is associated with volume increase of 1.24% (Clifton & Pommersheim, 1994). Since calcium hydroxide is very abundant in the hardened cement paste, up to approximately 20% by volume (Hobbs & Taylor, 2000), this reaction will generally continue if there is a supply of sodium sulfate (unless calcium hydroxide is leached out) (Neville, 2004). Gypsum continues to react and leads to SEF deterioration via the reactions discussed above. Sodium sulfate can also react with calcium hydroxide and C₃A to form ettringite directly according to the following equation:



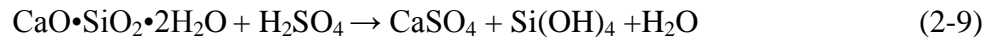
The reaction in equation (2-7) is associated with a volume increase of 283% (Clifton & Pommersheim, 1994). Thus, a similar level of expansion should be expected whether gypsum is part of the reaction or not based on stoichiometric volumes.

2.2.1.3 Sulfuric Acid

Sulfuric acid (H_2SO_4) is very corrosive to concrete as it can attack the durability of concrete in 2 different ways. The first attack is the result of the sulfuric acid reacting to form gypsum, this can happen in 2 different ways; sulfuric acid will react primarily with the calcium hydroxide found in concrete to form gypsum, according to the following equation (Monteny et al., 2000):



The gypsum can then go on to react with the cement and form ettringite, as discussed above. If the calcium hydroxide in the concrete becomes depleted, either through reactions or leaching, sulfuric acid can also react with the calcium silicate hydrates, releasing calcium ions to form gypsum according to the following equation (Monteny et al., 2000):



The second method of attack is caused by the hydrogen ions of the acid reacting with the cement and causing the dissolution of ferrite and aluminate hydrates ions (O'Connell, McNally, & Richardson, 2010). This reaction is slower however, and would happen at a much lower pH than the previous reactions (Beddoe & Dörner, 2005).

2.2.1.4 Delayed Ettringite Formation

Delayed ettringite formation (DEF) is considered as a type of secondary ettringite formation (SEF) in hardened concrete. It is caused by sulfates that originated from the cement paste only, therefore it is also a type of internal sulfate attack (ISA). Typical, primary ettringite formation may be suppressed if the concrete is heated above about 70°C during curing, because ettringite is not stable above that temperature. Instead, the sulfate ions are adsorbed on the C-S-H phase at the elevated temperature (Collepari, 2003). The exact temperature to which this occurs seems ambiguous, and some researchers report it as greater than $60^\circ\text{C}/70^\circ\text{C}$ (Bouzabata, Multon, Sellier, & Houari, 2012; Leklou, Aubert, & Escadeillas, 2012). It is generally agreed that curing temperatures above 70°C will cause DEF with typical cases; some researchers have found that the effects of DEF can be seen at lower temperatures, but this is usually associated with a special circumstance (Bouzabata et al., 2012; Taylor, Famy, & Scrivener, 2001). Upon cooling, the

sulfates are free to react with the aluminate phases in the cement paste, and cause the delayed formation of ettringite (Taylor et al., 2001). DEF and SEF from ISA are often referred to as the same phenomenon, but will be differentiated between here; DEF occurs only from sulfates derived from the cement paste, where SEF includes all internal sulfate sources.

2.2.1.5 *Secondary Ettringite Formation*

Secondary Ettringite Formation (SEF) can be considered as all other internal sulfate attack mechanisms, which promote ettringite formation in the concrete after hardening. Sulfates for this type of attack are provided by internal sources (ISA) or external sources (ESA) as discussed previously; this section will focus on SEF from ISA. The difference between SEF and DEF is that primary ettringite is allowed to form with SEF while it is not with DEF. It is important to distinguish between them, because SEF can occur in any concrete, regardless of curing temperatures. Therefore, similar characteristics are expected here as was discussed above with DEF. In the most currently accepted understanding of the mechanism producing SEF, 3 requirements must be present; micro-cracking, late sulfate release, and exposure to water. The late sulfate release could be from any of the following sources: sulfate release from aggregates, thermal decomposition of primary ettringite, or from adsorbed on C-S-H (for DEF). Researchers have demonstrated that significant expansion and cracking can be caused in concrete upon heating and cooling cycles to 80°C, caused by the dissolution of sulfoaluminates (monosulfate or ettringite) formed during concrete hardening (Fu & Beaudoin, 1996; Grabowski, Czarnecki, Gillott, Duggan, & Scott, 1992).

2.2.2 Thaumasite

Thaumasite ($\text{CaSiO} \cdot \text{CaSO}_4 \cdot \text{CaCO}_3 \cdot 15\text{H}_2\text{O}$) is another reaction product associated with severe cases of ESA; this mechanism is known as thaumasite sulfate attack (TSA). The thaumasite is able to cause deterioration in the concrete in 2 ways; expansion caused by volume increase associated with reaction products, and the attack of the C-S-H in the cement paste (Brown, 2002). Thaumasite formation weakens the cement paste and turns it too mush in severe cases (Kohler, Heinz, & Urbonas, 2006). Thaumasite requires the calcium and silica of the paste, and also the presence of sulfates, carbonates, and moisture (Shi et al., 2012); carbonates may be present in concrete from either carbonation or cement fillers such as limestone. Thaumasite

formation requires temperatures below 15°C, and favours low temperatures compared to ettringite; 5°C is thought to be the optimal temperature to promote thaumasite sulfate attack (TSA). Deterioration caused by thaumasite is often more severe than that caused by ettringite (Shi et al., 2012), and it also occurs more rapidly. Ettringite is thought to be a necessary precursor to thaumasite formation, but that is still an area of debate. One researcher found that thaumasite forms through a heterogeneous nucleation on the surface of ettringite (Kohler et al., 2006). There is also thought to exist an ettringite/thaumasite solid solution, where evidence of both phases are present, this has been reported to form in a massive type formation (Barnett, Adam, & Jackson, 2000; Brown, 2002).

2.3 Physical Salt Attack

When salts are allowed to enter concrete and experience drying, the water evaporates and leaves behind the salt crystals. When enough water evaporates, super-saturation is achieved in the remaining solution, and the salt crystals are allowed to precipitate inside the concrete. Upon subsequent wetting and drying, the crystals can swell and grow; this can put pressure on the concrete and cause cracking, a phenomenon known as salt weathering (Neville, 2011). This process is known to occur with sea water in tidal zones and with de-icing salts as a contribution to salt scaling. Salt weathering can affect the coarse aggregate particles also, if they are sufficiently porous. There are many different types of salt that can cause a varying amount of damage to concrete upon wet/dry cycles. The following section will focus only on the effects of sodium chloride.

2.3.1 Sodium Chloride (NaCl)

Sodium chloride (NaCl) is known to cause some salt weathering in concrete, especially when the w/c is high. While sodium chloride is not as aggressive as the other salts, it has been shown to cause distress in concrete tested at 40°C (Haynes, O'Neill, Neff, & Kumar Mehta, 2010). Relatively high concentrations of NaCl are required to cause damage; a NaCl solution of 15% (~2.6M) was found to cause severe damage to concrete, while a solution of 3% (~0.5M) was found to result in much less damage (Darwin, Browning, Gong, & Hughes, 2008). Sodium chloride salt crystals are hygroscopic, and thus, have the ability to swell upon absorption of moisture from the environment. This means that upon repeated wetting and drying cycles, the

salt crystals will re-hydrate and continue to grow, which can exert pressure on the concrete and cause cracking. Also, they may undergo dissolution/crystallization cycles if the relative humidity (RH) in the environment crosses the crystallization RH of the salt, which was found to be between 75-80% for NaCl (Langlet et al., 2011; Lubelli, van Hees, & Groot, 2006). It has also been found that NaCl salts seem to have a preferential formation location at the aggregate paste interface in mortar (Lubelli et al., 2006). It has been observed that NaCl salts form crystalline salt columns reminiscent of ice needles in concrete, which resulted in physical salt attack (Brown, 2002).

2.4 Chlorides in Concrete

It is known from reinforcement corrosion understanding, that when Friedel's salt is present in concrete, sulfate attack can cause the formation of ettringite and release of chlorine. A reverse reaction may also occur, where if ettringite is present and excess chlorides are introduced, Friedel's salt will be promoted; chlorides will be consumed and sulfates will be released during this reaction (A. M. Neville, 2011). Friedel's salt itself is not associated with causing damage to concrete, and thus, chlorides may have the ability to mitigate expansion associated with sulfate attack. The following section focuses on the later reaction and subsequent interactions.

2.4.1 Friedel's Salt

Cement itself has the ability to react with a certain amount of chlorides; the amount depends on the composition of the cement. Ettringite is also known to possess the ability to react with chlorides and promote the formation of Friedel's salt and the release of sulfates (Ekolu, Thomas, & Hooton, 2006; Yee-Ching, 2012). It seems that the chlorides will first react with any available C_3A , then with any monosulfate in the cement, and if the concentration of chlorides is strong enough, it will then go on to react with any ettringite present to form Friedel's salt ($3CaO \cdot Al_2O_3 \cdot CaCl_2 \cdot 10H_2O$) (Ekolu et al., 2006; Jones et al., 2003). When the chlorides react with monosulfate, they will first produce Kuzel's salt; ($3CaO \cdot Al_2O_3 \cdot \frac{1}{2}CaSO_4 \cdot \frac{1}{2}CaCl_2 \cdot 10H_2O$). Then, if the chloride concentration is higher than about 1M, the monosulfate will transform completely into Friedel's salt. It is not until the chloride concentration is above 2M that the ettringite will react to form Friedel's salt (Zibara, 2001). Others have found that ettringite can react with chlorides present at lower concentrations to form Kuzel's salt, but the rate of reaction

is very slow (Yee-Ching, 2012). There are several theories discussed that describe the exact mechanism involved in the formation of Friedel's salt, the most generally accepted is described here. When NaCl enters concrete, it acts as 2 separate components; Na^+ and Cl^- . When the chloride ion reacts to form Friedel's salt, the free Sodium is then absorbed in the C-S-H, which leads to the release of OH^- ions (Jones et al., 2003; Yee-Ching, 2012). Sulfur is dissolved during this reaction and may react with the calcium hydroxide in the cement to form gypsum, and may be removed from the concrete as with marine exposure. It is known from the effects of sea water on concrete that both ettringite and gypsum are soluble in the presence of chlorides, and can be leached out by the sea water (Neville, 2011). Friedel's salt is dependent on the amount of C_3A in the cement; either unreacted, or decomposed from monosulfate or ettringite. Once all of the C_3A is reacted, Friedel's salt production will reach completion. Researchers found that Friedel's salt and gypsum were the final phase products when concrete was exposed to chlorides in high concentration (2.8M) and DEF was induced (Ekolu et al., 2006).

2.5 Wetting and Drying Cycles

Wet/dry cycles have been known to cause some expansion and damage in concrete, the reason for the expansion could be from many sources. It has been demonstrated that wet/dry cycles will cause micro-cracking in concrete, after only 5 cycles (Leklou et al., 2012). The damage mechanism is believed to be mechanical, and is attributed to the action of water penetrating into the very small pores and cracks of the concrete and exerting pressure (Batic, Milanese, Maiza, & Marfil, 2000). Wetting of concrete occurs very rapidly, while drying happens much more slowly, and the core of the concrete may never completely dry (A. M. Neville, 2011). Thus, subsequent wetting and drying cycles may cause further ingress of water into the core of the concrete. Wet/dry cycles have been found to accelerate the expansion caused by SEF, a mortar sample with regular cement experienced expansion of 0.059% after 12 months from wet/dry cycles at with drying at 38°C and soaking at 20°C . This expansion was achieved with type GU cement with SO_3 content of 2.0%, and the researchers concluded that the damage was not caused entirely by the moisture conditions; they suspected massive ettringite of contributing (Batic et al., 2000). It has been well documented that wet/dry cycles with drying at 80°C will increase the rate of expansion caused by DEF (Leklou et al., 2012). Also, it has been found that heating cycles to

80°C with moisture will cause damage in concrete that would not have suffered from DEF (Fu & Beaudoin, 1996; Grabowski et al., 1992).

2.6 Mix Design Parameters

2.6.1 Water-to-Cement Ratio (w/c)

Water-to-Cement ratio (w/c) is known to control both strength and porosity of the concrete. Therefore, selection of the appropriate w/c is a very important property with regards to concrete durability. A minimum w/c is specified for each exposure class when proportioning a concrete mixture according to the procedure outlined by ACI committee 211.1 (ACI Committee 211, 1991). A low w/c (<0.45) would produce a relatively strong and durable concrete with less porosity and lower permeability, but workability may be poor unless a plasticizer is used. Conversely, a high w/c (>0.6) would produce a very workable concrete that is relatively weak and has high porosity, and thus poor durability. A lower w/c would require a higher cement content to maintain a proper consistency, which contributes to the increased durability (Kosmatka, Kerkhoff, Hooton, & McGrath, 2011).

2.6.2 Cement Content

The cement content of concrete affects properties in several different ways; concrete strength, permeability, and consistency are all dependent on cement content. When selecting cement content, several factors need to be considered. Applications that require improved durability require higher cement content; examples of durability issues affected by cement content are: finishability, wear/abrasion resistance, aesthetic appearance, freeze-thaw resistance, de-icer resistance, and sulfate exposure. Minimum cement content requirements are specified for each of the previous cases mentioned when proportioning concrete mixtures according to ACI 211.1 (ACI Committee 211, 1991). High cement content will produce a relatively strong concrete, which has a more dense and less permeable cement matrix. Conversely, low cement content will produce a relatively weak concrete with higher permeability (Kosmatka et al., 2011).

2.6.3 Silica Fume

Silica fume is a by-product of the processes used to produce silicon and silicon containing alloys. It is considered as a supplementary cement material; it has a specific gravity of 2-2.5 and can provide added durability to concrete. It will provide cementing properties upon a hydration process known as a pozzolanic reaction; where it will react with either water or the calcium hydroxide produced during cement hydration, to produce additional hydration products that contribute to strength development. The small particle size of silica fume compared to cement means that it has a much greater surface area, and will promote the formation of a more densely packed cement paste. The increased surface area allows the reaction to proceed very quickly, and the result is a cement paste that develops an increased rate of strength gain, and has a relatively very low permeability. Therefore, silica fume is used in applications that require high early strength or very low permeability. It is recommended to not exceed a silica fume content of 15% by weight in typical concrete applications; applications such as shotcrete may require higher silica fume content. It is typically added to concrete at up to 10% replacement of the cement, but is recommended around 8% to balance economy and ease of concrete placement. Silica-Fume is known to increase water demand and decrease air content, therefore it will also produce a concrete with less slump than that of a mixture with the same proportions and no silica fume (Kosmatka et al., 2011).

2.6.4 Air-Entraining Admixture

Air-entraining admixture is added to concrete to introduce microscopic stabilized air bubbles into the concrete. These bubbles are uniformly distributed throughout the cement paste and the optimum amount has been found to be 6-8% by volume of concrete. This is known to improve resistance to damage associated with freeze-thaw cycles, and may also help reduce damage caused by salt weathering. Air-entraining admixture is known to significantly improve workability, and reduce or eliminate segregation and bleeding in fresh concrete (Kosmatka et al., 2011).

3 Experimental Procedures

3.1 Scope of Work

3.1.1 Test Development

There is currently very little information available regarding the promotion of iron sulfide oxidation in a laboratory. Information and ideas may be adopted from sulfate attack testing, to aid in the promotion of ettringite and thaumasite. Also information may be adopted from alkali silica reaction (ASR) testing, where the oxidation and ASR reactions share some similarities. Both involve a reaction with a mineral found in the aggregates, and both require a certain moisture level for the reaction to proceed. The difference is that ASR requires high alkalinity within the concrete, while the iron sulfides require a certain amount of oxygen for the oxidation reaction to proceed. Therefore, test development will be designed with an understanding of other reaction mechanisms, and the processes that accelerate reactivity. A successful test will be able to show expansion with the iron sulfide bearing aggregate, and no expansion with aggregates that contain no iron sulfides. In order to be considered as an accelerated test, definitive results within 6 months to a year would be expected. The only reference available to measure the success of the test development with regards to producing the desired reaction mechanism, is the actual foundations that were sampled from and tested. Thus, a successful test would be expected to produce damage upon the formation of ettringite, thaumasite, and iron oxyhydroxides in the concrete, as was observed in the foundations. It was decided to make all testing cycles based on a weekly routine, some as 7-day cycles, with others as 14-day cycles. Making the scheduling repetitive in such a manner was done to aid in repeatability and to be more operator friendly with regards to keeping track of the cycles.

3.1.2 Sample Preparation

A sample used in all testing is comprised of 3 individual specimens, the specimens used were concrete prisms that measured 76x76x264mm (3"x3"x11-1/4"). Each prism was equipped with a gauge stud in each end that was used for measurements. All gauge lengths were adjusted to 254mm. All samples were made in accordance with ASTM C192 - Standard Practice for Making and Curing Concrete Test Specimens in the Laboratory. A length comparator was used to take

measurements, and all measurements were compared against an invar bar. This invar bar was calibrated monthly against a reference bar, and all measurements are adjusted for the difference, which was relatively substantial in this type of testing, where bleach was involved. All measurements were taken as per ASTM C490 - Standard Practice for Use of Apparatus for the Determination of Length Change of Hardened Cement Paste, Mortar, and Concrete. A standard 10 minute mixing procedure was used for all sample preparation, with a detailed description shown below; the air-entraining admixture was added with the second portion of water.

1. Add aggregates, mix for 1min
2. Add ½ of water, mix for 1 min
3. Rest for 2 min
4. Add cement and remaining water, mix for 2 min
5. Rest for 2 min
6. Mix for 2 min
7. Rest for 2 min
8. Mix for 2 min

3.2 Materials

3.2.1 Aggregates

There were 2 coarse aggregates used throughout testing, discussed below. Sulfide is the problematic aggregate that is the focus of this study, while Dolostone is the control aggregate. There was only one type of fine aggregate used for all testing, thus it will not be discussed further than this section.

3.2.1.1 Sulfide

The sulfide-bearing coarse aggregate is the aggregate under question in this study; it was quarried in the St. Boniface area, near Trois-Rivières, in Quebec, Canada. It will be referred to as “Sulfide” in this paper; it has also been named Maskimo (MSK) in the past. It contained iron sulfides, such as pyrite and pyrrhotite, and was known to be detrimental to concrete when used as an aggregate. It was an anorthositic gabbro type igneous rock, with a bulk relative density of 2860kg/m³. The properties of all aggregates used are shown in Table 3.2.1. This type of rock had

good mechanical typically and in the past was considered as a good quality aggregate for use in concrete. This particular formation contained large intrusions of pyrrhotite and pyrite, with a relatively very large pyrrhotite grain size, which is thought to be related to the concrete deterioration. The amount of iron sulfide varied from particle to particle, but could reach up to 5%-7% (Duchesne & Fournier, 2011). Upon shipment of the Sulfide aggregate to the lab, it was fully submerged in water. This was done to prevent any further oxidation of the coarse aggregates; the water will not allow oxygen to reach the iron sulfides, and they will not be able to oxidize further.

3.2.1.2 Dolostone

The Dolostone coarse aggregate was used as a control in this study; it was a dolomitic limestone that was generalized to be named “Dolostone”. It was of Silurian age (Amabel Formation) quarried from the Niagara Escarpment in the Hamilton area in Ontario, Canada. It was a standard aggregate that was commonly used in commercial concrete in the southern Ontario area, it was considered as a high quality concrete aggregate. It had a bulk relative density of 2570kg/m³, and absorption of 2%, shown in Table 3.2.1. While this aggregate was relatively very porous, it had proven to be successful to produce durable concrete.

Table 3.2.1: Aggregate properties

	BRD (kg/m ³)	Absorption (%)
Sulfide	2862.70	0.38
Dolostone	2571.11	2.08
Sand	2628.77	1.15

3.2.1.3 Fine Aggregate

The fine aggregate used in this study was natural river sand, which had a fineness modulus of 2.7 and a bulk relative density of 2630kg/m³. It was quarried in the Caledon area near Toronto, Ontario, Canada, and is used in commercial concrete in the southern Ontario area. It had a good track record of past performance, and is considered high quality concrete sand.

3.2.2 Cementing Materials

3.2.2.1 *General Use Portland Cement*

Most testing in this study was done with type GU Portland cement, produced at the Holcim plant in Mississauga. It has a chemical analysis shown in Table 3.2.2, the SO₃ was found to be 3.93%.

Table 3.2.2: Chemical analysis of GU cement used in samples

Compound	Amount (%)	Compound	Amount (%)
LOI	2.35	C3S	56.13
SiO ₂	19.47	C2S	13.49
Al ₂ O ₃	5.28	C3A	9.85
Fe ₂ O ₃	2.45	C4AF	7.46
CaO	62.47		
MgO	2.41		
SO ₃	3.93		
Total Alkali	0.97		
Free Lime	1.05		

3.2.2.2 *High Silica Fume Cement (HSF)*

The high silica fume content (HSF) cement is a blended cement; it is made from 92% type GU cement and 8% silica fume. It was used in Phase II as a possible mitigation technique; there were only 4 samples tested with this cement.

3.2.3 Solutions

There were several solutions used to saturate the concrete samples at different stages of testing. Each was used for a different specific purpose, but each purpose was aimed at the same goal; to oxidize the Sulfide aggregate.

3.2.3.1 Bleach

Bleach is an oxidizing agent, it was used in this study to provide moisture and oxygen to the Sulfide aggregates simultaneously. It was also used to replace mixing water in some mixtures in Phase II. It has a high pH between 12-13, and a specific gravity of 1.1. The active ingredient is sodium hypochlorite, and was used at a 6% concentration in this study. Sodium hypochlorite at 6% (w/v) was calculated to be 0.8M NaClO in solution. Bleach is known to decompose upon heating above 40°C (ERCO, 2012). The primary pathway for the decomposition of bleach is shown in Equation (3-1), where 3 moles of bleach will produce 2 moles of sodium chloride (NaCl) and 1 mole of sodium chlorate (NaClO₃) (Hove, 2011).



If bleach is allowed to react with sulfuric acid, it will promote a sodium sulfate solution and hypochlorous acid, as per Equation (3-2) (Jacobson, 2013).



3.2.3.2 Hydrogen Peroxide

Hydrogen peroxide (HP), H₂O₂, was used in Phase I as an oxidizing agent to replace mixing water. It was used at a concentration of 3% in this study. The pH of hydrogen peroxide can be in the range from 4.5-6 and it has a specific gravity of 1.1.

3.2.3.3 Hydrogen Peroxide Bleach (HPB)

Hydrogen peroxide bleach was a store bought “chlorine-free bleach”, also known as “active oxygen bleach”. It was used in Phase II as an oxidizing agent during soaking and to replace mixing water occasionally. The active ingredients are citric acid and hydrogen peroxide; the exact percentages could not be reported due to confidentiality.

3.2.3.4 Lime Solution

Lime solution was used throughout this study, as a type of control solution. It was made from water saturated with calcium hydroxide, Ca(OH)₂ which saturates at about 0.15% (w/v). It was

used to provide moisture to the concrete, without leaching alkalinity. Since lime solution has a pH of between 12 and 13 and it is made from calcium hydroxide, it will not react with the concrete in any way other than providing moisture.

3.2.4 Air-Entraining Admixture

The air-entraining admixture used in this study was Darex AEA, made by Grace Concrete Products. It meets the requirements of ASTM C260, and has a specific gravity of 1.02. It was found that a dosage rate of 70ml/100kg of cement was sufficient to provide 6-8% air content.

3.3 Methodologies

3.3.1 Mix Design

During testing, there were 2 main parameters that were adjusted with regards to concrete mix design; the coarse aggregate type, and the water-to-cement ratio (w/c). All other parameters remained relatively constant during testing, although Phase I and Phase II samples were made with different mixtures, which will be discussed in the following sections. Samples made with Sulfide aggregates used as their coarse aggregates will be referred to as the Sulfide samples, likewise, the samples made with the Dolostone aggregates will be referred to as the Dolostone samples from here forward. Also, w/c is commonly referred to during discussion, to aid in reference it will be included in the title of the sample. For example, if a sample was made with the Sulfide aggregate and had a w/c of 0.45 it will be referred to as Sulfide-0.45. In all testing, the moisture condition of each aggregate was monitored, and compared against its maximum absorption found in Section 3.2.1. The amount of mixing water was adjusted to accommodate for the absorption of the aggregates. Since the Sulfide aggregate was stored in a saturated condition, the free water present on its surface was adjusted for.

3.3.1.1 Phase I

The ASR mix design was adapted for Phase I testing, even the alkalinity was posted to 1.25%. Phase I testing began immediately upon receipt of the coarse aggregate, before strength testing could be conducted. Thus, these samples were made directly following ASR testing procedures. The cement content of 420kg/m³ is considered very high, and produced a concrete with relatively

high quality and a cement matrix with low permeability. The fine to coarse aggregate ratio was kept constant at 2:3. There was 2 different w/c's employed in Phase I; 0.45 and 0.62. The first was used to test concrete with low porosity; any lower would require the use of a plasticizing admixture to achieve a reasonable slump. The second was used to test concrete with high porosity, this was thought to be a safe w/c to use, without promoting segregation of the concrete. A mix design was developed for Phase II that was of lower quality with regards to strength and durability, compared to what was used in Phase I. The exact proportions used for all concrete mixtures can be found in Appendix B.

3.3.1.2 Phase II

After casting Phase I, it was felt that concrete tested in the lab should be made to closely represent the concrete in the foundations. The mix design used in the foundations was acquired and tested, and it gave higher strength results than was provided with the mix design. The mix design specified 20MPa concrete, and when we tested the mix in the lab we got around 30MPa; the difference was thought to be caused by a difference in cement properties. Therefore, we decided to develop a mixture that would achieve a maximum of 20MPa at 28-days. The mixture was designed as per the absolute volume method as described by ACI committee 211.1 (ACI Committee 211, 1991; Kosmatka et al., 2011). Several different mixtures were tested, and the final design achieved 17MPa at 28-days. The mixture proportions for this design, with w/c of 0.65, are shown in Table 3.3.1 and in Appendix B. There was air-entraining admixture used in the foundations, so air-entraining admixture was provided in this design also, the amount was adjusted until 6-8% was achieved via pressure testing. This mixture was used in all Phase II testing of samples with w/c of 0.65, although some adjustments were made to test at w/c of 0.45. Other than the amount of water used, the cement content was adjusted to provide a mix with the proper consistency. This of course meant that the amount of fine aggregate also needed adjustment, as per absolute volume method, these mixture proportions are found in Table 3.3.2 and Appendix B. The reasoning for the w/c selection is similar here to what was described for Phase I. There were several mixtures tested with oxidizing agents used as mixing water, strength testing was conducted on the samples to investigate possible alterations to the concrete. When bleach was used, the 28-day compressive strength was reduced to 13MPa, while the hydrogen peroxide bleach (HPB) reduced compressive strength to only 8MPa.

Table 3.3.1: Phase II concrete proportions for 0.65 w/c mix

	Mass (kg/m ³)
Water	176
Cement	250
Coarse Aggregate	1078
Fine Aggregate	819

Table 3.3.2: Phase II concrete proportions for 0.45 w/c mix

	Mass (kg/m ³)
Water	157.5
Cement	350
Coarse Aggregate	1078
Fine Aggregate	749

3.3.2 Moisture Conditions

The moisture condition of the concrete being tested was an important factor to consider when trying developing a testing regime that was the most effective. This information was particularly important here as the oxidation reaction may be dependent on relative humidity (RH) within the concrete. If the RH is too high, there may not be enough oxygen for the reaction to proceed. Similarly, if the RH inside the concrete is too low, there may not be enough moisture inside the concrete for the reaction to occur. The rate of saturation and rate of drying will vary for different w/c and different drying temperatures, therefore several samples were tested.

3.3.2.1 *Absorption and Drying*

There were 4 samples prepared and tested for absorption and drying testing. Each sample was comprised of 3 identical concrete prism specimens that measured 76mm x 76mm x 254mm. Two samples were made with w/c of 0.45, and 2 were made with w/c of 0.65, using the concrete mix

designs described above. The samples were allowed to cure for 7-days in a controlled room with RH of greater than 95% and temperature of 23°C. The samples were then placed in an environment to promote dry shrinkage for 14-days; RH of 50% and temperature of 23°C. The samples were then allowed to dry for an additional 7-days in a drying oven at their respective temperatures. 2 samples were dried at 40°C, and 2 samples were dried at 60°C for this testing.

After spending 7-days in the oven, before testing began, the samples were weighed, and this was considered their zero reading. The samples were then immersed in water for pre-determined lengths of time. The samples were then removed from the water and dried to a saturated surface dry (SSD) condition, before taking the subsequent weight measurements. All subsequent measurements were taken in this condition until 7-days was reached.

After the saturation testing was complete, the drying measurements were taken. Here, the last saturation reading is considered as the zero reading. The samples were then placed in the drying ovens for pre-determined lengths of time. The samples were removed from the oven and weighed in a heated condition. These measurements were continued until 7-days was reached. 7-days was chosen as the maximum testing time for these tests because it was a practical time for repetitive cycles in the development of a performance test.

3.3.2.2 Relative Humidity

After completion of the absorption and drying testing described above, the same samples were then allowed to stabilize in a room at 50% RH and a temperature of 23°C for 14-days. After this time 2 of the samples were selected for RH testing and were equipped with a relative humidity sensor probe. Relative humidity values were taken with the Wagner Rapid RH 4.0 EX moisture test kit. Smart sensors were installed inside of these concrete prisms at a depth of 38mm, which is at the centre of the 76mm x 76mm cross-section. All RH measurements are taken after the specimens have stabilized at room temperature for 24-hours.

Preliminary RH testing involved fully immersing the concrete prisms in tap water for 2-hours. After this time the concrete prisms were toweled off to an SSD condition and placed in the oven at 60°C for 24-hours. At this time the specimens were removed from the oven and wrapped in plastic wrap to prevent moisture transfer, they were then allowed to stabilize for 24-hours at a

temperature of 23°C. At this time the plastic was removed and the specimens were further allowed to stabilize for 2-hours, at which time stabilization of the RH reading was considered sufficient. This process was repeated twice more, until a time of 72-hours of drying time in the oven was reached.

Subsequent testing of these samples involved exposure of the concrete prisms to Phase I and Phase II conditions, except performed with tap water as the soaking solution. The RH readings were taken at the same time as the Phase I and Phase II readings, after stabilization at 23°C and 50% RH for 24-hours. The RH testing was completed side by side with Phase I for a period of 28-days, at which point the readings were considered to have reached equilibrium. The same samples were then tested side by side with Phase II testing conditions for a period of 28-days.

3.3.3 Phase I

Phase I testing was designed to promote oxidation within the sample, and maintain conditions to encourage the formation of ettringite and thaumasite. Since there is currently very little information on the topic of iron sulfide degradation of concrete, some testing methods are the result of an educated trial and error. In Phase I we decided to heat the samples to 150°C and 60°C in an attempt to accelerate to oxidation process within the concrete. These temperatures were chosen for different reasons; 150°C is thought to be the maximum safe temperature to heat concrete, above which the cement starts to degrade. 60°C was chosen because it is generally accepted that ettringite is stable at this temperature, at and above around 70°C we can expect to see the effects of SEF upon heating and cooling cycles (Collepari, 2003). The heating period can also be considered as a drying period, because the RH in the drying ovens is very low, and the RH within the samples is reduced during heating. All Phase I samples were cured for 7-days, followed by 7-days in a room at 50%RH and 23°C; the zero reading was taken after. This was done to allow the samples to experience some dry shrinkage before they were placed in the oven, in order to compensate for the dry shrinkage in the results. It can be noted again here that both Phase I and Phase II testing programs were designed before the completion of the moisture content testing described in the previous sections. It is presented in this order to aid discussion in the following sections. All hot/cold cycles are 6-days long, followed by a 24-hours period at 50%RH and 23°C. All dry measurements are taken immediately following the 50%RH and 23°C

time period. The 24-hours was considered sufficient to stabilize the temperature and RH throughout the specimens, this provides for consistent and comparable measurements in a clear, repeatable manner. Upon completion of the dry measurements, some samples undergo a soaking period, while some samples are returned to the oven.

Table 3.3.3: Phase I testing program

Exposure		Mixture			
7-Day Dry Cycle (°C)	7-Day Wet Cycle (°C)	Sulfide (0.45)	Dolostone (0.45)	Sulfide (0.62)	Dolostone (0.62)
150	-	✓	✓	✓	✓
150	23	✓	✓	✓	✓
150	5	✓	✓	✓	✓
60	-	✓	✓	✓	✓
60	23	✓	✓	✓	✓
60	5	✓	✓	✓	✓
60	-	✓ (HP)*	✓ (HP)*	✓(HP)*	✓(HP)*

* 3% hydrogen peroxide (HP) was used in place of mixing water

In Table 3.3.3 we can see the 28 samples that were tested in Phase I, each check mark corresponds to a sample that consists of 3 concrete prism specimens. The samples shown in rows 1, 4 and 7 are only tested dry, which is no soaking period, after their dry measurements they were returned to the oven. Therefore, these samples have 1 hot/cold cycle every week. A diagram of a typical month of testing Phase I dry conditions is shown in Appendix A. Also, in Figure 3.3.1-A) a heating schematic is shown for Phase I dry testing for comparison to the other types of testing. Since no additional moisture is provided, these samples were tested to see if the moisture provided at mixing and during curing is enough to promote oxidation in the coarse aggregate. Testing conditions shown in row 4 and 7 in Table 3.3.3 are identical, although in row 7 we used 3% hydrogen peroxide (HP) solution as the mixing water when preparing the samples. Mixing with HP solution instead of water was done in an attempt to accelerate the oxidation reaction, and to also test whether providing an agent at the time of mixing was sufficient to promote oxidation of the aggregates. In the remaining rows shown in Table 3.3.3, rows 2, 3, 5,

and 6 all correspond to wetting and drying testing. The soaking was done for 7-days in all samples, and at 2 different temperatures; 23°C and 5°C.

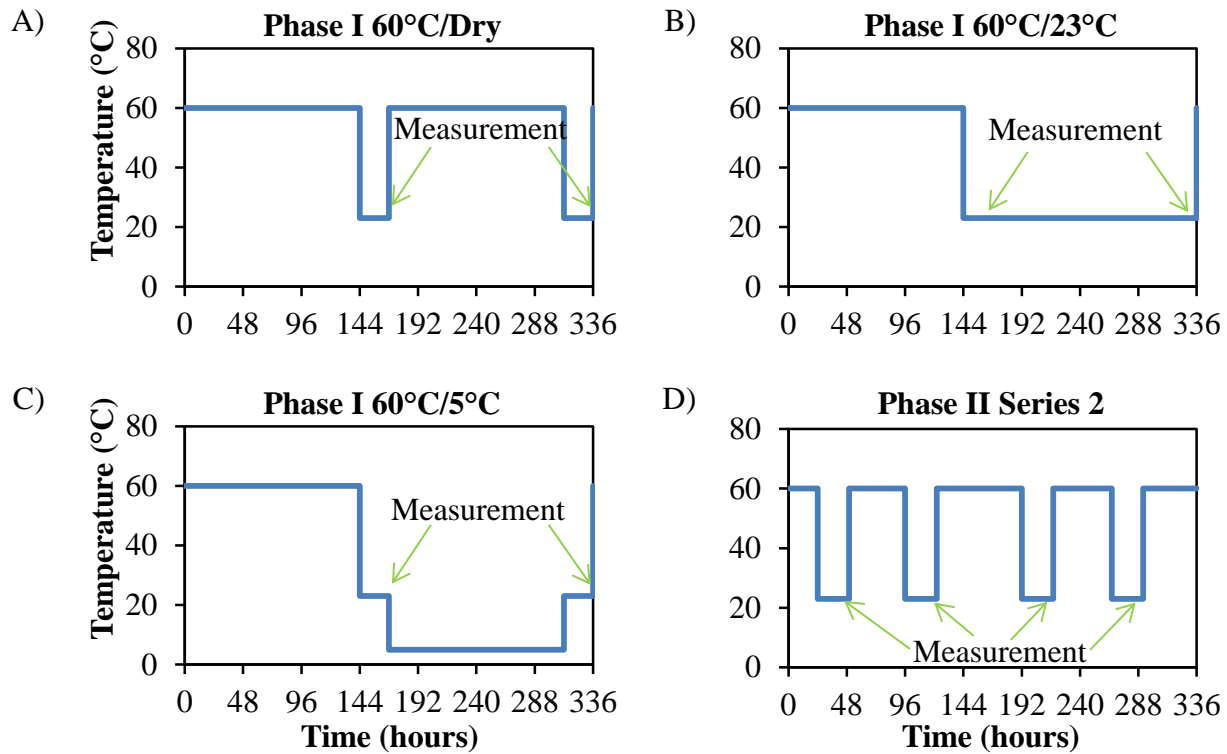


Figure 3.3.1: Heat cycle schematics for different testing regimes over 14-days – Samples were soaked in solution (lime or bleach) while at temperatures of 5°C or 23°C, except A) Phase I 60°C/Dry

The samples that were soaked at 23°C spend 7-days at 23°C, and were towelled off and dried to an SSD condition before taking their wet measurements. The samples that are soaked at 5°C spend 6-days at 5°C, and are then moved, while remaining in solution, to 23°C for 24-hours. The heating schematics for these testing regimes are shown in Figure 3.3.1-B)&C), for 60°C/23°C and 60°C/5°C respectively. After the 24-hour period, the samples are measured in the same manner as the other Phase I wet/dry testing described above; the time of measurements are shown in Figure 3.3.1. Thus, for all wet/dry testing mentioned here for Phase I, it takes 14-days to complete 1 wet/dry and 1 hot/cold cycle. A diagram of a typical month of testing for a Phase I wet/dry sample is shown in Appendix A to clarify the weekly cycles. It was decided to soak the samples in lime solution to provide extra moisture to the concrete samples. Soaking of the samples will provide the moisture that is needed for the oxidation of the iron sulfides in the coarse aggregates. Also, ettringite formation is dependent on the presence of moisture, thus, if

extra moisture is not provided, we will likely not get ettringite after the first heating cycle. The soaking temperatures of 23°C and 5°C were chosen for specific reasons. 23°C is a very favourable condition to promote the formation of ettringite. While we may get ettringite forming in the temperatures ranging from about 5°C to about 70°C (Collepari, 2003), we are most likely to form the greatest amount of ettringite at around ambient room temperature (23°C). Thaumasite formation most favours 5°C, thus it was chosen for a soaking condition to aid its formation. Therefore, the effects of the ettringite and thaumasite formation can be directly compared when comparing the results from soaking at these 2 temperatures. While these temperature are being referred to as the soaking temperatures, this period of time outside of the oven will allow for the formation of significant sulfide expansion products, which cannot form at the elevated temperatures.

3.3.4 Phase II

Phase II involved the introduction of oxidizing agents with the hopes of accelerating the oxidation reaction of the iron sulfides in the coarse aggregate. Some samples were made with the oxidizing agent used as the mixing water, and others were soaked in the agent for different lengths of time. In Phase II, a different concrete mix design was used than in Phase I, this was discussed in Section 3.3.1. That soaking cycles consisted of fully submerging the sample in its respective solution, this was always done at 23°C, after the samples have been stored at 23°C and 50%RH for 24-hours; something that was consistent throughout all testing. With the exception of some samples that were measured in a wet condition, these include: Series 1 Exposure #9, Series 3 and Series 4. This was done to ensure that samples had sufficient time to reach equilibrium to avoid possible thermal stresses cause by soaking temperature differentials. Also, all measurements were taken at 23°C, after the samples were stored at 23°C and 50%RH for 24-hours, this was done to try to minimize the effects of different environmental conditions, and ensure that length change being measured is not influenced by thermal expansions. All samples were cured for 7-days, followed by 14-days at 23°C and 50%RH. This was done to allow sufficient strength gain, followed by drying shrinkage. Since there are different drying cycles, all samples experience the same initial shrinkage to provide a consistent starting point. Zero measurements were taken at the end of the 14-day drying period for most samples. For the

samples that were measure in a wet condition, the reading after 7-days curing was considered as zero.

3.3.4.1 *Series 1*

Six different concrete mixtures were used in Series 1, all with the same proportions and w/c of 0.65, but with different solutions used as mixing water. There were 9 different exposure regimes that were tested in this series, the combinations of mixture and exposures that were tested are shown with a check mark in Table 3.3.4 for comparison.

Exposure #1 was considered as a control exposure, where it was maintained at 50% RH and 23°C at all times. Sulfide samples were made with bleach, and with hydrogen peroxide bleach (HPB) as mixing water, to see if this would be enough to promote oxidation of the iron sulfide. The same was done with the Dolostone sample for comparative reasons.

Exposure #2, #3, and #4 all consisted of a 50% RH and 23°C dry cycle, with 2 wetting cycles per week. They were soaked in their respective solutions for 2-hours for each of their wetting cycles. These samples were measured dry at the end of each 50% RH dry cycle, twice a week.

Exposure #5 had very similar testing to exposure #3, only with heating to 60°C during the dry cycle. Relative Humidity in the drying ovens is considered as being very low. Samples spent either 42-hours or 72-hours in the oven each cycle (to allow for 7-days repetition) followed by 24-hours at 50% RH and 23°C to allow for consistent measurements. A heating schematic of this testing regime is shown in Figure 3.3.1-D).

Exposure #6, #7, #8, and #9 all had 7-day testing cycles; both the drying and the wetting cycles consisted of 7-days, after each of which, a reading was taken. A wet reading was taken at the end of the wet cycle, and a dry reading was taken at the end of the dry cycle; 1 reading per week. The 2 sets of readings were kept separate, and comparisons were made only against readings of a similar condition. Therefore, these samples experienced 1 wetting cycle every 2-weeks.

Exposure #6 and #7 had a wetting cycle that consisted of storing the samples at >95% RH and 23°C for 7-days. Exposure #6 had a 60°C dry cycle, similar to that of Exposure #5. While Exposure #7 had a drying cycle similar to Exposures #2, #3, and #4

Exposure #8 and #9 had a wetting cycle that consisted of soaking the samples in bleach solution for 7-days at 23°C. Exposure #8 had a drying cycle similar to Exposures #2, #3, #4, and #7. While Exposure #9 had a “dry cycle” that was the same as the wet cycle for Exposure #6 and #7. All of these exposures are summarized in Table 3.3.4 to allow for comparison.

Table 3.3.4: Phase II Series 1 testing program; all soaking was after stabilization at 23°C, and all samples had 0.65 w/c

Exposure #	Dry Cycle (RH / Temp)	Wet Cycle (Sol'n / length)	Mixture					
			Sulfide			Dolostone		
			-	Bleach	HPB	-	Bleach	HPB
1	50% / 23°C	- -	✓	✓	✓	✓	✓	✓
2	50% / 23°C	Lime / 2-hrs	✓					
3	50% / 23°C	Bleach / 2-hrs	✓					
4	50% / 23°C	HPB / 2-hrs	✓					
5	Uncontrolled% / 60°C	Bleach / 2-hrs	✓					
6	Uncontrolled% / 60°C	>95%* / 7-day	✓	✓	✓			
7	50% / 23°C	>95%* / 7-day	✓	✓	✓			
8	50% / 23°C	Bleach / 7-day		✓				
9	>95% / 23°C	Bleach / 7-day		✓				

*Samples were stored at RH of greater than 95% instead of soaking

3.3.4.2 Series 2

Series 2 is a continuation of Series 1, Exposure #5; it produced promising preliminary results, so testing was focused here and several samples were tested to check some fine points. In Table 3.3.5 we can see the different testing conditions and type of concrete that was tested, each checkmark represents a sample. All testing cycles are the same as they were described in detail in the previous section for Exposure #5. A diagram showing the first month of testing for a typical Phase II Series 2 sample is shown in Appendix A.

Table 3.3.5: Phase II Series 2 testing program; cycles included drying at 60°C with soaking at 23°C for 2-hours, twice a week; humidity was uncontrolled (low) during heating/drying

Exposure		Mixture			
Dry Cycle (°C)	Wet Cycle (2-hrs)	Sulfide (0.45)	Dolo (0.45)	Sulfide (0.65)	Dolo (0.65)
60	Bleach	✓	✓	✓✓*	✓*
60	Lime	✓	✓	✓	✓
40	Bleach	✓	✓	✓✓*	✓*
40	Lime			✓	✓

*Samples made with 6 specimens for simultaneous testing in Phase II Series 3

Table 3.3.6: Phase II Series 2 testing program with alternate cement; cycles included drying at 60°C with soaking at 23°C for 2-hours, twice a week; humidity was uncontrolled (low) during heating/drying

Exposure		Mixture			
Dry Cycle (°C)	Wet Cycle (2-hrs)	Sulfide (HSF 0.45)	Dolo (HSF 0.45)	Sulfide (HSF 0.65)	Dolo (HSF 0.65)
60	Bleach	✓	✓	✓	✓

Since this testing regime was important, the heating schematic was shown in Figure 3.3.1-D) along with that of Phase I for comparison. Where it is seen that Phase II Series 2 testing has 2 wet dry cycles every 7-days, which is 4 times as many as in Phase I wet/dry testing. In addition to repeating Exposure #5 twice, a Sulfide-0.45 sample was tested, and a Dolostone control sample was prepared for each of these. Other samples were tested at 40°C, and in lime solution

for comparison. 40°C was chosen to see if that would be enough heat to accelerate the reactions, the same drying ovens were used, so the relative humidity was uncontrolled, and very low. Standard ASR testing uses rooms at 38°C, so utilizing the same temperature would allow for easier acceptance of the test, by the industry. Also, Ettringite is more stable at 40°C, so there is less chance of promoting SEF in samples tested at 40°C. Samples were tested in lime solution to see if we could promote a reaction to occur without using an oxidizing agent, this would be beneficial because the agents may affect the concrete in other ways or promote different, unwanted reactions. The samples marked with an asterisk were made of 6 specimens, they were hopeful test candidates at that time, and so were selected for Series 3.

In addition to these concrete mixtures, another set of samples was made with High Silica Fume Cement (HSF Cement). This was done to see if the silica fume would be able to prevent the expansion of the concrete during this exposure condition. The Silica Fume has a very small particle size, so it will fill spaces between the cement particles and provide a less permeable cement matrix and concrete. The samples that were tested with HSF cement are shown in Table 3.3.6.

3.3.4.3 *Series 3*

For this series, some Series 2 samples were made with six specimens; they are highlighted with an asterisk in Table 3.3.5. They were tested in Series 2 until the Sulfide-0.65 sample reached an expansion of 0.7. At that point, 3 of the specimens were moved to Series 3, while the other 3 specimens remained in Series 2. These new Series 3 samples were placed in a lime solution bath and stored at 5°C for 6-days a week, on day 7 the samples were stored at 23°C for 24-hours. Measurements were then taken in a wet condition, and the samples were returned to the fridge in a new, previously prepared solution. The reason this Series is tested in such a way is to try to promote thaumasite formation. Since thaumasite was found in the examined foundations, this type of testing was designed to mimic actual field exposure; where it is possible that a buildup of sulfuric acid could occur during the summer months, followed by colder temperatures and optimal conditions for thaumasite formation. If oxidation was occurring in the Series 2 samples, and excess sulfuric acid was present, it could be expected that Series 3 testing would promote, and show signs of thaumasite attack, after being allowed to expand 0.07% in Series 2.

3.3.4.4 Series 4

The Series 4 samples were tested under the same cycles as Series 2, with heating to 60°C and soaking in bleach. Samples tested are shown in Table 3.3.7. The only difference with this series is that the samples were tested in a container, with the RH maintained at 100%, at all times. The only time they were removed from the containers was for measurement, and soaking.

Table 3.3.7: Phase II Series 4 testing program with humidity maintained at 100%; cycles included heating to 60°C above water in containers, with bleach soaking at 23°C for 2-hours, twice a week

Exposure		Mixture	
Heat Cycle (temp / RH)	Wet Cycle (2-hrs)	Sulfide (0.65)	Dolo (0.65)
60°C / 100%	Bleach	✓	✓

This series was developed in light of observations made during scanning electron microscopy investigation of Series 2, where an abundance of salt crystals had formed inside of the samples. It is possible that these crystals formed as a result of a solution evaporating during heating. When these salt crystals form, they are likely putting pressure on the surrounding concrete. If this pressure was great enough, it could cause cracking of the concrete. The relative humidity of the Series 4 samples was maintained at 100%, inside of a container during heating. This was done to prevent evaporation of any solutions, and test the theory stated above. If expansion occurs under this testing, the damage is not a result of evaporation, and would occur regardless of the relative humidity.

3.3.5 Phase III

Phase III was designed to expose the samples to more bleach each week. It was thought that the bleach will provide more oxygen to the aggregate and cause it to react in a more accelerated manner. These samples were soaked for 2-days over the weekend. On Monday they were removed from solution and measured in an SSD condition, they were then heated for 24-hours. On Tuesday the samples moved from the oven to the 50%RH 23°C room for 24-hours. On Wednesday they would move from 50%RH 23°C room to their solution for 24-hours. On

Thursday the samples were again measured wet and placed in the oven for 24-hours. On Friday the samples were moved to the 50%RH 23°C room for 6-hours, after which they were moved to their solutions for the weekend. In Phase III the samples spend more time in bleach, and less time in the oven compared to Phase II.

Table 3.3.8: Phase III testing program; cycles included soaking at 23°C for 24-hours twice a week; humidity was uncontrolled (low) during 24-hours of heating/drying twice a week

Exposure		Mixture			
Dry Cycle (°C)	Wet Cycle (24-hrs)	Sulfide (0.45)	Dolo (0.45)	Sulfide (0.65)	Dolo (0.65)
60	Bleach			✓	✓
60	Lime	✓	✓	✓	✓
40	Bleach	✓	✓	✓	✓
40	Lime			✓	✓

3.3.6 Phase IV

Phase IV was designed to be similar to Phase I testing, but more accelerated. They are in the oven for a similar length of time, and have soaking that should cause similar saturation levels, but Phase IV was twice as fast as it had 1 cycle per week, where Phase I experienced 1 cycle every 2-weeks. The difference being that Phase IV only spent 24-hours per week at 23°C, where Phase I spent a full 7-days at 23°C. Since these samples were recycled from Phase III, Sulfide-0.45 was not tested in lime in Phase IV.

Table 3.3.9: Phase IV testing program; cycles included soaking at 23°C for 24-hours once a week; humidity was uncontrolled (low) during 5-days of heating/drying at 60°C each week

Exposure		Mixture			
Dry Cycle (°C)	Wet Cycle (24-hrs)	Sulfide (0.45)	Dolo (0.45)	Sulfide (0.65)	Dolo (0.65)
60	Bleach	✓	✓	✓	✓
60	Lime			✓	✓

3.3.7 Scanning Electron Microscopy (SEM)

The microstructure of the concrete was examined using an SEM made by JEOL model JSM-6380-LV. It can performed backscatter electron images (BSE), or secondary electron images (SE). This microscope is capable of providing energy dispersive X-ray spectroscopy (EDS). During EDS analysis, electrons penetrate into the surface of the samples, and the electron beam has a minute diameter that can be focused. Thus, the EDS results often include electrons that penetrated to a depth inside the surface of the sample and in a circle around the point of interest. A circle was shown in the SEM images instead of a point to represent an estimation of the maximum size of the electron beam. It is reasonable to say that the maximum diameter of the electron beam is 5 micron for most analyses, so the circles shown in the images are made roughly 4 or 5 microns, based on the scale on the image. When a sample was selected for SEM analysis, 1 specimen was sacrificed to provide a representative SEM sample. A pair of identical SEM samples was taken from the same specimen to allow for a larger investigation area, they are considered as the same and will not be differentiated between from here on. These SEM samples were cut and polished to be very smooth. They were then coated with either carbon or gold.

3.3.8 Other Testing Procedures

Coarse aggregate testing was done in accordance with ASTM C127 - 12 Standard Test Method for Density, Relative Density (Specific Gravity), and Absorption of Coarse Aggregate (ASTM C127, 2012). Fine aggregate testing was done in accordance with ASTM C128 - 12 Standard Test Method for Density, Relative Density (Specific Gravity), and Absorption of Fine Aggregate (ASTM C128, 2012). Air content pressure testing was done as per ASTM C231 – 10 Standard Test method for Air Content of Freshly Mixed Concrete by the Pressure Method (ASTM C231, 2010). Compressive strength testing was done in accordance with ASTM C39 – 12a Standard Test Method for Compressive Strength of Cylindrical Concrete Specimens (ASTM C39, 2012) Split tensile strength testing was done as per ASTM C496 - 11 Standard Test Method for Splitting Tensile Strength of Cylindrical Concrete Specimens (ASTM C127, 2011)

4 Results and Analysis

4.1 **Moisture Conditions**

The development of an effective testing program is dependent on understanding the relative amount of moisture within the concrete prism samples at a given time. To properly analyze the effects of the different testing regimes, the amount of time needed to saturate the samples, and the amount of time needed to dry the samples must be known. This information was used to estimate the degree of saturation of the samples at the different stages of testing of Phase I and Phase II, in the following sections. This testing was done subsequent to Phase I and Phase II testing, as a method to investigate the moisture conditions inside of the concrete; it is presented here to aid in the analysis of Phase I and Phase II during analysis.

4.1.1 Absorption and Drying

Before this testing was conducted, the samples were conditioned in the same manner as in Phase II, followed by a drying period of 7-days in an oven at their respective testing temperatures. The absorption and drying results for samples that were tested at 60°C are shown in Figure 4.1.1 and Figure 4.1.2 respectively. In Figure 4.1.1 the saturation trends for 24-hours are shown, it is seen that the sample with w/c of 0.65 reached a higher degree of saturation than that of the sample with w/c of 0.45. The higher porosity in the sample could have contributed to this difference in several ways. During the 7-day drying period prior to testing, the higher porosity would have allowed the sample with w/c of 0.65 to dry more. This means the initial weight measurement may have been taken at a dryer condition compared to the sample with w/c of 0.45. The higher porosity also means that the pores are relatively larger, and would have allowed for water to enter the void system more easily. Thus, the water would be allowed to migrate further into the sample with higher w/c, over the same time period. What can also be noted here is the amount of time necessary to saturate the samples; when examining Figure 4.1.1 and Figure 4.1.3 at 12-hours and 24-hours of testing, the samples reached 91.8% and 94.3% of the 7-day saturation level, respectively. Another point of interest here is the soaking time used in Phase II, which is 2-hours. At 2-hours of testing the sample with w/c of 0.45 reached an average of 56.9% of the 7-day saturation level, while the sample with w/c of 0.65 reached 59%.

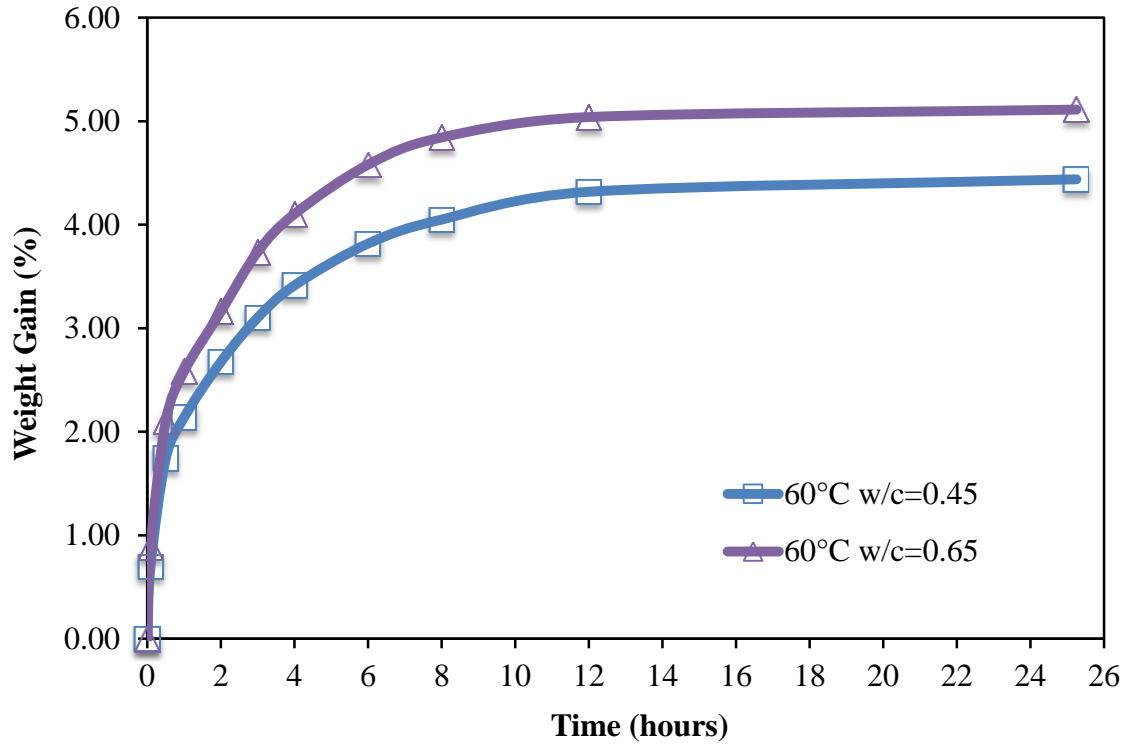


Figure 4.1.1: Absorption of 76x76x256mm prisms with water over 24-hours

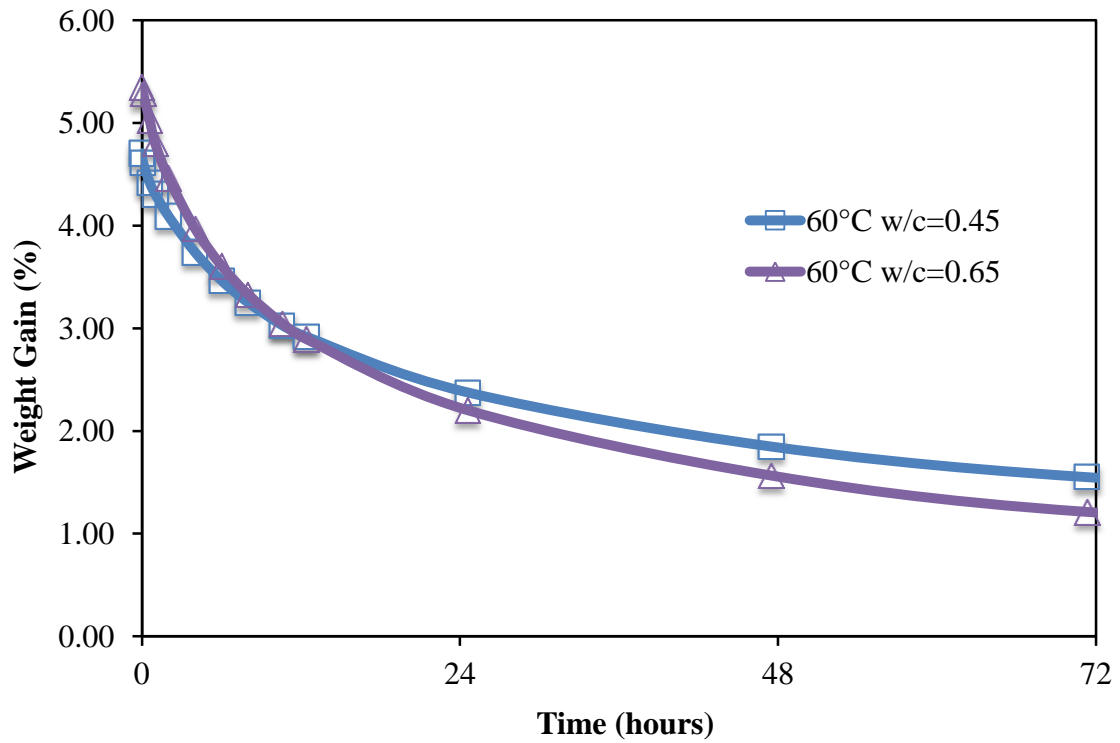


Figure 4.1.2: Drying of 76x76x256mm prisms over 72-hours

In Figure 4.1.2 the drying curves over 72-hours are shown for the 2 samples dried at 60°C. These samples were tested for 7-days in the drying oven, and are shown with their initial reading being their 7-day saturation levels. What is clear from Figure 4.1.2 is that the sample with w/c of 0.65 dried at a faster rate than the w/c of 0.45 sample, especially during the first 24-hours. Also, the sample with w/c of 0.65 started at a higher degree of saturation, and over 24-hours, dried to a lower degree of saturation, when compared to the sample with w/c of 0.45. Once again, these results can be explained by the relative porosity of the samples. Just as it was easier to saturate the more porous sample, it was also easier to dry it out. The relatively large pores allow water to migrate through the sample more easily. Another interesting point in Figure 4.1.2 and Figure 4.1.4 is that the samples do not dry out completely back to their initial readings. Even after 1-week of drying 10% to 20% of the water remains inside the sample.

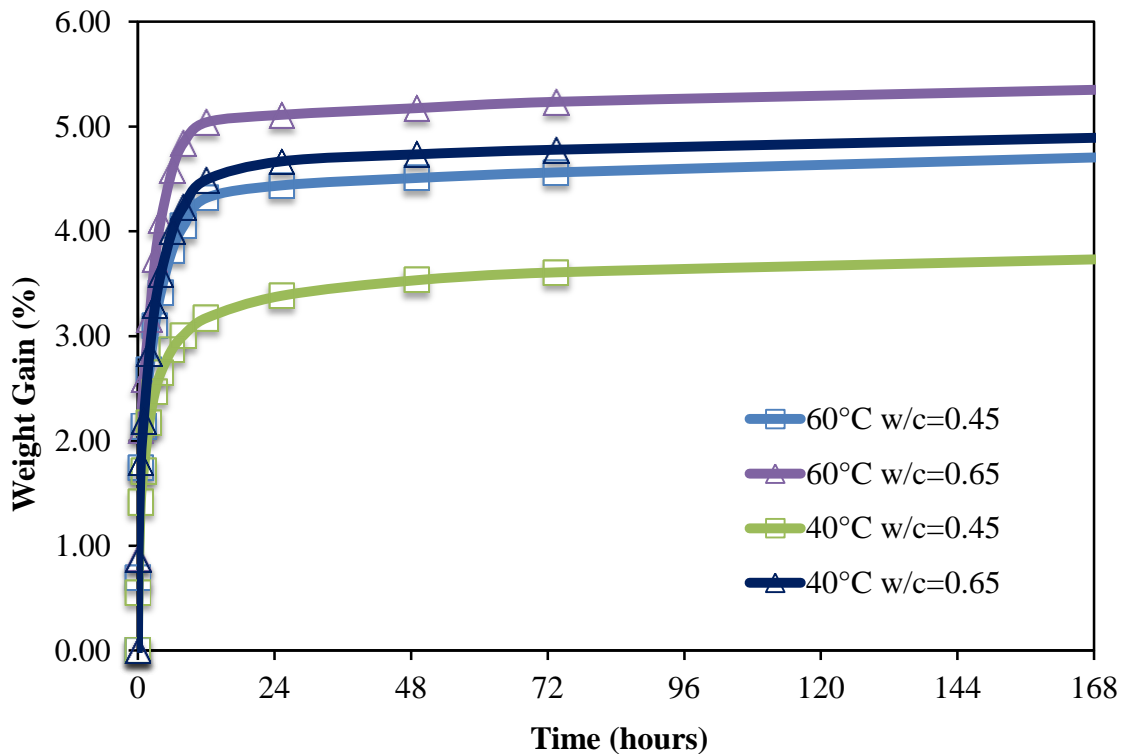


Figure 4.1.3: Absorption of 76x76x256mm prisms with water over 7-days

These results indicate that all samples will saturate at a faster rate than they will dry, and thus, they will retain some extra water each cycle, which may continue until the samples reach an equilibrium saturation level to where they dry to each cycle. This will be discussed further in the following sections. The saturation and drying curves are shown in Figure 4.1.3 and Figure 4.1.4

respectively, for 7-days of testing at both 60°C and 40°C drying temperatures. Similar trends are seen here with the 40°C samples, as were discussed above with the 60°C samples. The 40°C samples reach a lower level of saturation at 7-days when compared to the 60°C samples, but dried to a very similar value after 7-days of drying. The difference in the level of saturation between the 2 temperatures is likely caused by the sample conditioning prior to testing. Since the samples were dried at their testing temperature before immersion in water, the samples dried at 60°C likely dried more before testing. The increased drying temperature would cause the water to evaporate more easily. Thus, the 60°C samples may have experienced a higher amount of weight gain because their zero reading may have been at a slightly drier condition. Seeing that all samples, regardless of drying temperature or w/c, dry to the same relative amount of weight gain after 7-days is interesting. This would lead one to think that the samples with lower ultimate weight gain in Figure 4.1.3 would in fact have a greater amount of moisture inside the samples, especially after several repetitive cycles.

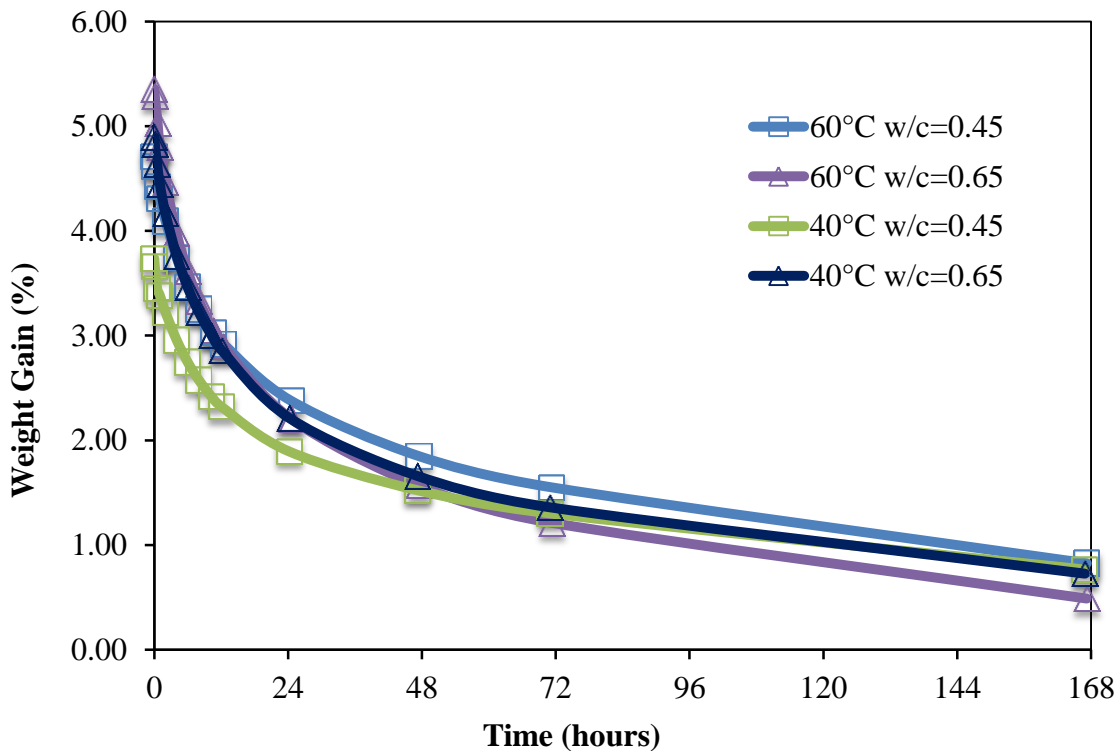


Figure 4.1.4: Drying of 76x76x256mm prisms over 7-days

4.1.2 Relative Humidity (RH)

Figure 4.1.5 shows the RH values for the samples with w/c of 0.45 and 0.65 after 24, 48, and 72-hours of drying. After 24-hours of drying the samples had an average RH of 87%, at this time there appeared to be no difference between the samples with different w/c. Since there was a high variability between specimens here, and the values reported are the averages from 3 identical samples, the results at 24-hours can be considered the same. After 48-hours of drying, the RH in the samples is seen to drop to 54% and 45% for the samples with w/c of 0.45 and 0.65 respectively. Variability was much less at 48-hours; these results highlight the effect of different w/c on the amount of drying of the entire sample, this trend continued to 72-hours of drying. At 24-hours the middle or core of the samples were not very affected by the drying as can be seen in Figure 4.1.5.

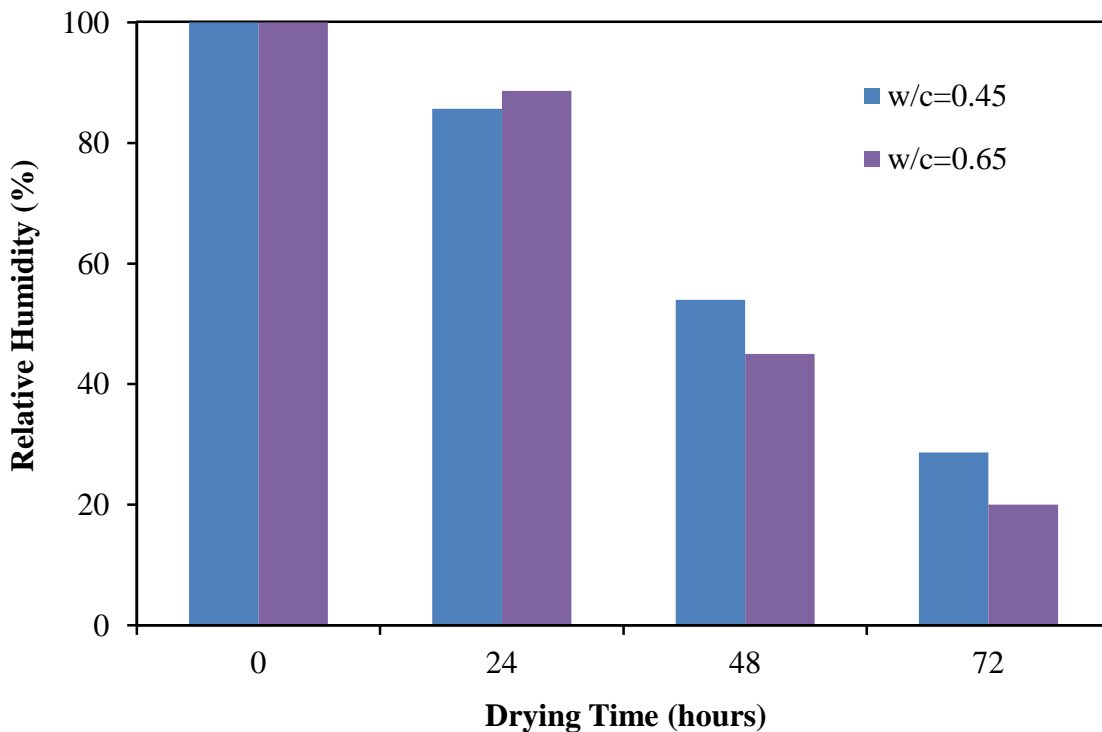


Figure 4.1.5: Relative humidity values for drying at 60°C over 72-hours

Conversely, at 24-hours there was a big difference in the rate of weight loss between the same samples, shown in Figure 4.1.2 in the previous section. It can be concluded that over the first 24-hours, the exterior of the sample was likely responsible for the large difference in drying rate,

while the interior of the samples remained in a similar condition. A clear difference is seen in the RH values after 72-hours of drying; which indicates that a higher w/c allows for a more complete drying, especially between 24 and 72-hours. It is worth mentioning that this difference is over just 1 cycle, multiple cycles may amplify this effect. In Figure 4.1.2 and Figure 4.1.4 it was seen that the samples retained some moisture after 7-days of drying. During actual testing cycles, there was likely residual moisture from previous cycles that could have possibly lead to an even higher degree of saturation. For this reason, the samples with RH probes were tested with the phase I cycles for 28-days, until equilibrium occurred. These values, along with that of Phase II, are presented in Figure 4.1.6.

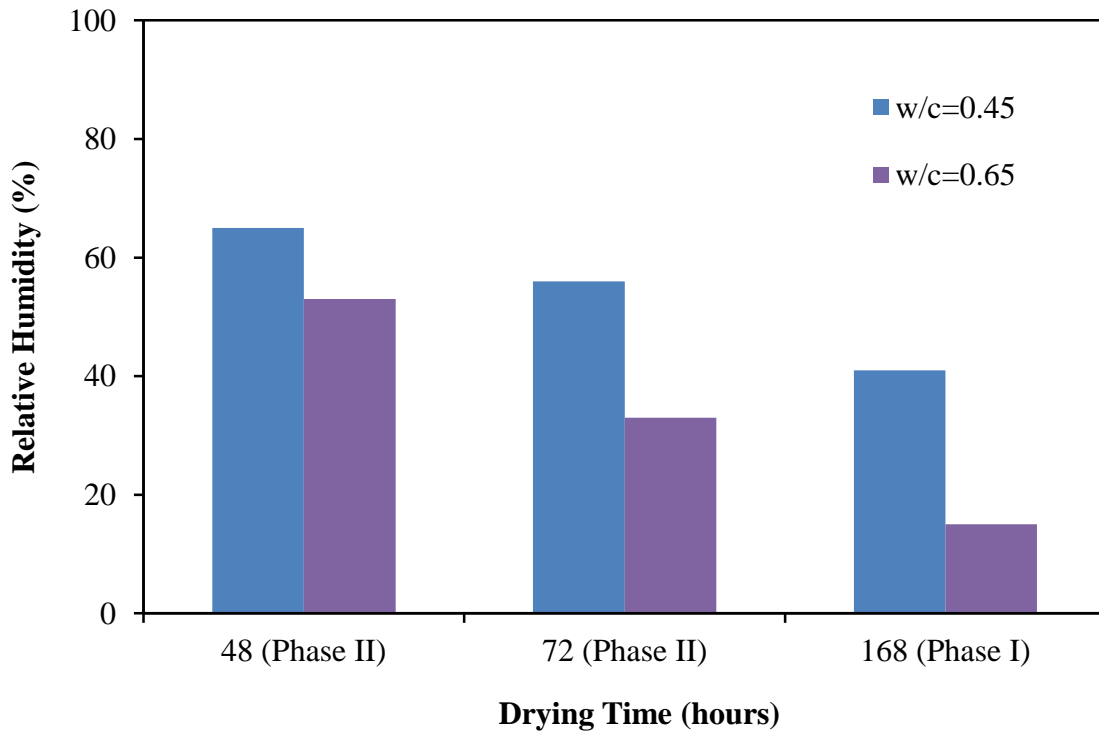


Figure 4.1.6: Equilibrium relative humidity values after 28-days of testing, all drying was at 60°C; RH measurements were taken adjacent to respective testing measurement, at the time of dry readings after stabilization for 24-hours

It was found that the samples tested in Phase I with w/c of 0.45 had an equilibrium RH of 41%, while the samples with w/c of 0.65 was only 15% at the time the readings were taken (following 7-days in the oven). The difference between these values, shown in Figure 4.1.6, and the values shown in Figure 4.1.5 is likely due to the residual moisture from many cycles. During each cycle, the samples became more saturated, and did not dry back to the same level. Thus, from Figure

4.1.6 the samples with w/c of 0.45 are seen to have RH conditions much more favorable for oxidation than that of the samples with w/c of 0.65 during their time in the oven throughout Phase I testing. Figure 4.1.6 also shows the RH values for the samples when they were tested under Phase II conditions. Since Phase II had 2 wet/dry cycles each week, there was 2 different drying times between each cycle; 48-hours and 72-hours. RH readings were taken at the end of each cycle, and their stabilization values at 28-days are shown in Figure 4.1.6. Here the sample with w/c of 0.45 is seen to have a similar RH level after each Phase II drying time. The RH in these samples never goes below 56%, while during Phase I testing the same sample experienced RH of 41%. This does not seem to follow the results shown in Figure 4.1.4 where at 72-hours the same sample dried to 33% of its maximum weight. From this, it seems apparent that the interior of the samples with w/c of 0.45 did not undergo the same severity of wetting and drying that the exterior portion of the samples did. The sample with w/c of 0.65 shows a trend in Figure 4.1.6 as would be expected to follow from Figure 4.1.4. The RH values even correspond with the relative saturation levels for the same amount of time tested. Therefore, the samples with w/c of 0.65 dried in a more uniform and complete manner than what was seen with w/c of 0.45. In Phase I the RH was seen as low as 15% in the sample with w/c of 0.65, this value is certainly too low to be able to promote oxidation inside the sample, even the RH value of 33% seen in Phase II is likely too low.

4.2 Phase I

Phase I was considered as preliminary testing, it included many different types of exposures to test for the possibility of iron sulfide oxidation. Heating to temperatures of 150°C and 60°C and soaking at 23°C and 5°C were adopted, some samples were also tested dry; results of which are shown in the following sections.

4.2.1 Heating to 150°C

4.2.1.1 150°C / Dry

The results from Phase I testing of heating to 150°C with no soaking are presented in Figure 4.2.1. The 3 distinct spikes in this graph are the result of a single specimens breaking, within their respective samples of 3 specimens each. All reported values in the following sections are an

average of all 3 specimens, until the time a specimen was rendered un-measurable, when the average of the remaining 2 specimens was taken and reported. Expansion in the Sulfide-0.45 sample is observed to begin after about 12-weeks of testing. It should be noted that this rise in average expansion was caused by a single specimen, which broke at an age of 22-weeks. The average of the remaining 2 specimens was about the same as the zero reading. An image of the fractured sample is shown in Figure 4.2.2.

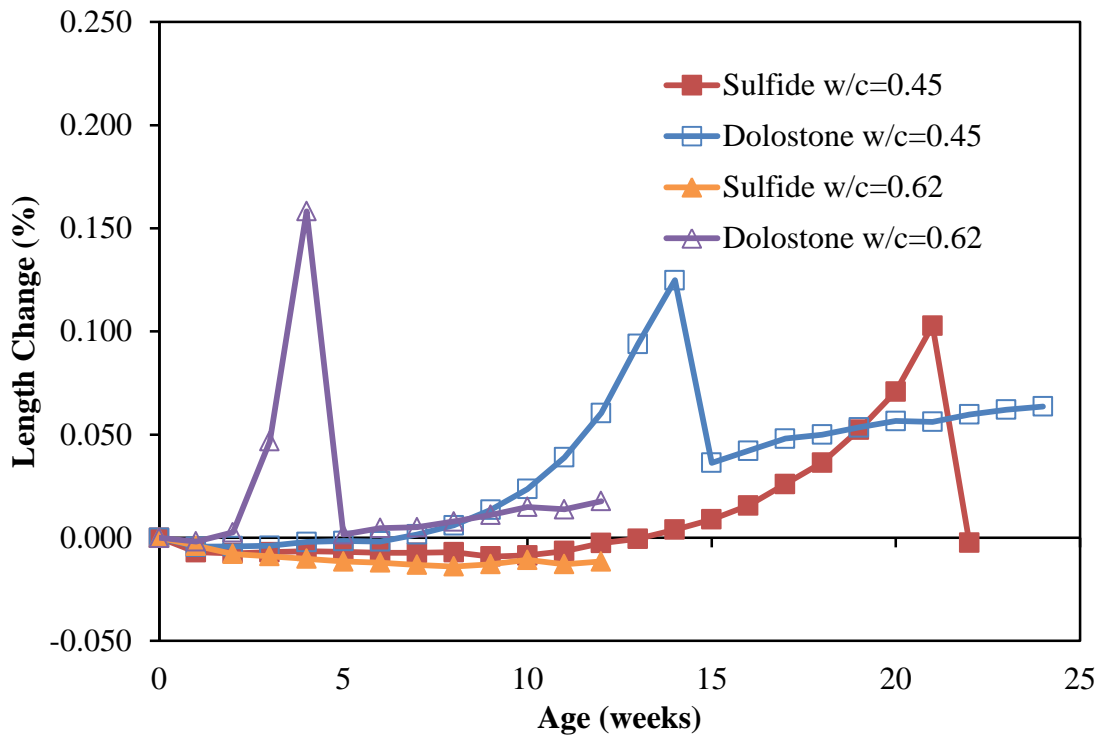


Figure 4.2.1: Phase I results from 1 heating/cooling cycle per week to 150°C/23°C and no wetting cycles; samples were measured after 24-hours stabilization at 23°C

The Sulfide-0.62 sample showed no expansion, nor did any specimens fracture over the 12-weeks they were tested. Outside of the single specimen that fractured, mentioned above, all other specimens with Sulfide aggregate tested dry at 150°C/23°C showed very consistent values in the low negative range (a small amount of shrinkage). All peaks in Figure 4.2.1 look to be in the same range, but because these values are an average of 3 specimens they are not representative of the true peak expansion. The expansion level experienced by the individual specimens that fractured, shown in Figure 4.2.1, were actually in the range of 0.3% to 0.5%. When looking at the Dolostone samples in Figure 4.2.1, a spike is immediately seen in both of the samples. In

both cases, this was the result of a single specimen expanding and eventually fracturing. Images of the fractured Dolostone samples are shown in Figure 4.2.3 through Figure 4.2.5. If the 2 peaks shown in the Dolostone samples in Figure 4.2.1 are ignored, it appears that these 2 samples follow a very similar expansion trend. This seemingly steady expansion is deceiving because the variability within the sample with w/c of 0.45 was very high. At 24-weeks the reported value of 0.064% is the average of 2 specimens, which had one value 4 times larger than the other (0.102% and 0.025%). Again, this large variability, and seeming instability, appears to be localized expansion caused by individual particles.



Figure 4.2.2: Image of Phase I Sulfide-0.45 sample tested under dry conditions with hot/cold cycles of 150°C/23°C

In the Dolostone-0.62 sample, the remaining 2 specimens were consistent and a steady increase in expansion was observed up to 12-weeks. The observed localized cracking which seemed to extend from a single particles location is shown clearly in Figure 4.2.3 and Figure 4.2.4.

Examination of these specimens revealed that a fractured and relatively very weak aggregate particle was the cause of cracking in each case. There was also a discolouration of the affected particles; some were slightly orange in colour, while others appeared black. These features were not seen in the raw aggregate before being used in concrete, therefore this alteration of individual coarse aggregate particles was obviously damaged by the hot/cold cycles of 150°C/23°C. This may lead one to believe that the expansion observed in Figure 4.2.1 was caused by the degradation of individual particles, and was not homogenous across the entire sample. The cause of this effect is currently unknown, but since a large variability was seen with both aggregate types, it can be concluded that it is likely not caused by the iron sulfides in the aggregate.



Figure 4.2.3: Image of Phase I Dolostone-0.62 specimen tested under dry conditions with hot/cold cycles of 150°C/23°C

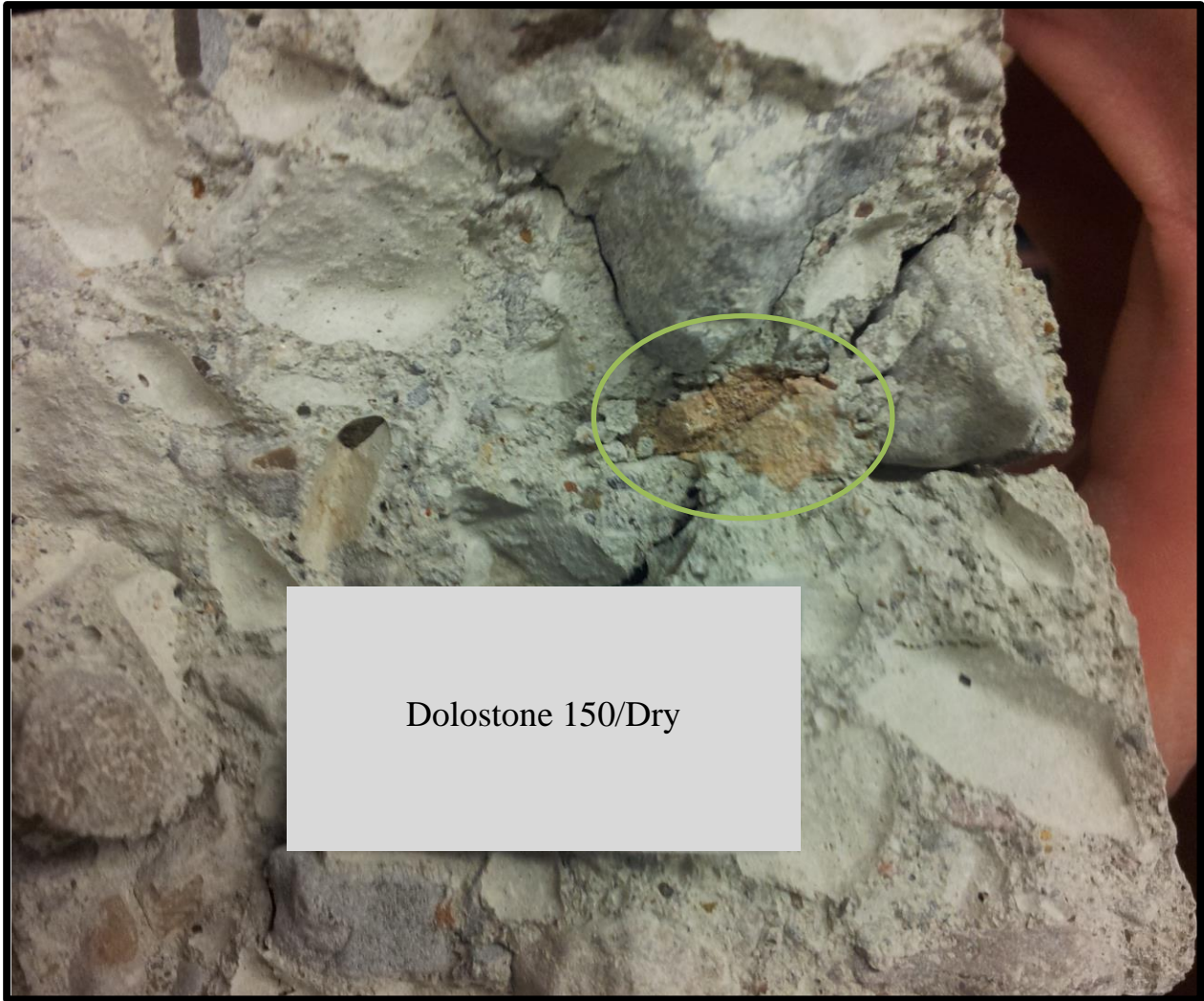


Figure 4.2.4: Image of fractured Phase I Dolostone-0.62 specimen tested under dry conditions with hot/cold cycles of 150°C/23°

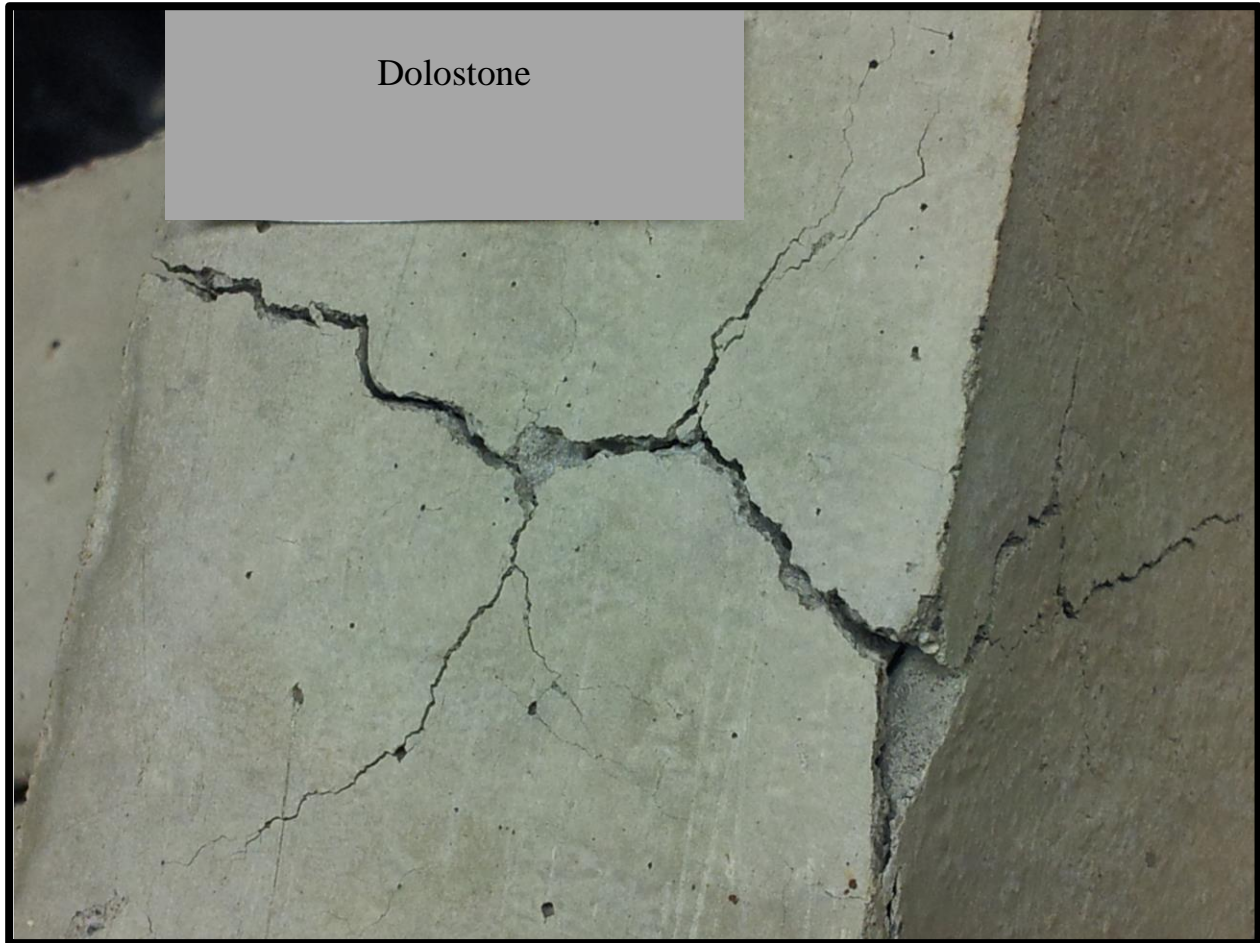


Figure 4.2.5: Image of severely cracked Phase I Dolostone-0.45 sample tested under dry conditions with hot/cold cycles of 150°C/23°C

4.2.1.2 150°C / 23°C Soaking

The Phase I results of heating to 150°C with soaking at 23°C are discussed here. It should be noted that the scale used here in Figure 4.2.6 is different to that used in Figure 4.2.1 and Figure 4.2.9 from the previous and next sections; the expansion in this testing was much greater here than in the others mentioned. Thus, the most apparent observation here is that the samples tested with soaking at 23°C produced much higher expansion than those soaked at 5°C, or not soaked at all. When comparing individual samples almost all values here are at least double their comparative 150°C testing samples. This very large difference is thought to be caused by ettringite formation, since other expansion types would have promoted more severe damage upon increasing the temperature differential. A secondary ettringite formation (SEF) type of expansion is possible here, promoted by heating to 150°C. Sulfoaluminates are not stable above

around 70°C, so any sulfoaluminates (either ettringite or monosulfate) present in the cement will decompose upon heating above 70°C. When the sample is returned to 23°C, the dissolved sulfate will form new, secondary ettringite, which can cause damage to concrete.

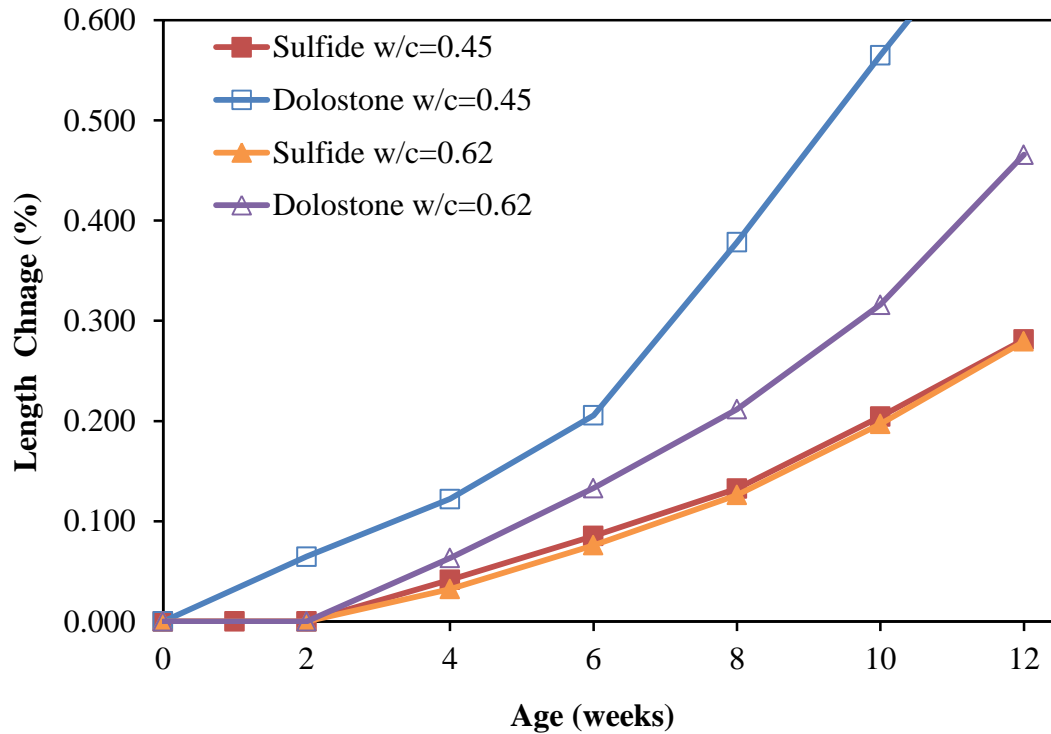


Figure 4.2.6: Phase I results from heating/drying to 150°C for 7-days and soaking cycles at 23°C for 7-days; thus 2 wet/dry cycles per 28-days were experienced

The moisture provided by the soaking, and longer amount of time of 23°C, would provide a better environment to promote ettringite formation, when compared to the testing with no soaking; dry samples spend only 24-hours at room temperature (23°C) per cycle, while 150°C/23°C testing with soaking cycles spend 7-days at room temperature. This testing cycle most favours ettringite production because it is reliant on the presence of moisture, and it is most stable near room temperature (23°C). This occurs with both aggregate types, so is likely not related to the iron sulfides in the aggregate. Testing at 150°C/23°C will be compared to testing at 150°C/5°C in the next section. The Sulfide samples shown in Figure 4.2.6 reveal that both samples experienced very consistent expansion. Only 1 of these specimens fractured, in the Sulfide-0.45 sample, although even its measurements were consistent with the others, and was in-fact not even the highest level of expansion in that sample, at that time. The Dolostone

samples shown in Figure 4.2.6 expanded much more than the Sulfide samples in both cases. All 3 of the Dolostone specimens with w/c of 0.45 fractured by 18-weeks of testing, while none of the Dolostone samples with w/c of 0.62 had fractured after their maximum testing age of 12-weeks. There was a brownish staining present on all Dolostone samples tested with wet conditions, an example of this is shown in Figure 4.2.7, where samples made with both aggregate types are shown for comparative reasons.

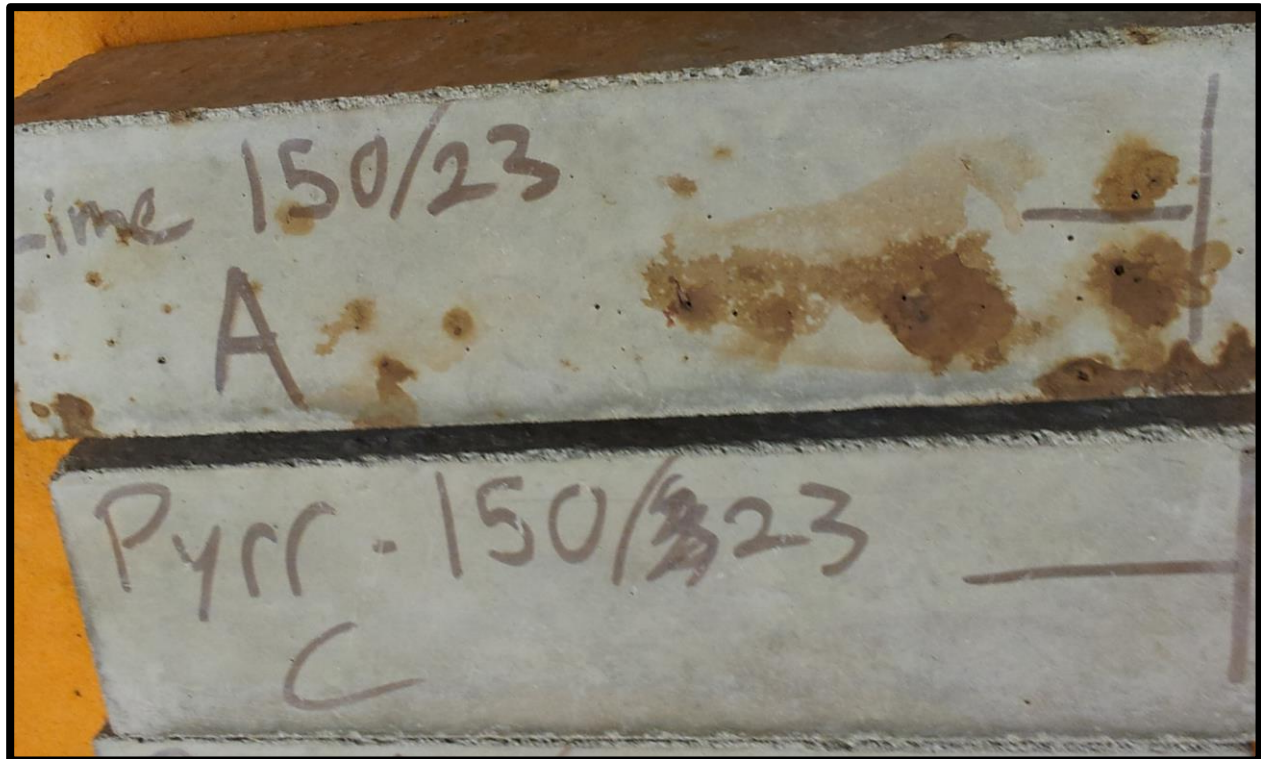


Figure 4.2.7: Image of Phase I samples with w/c of 0.45 tested with 7-days heating/drying at 150°C and soaking at 23°C, the Dolostone sample with staining is shown on top, and the Sulfide sample is below

The Dolostone sample with the aforementioned brownish staining is shown at the top of Figure 4.2.7, and the Sulfide sample is shown below with no staining. After examining the fractured specimens it was apparent that the fractures were again caused by individual aggregate particles, although here in contrast to the dry testing, many of the particles appeared to be reacting. The specimen pictured in Figure 4.2.8 details such a fracture that occurred in the Dolostone-0.45 sample at an age of 6-weeks of testing. In images A) and C) in Figure 4.2.8 it can be seen how the aggregate particle caused the fracture in the specimen. In image B) the particle is seen removed from the concrete, which experienced a bright orange and brown discolouration and

severe expansion, as mentioned earlier. This bright colouration was found on many of the particles that caused their concrete specimen to fracture. The cause of this transformation is currently unknown, but seems to be caused by the heating of the samples to 150°C while the aggregates were saturated. Since this staining and severe expansion was observed only in the Dolostone sample, it would seem to be a property of this specific type of aggregate.

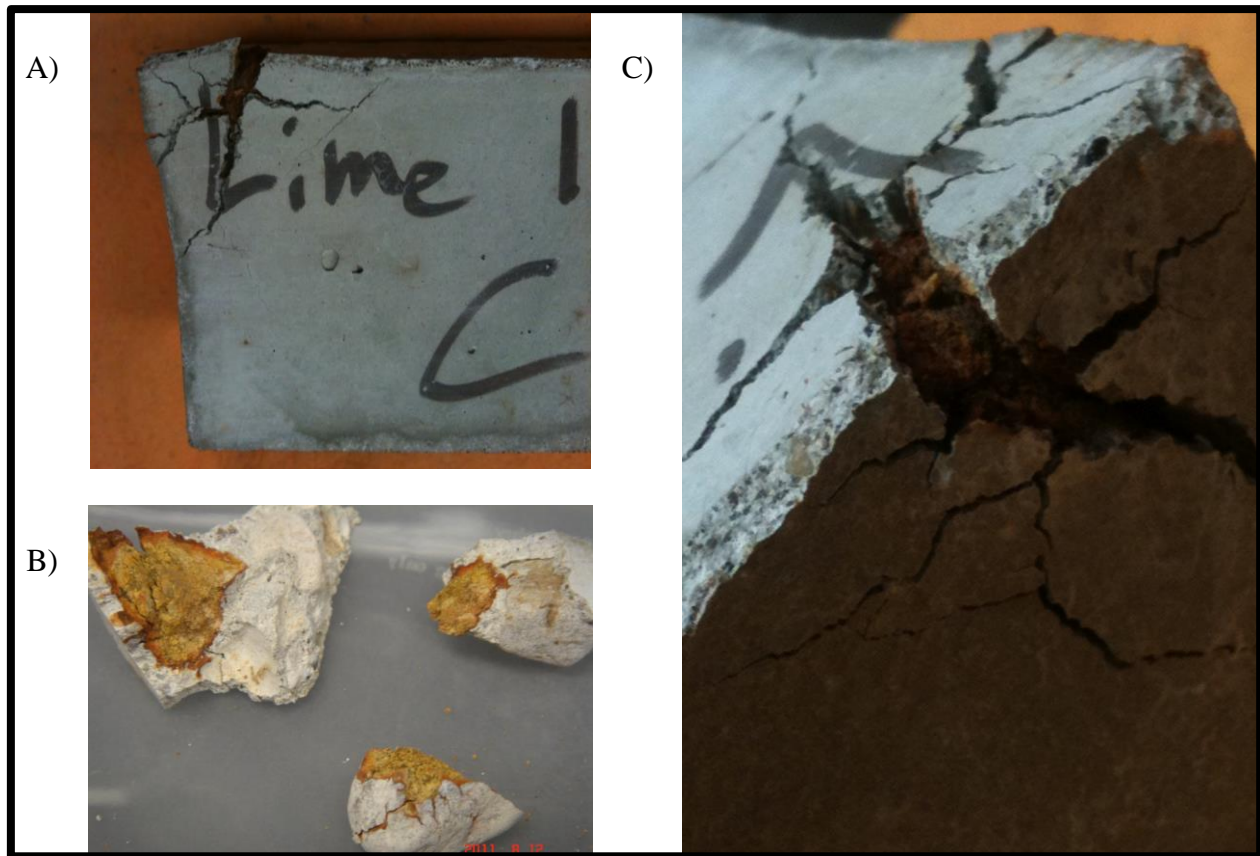


Figure 4.2.8: Images of fractured specimen from Phase I Dolostone-0.45 sample tested with 7-day heating/drying at 150°C and 7-day soaking at 23°C; fractured concrete sample shown in A) and C), removed aggregate particle causing fracture shown in B)

4.2.1.3 150°C / 5°C Soaking

The expansion values presented in Figure 4.2.9 are on a different scale, and are much less than what was observed with testing at 23°C, but both figures show very similar trends. Again, only 1 out of 6 Sulfide specimens fractured, and the expansion values of the other 5 specimens were relatively constant. The 3 Dolostone-0.45 specimens all fractured within 12-weeks of testing, and none of the specimens with w/c of 0.62 fractured after 14-weeks of testing. The values are

thought to be less here than in the previous section because these samples are soaked at 5°C compared to 23°C. These conditions were tested to explore the promotion of thaumasite formation within the samples. This means that while thaumasite was more likely to form here, ettringite was less likely to form. Thus, by comparing Figure 4.2.6 and Figure 4.2.9, it is apparent that greater expansion, and a faster rate of expansion, occurred when conditions to promote ettringite were provided, versus thaumasite.

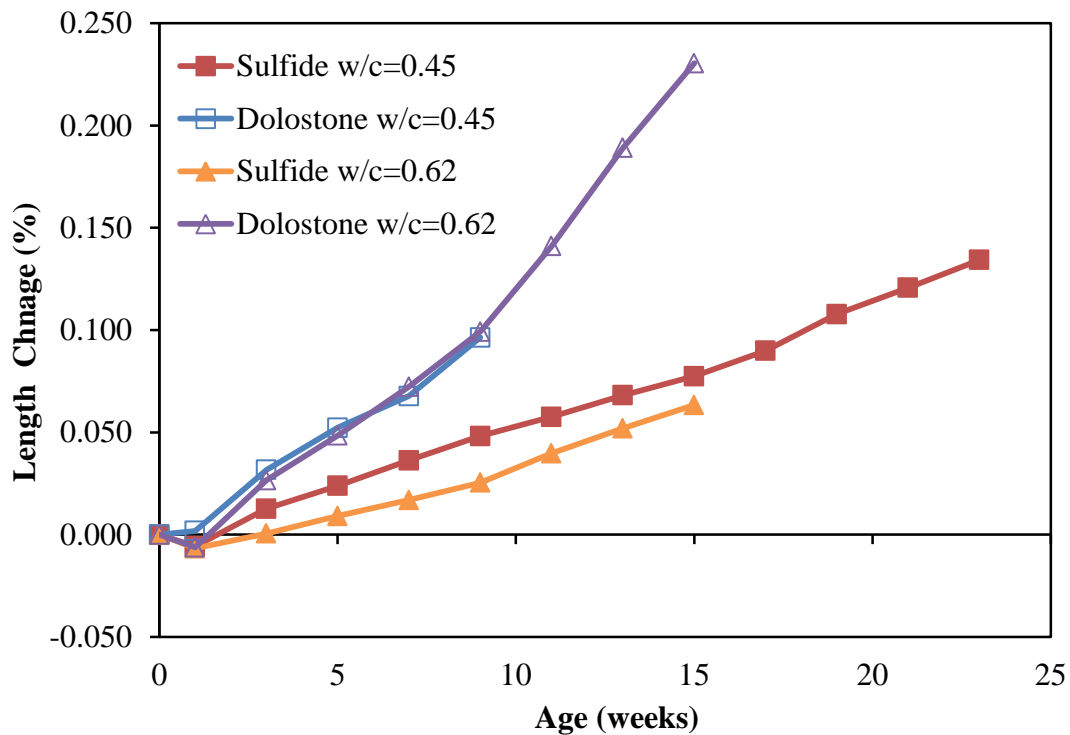


Figure 4.2.9: Phase I results from 7-days heating/drying to 150°C and 7-days soaking cycles at 5°C, thus 2 wet/dry cycles per 28-days was experienced

Therefore, since relatively much more ettringite was present compared to thaumasite, it is suspected that the expansion observed here was likely not caused by the oxidation of the iron sulfides. Since thaumasite was observed in the actual foundations, and was thought to be caused by the oxidation of the iron sulfides, a similar trend would have been expected here. Thus, it is suspected that the expansion observed in Figure 4.2.6 and Figure 4.2.9 with the Sulfide samples was likely caused by an SEF related expansion, and not oxidation of the iron sulfides. As before, the expansion of the individual Dolostone particles seen here is thought to be associated with the

heating of the saturated samples to 150°C. A fractured specimen is shown in Figure 4.2.10; it had nearly identical properties to the specimen shown in Figure 4.2.8 in the previous section.

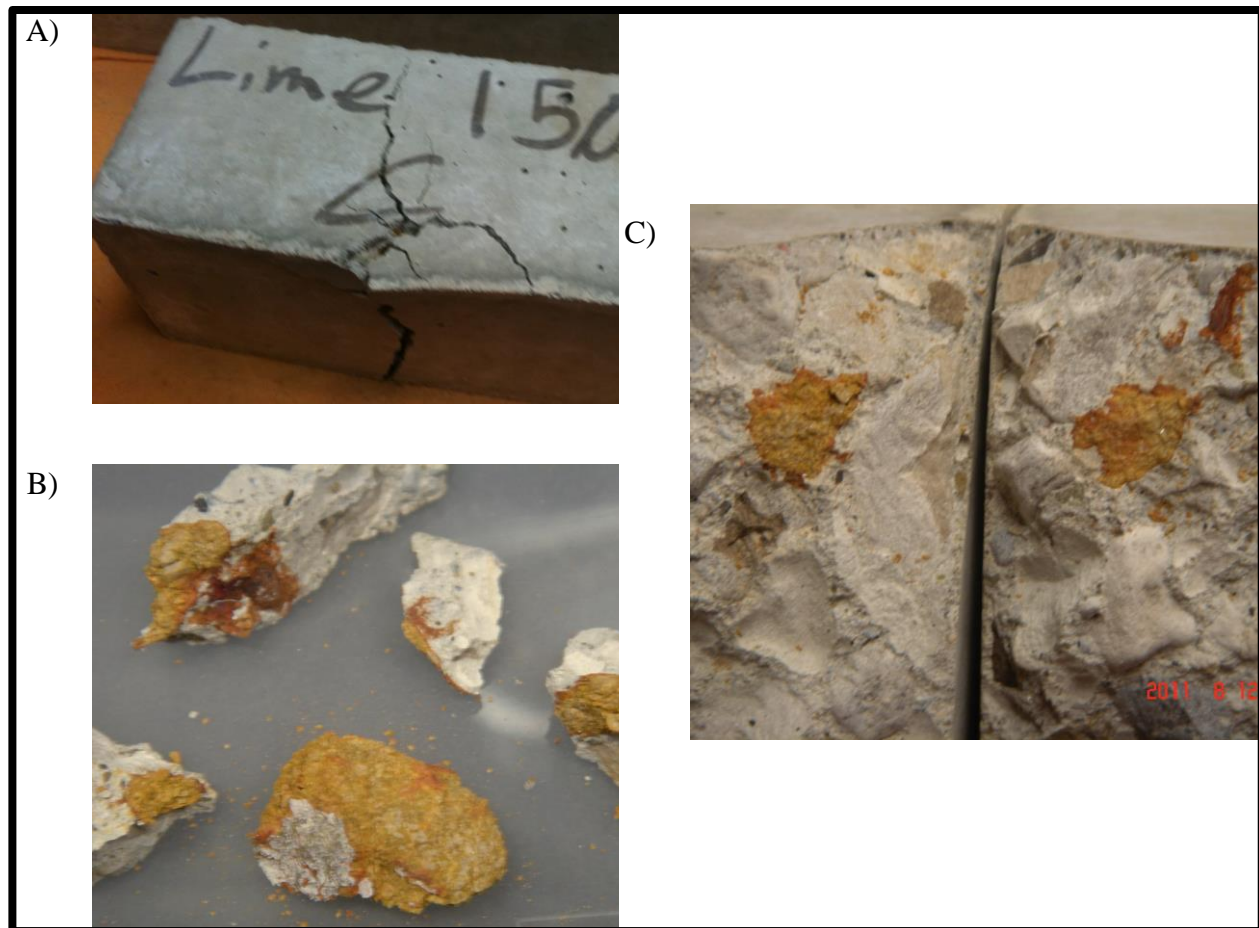


Figure 4.2.10: Images of fractured specimen from Phase I Dolostone-0.45 sample tested with 7-days heating/drying at 150°C with 7-days soaking at 5°C; fractured concrete sample shown in A) and C), removed aggregate particle causing fracture shown in B)

The reason more fractures were observed in the Dolostone samples with lower w/c may be associated with the porosity of the samples. The higher w/c would mean higher porosity and this could better accommodate the release of the water vapors from the concrete. The lower w/c may cause a build-up of vapor pressure within the concrete, or an aggregate particle with high porosity. This could have caused the breakdown and alteration of the Dolostone aggregate. Since large expansions were observed with the Dolostone aggregates both here and in the previous section, it can be concluded that heating the samples to 150°C in a saturated condition was likely

too aggressive to be able to indicate or monitor any effects of the oxidation when comparing to the Sulfide sample.

4.2.2 Heating to 60°C

4.2.2.1 60°C/Dry

The results from Phase I testing at 60°C with no wet cycles are shown in Figure 4.2.11, where no expansion was observed in any of the samples. All samples tested under these conditions experienced drying shrinkage, with a maximum value in the range of -0.040% to -0.050%. A greater amount of shrinkage was seen in the samples made with hydrogen peroxide (HP). It can be noted again here that these samples were exposed for 7-days in a room with 50% RH and 23°C before their zero reading in order to allow for some initial dry shrinkage to occur.

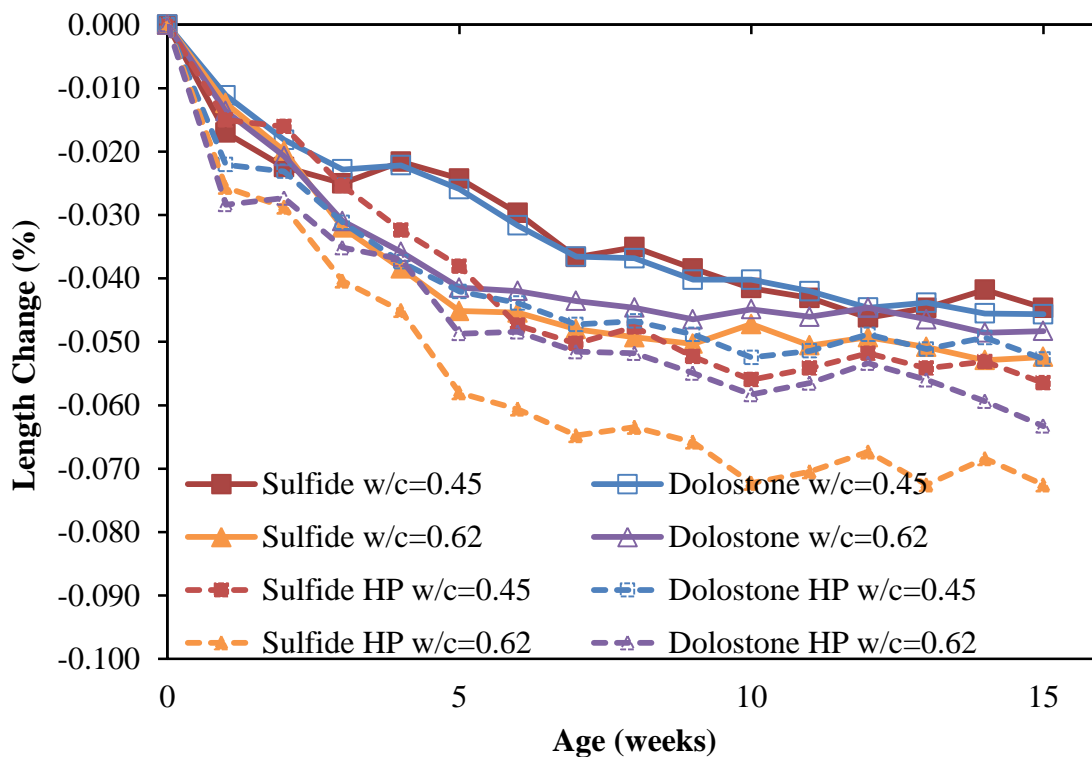


Figure 4.2.11: Phase I results from heating/cooling cycles to 60°C/23°C and no wetting cycles

What can be seen from Figure 4.2.11 is that, for each type of aggregate, the samples made with higher w/c experienced shrinkage at a faster rate, and had a higher ultimate amount of shrinkage. These results indicate that this type of testing is likely not promoting any oxidation in the Sulfide

aggregates. Since these samples were always stored in a dry condition, it seems that the moisture provided from the concrete mixture and curing were not enough to promote oxidation in these samples. After the first couple days in the oven at 60°C, the relative humidity inside the concrete, even at the center of the sample, likely dropped below the effective range to allow oxidation. Referring back to Figure 4.1.5; the RH in the samples was likely below 30% in all samples after just 72-hours, thus, after only 3-days in the oven there was not enough moisture for the oxidation reaction to occur. There was no expansion seen in the samples made with hydrogen peroxide solution as their mixing water. This means that providing an oxidizing agent such as this, at the time of mixing, was not enough to promote oxidation of the iron sulfide either.

4.2.2.2 60°C /23°C Soaking

The results from 7-days heating to 60°C followed by 7-days soaking in lime solution at 23°C are presented in Figure 4.2.12.

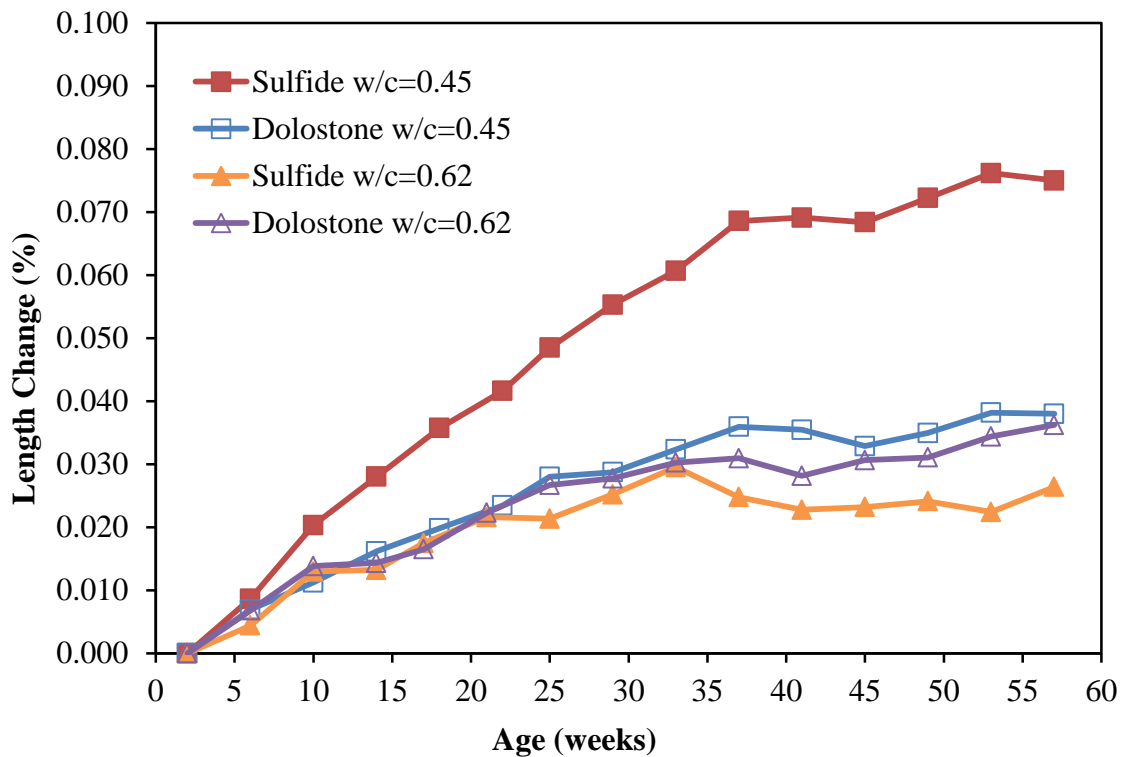


Figure 4.2.12: Phase I results from heating/drying to 60°C for 7-days and soaking cycles at 23°C for 7-days; thus 2 wet/dry cycles per 28-days were experienced

They are 14-day cycles involving heating for 6-days, and soaking for 7-days. The values presented here are considered as wet measurements, because they were measured in a fully saturated condition. Since the zero reading for the wet measurement was taken after the first drying cycle, the values in Figure 4.2.12, and in Figure 4.2.28, start at the age of 1-week. It is clearly seen in Figure 4.2.12 that the Sulfide-0.45 sample expanded much more than the other samples tested under the same conditions. Compared to the Dolostone-0.45 sample, the Sulfide-0.45 sample produced expansion values of nearly double. While the Sulfide-0.45 sample expanded significantly, the Sulfide-0.62 sample actually showed the least amount of expansion for this testing regime. The higher w/c would produce a sample that is relatively very porous, this porosity could be affecting the results in several ways. The increased porosity would have allowed the sample to dry out faster while in the oven (observed in Section 4.1); resulting in less time at an effective relative humidity to promote oxidation within the sample. Also, the increased porosity may have allowed for areas of stress relief; possible expansive reaction products may have been able to form in the more abundant air void system, where they did not put as much pressure on the sample. Also, the lower w/c and lower amount of voids means that there was relatively more cement paste, and therefore more sulfoaluminates available in the sample, which equates to more reactants to produce SEF related expansion. The large difference in expansion values between Sulfide-0.45 and Dolostone-0.45 samples must have been caused by a reaction involving the Sulfide coarse aggregate, as all other parameters are constant between these 2 samples. For this reason, the Sulfide-0.45 and Dolostone-0.45 samples were selected for examination under the SEM; these SEM samples will be referred to as I-S60/23 and I-D60/23 respectively in the following sections. Another feature seen in Figure 4.2.12 is that the expansion of these samples appears to have slowed significantly after 38 or 40-weeks. This finding was most pronounced in the expansion results from the Sulfide-0.45 sample, although similar effects were seen across all samples. It is possible there were several contributors to this trend; the wet/dry cycles may cause micro-cracking inside the concrete. This micro-cracking may take several weeks to come to completion, especially in Phase I, since there was only 1 wet/dry cycle every 2-weeks. This translates into 19 or 20 wet/dry cycles until the related expansion had stopped. One may suspect that this micro-cracking showed more expansion in the Sulfide-0.45 in Figure 4.2.12 when compared to the Sulfide-0.62 sample. While this may be possible, it is also thought that the micro-cracking would actually allow more water and oxygen to reach the

reactive coarse aggregates. There is a possibility that heating cycles, even to 60°C, may have caused some breakdown of previously formed sulfoaluminates. Upon cooling to a less aggressive temperature, the reformation of ettringite may have occurred, a phenomenon known as secondary ettringite formation (SEF) (Collepari, 2003). A single hot/cold cycle to 60°C would likely not cause much damage, but many repetitive cycles may have caused the eventual decomposition of enough sulfates to cause some damage to the concrete. This type of expansion is known to proceed further upon heating cycles to 80°C (Fu & Beaudoin, 1996; Grabowski et al., 1992), but may level off upon heating to only 60°C; this type of expansion may have reached a point when there were no more sulfoaluminates free to dissolve at 60°C, which may have caused the expansion to cease in all samples.

Scanning Electron Microscopy on I-S60/23

This sample was made with Sulfide coarse aggregate and a w/c of 0.45; it was tested with 7-days heating to 60°C followed by 7-days soaking in lime solution at 23°C. When examining the I-S60/23 sample under the SEM it was soon apparent that ettringite could be readily found throughout the sample. It was easy to locate concentrated areas of ettringite in the sample, surrounding both the coarse and fine aggregate particles. There were also areas near pyrrhotite inclusions in the coarse aggregate particles that were abundant in ettringite. An image of such an area is shown in Figure 4.2.13 and Figure 4.2.14, where the edge of the coarse aggregate particle is seen in the bottom of the image. An area where iron may have reacted and migrated into the paste, is located in the bottom right corner of the rectangle in Figure 4.2.13, which represents the area that was magnified to in Figure 4.2.14. The darker area in the images shows a void or crack that has formed around the coarse aggregate, likely to be associated with the interfacial transition zone (ITZ). In Figure 4.2.13, the area immediately surrounding the coarse aggregate looks to be less dense than the bulk cement paste matrix; a feature known to be associated with the ITZ, especially in cases involving SEF. A lower w/c would mean that there was more cement and fewer voids in the sample. More cement means that there is a larger relative amount of sulfoaluminate formed inside the sample. Thus, there is a greater possibility for SEF formation to present itself more noticeably within the sample with w/c of 0.45 compared to that of 0.62. This could follow the association of SEF as being more pronounced in high quality concrete with lower w/c. In Figure 4.2.14 an SEM image is shown along with an EDS analysis, where the

analysis area is shown as a circle. A circle is used instead of a point to account for the total analysis area that may have been displayed in the EDS output. In the EDS analysis in Figure 4.2.14, the three distinct peaks of ettringite are seen; calcium (Ca), sulfur (S) and aluminium (Al). The little bit of silicon (Si) that was present in the analysis is considered to be background, and likely not occurring in the feature shown in the image. Large pockets of ettringite can be seen all through Figure 4.2.14, when formed in a restricted space, such as the cement matrix, ettringite grows in a condensed form. The crystal shaped needles typically associated with the presence of ettringite are formed in the air voids, where they have the space to form in a stress free environment. Images of ettringite needles seen in the same sample are shown in Figure 4.2.15 and Figure 4.2.16.

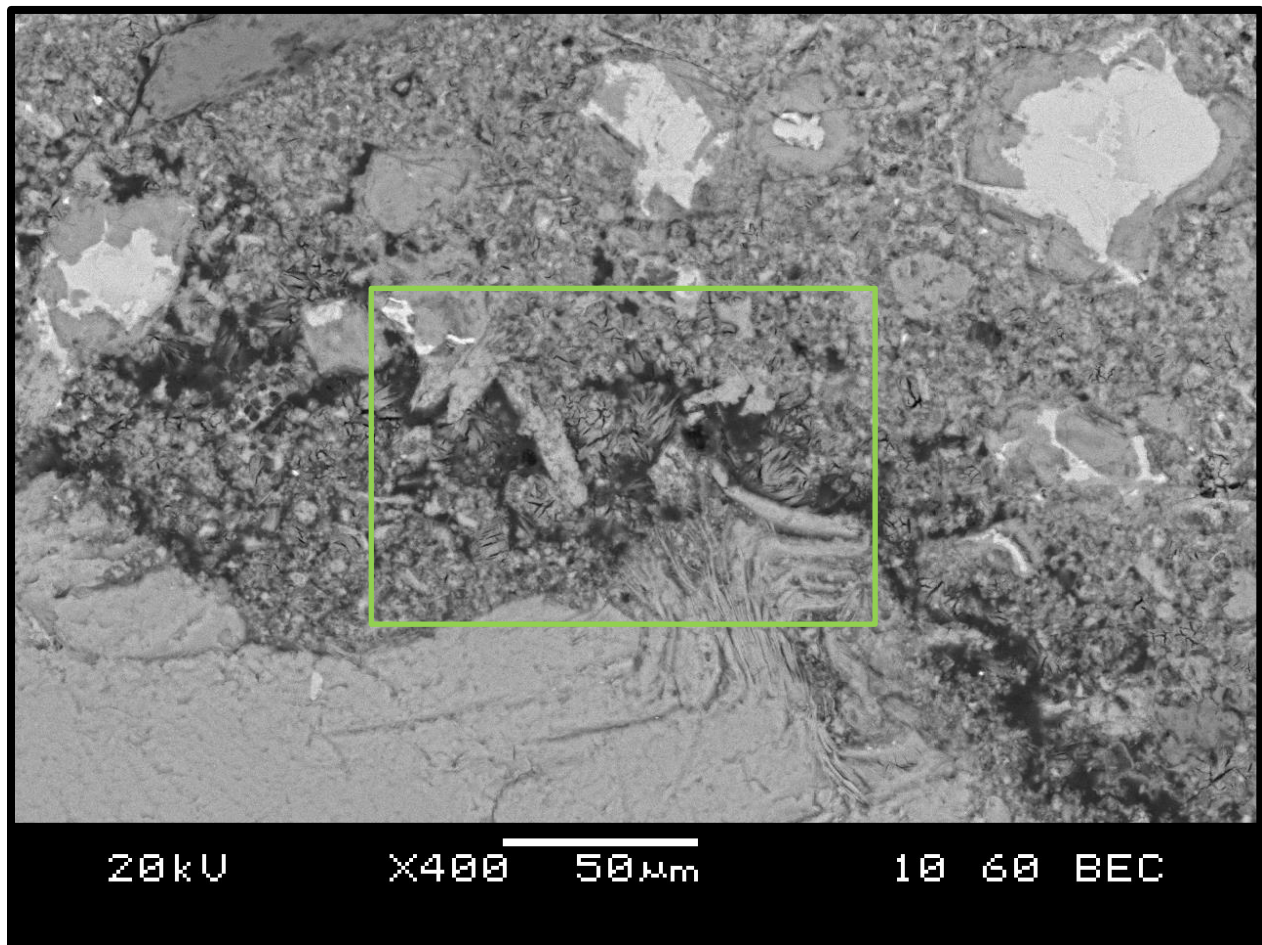


Figure 4.2.13: SEM image of Phase I Sulfide-0.45 sample showing ettringite in paste at 57-weeks of testing; made with Sulfide aggregate, 0.65 w/c, and tested with 7-days drying at 60°C and 7-days soaking at 23°C

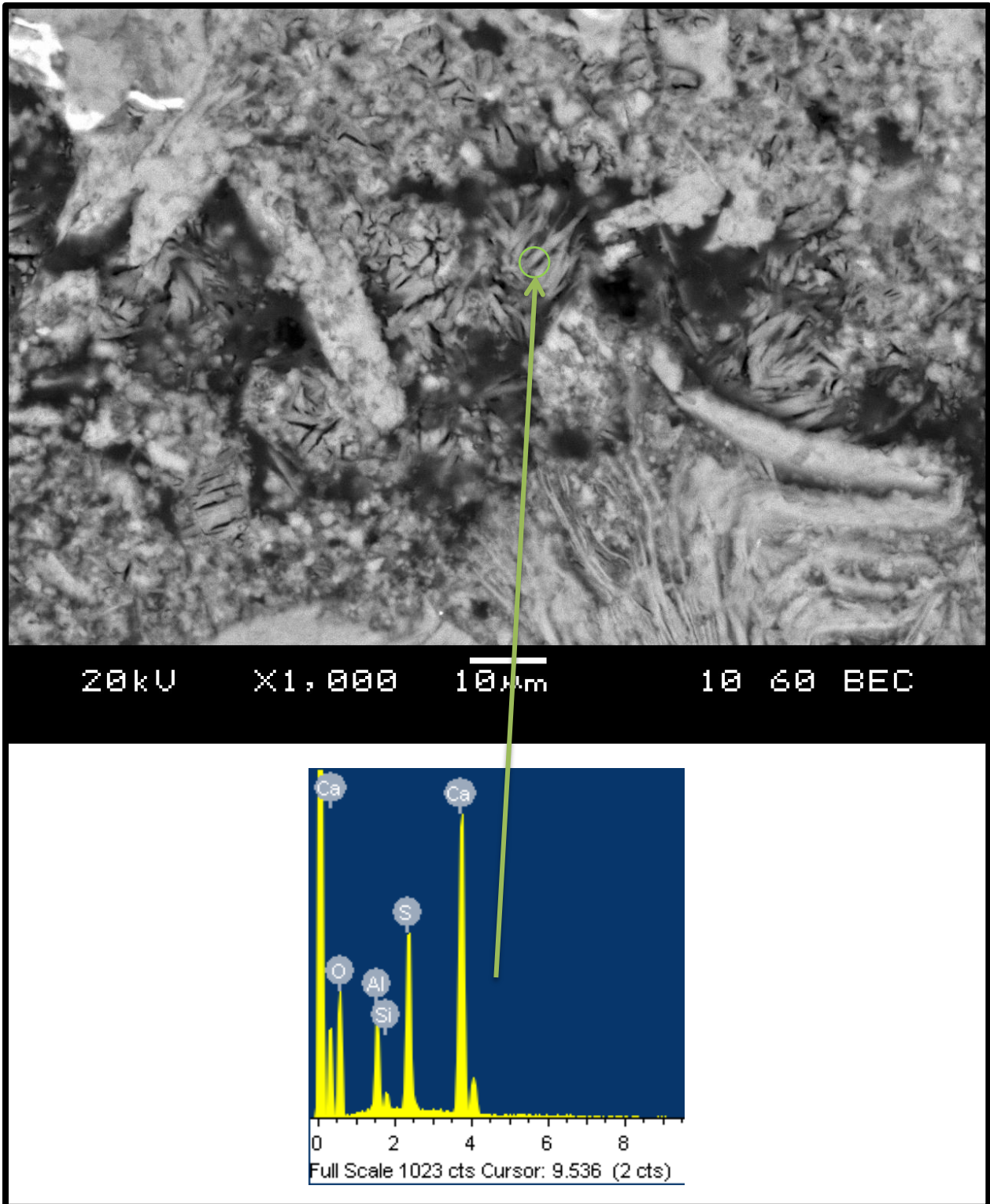


Figure 4.2.14: SEM image and EDS analysis of Phase I Sulfide-0.45 sample showing condensed ettringite at 57-weeks of testing; made with Sulfide aggregate, 0.65 w/c, and tested with 7-days drying at 60°C and 7-days soaking at 23°C

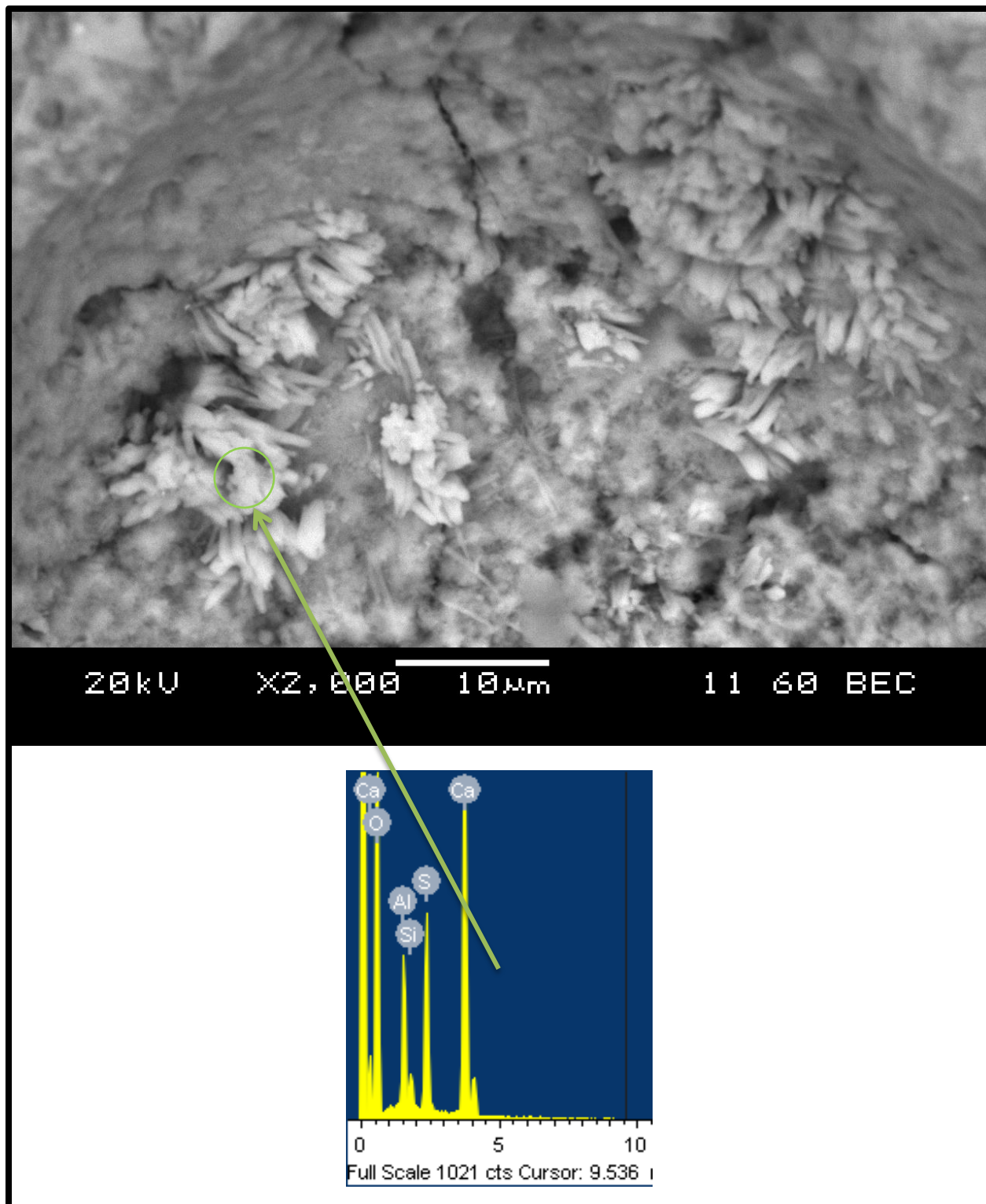


Figure 4.2.15: SEM image and EDS analysis of Phase I Sulfide-0.45 sample showing ettringite crystals in an air void at 57-weeks of testing; made with Sulfide aggregate, 0.65 w/c, and tested with 7-days drying at 60°C and 7-days soaking at 23°C

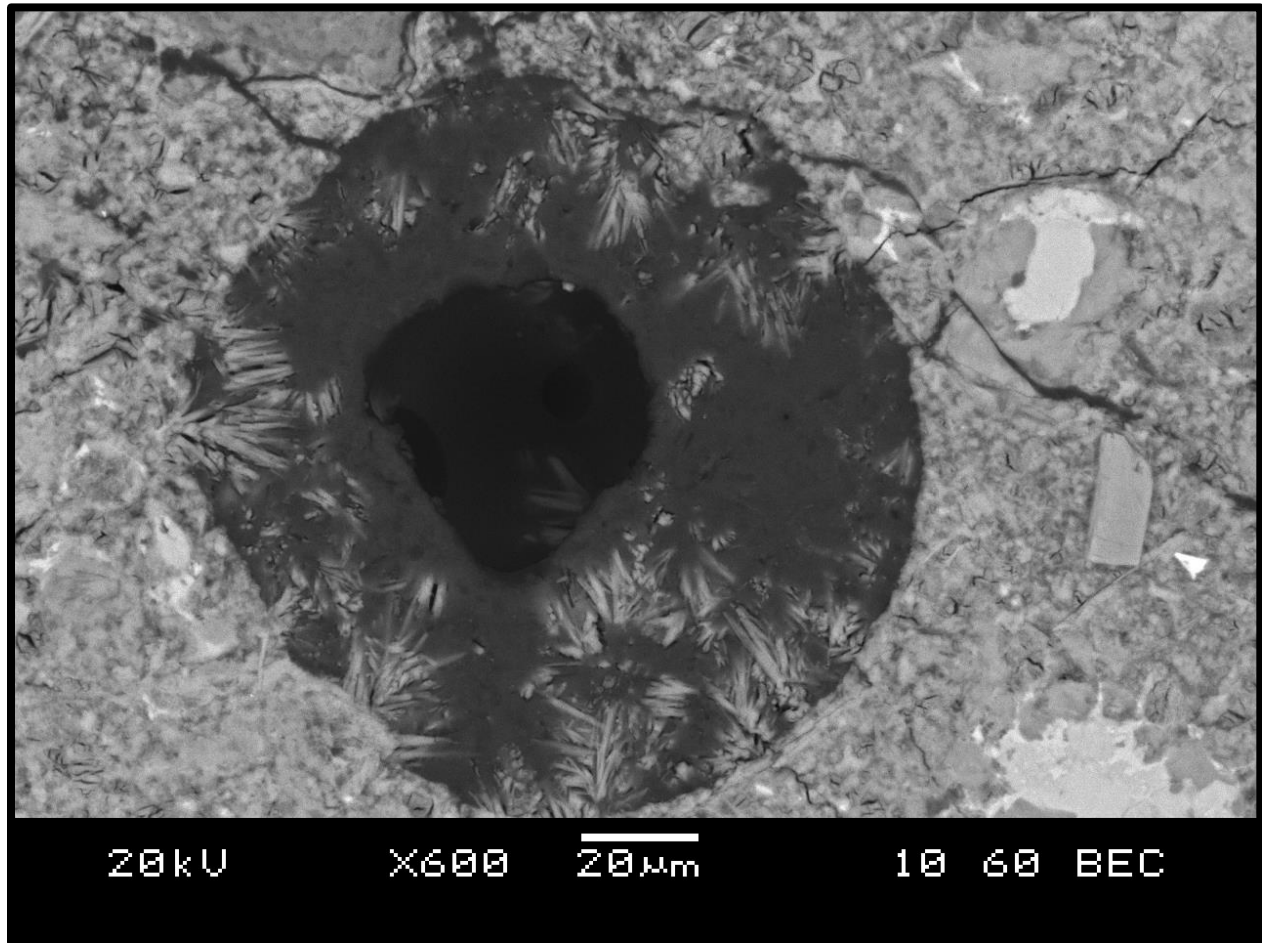


Figure 4.2.16: SEM image of Phase I Sulfide-0.45 sample showing ettringite crystals in an air void at 57-weeks of testing; made with Sulfide aggregate, 0.65 w/c, and tested with 7-days drying at 60°C and 7-days soaking at 23°C

An example of smaller ettringite concentrations is shown in Figure 4.2.17, along with EDS analysis of the 2 locations highlighted on the image. Analysis at location A) shows an area that can be positively identified as ettringite from the peaks shown in the analysis. At location B) similar peaks are seen, ettringite could be suspected, but no conclusions were drawn since silicon was present in the analysis. Again, this silicon is likely from background analysis of the cement paste; with a small ettringite concentration such as this some silicon was expected in the analysis. There is also the possibility that the silicon was a part of an ettringite/thaumasite solid solution. Ettringite was found in large concentrations near coarse aggregates, especially where iron sulfide was present, such an area is shown in Figure 4.2.13, Figure 4.2.14, and Figure 4.2.18. Areas such as this provide an excellent spot for analysis because the large size of the concentrations accommodates for the relatively large analysis area required by the EDS, as discussed earlier.

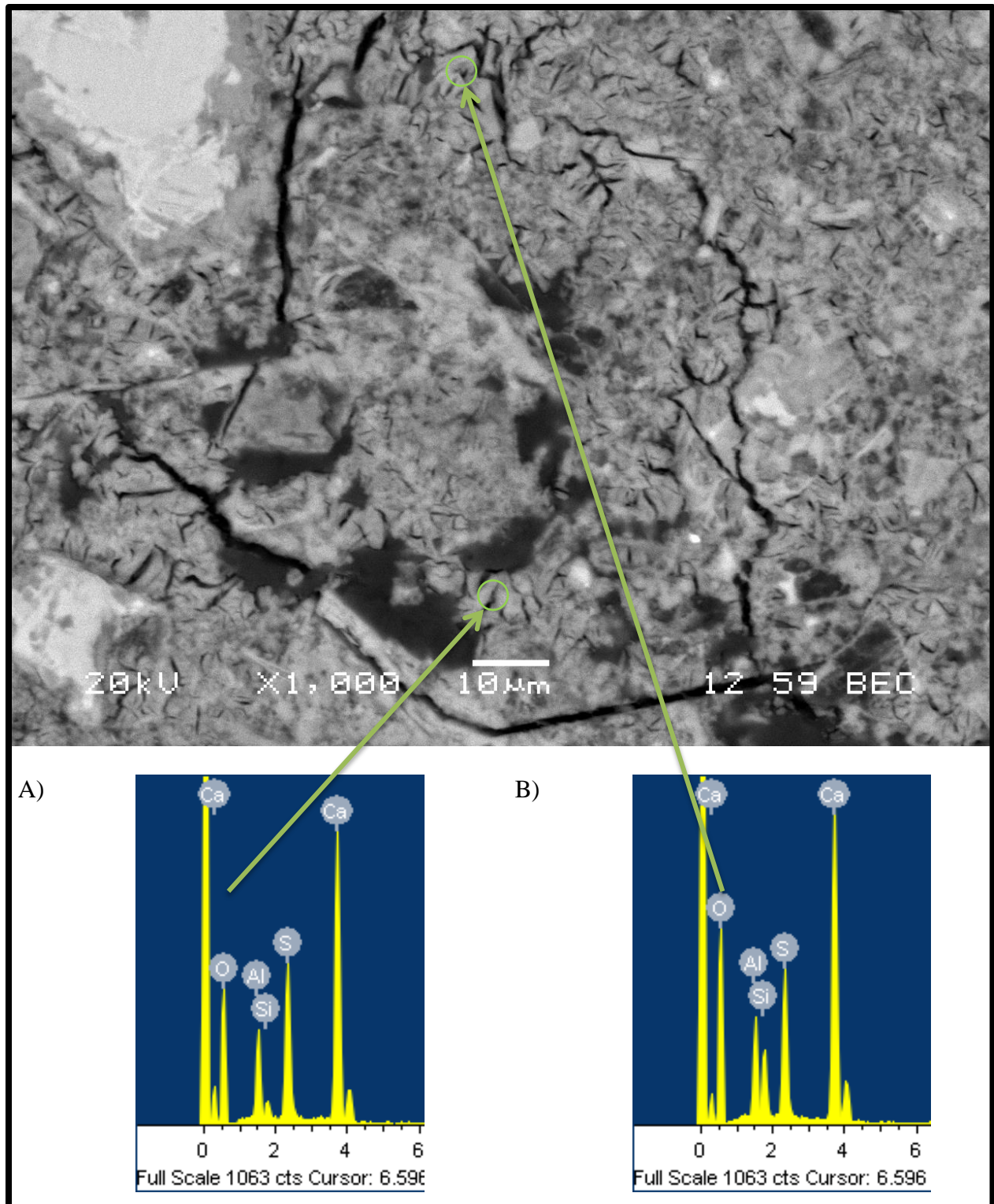


Figure 4.2.17: SEM image and EDS analysis of I-S60/23 showing condensed ettringite within the cement matrix; made with Sulfide aggregate, 0.65 w/c, and tested with 7-days drying at 60°C and 7-days soaking at 23°C

EDS Mapping: I-S60/23

In order to better illustrate the pockets of condensed ettringite in Figure 4.2.14 in a definitive way, EDS mapping was employed, results of which are shown in Figure 4.2.18. Here the area was analyzed many times, randomly over the entire area, and all the results were combined to produce a map style image of where each element was present, and their relative abundances. For example, in Figure 4.2.18-B) the EDS mapping result is shown for sulfur, the spots that are coloured white represents areas where sulfur was present in the analysis, while the spots that are black represent areas where no sulfur was present. EDS mapping is a good way to get an overall analysis image of the sample according to atomic mass, and it provides the true shapes of the features present. An identical set of ovals was set as an overlay on top of each of the EDS result images in Figure 4.2.18; these are included as a reference to highlight the regions of interest with regards to ettringite. In the SEM image shown in Figure 4.2.18-A) the features within the ovals all appear somewhat similar in their composition. This image gives us great insight into the appearance of condensed ettringite, which can be characterized as circular or oval shapes that contain short discontinuous black lines of varying thickness. They are typically found as smaller diameter concentrations that are more numerous throughout the sample, but here the condensed ettringite features are seen in large concentrations, bound by the overlain ovals. The sulfur analysis in Figure 4.2.18-B) shows that sulfur was concentrated within the oval. In Figure 4.2.18-D) aluminum was also seen to be present and concentrated within the ovals. As expected, aluminum was also present in other forms throughout the cement matrix, it is interesting however to note the concentration of aluminium in the bottom right corner of the image. In Figure 4.2.18-F) the results from the silicon analysis are shown, here areas with very little or no silicon at all are seen within the ovals. This, along with Figure 4.2.18-E) to show the presence of calcium, is very strong evidence to prove that the formations described above are in-fact concentrated areas of condensed ettringite. Even though very little silicon was seen within the ovals, it may be associated with an ettringite-thaumasite solution (Barnett et al., 2000). Another thing found in the mapping results of iron in Figure 4.2.18-C) is that the area in the bottom right of the image is rich in iron.

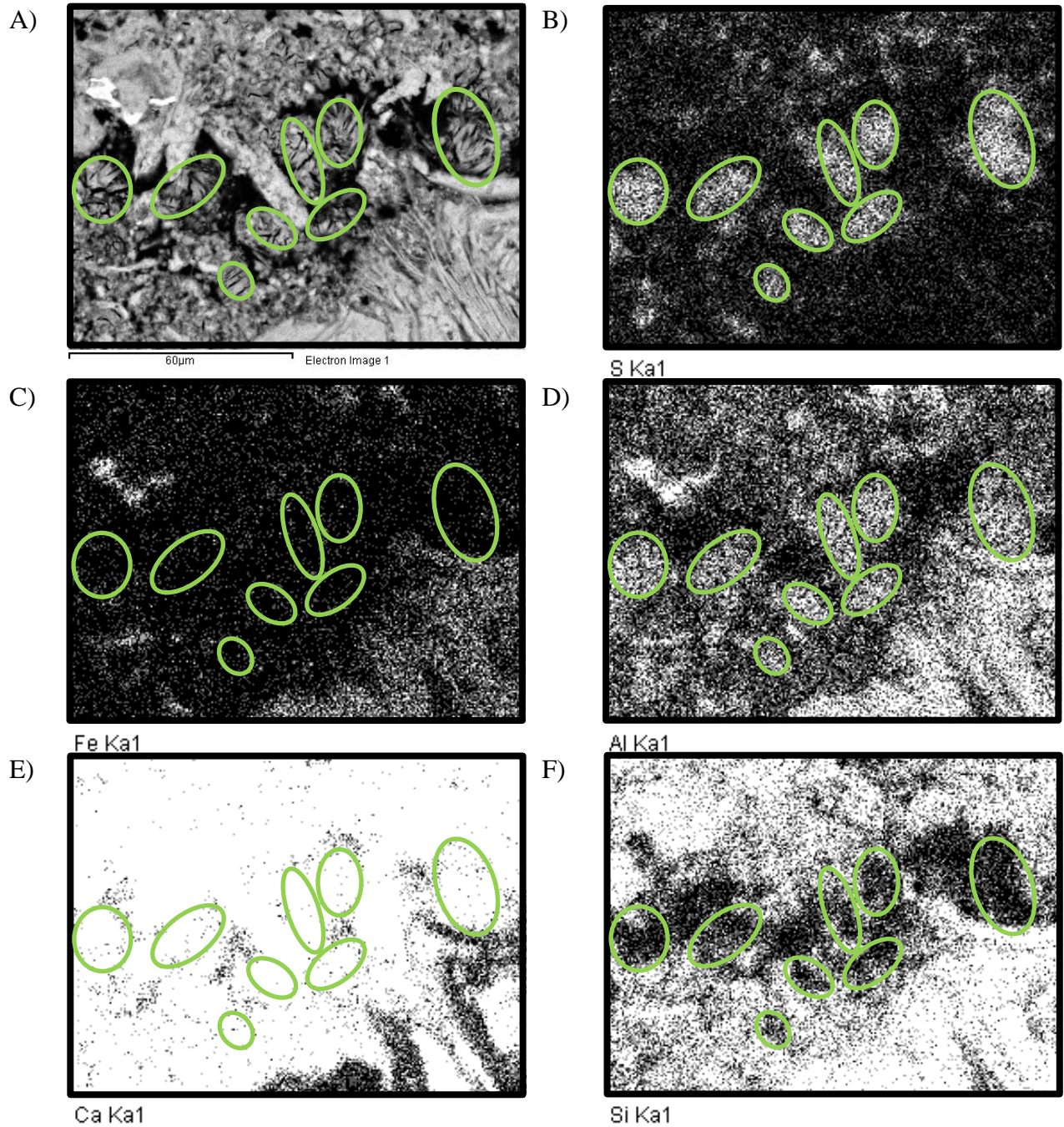


Figure 4.2.18: I-S60/23 EDS mapping analysis results A)SEM Image of area B)Sulfur C)Iron D)Aluminium E)Calcium F)Silicon; made with Sulfide aggregate, 0.65 w/c, and tested with 7-days drying at 60°C and 7-days soaking at 23°C

Iron Sulfide Oxidation

An important aspect of this research work was to evaluate the degree to which the oxidation of the iron sulfide, namely pyrrhotite, was occurring within the concrete. For this reason, all samples examined under the SEM were inspected for pyrrhotite of any state, either un-oxidized, partially, or nearly fully oxidized. It was seen in the EDS mapping in the previous section that iron appeared to have migrated into the paste, this was likely the result of the iron undergoing a reaction. Also, it was observed that sulfur reacted with the paste in this area and formed ettringite. This may lead one to believe that this area, where the iron was mobilized, is the type of reaction that was desired. It should be noted here that sulfur was not seen directly in the area where the iron seemed to be reacting. An image of the same area in sample I-S60/23 is shown less magnified in Figure 4.2.19, unfortunately an EDS analysis was not done to investigate the composition of this iron inclusion. Some pyrrhotite was located at the exterior surface of a coarse aggregate in sample I-S60/23, shown in Figure 4.2.20. On the left side of the image the cement paste is seen, and on the right side of the image the coarse aggregate particle is seen. The big white shape on the edge of the coarse aggregate is a pyrrhotite intrusion. The EDS analysis shows that, at both locations shown, familiar peaks of un-oxidized pyrrhotite are seen. In the EDS analysis A) shown on the left, a bit of nickel was present, thus the areas within the intrusion that show a slightly brighter shade of white represent areas that include nickel. This area that includes nickel is thought to be a mineral other than pyrrhotite, which was also found in other areas in the Sulfide aggregate. In Figure 4.2.20, the edge of the pyrrhotite intrusion shows oxidation, the bottom left corner of the intrusion separated and likely caused the crack in the immediate vicinity. It seems that the oxidation did not penetrate much past the surface of the aggregate in this image. There was also another larger crack that is shown in the image, which does not look as though it was related to the iron sulfide. It should be noted here that the cement paste in this area is very rich in ettringite. If this was an area where pyrrhotite was undergoing oxidation, gypsum would be expected in the immediate vicinity. Since no such gypsum was found, it is suspected that either the oxidation has ceased or is very slow, and the gypsum has fully reacted to form ettringite, or there was no oxidation and this ettringite formed from sulfoaluminates dissolved from the cement in a SEF type manner. Since the Sulfide-0.45 sample expanded more than Dolostone-0.45 sample, it is thought that the iron sulfide contributed to the formation of the previously discussed ettringite. This ettringite may have de-composed during

the 7-day heating cycles, and then caused any contribution by the iron sulfides to be amplified by subsequent reformation and dissolving of ettringite, cause by the heating cycles to 60°C with saturation in lime solution at 23°C.

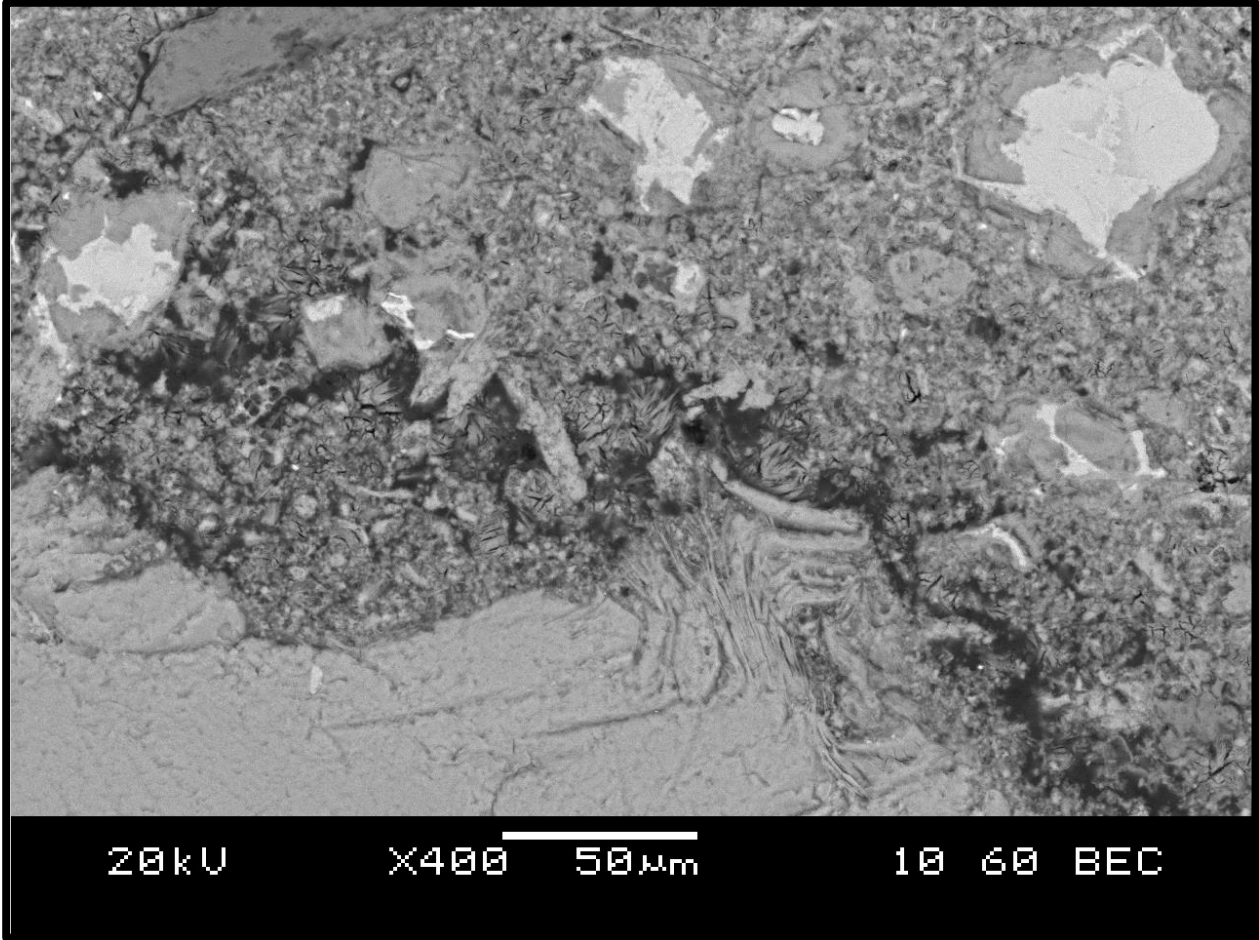


Figure 4.2.19: SEM image of I-S60/23 showing iron interaction with paste; made with Sulfide aggregate, 0.65 w/c, and tested with 7-days drying at 60°C and 7-days soaking at 23°C

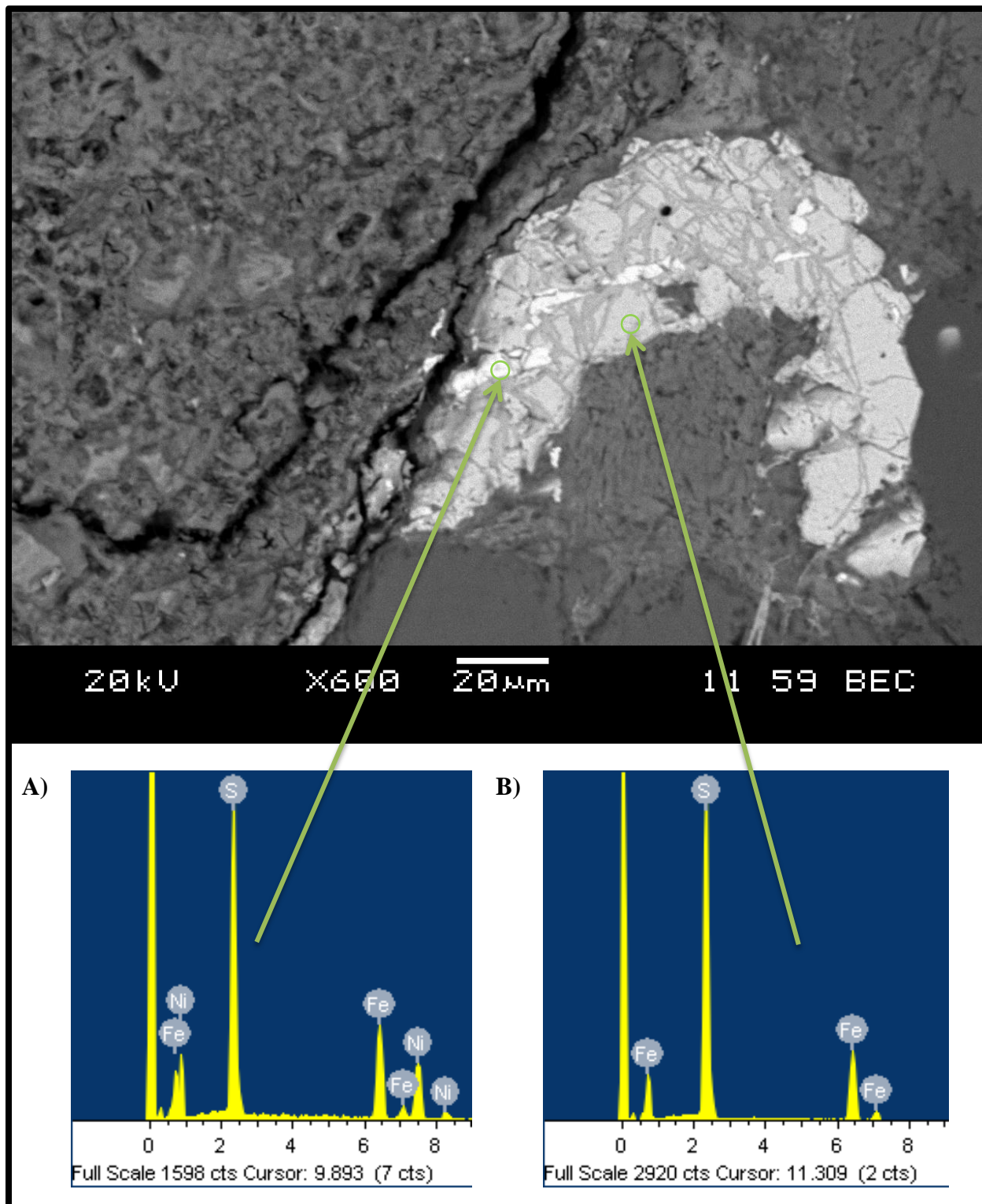


Figure 4.2.20: SEM image and EDS analysis of I-S60/23 showing a pyrrhotite inclusion with very little oxidation; made with Sulfide aggregate, 0.65 w/c, and tested with 7-days drying at 60°C and 7-days soaking at 23°C

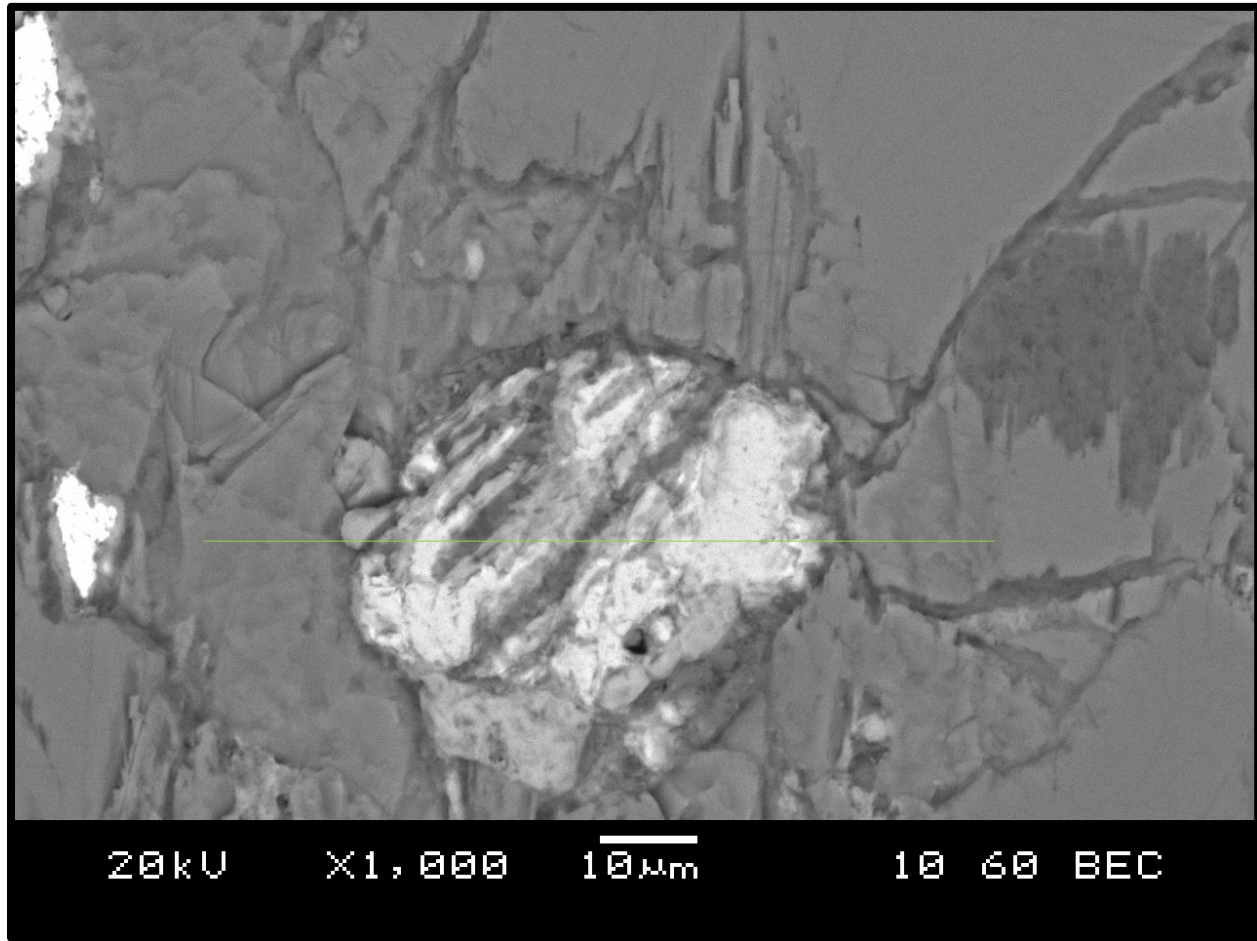


Figure 4.2.21: SEM image of I-S60/23 showing a partially oxidized pyrrhotite inclusion that was examined via a line scan in Figure 4.2.22; made with Sulfide aggregate, 0.65 w/c, and tested with 7-days drying at 60°C and 7-days soaking at 23°C

In Figure 4.2.21 and Figure 4.2.22 another pyrrhotite inclusion is seen, it appears as though it could have been partially oxidized. Figure 4.2.22 is an EDS line scan analysis, which shows the relative amount of each element across the line shown in A) and the line in Figure 4.2.21. In B), C), and D) the EDS output for sulfur, oxygen, and iron are shown respectively. Where there were high peaks of sulfur, there was iron and no oxygen; this corresponds to the bright white areas in Figure 4.2.21. In the light grey areas there was iron and oxygen, but no sulfur. Thus, one may suspect the light grey areas of showing signs of oxidation. This idea will be discussed further in Section 4.3.2.1. It was noticed that this inclusion was not at the surface of the coarse aggregate, and it is possible that if this is oxidation it may have occurred previously to being mixed into the concrete. The peak on the far left side of the image, shown in purple, represents titanium (Ti), considered as another impurity in the iron.

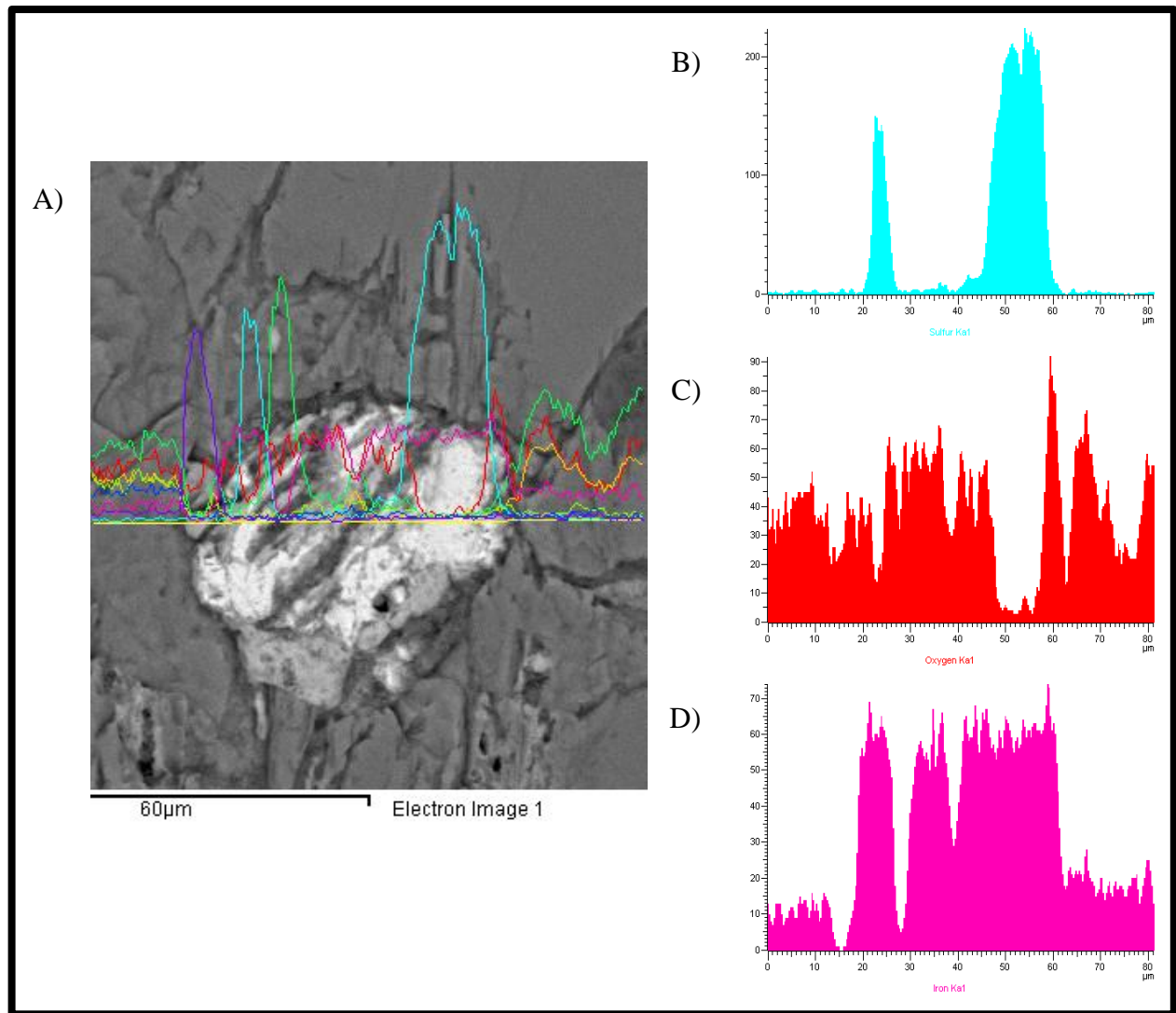


Figure 4.2.22: Line scan of I-S60/23 showing A) a partially oxidized pyrrhotite inclusion, and the relative amounts of the analysis results for B) Sulfur C) Oxygen and D) Iron; made with Sulfide aggregate, 0.65 w/c, and tested with 7-days drying at 60°C and 7-days soaking at 23°C

Scanning Electron Microscopy on I-D60/23

The control aggregate sample corresponding to the previous section, known here as I-D60/23, was also examined under the SEM; made with Dolostone coarse aggregate and a w/c of 0.45; it was tested with 7-days heating to 60°C followed by 7-days soaking in lime solution at 23°C. It was immediately apparent that this sample contained many similar features to what was seen in the previous section, with the exception of the oxidation and iron sulfides. There were also areas with large concentrations of condensed ettringite, formed in the void space created around the coarse aggregate particles, as shown in Figure 4.2.23. Both concentrations that were analyzed in Figure 4.2.23 were large enough to give great EDS analysis results to show ettringite definitively. In analysis A) the familiar ettringite peaks are seen along with a very small peak for silicon, while in analysis B) there was no silicon, just pure ettringite peaks. It can be noted that these large concentrations in Figure 4.2.23 were formed in the ITZ around a coarse aggregate particle. There were also areas with smaller concentrations of ettringite, and cracks that were lined with ettringite, shown in Figure 4.2.24. In both analysis A) and B) here a small amount of silicon was present, although again, this was considered to be background from the surrounding paste. Ettringite crystals were also observed in the air voids in in this sample, shown in Figure 4.2.25. This shows again that the perfect ettringite crystals will form inside of the air voids in the concrete, even here in a sample that does not contain iron sulfide in the coarse aggregates. What can be said in comparison between this sample, Dolostone-0.45, and the previous sample, Sulfide-0.45, is that there is relatively less ettringite found throughout the Dolostone sample. Both samples included the same features (except for iron sulfide oxidation), but when examining the samples it was apparent that the Sulfide sample had ettringite spread throughout the entire cement matrix. While in the Dolostone sample, ettringite was observed only in the ITZ around aggregates, and along the edges of some cracks. These findings are promising for test development, and future testing without the aid of an oxidizing agent.

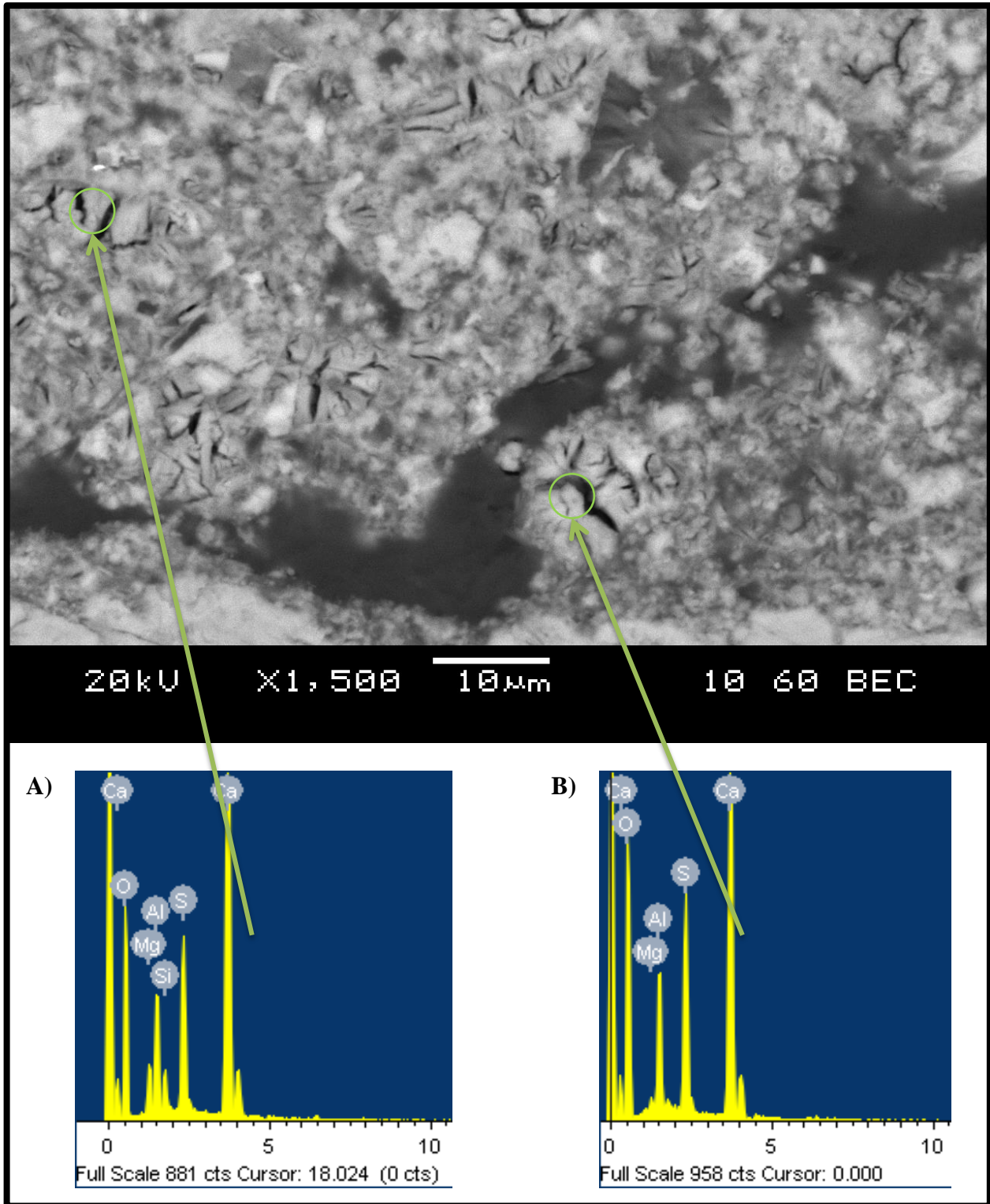


Figure 4.2.23: SEM image and EDS analysis of I-D60/23 showing condensed ettringite in large concentrations in cement matrix; made with Dolostone aggregate, 0.65 w/c, and tested with 7-days drying at 60°C and 7-days soaking at 23°C

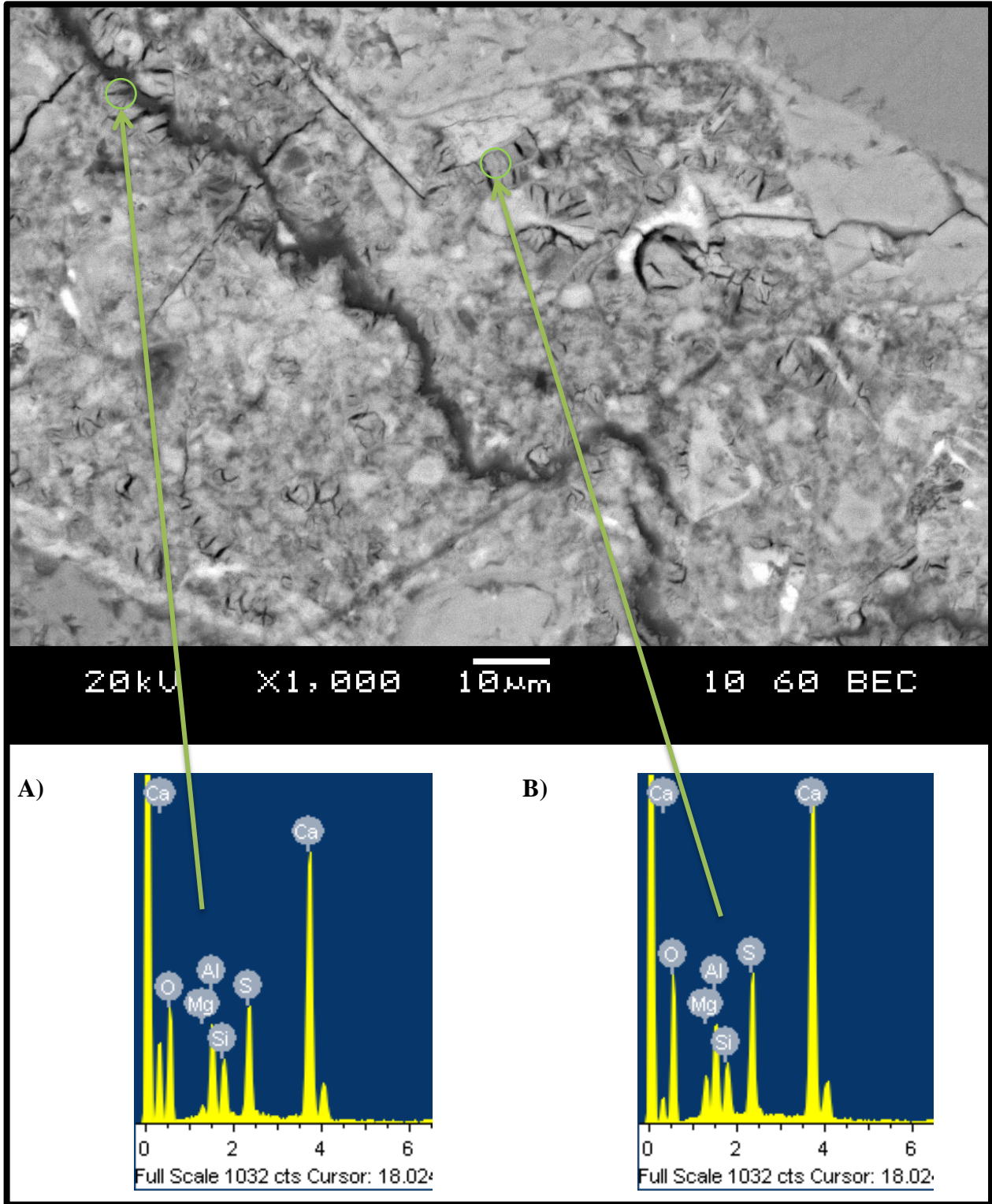


Figure 4.2.24: SEM image and EDS analysis of I-D60/23 showing condensed ettringite in cement matrix; made with Dolostone aggregate, 0.65 w/c, and tested with 7-days drying at 60°C and 7-days soaking at 23°C

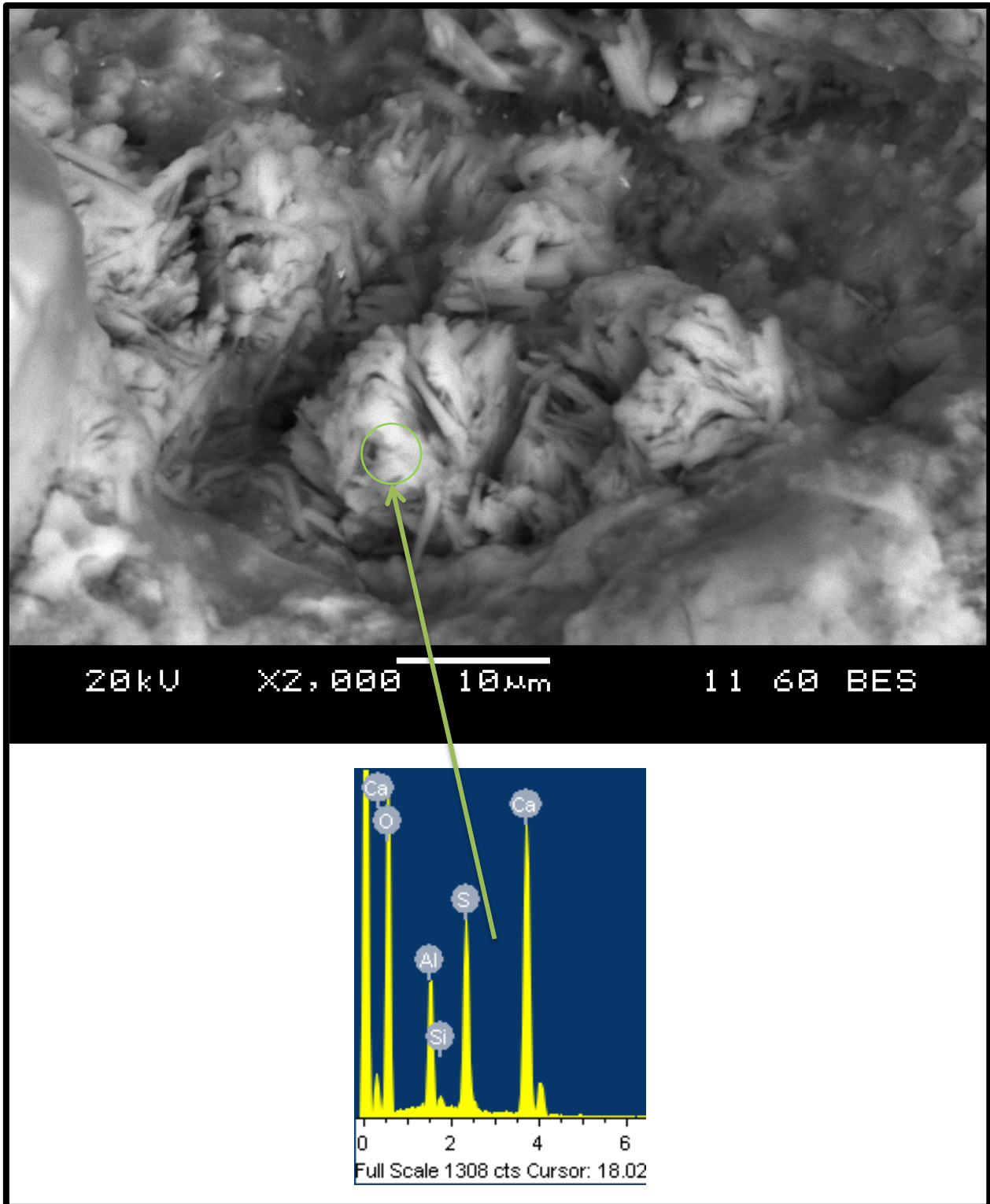


Figure 4.2.25: SEM image and EDS analysis of I-D60/23 showing ettringite crystals in an air void; made with Dolostone aggregate, 0.65 w/c, and tested with 7-days drying at 60°C and 7-days soaking at 23°C

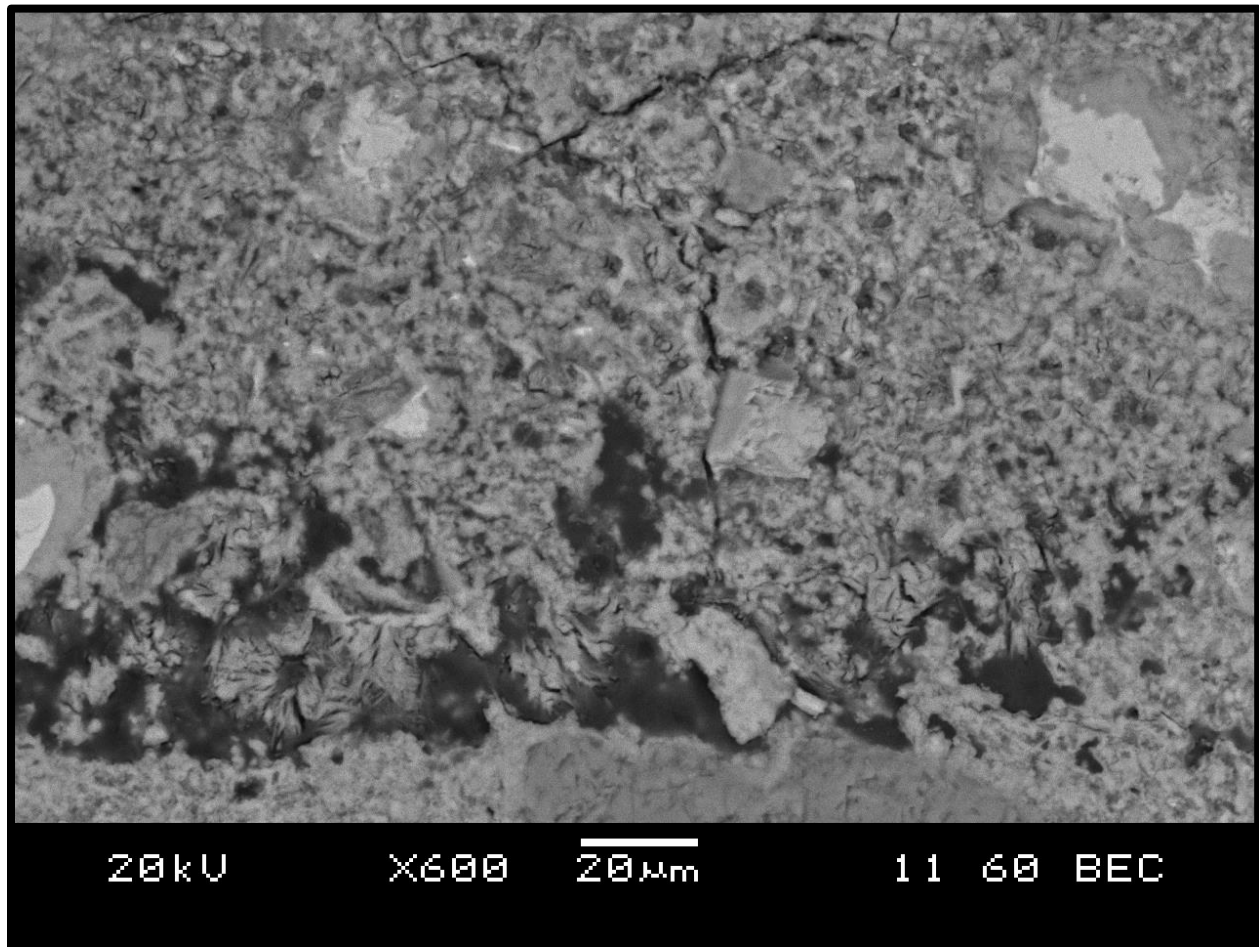


Figure 4.2.26: I-D60/23 SEM image of mapping area; made with Dolostone aggregate, 0.65 w/c, and tested with 7-days drying at 60°C and 7-days soaking at 23°C

EDS Mapping was also done on the Phase I Dolostone-0.45 sample; I-D60/23. The results are shown in Figure 4.2.27. A very similar analysis was done here as before, and again the presence of ettringite was confirmed within the sample containing the Dolostone aggregate. An identical set of ovals were overlain here on Figure 4.2.27-A) through Figure 4.2.27-F), and they highlight the areas where ettringite can be clearly seen and confirmed. Figure 4.2.27-B) confirmed the strong concentration of sulfur, Figure 4.2.27-D) confirmed the presence of aluminium in each of the ovals, and Figure 4.2.27-F) shows that there was little or no silicon within the ovals.

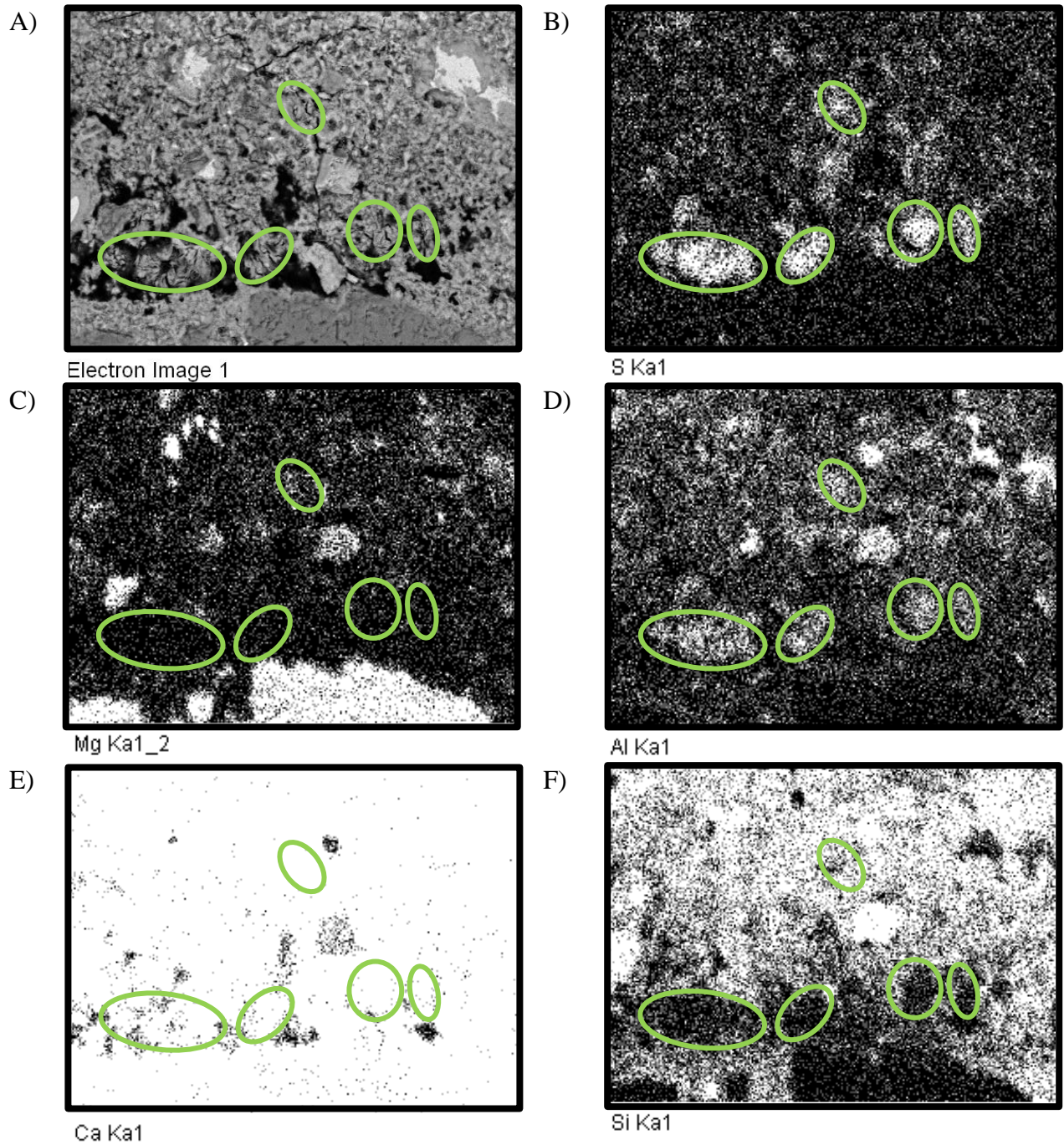


Figure 4.2.27: I-D60/23 mapping analysis results A) SEM image of area B) Sulfur C) Magnesium D) Aluminium E) Calcium F) Silicon; made with Dolostone aggregate, 0.65 w/c, and tested with 7-days drying at 60°C and 7-days soaking at 23°C

4.2.2.3 60°C/5°C Soaking

The results from testing cycles of 6-days drying in the oven at 60°C followed by soaking in lime solution for 6-days at 5°C are presented in Figure 4.2.28. Also presented here in Figure 4.2.29 is a side-by side comparison of Figure 4.2.28 and Figure 4.2.12 from the previous section to aid in comparative observations.

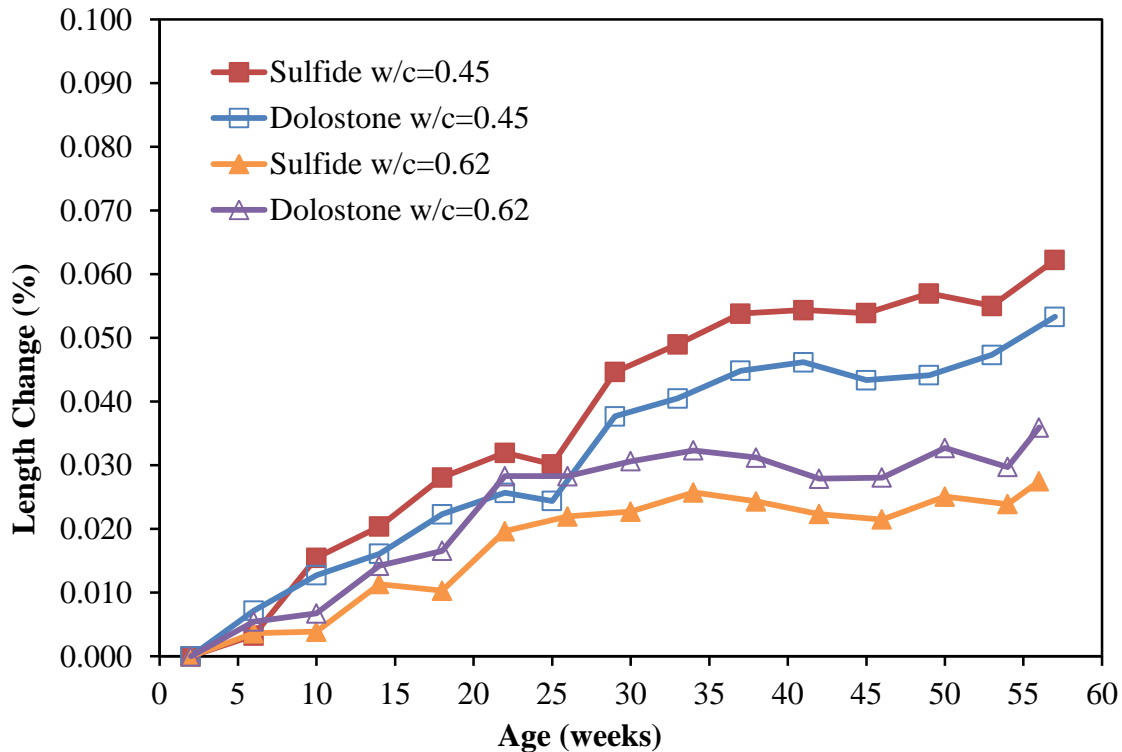


Figure 4.2.28: Phase I results from heating/drying to 60°C for 7-days and soaking cycles at 5°C for 7-days; thus 2 wet/dry cycles per 28-days were experienced

In Figure 4.2.12, the maximum expansion experienced by the Sulfide sample with 0.45 was 0.076%. Here in Figure 4.2.28 the maximum with the Sulfide sample was 0.062%, and was 0.053% with the Dolostone sample, when examining samples with w/c of 0.45. All of these values are very consistent across their respective samples, and are quite comparable considering a testing age of over 1 year. The Sulfide-0.45 samples in these 2 figures show a similar trend, perhaps at a slightly slower rate at 5°C soaking, but will likely reach the same ultimate value. The expansion in all of these samples seemed to slow or stop after about 38-weeks. It appears there was a possible false final reading with the samples in Figure 4.2.28, as a distinct jump is seen across all samples on the right side of the graph. Again here, the Sulfide-0.62 sample did

not show any significant expansion. The separation between the similar samples with different w/c is clear in Figure 4.2.28 for both aggregate types. Therefore, it is seen clearly here that the lower w/c is produced a greater amount of expansion, likely for the same reasons discussed earlier in section 4.2.2.2. When these results are compared with the RH testing of section 4.1, it can be seen that the sample with high w/c dried out very fast compared to the 0.45 w/c sample.

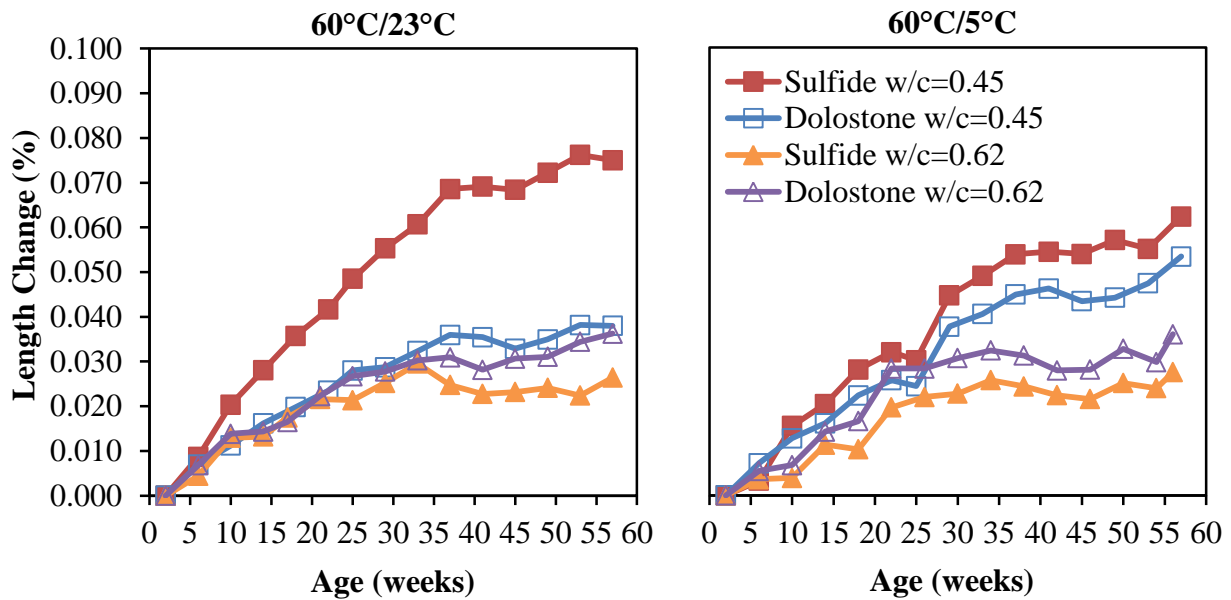


Figure 4.2.29: Side-by-side comparison of Phase I testing with 7-days soaking at 23°C from Figure 4.2.12 and 7-days soaking at 23°C from Figure 4.2.28; tested with 7-days drying at 60°C

The Dolostone-0.45 sample in Figure 4.2.28 showed a similar trend to that of Figure 4.2.12. The Dolostone-0.45 sample tested at 5°C actually reached a slightly higher ultimate value, the opposite to what was observed with the Sulfide sample. As discussed previously in Section 3.3.3 and Section 4.2.1.3, the testing conditions described in this section are designed to promote thaumasite formation, when compared to the previous section, which was designed to promote ettringite formation. So weather thaumasite was being promoted here in the Sulfide sample, or just ettringite at a slower rate, because of the reduced temperature, is not currently known. As previously stated, these samples were not selected for SEM analysis, due to their lower ultimate expansion value at the time of selection. Since the Dolostone-0.45 sample showed higher expansion with the 5°C soaking one may speculate that thaumasite had formed here, or an ettringite/thaumasite solid solution, related to an SEF type reaction. This seems possible since

there is no other reason to see this difference in the expansion levels between the Dolostone-0.45 samples in these 2 testing regimes. It is observed in all samples in both Figure 4.2.12 and Figure 4.2.28, that the expansion seems to level off after around 38-weeks. This may suggest that oxidation was no longer being promoted here in the Sulfide samples, or promoted at a relatively very slow rate. It is possible that the SEF type reaction may have reached a completion and ceased to cause further expansion. When comparing Figure 4.2.12 and Figure 4.2.28 the Sulfide samples are seen as the lowest and highest lines in both figures. From this one may speculate that if ettringite was causing expansion, it was worse in the samples that was the strongest and most sound; the Sulfide samples. Since the Dolostone aggregate is known to be a more porous stone than the Sulfide aggregate, it may have been able to accommodate for a certain amount of pressure or stress relief upon the formation of ettringite. Therefore, it is possible to conclude that the Sulfide aggregate samples performed worse (more expansion) when ettringite is more of a factor, but better (less expansion) when it was not. This finding may help to explain the large difference seen between the Sulfide-0.45 and Dolostone-0.45 samples in Figure 4.2.12, if in-fact there was very little or no oxidation. One may venture to the notion that the Dolostone aggregate experienced relatively more damage from the wet/dry damage; where ettringite was not as much of a factor. It would follow that the more severe temperature gradient, in testing at 5°C, would likely have caused slightly worse damage when considering the effects of micro-cracking caused by thermal expansions. Some possible evidence to this was seen as the greater expansion of the Dolostone-0.45 sample shown in Figure 4.2.28 compared to Figure 4.2.12.

In the Sulfide-0.45 sample in Figure 4.2.12 it is likely that these results indicate expansion from a combination of some oxidation, amplified by some SEF. In all other samples in Figure 4.2.12 it appears as though the effects of SEF are seen. Therefore, most of the expansion results presented in section 4.2.2, pertaining to 60°C testing, was likely caused by either SEF, wet/dry, thermal related expansions, or a combination thereof. The one exception being the Sulfide-0.45 sample, where some expansion related to iron sulfide oxidation may have been seen, the results of which were likely amplified through cycles of de-composition and re-formation. It cannot be concluded that this expansion was in-fact caused by iron sulfide oxidation, even though there was evidence of oxidized pyrrhotite found in the sample; one cannot be certain as to whether it was oxidized previously too, or during testing. In both aggregate types, concentrations of ettringite were found in the cracks formed in the ITZ around the aggregates. This suggests that the ettringite

concentrations formed for a reason other than iron sulfide oxidation in the Dolostone sample. Some expansion caused by the wet/dry cycles was expected, but not to the extent seen in Figure 4.2.12 and Figure 4.2.28. A significant amount of ettringite was seen in the ITZ in both aggregate types, and cracking patterns were observed, both of which are known to be associated with SEF damage. Comparative lab studies and field trials will need to be carried out in order to relate the accelerated expansion observed in the lab with actual damage to concrete in practice.

4.3 Phase II

Phase II involved many different testing cycles, and was completed in several stages. For this reason, Phase II has been separated into 4 different series', which are characterized by the type of testing exposure conditions used. It should be noted that the scale used in all Phase II graphs here, is 3 times as large as the scale used in the Phase I 60°C graphs from the previous sections.

4.3.1 Series 1

In Series 1 several different temperatures and humidity levels were tested, along with many different types of exposure conditions (cycles of heating and soaking). The results from many of these are shown in Figure 4.3.1, Exposures #8 and #9 that were described in Table 3.3.4 are not shown here, but followed the same trend of no expansion as did most of the others. All of the samples shown in Figure 4.3.1 are made with the Sulfide aggregate and all have a w/c of 0.65, although Exposure #6 and #7 were made with bleach as their mixing water. What is obvious when looking at Figure 4.3.1 is that only 1 exposure condition has shown any expansion whatsoever; Exposure #5: 2-hours soaking in bleach, twice a week. From Figure 4.3.1 one could conclude that heat was necessary to accelerate the expansion; when comparing Exposures #3 and #5 it is seen that even after a year of exposure, no expansion occurred in Exposure #3, which was soaked with the same cycles but never heated. The heat is thought to have acted as a catalyst to the oxidation reaction; it may have increased the rate of the reaction. When comparing Exposure #5 in Figure 4.3.1 to the 60°C/Dry and 60°C/23°C results from Phase I in Section 4.2.2, one could suspect that the bleach is also playing a part in the expansion of Exposure #5. Phase I and Phase II samples cannot be compared directly, as they were made with a different concrete mixture design, so samples were made to investigate this, and were tested in Phase II- Series 2. Series 1 was considered as a trial and error type of testing, so not many conclusions can be

drawn from these results. Since Exposure #5 showed promising expansion results here, it was selected for further testing in Series 2.

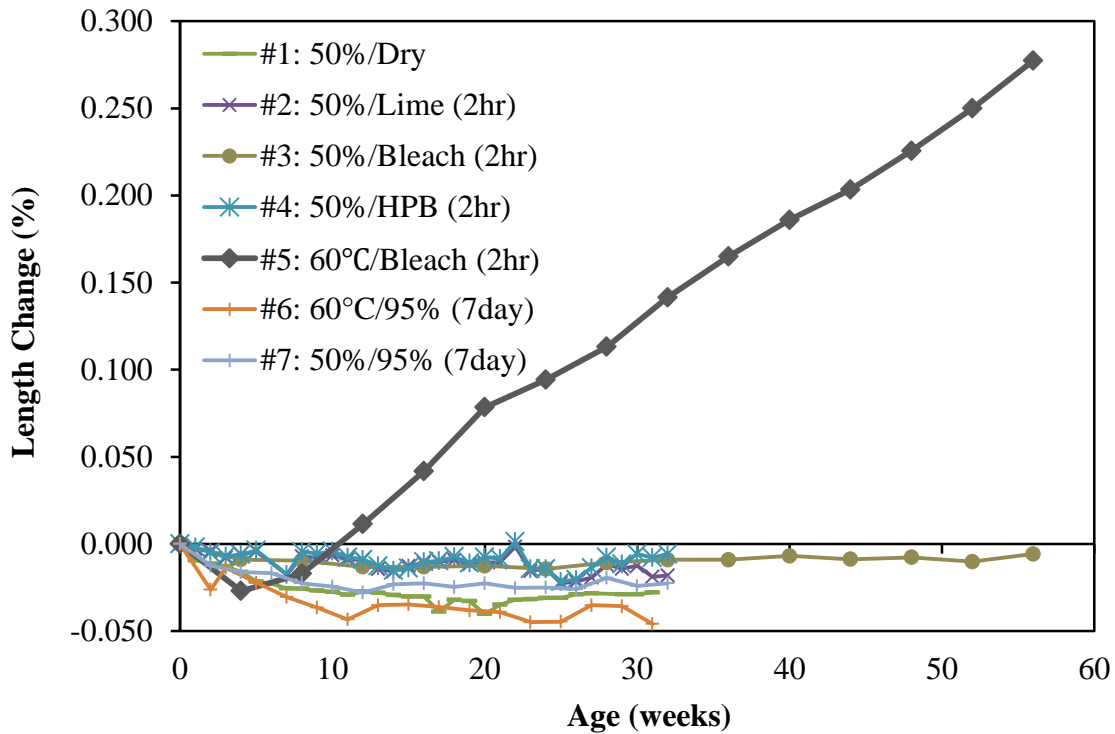


Figure 4.3.1: Phase II Series 1 results for sulphide aggregate with w/c of 0.65; all soaking was at 23°C after 24-hours stabilization

4.3.2 Series 2

Series 2 was designed to focus in on Exposure #5 from the last section, and test different samples to determine the fine points behind the expansion. The same exposure regime was used here as in Exposure#5 from Series 1; a 2-hour soaking, twice a week, but many other parameters were adjusted. Samples were tested at 40°C and 60°C, to see if 60°C was necessary to accelerate expansion. Samples were tested with their soaking cycles in both lime and bleach solutions, to test the adequacy of an oxidizing agent. Also, all samples were repeated with the Dolostone aggregate, to be used as a control, to check if the expansion will occur only with the Sulfide aggregate. The Series 1 Exposure #5 was repeated here twice to confirm the results, which are shown below.

4.3.2.1 Bleach Soaking

In Figure 4.3.2 the results from the repeated Series 1 sample, Sulfide 60°C, along with its control and their corresponding 40°C samples are shown. All samples shown here in Figure 4.3.2 were made with the same concrete mixture and have the same w/c of 0.65. The repeated Sulfide 60°C sample showed a very similar trend as in Series 1, but at a slightly faster rate. This sample was repeated a second time, but the results are not shown as they once again confirm the same trend.

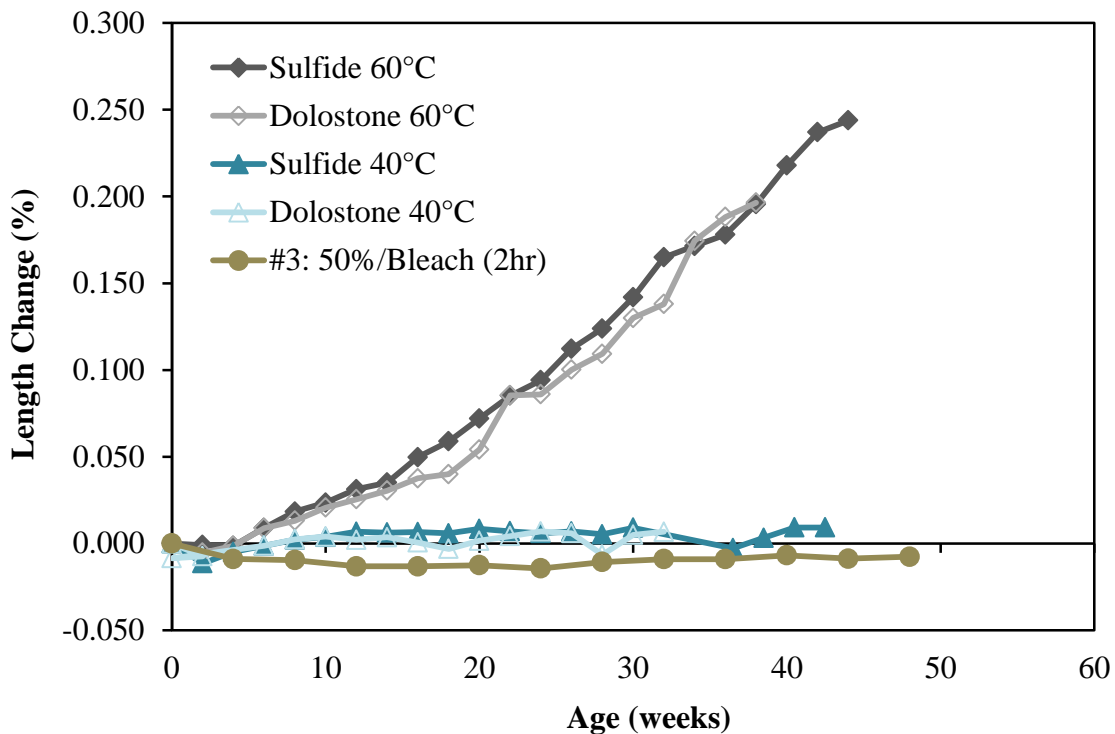


Figure 4.3.2: Phase II Series 2 results; all samples have w/c of 0.65 and were tested with 2-hours soaking in bleach at 23°C twice a week

The samples tested at 60°C expanded much more than the samples tested at 40°C, in fact, the samples tested at 40°C showed a similar inactivity as the samples tested with no heating from Series 1, shown here in Figure 4.3.2 for comparison. Therefore, one could conclude that this expansion only occurred upon heating to 60°C, and thus, heating to 60°C was necessary to accelerate this type of expansion. What is also apparent in Figure 4.3.2 is that the Dolostone sample tested at 60°C showed a result very similar to the Sulfide sample tested at 60°C. At 18-weeks of testing the 2 samples started to show a separation, but this difference was soon recovered and the expansion continued very similar. This suggests that the expansion seen in

Figure 4.3.2 was not a product of the sulfides in the aggregate, but perhaps some other sort of expansion was promoted here. To further investigate the cause of this expansion, the Sulfide and Dolostone samples tested at 60°C from Figure 4.3.2 were selected to be examined under the SEM, results of which are discussed in the following sections.

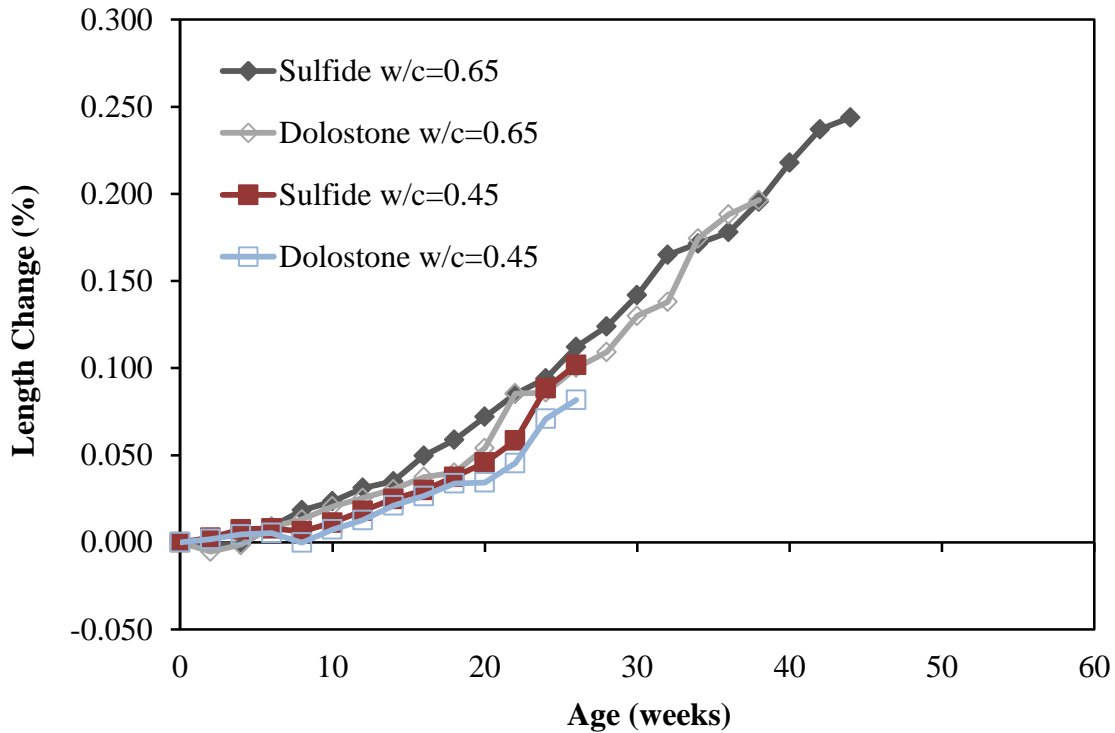


Figure 4.3.3: Phase II Series 2 Results; all samples tested with drying at 60°C and 2-hours soaking in bleach at 23°C twice a week

In Figure 4.3.3 the 2 samples from Figure 4.3.2 are shown again, along with their equivalent 0.45 w/c samples. It is seen that all samples shown in Figure 4.3.3 all followed a similar expansion trend. Therefore, it seems that for this specific testing condition, the expansion will occur regardless of the w/c of the concrete. It may have occurred a bit sooner with a higher w/c, but all samples seemed to have a similar rate of expansion once it began. Since all 4 samples in Figure 4.3.3 followed the same trend, one could conclude that the expansion seen in Figure 4.3.2 and Figure 4.3.3 was likely not related to the iron sulfides in the coarse aggregate, and is therefore likely not the reaction that was desired. In Figure 4.3.4 the results for the samples made with HSF cement are shown, samples with w/c of 0.65 and 0.45 were made for both aggregate types. There was no expansion here at all, under the exact same testing conditions as the results shown

in Figure 4.3.2. The silica fume in the cement provided a less permeable surface and more densely packed cement paste. This likely prevented the bleach from reaching the coarse aggregate, or at least slowed down the migration of the bleach. Therefore, it seems that adding Silica Fume to the cement may be effective to prevent the expansion caused by this test.

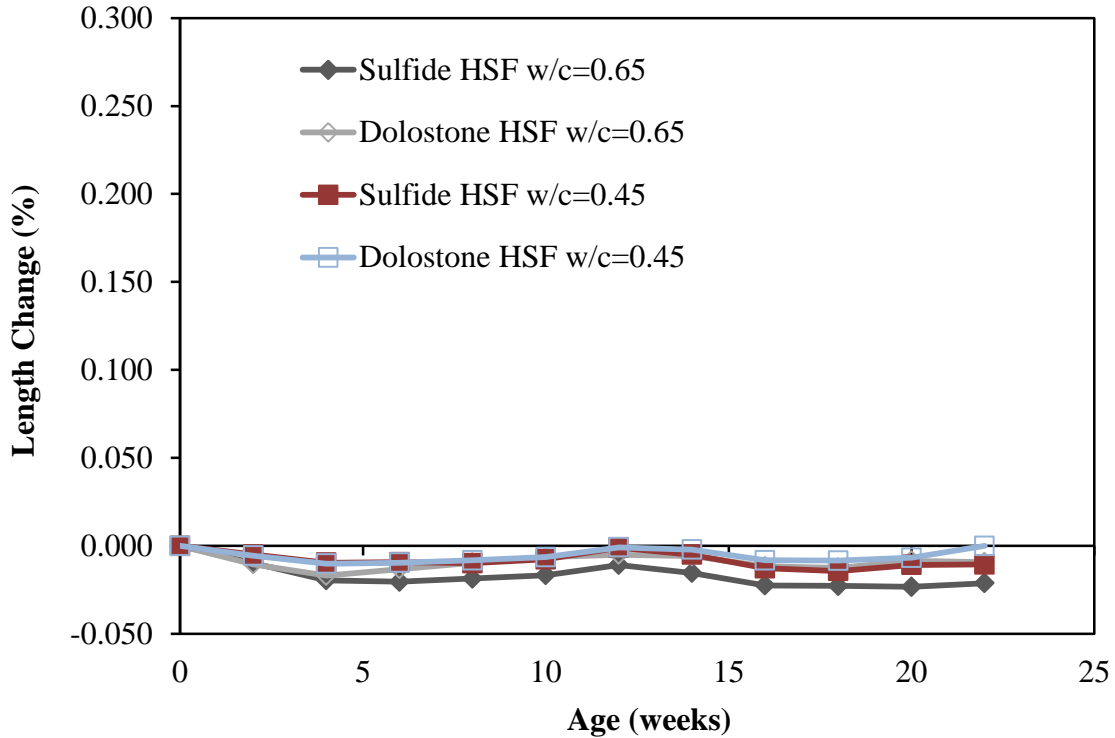


Figure 4.3.4: Phase II Series 2 Results; all samples made with HSF cement and tested with drying at 60°C and 2-hours soaking in bleach at 23°C twice a week

These results suggest that the damage observed in Figure 4.3.2 is a result of the bleach penetrating inside the concrete, and reacting in some way. Therefore, one may speculate that it is not the hot/cold cycles that caused any damage, but instead it was the wet/dry cycles that caused damage. While the silica fume prevented the inflow of moisture, it also prevents the moisture from escaping, and would therefore likely dampen the range of relative humidity inside the sample. The slight hump in the lines starting at week 12 was caused by a pause in testing for several weeks.

Scanning Electron Microscopy

In the following sections, 4 separate SEM samples are analyzed; they were made from the 2 samples that showed expansion in Figure 4.3.2. SEM samples were taken at different ages of testing, each age was examined separate, and will be differentiated between in the following sections. The different sample ID's, their age and expansion at time of sampling are shown in Table 4.3.1. When a specimen was sacrificed for SEM analysis a small sample was taken from the interior of the concrete, towards an end of the prism. The remaining portion was then returned to testing to undergo exposure cycles, but was no longer able to be measured; this was done to provide representative samples for future SEM analysis, without sacrificing another sample. Therefore, the results shown in Section 4.3.2, from the first sample date in Table 4.3.1 onward is the average of 2 specimens instead of 3. Variance was very low across all samples, so there was no change in the average value after a specimen was sacrificed for SEM analysis.

Table 4.3.1: Phase II SEM samples I.D. and related information

SEM I.D.	Exposure ID	Age (weeks)	Expansion (%)
II-S60A	Sulfide-0.65 60°C/Bleach	31	0.143
II-S60B	Sulfide-0.65 60°C/Bleach	59	0.308
II-D60A	Dolostone-0.65 60°C/Bleach	22	0.078
II-D60B	Dolostone-0.65 60°C/Bleach	26	0.111

II-S60A

SEM sample II-S60A was made from with the Sulfide aggregate and had a w/c of 0.65, and was tested in Phase II Series 2; drying at 60°C and 2-hours soaking in bleach at 23°C twice a week. This sample was taken at an age of 31weeks of testing, and had and expansion of 0.143% at that time. When examining this sample, the first target was to look for any signs of pyrrhotite, and then search in the immediate vicinity for evidence of a reaction or reaction products. In **Error! Reference source not found.** an SEM image that shows such a partially oxidized pyrrhotite inclusion can be seen. The EDS analyses presented with it indicate that the brightest white area

contained iron, along with a high concentration of sulfur; this relates to an area of pyrrhotite that had not been oxidized. Surrounding this, a greyish area can be seen that shows closely spaced lines running parallel to the interface. The EDS analysis in this area revealed that there was no sulfur here in the greyish zone. When iron sulfides oxidize, they are known to release sulfuric acid, thus, after oxidation we expect to see no sulfur present in the EDS analysis. There are cracks extending out from this location, therefore it would seem intuitive to suspect that this reaction was creating a pressure on the surrounding concrete. In Figure 4.3.6 the same SEM image is seen, along with 2 EDS analyses of the cement paste, which show an elemental signature similar to gypsum, but with other elements also present. There appeared to be sulfur present throughout this immediate area, and signs of gypsum found in localized places. Gypsum crystals were confirmed in an air void nearby shown in Figure 4.3.7. Therefore, the combination of partially oxidized pyrrhotite, presence of gypsum, and abundance of sulfur in the area, would lead one to think that sulfate attack had in-fact been induced, as a result of pyrrhotite oxidation, in this area. In Figure 4.3.7 gypsum crystals are seen to have formed in an air void in relative proximity to the partially oxidized, which is shown at lower magnification in Figure 4.3.8 and Figure 4.3.9. The EDS analysis A) in Figure 4.3.7 shows a massive form of gypsum that seems to have formed within the cement paste matrix. EDS analysis B) confirms the elements of gypsum are present in the crystals, which show the aspect ratio expected of gypsum. What can also be seen in Figure 4.3.9 is that some of the aggregate particles seem to have a black ring or halo around them, in the ITZ. This feature is not considered typical to concrete, and it has been associated with DEF formation in the past (Taylor et al., 2001).

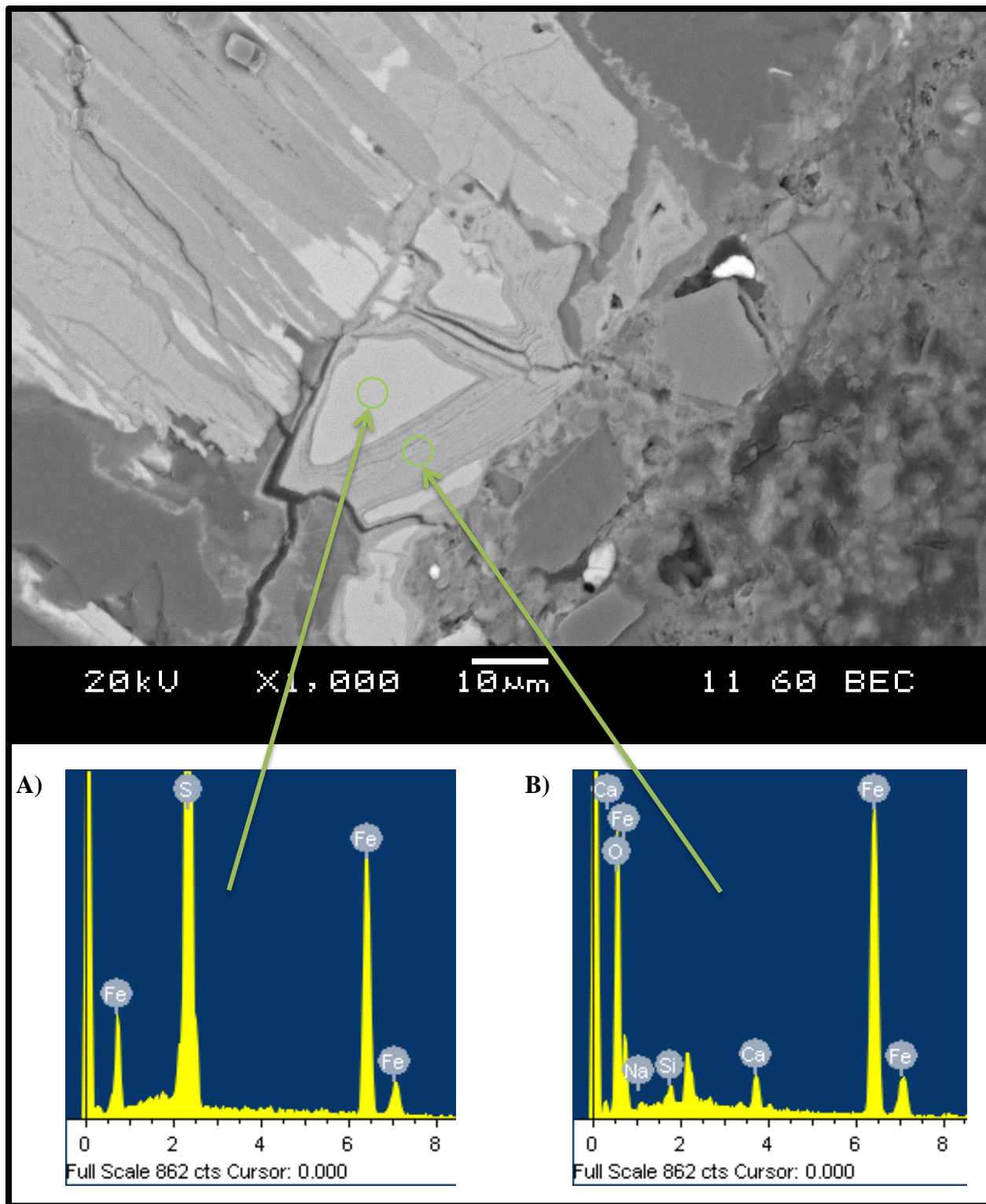


Figure 4.3.5: SEM image and EDS analysis for II-S60A showing oxidation; made with Sulfide coarse aggregate, w/c of 0.65, and tested with drying at 60°C and 2-hours soaking in bleach at 23°C twice a week

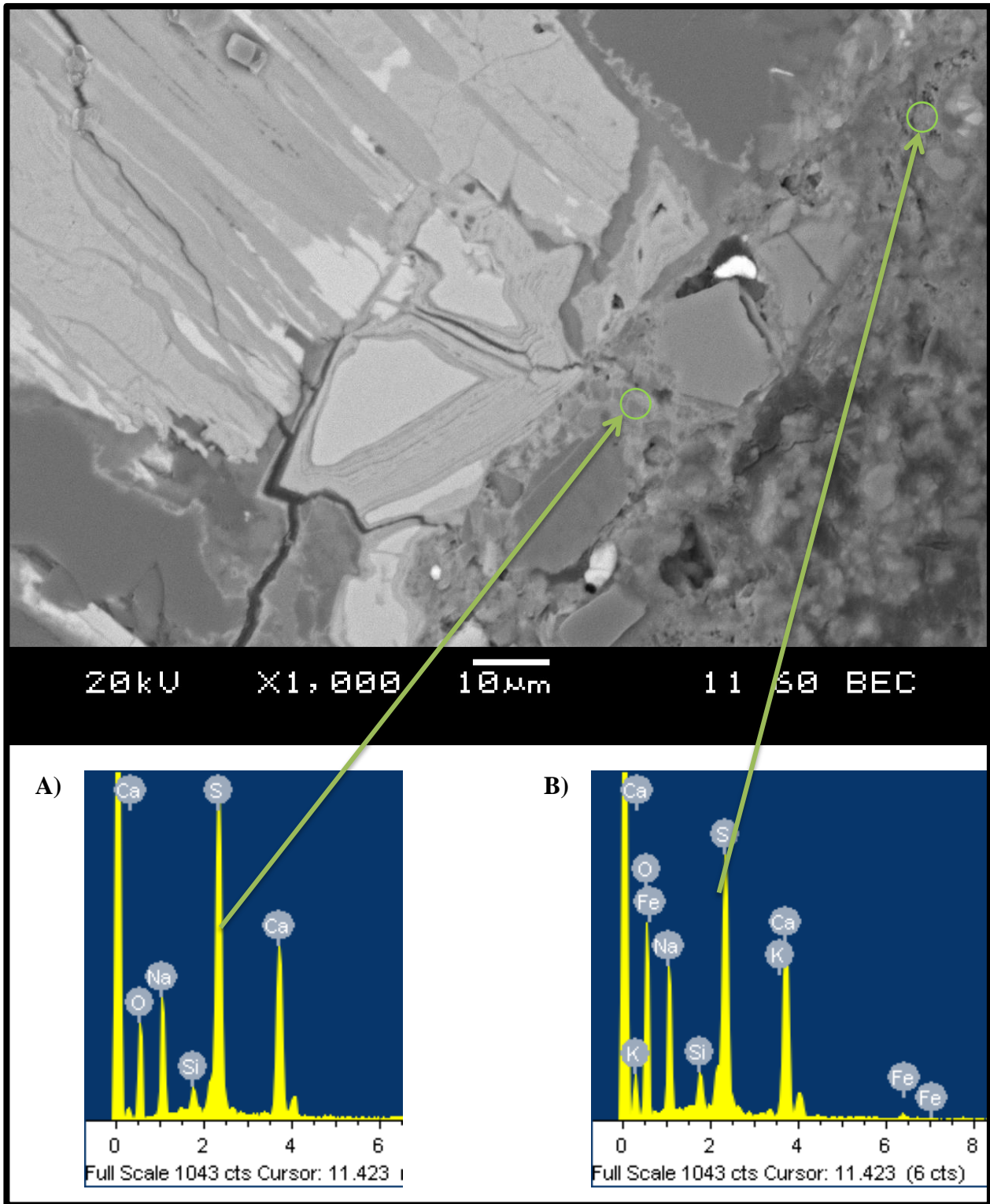


Figure 4.3.6: SEM image and EDS analysis for II-S60A showing gypsum; made with Sulfide coarse aggregate, w/c of 0.65, and tested with drying at 60°C and 2-hours soaking in bleach at 23°C twice a week

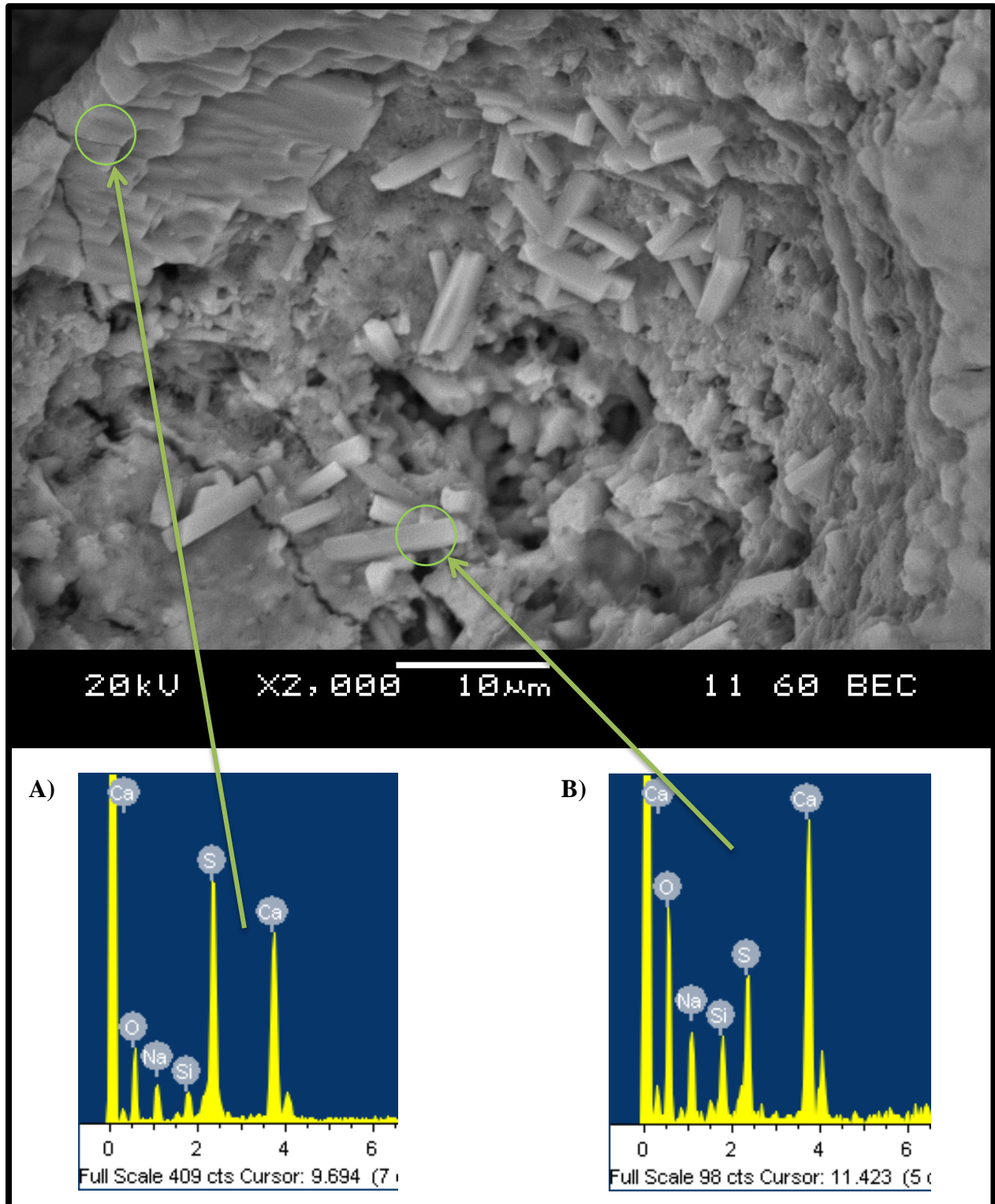


Figure 4.3.7: SEM image and EDS analysis for II-S60A showing gypsum crystals; made with Sulfide coarse aggregate, w/c of 0.65, and tested with drying at 60°C and 2-hours soaking in bleach at 23°C twice a week

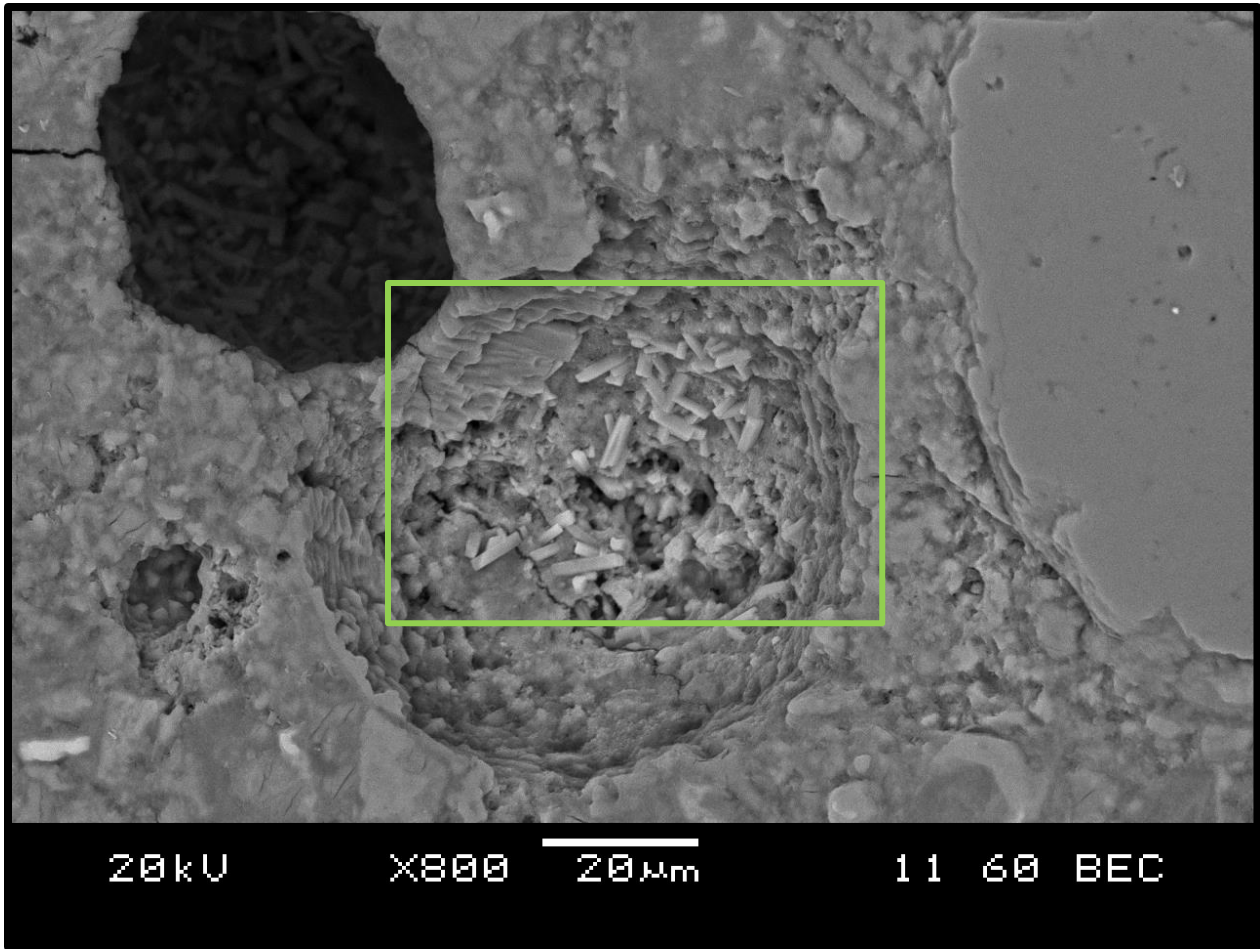


Figure 4.3.8: SEM image for II-S60A showing gypsum crystals; made with Sulfide coarse aggregate, w/c of 0.65, and tested with drying at 60°C and 2-hours soaking in bleach at 23°C twice a week

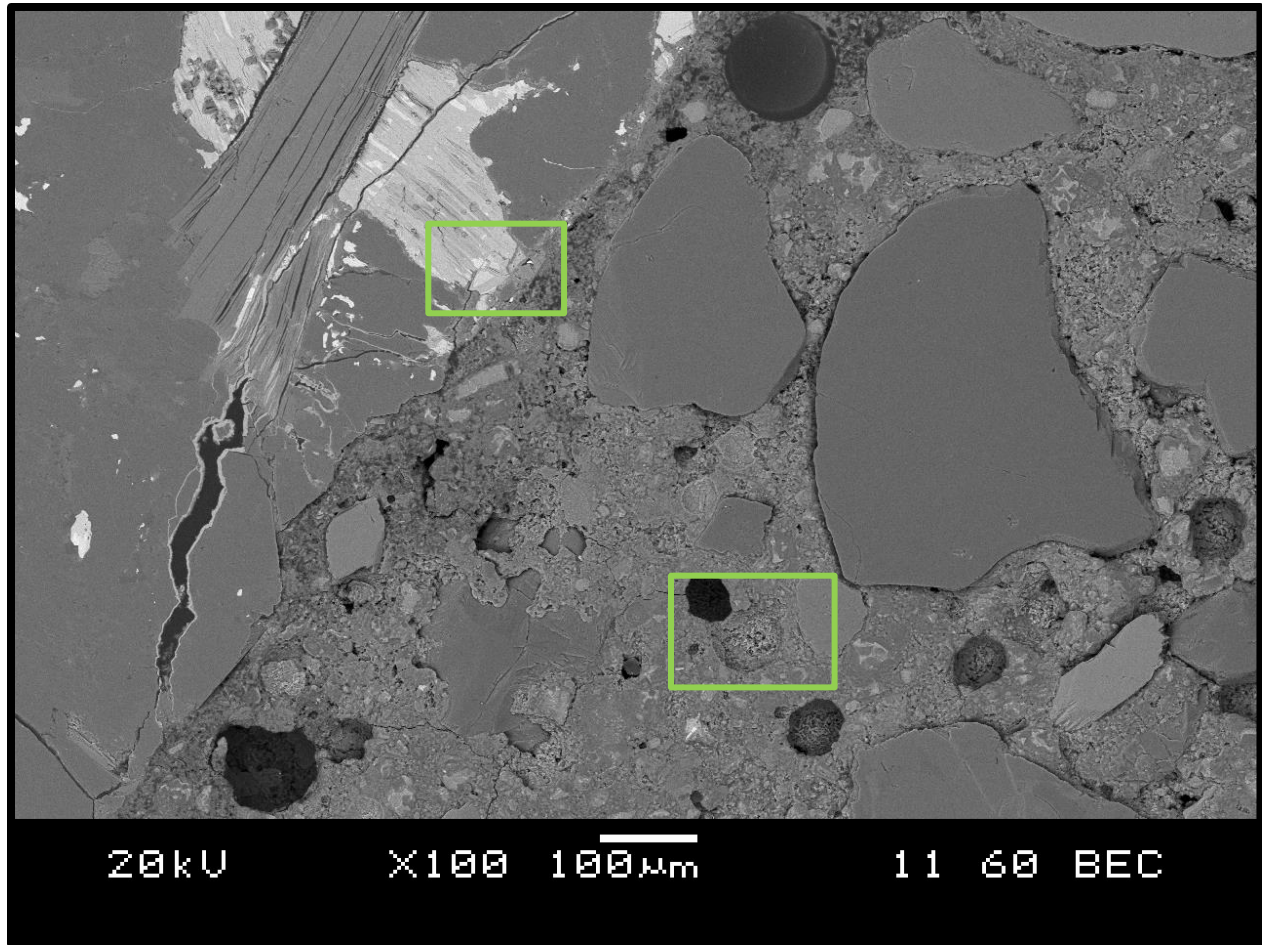


Figure 4.3.9: SEM image for II-S60A showing large analysis area; made with Sulfide coarse aggregate, w/c of 0.65, and tested with drying at 60°C and 2-hours soaking in bleach at 23°C twice a week

Another large pyrrhotite inclusion was found in a different area of the same sample, and similar features were found, shown in Figure 4.3.10 through Figure 4.3.16. In Figure 4.3.10 the area under analysis is seen at low magnification; the rectangles highlight the specific area which was magnified to in the following figures. In the upper right corner of Figure 4.3.10, a large pyrrhotite inclusion is seen at the surface of the coarse aggregate particle. The coarse aggregate is seen across the top half of the image, while the cement paste is seen in the bottom half of the image. In Figure 4.3.11 the EDS analysis B) shows that the brightest white area contains sulfur and the area highlighted in analysis A) is where oxidation was suspected to have occurred, and no sulfur was present; although the small unmarked peak appears to be a small amount of sulfur that was not recolonized. In Figure 4.3.12 EDS analysis B) shows an area on the same image, but just inside of the cement paste, immediately adjacent to the suspected oxidation. It shows that

there was a high concentration of iron in the paste, at this location. Therefore, it can be concluded here that there is definitely a reaction occurring between the cement paste and the iron sulfide in the coarse aggregate here. There are also see some cracks in the area, but one could not say definitively that this particular reaction caused the cracking and expansion of the concrete. In Figure 4.3.13 another area of the same sample is shown, this area is not shown in Figure 4.3.10, but is relatively very close and just off of the left side of the image. The large peaks of calcium and sulfur that are associated with gypsum are seen in both EDS analyses in Figure 4.3.13, and some crystals are seen within the cement paste that showed the same signs of gypsum. In both analyses, many other elements are present, which were considered to be “background” detection, as was expected due to the size of the crystals and relatively large analysis area of the EDS in these images. The area inside the rectangle in Figure 4.3.13 was magnified to Figure 4.3.14, which shows a secondary electron image of the area. The circle shown in this figure represents the analysis area for the EDS analysis B) in Figure 4.3.13. Gypsum crystals are clearly seen, and also the analysis area appears to likely include some background cement paste in the vicinity. The secondary electron image is shown here to highlight the crystals in the image as it shows better depth of field. It is possible that these crystals were transported here from an air void during polishing, as crystals of this nature are not necessarily expected in the paste like this. In Figure 4.3.15 the area from the other rectangle in Figure 4.3.10 was magnified to. Many gypsum crystals are seen scattered throughout the area, and the EDS analyses show that sulfur was present in the lighter grey areas in the image. While sulfur was present in these analyses, varying amounts of aluminum and silicon were also seen, and so, no conclusions can be made about which compounds are present here. In Figure 4.3.16 another image of the same area is shown, although again not shown in Figure 4.3.10, it clearly shows a gypsum crystal in analysis B). An interesting feature can be seen in analysis A) in Figure 4.3.16; from previous experience with Phase I analysis, one would have expected to find ettringite at this location. While the familiar peaks of calcium, sulfur, and aluminum were present as expected, peaks of sodium and chlorine were also seen. This phenomenon is thought to be associated with a reaction between the bleach and ettringite. Since it was very hard to find pure ettringite anywhere in this sample, the chlorine is suspected of dissolving the sulfur from these crystals and converting them into Friedel’s salt. The presence of Friedel’s salt will be discussed further with the following figures below.

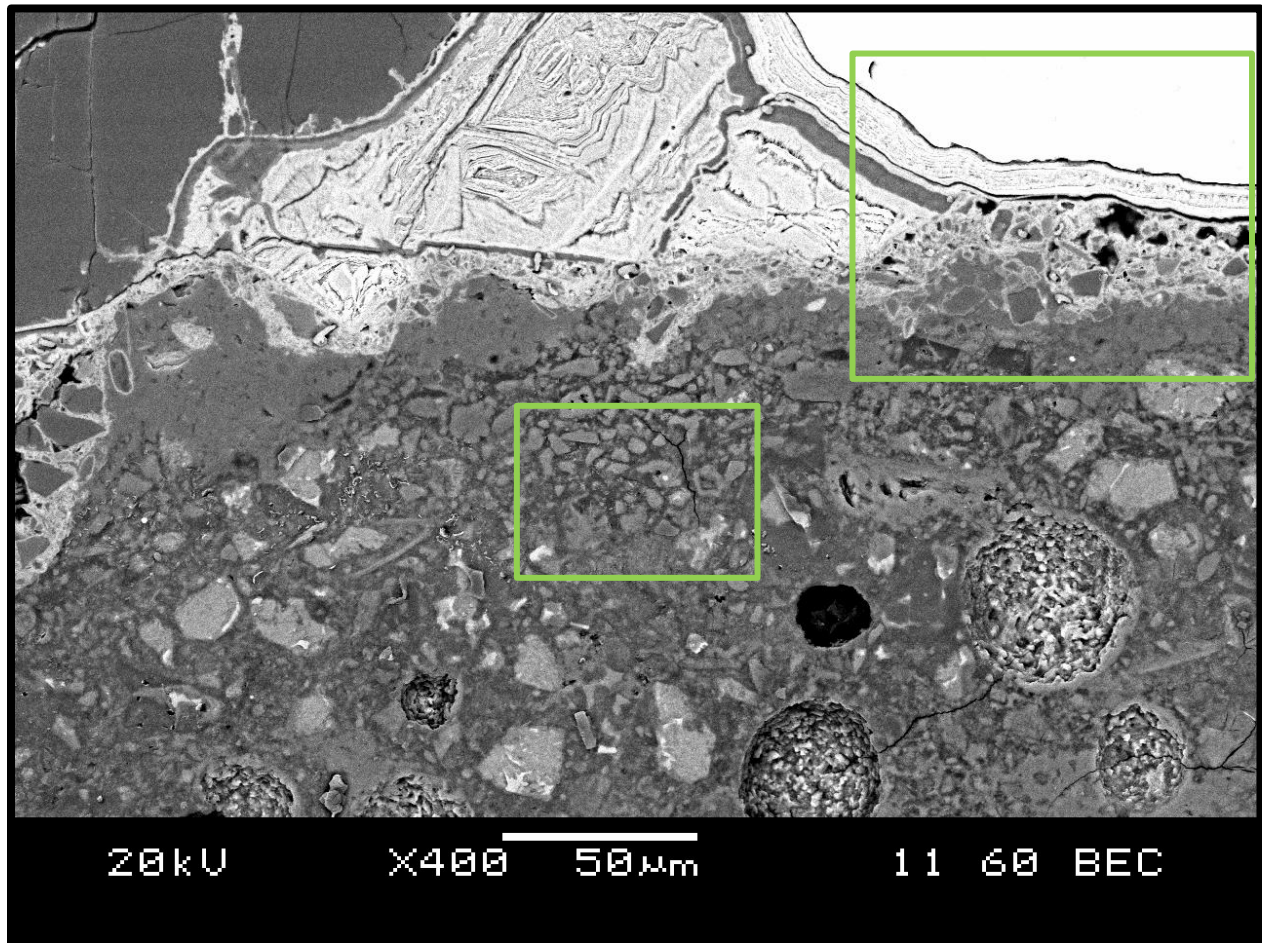


Figure 4.3.10: SEM image and EDS analysis for II-S60A showing gypsum and large area; made with Sulfide coarse aggregate, w/c of 0.65, and tested with drying at 60°C and 2-hours soaking in bleach at 23°C twice a week

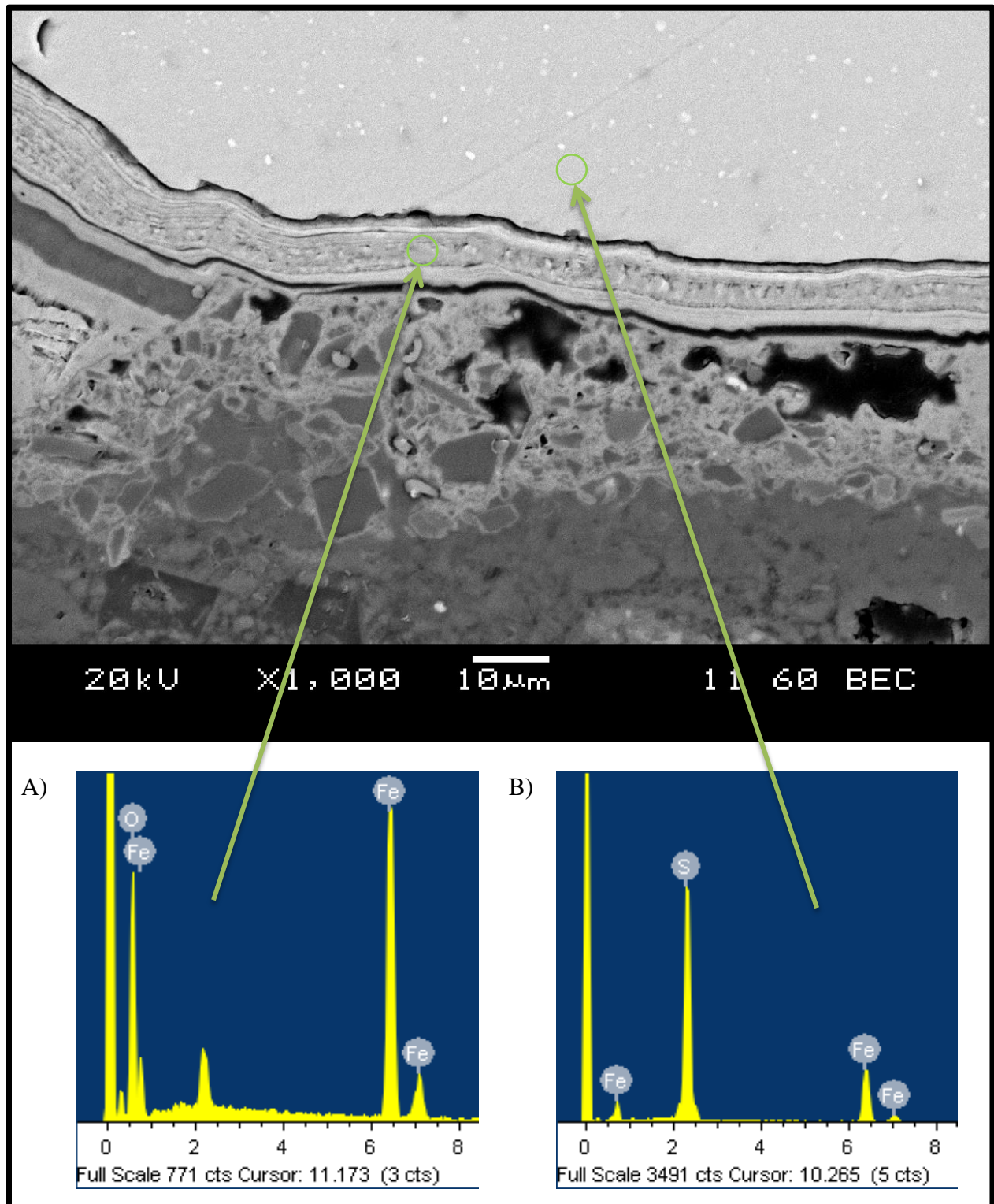


Figure 4.3.11: SEM image and EDS analysis for II-S60A showing oxidized pyrrhotite; made with Sulfide coarse aggregate, w/c of 0.65, and tested with drying at 60°C and 2-hours soaking in bleach at 23°C twice a week

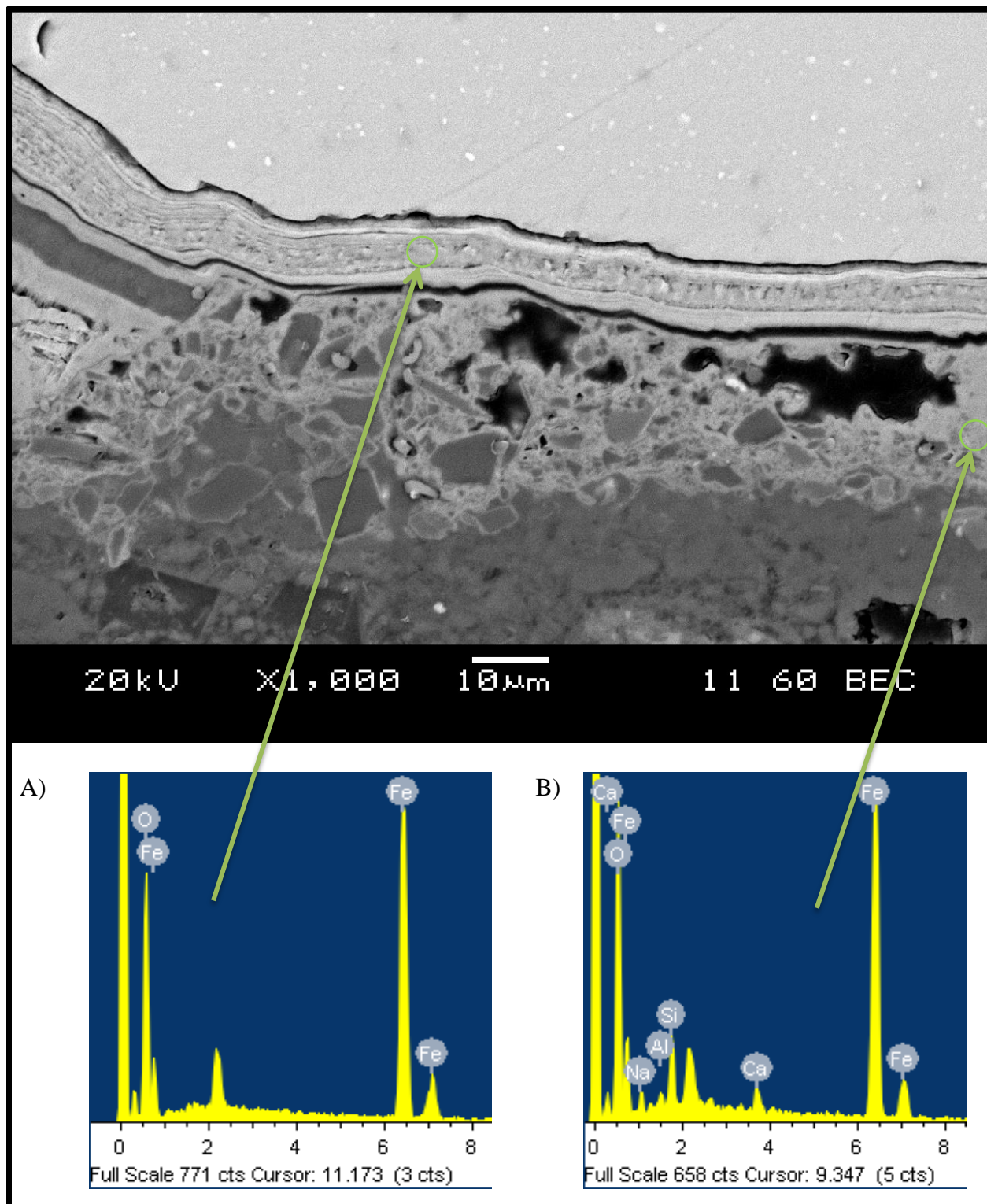


Figure 4.3.12: SEM image and EDS analysis for II-S60A showing oxidized pyrrhotite; made with Sulfide coarse aggregate, w/c of 0.65, and tested with drying at 60°C and 2-hours soaking in bleach at 23°C twice a week

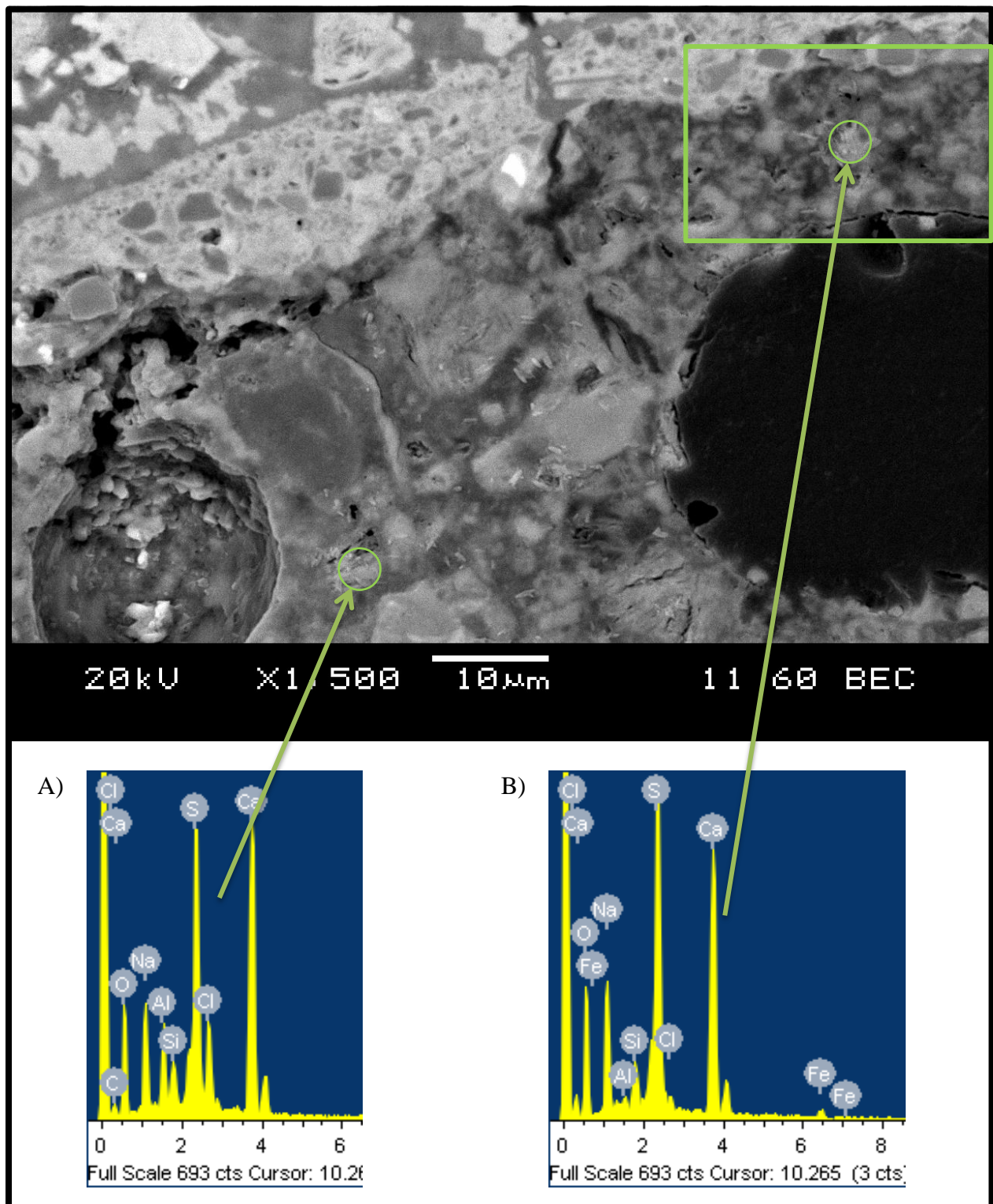


Figure 4.3.13: SEM image and EDS analysis for II-S60A showing gypsum; made with Sulfide coarse aggregate, w/c of 0.65, and tested with drying at 60°C and 2-hours soaking in bleach at 23°C twice a week

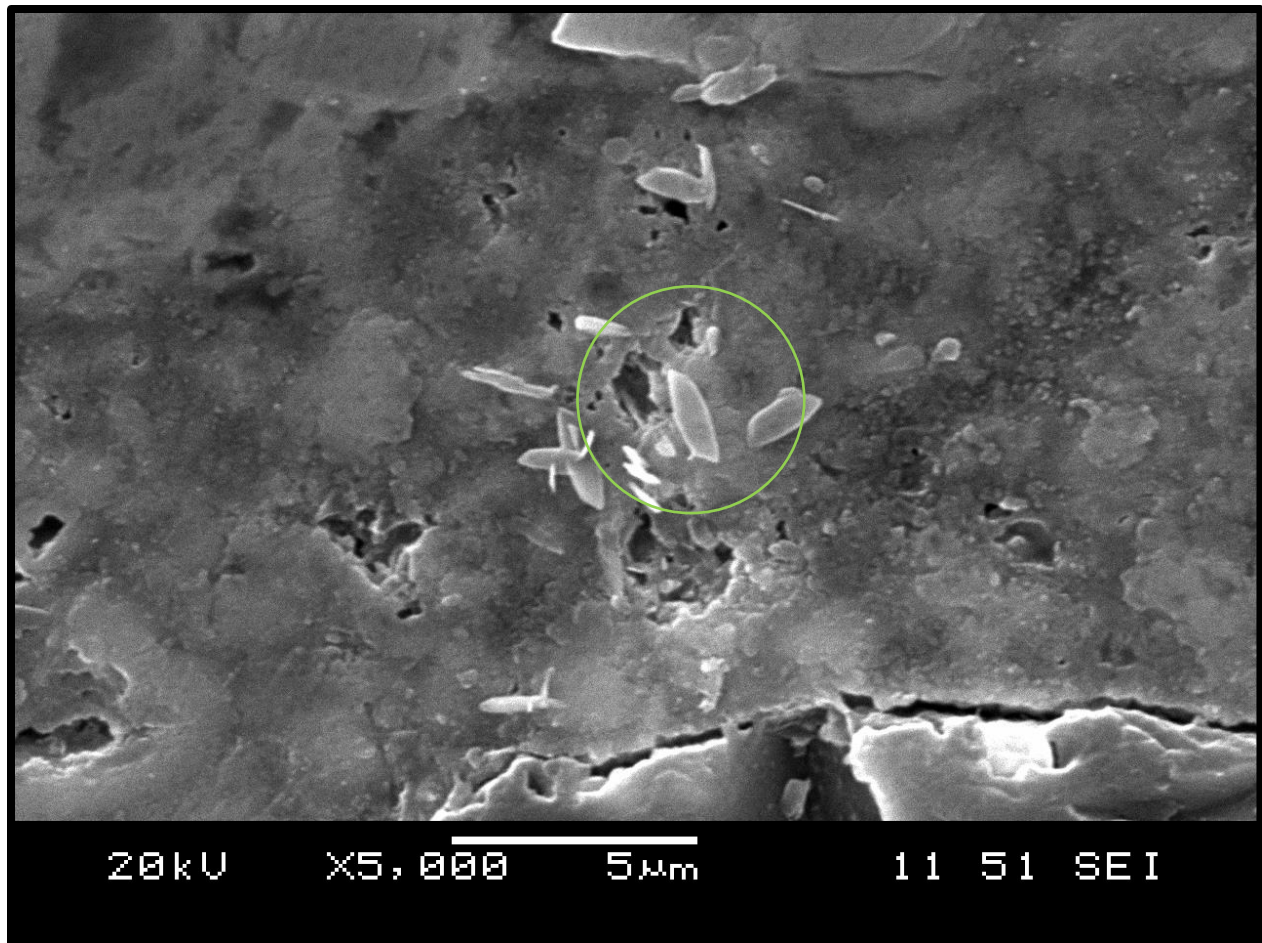


Figure 4.3.14: Secondary electron image of gypsum crystals in cement paste in II-S60A; made with Sulfide coarse aggregate, w/c of 0.65, and tested with drying at 60°C and 2-hours soaking in bleach at 23°C twice a week

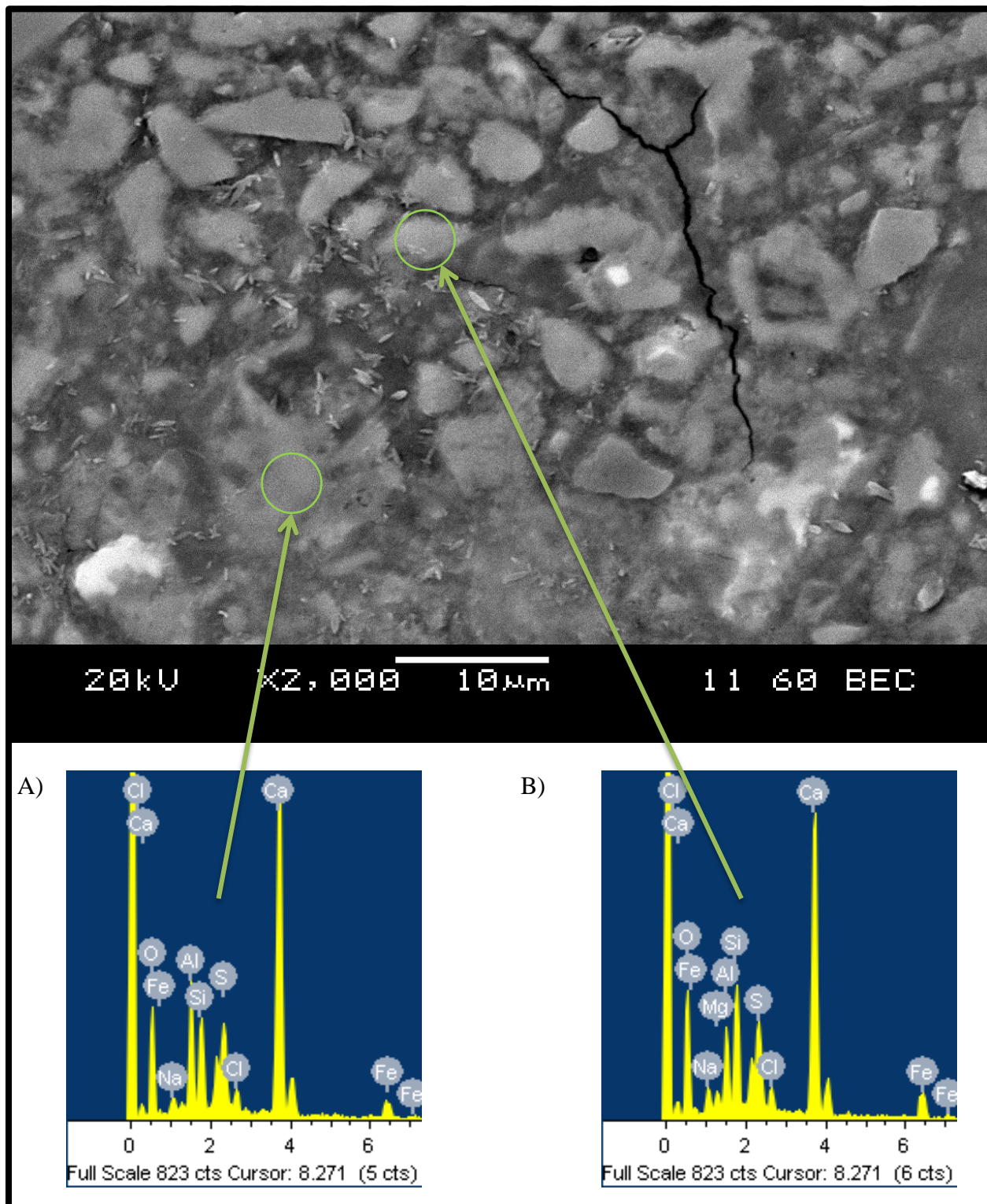


Figure 4.3.15: SEM image and EDS analysis for II-S60A showing presence of sulfur; made with Sulfide coarse aggregate, w/c of 0.65, and tested with drying at 60°C and 2-hours soaking in bleach at 23°C twice a week

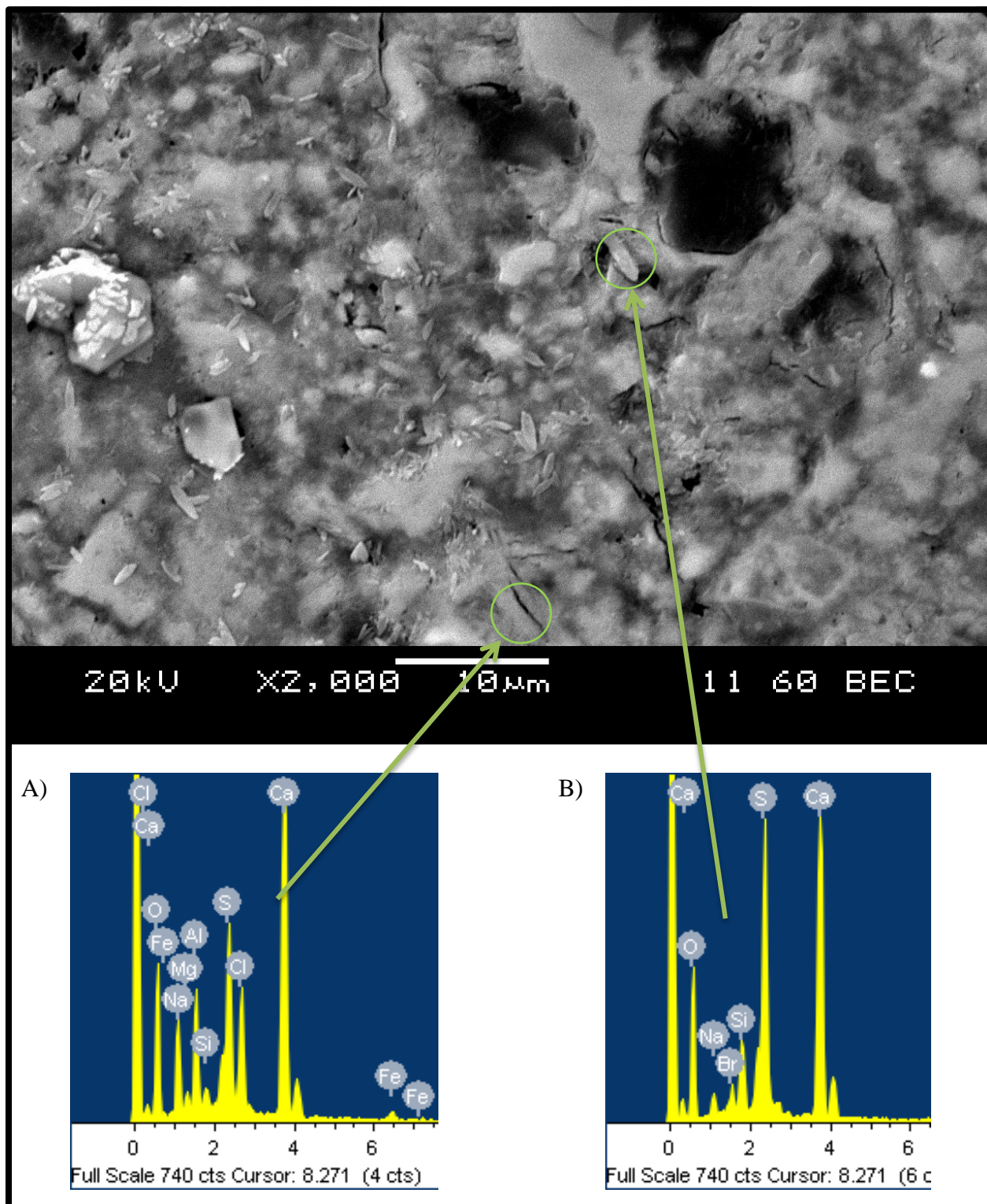


Figure 4.3.16: SEM image and EDS analysis for II-S60A showing gypsum and Friedel's salt; made with Sulfide coarse aggregate, w/c of 0.65, and tested with drying at 60°C and 2-hours soaking in bleach at 23°C twice a week

A different area of the same sample is shown in Figure 4.3.17 through Figure 4.3.19. In Figure 4.3.17 and Figure 4.3.18 all analysis points have strong peaks of calcium, chlorine, and aluminium. In Figure 4.3.17, the same short discontinuous black lines are seen at the analysis locations, which were previously associated with ettringite. In Figure 4.3.18, a different style of crystals is seen to have formed in the ITZ around an aggregate particle. In the EDS analyses in Figure 4.3.19, the strong peaks of calcium aluminum and chlorine that are associated with Friedel's salt are seen. In both of these analyses there appears to be some sulfur also present that was not recognized. These features are suspected of being a mixture of ettringite and Friedel's salt, but since other elements are also present no conclusions can be drawn. Ettringite is known to react with chlorides, which results in the formation of Friedel's salt and gypsum (Zibara, 2001). During this reaction, the ettringite exchanges its sulfur for chlorine and becomes Friedel's salt. The sulfur goes on to react with the calcium hydroxide in the cement to form gypsum.

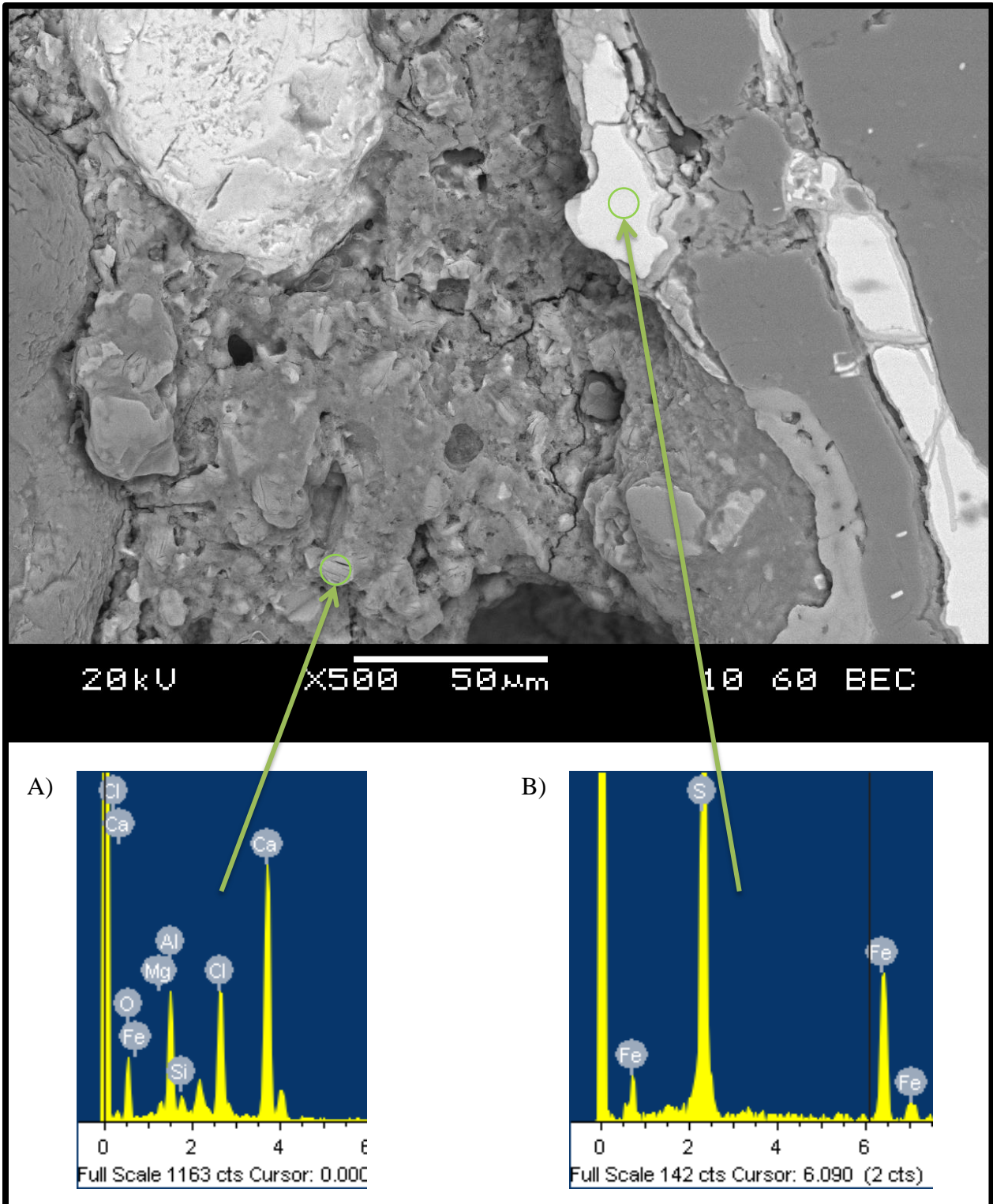


Figure 4.3.17: SEM image and EDS analysis for II-S60A showing Friedel's salt; made with Sulfide coarse aggregate, w/c of 0.65, and tested with drying at 60°C and 2-hours soaking in bleach at 23°C twice a week

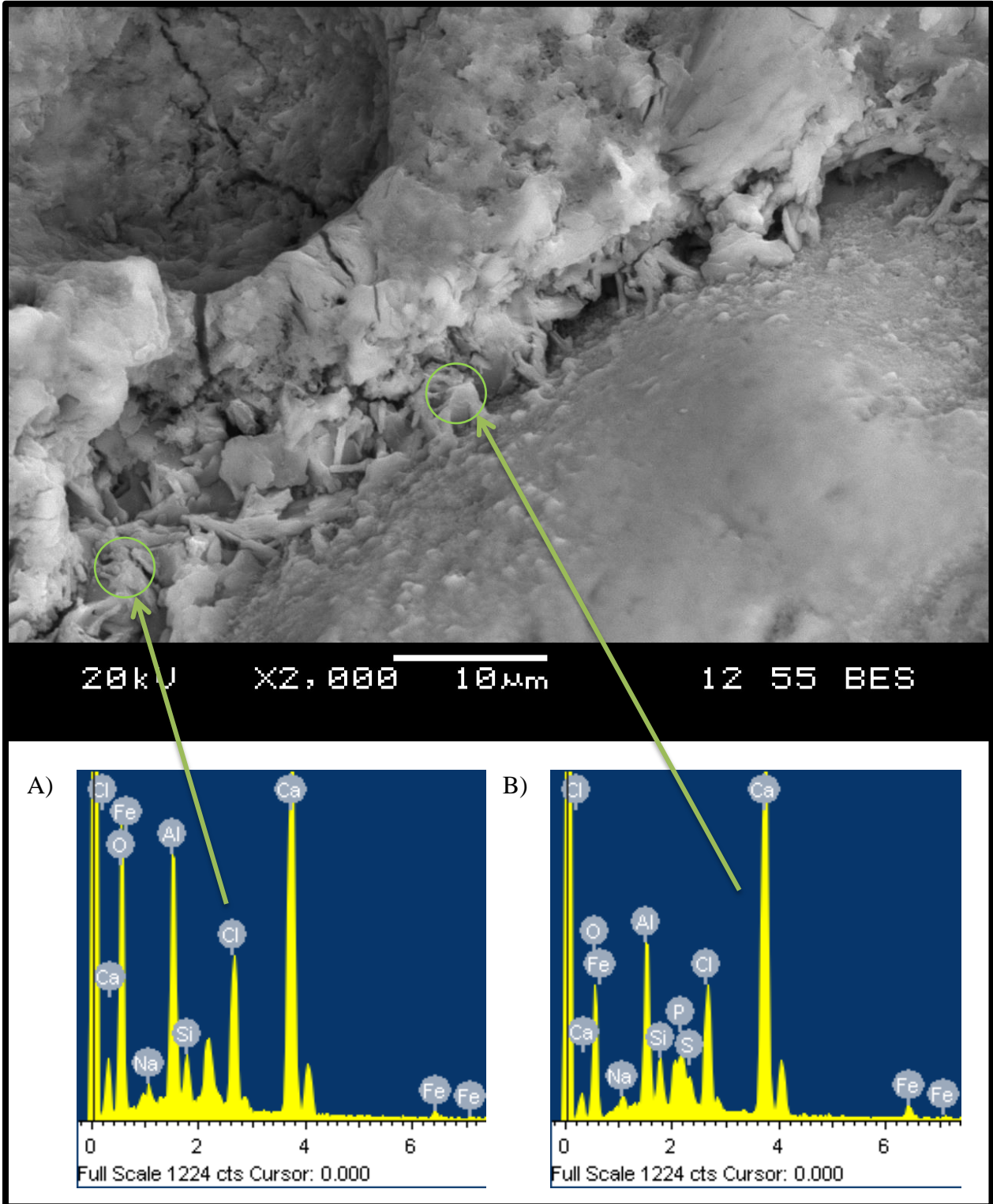


Figure 4.3.18 SEM image and EDS analysis for II-S60A showing Friedel's salt; made with Sulfide coarse aggregate, w/c of 0.65, and tested with drying at 60°C and 2-hours soaking in bleach at 23°C twice a week

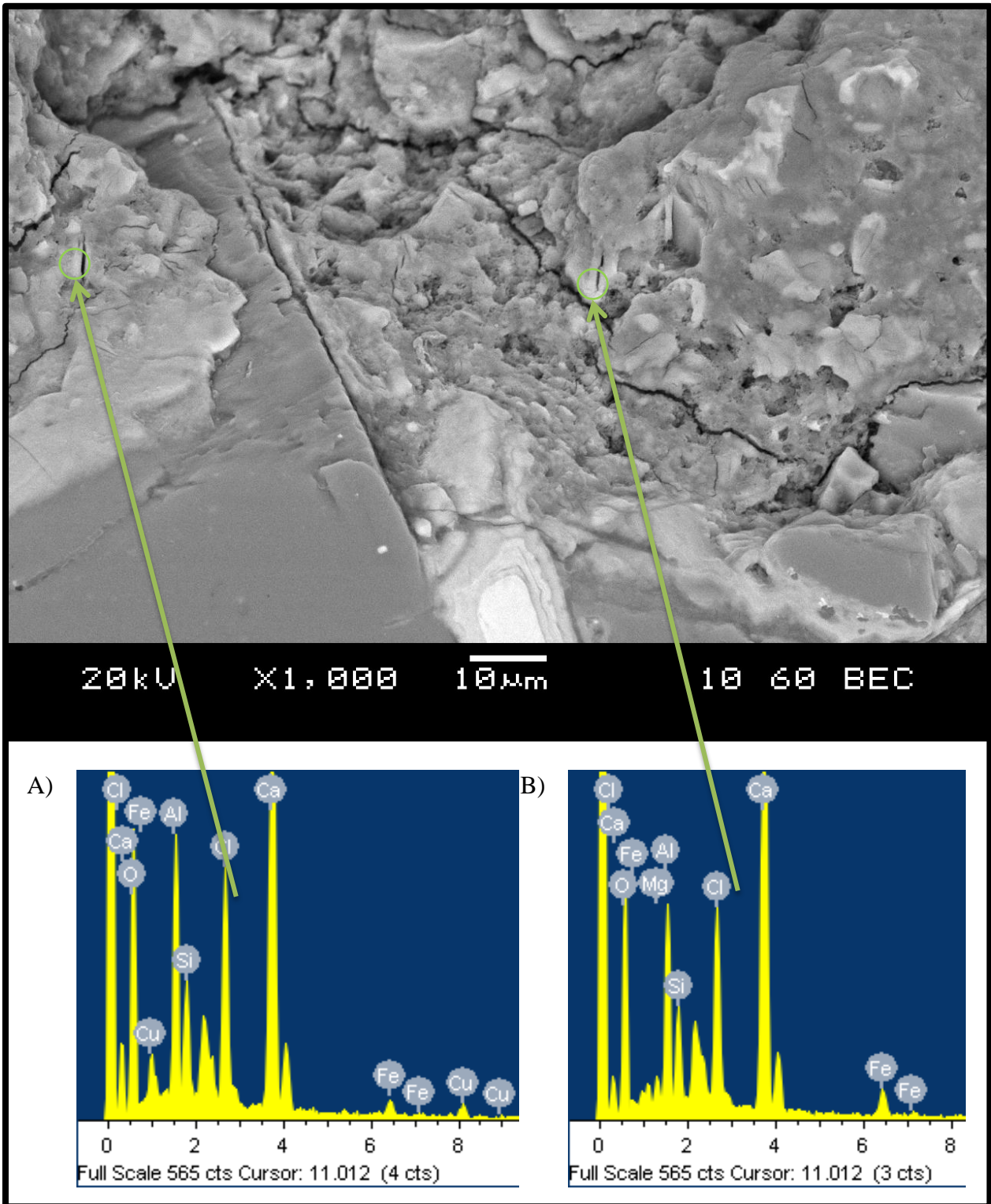


Figure 4.3.19: SEM image and EDS analysis for II-S60A showing Friedel's

II-S60B

This SEM sample was taken from a different specimen than II-S60A was, but both were from the same sample. II-S60B was tested for much longer than II-S60A, and showed more than twice the amount of expansion, presented in Table 4.3.1. At this age there was a very large amount of sodium chloride (NaCl) salt found throughout this sample, which is shown in Figure 4.3.20. Here the salts completely filled the cracks in the ITZ around a coarse aggregate, and many of the air voids were partially, or completely filled with NaCl salts as well. EDS analysis A) in Figure 4.3.20 confirms that the salt was pure sodium and chloride, NaCl salt is known to be a product of bleach decomposition. The active ingredient in bleach is sodium hypochlorite, which when left to evaporate will primarily breakdown into sodium chloride (NaCl) and sodium chlorate (NaClO) salts (Hove, 2011); since there was no oxygen present in the analyses it can be concluded that this is sodium chloride and not sodium chlorate. When salt crystals formed in a condensed fashion within the concrete matrix, or within an aggregate particle, they may have put pressure on the surrounding concrete, in a process known as salt weathering. NaCl salts are known to cause a certain amount of damage when they form inside concrete, if sufficient conditions are provided NaCl salts are capable of causing significant damage (Darwin et al., 2008). Therefore, these NaCl salts are suspected of causing the expansion of the concrete seen in Figure 4.3.3, as a result of the bleach evaporating. Analysis B) shows that iron was present in the coarse aggregate, at its surface, where the cracks were found. No sulfur was found in this area, so no definitive statements can be made towards iron sulfides. What can be noted here is that the samples taken at 31-weeks (II-S60A) showed hardly any salt crystals, but here at 59-weeks (II-S60B) a very large and important amount of salt was found. A very large crack was found packed full of NaCl salt, which is shown in Figure 4.3.21. This crack extended from the interior of the aggregate into the paste. There are 2 possibilities for how this feature came to be, one cannot be certain which took place. It is possible that the crack formed first on its own, and the salt migrated into the crack after and contributed to expansion. Or, it is also possible that the salt contributed to the formation of the crack, and caused the expansion. The nature of the crack would suggest that the NaCl salt extended the crack to the size observed, but no conclusions could be drawn. In Figure 4.3.22 the EDS signature that is associated with gypsum was found once again, it was located at the edge of the ITZ in a very large crack around a coarse aggregate particle. There were many elements present in the EDS analysis and no crystals were found, so one could not necessarily

conclude that this was gypsum. All that can be said is that there is an important amount of sulfur found in this analysis. Figure 4.3.23 shows a less magnified view of the area to confirm the presence of NaCl salts close by. Again in this sample, there are features that show the possibility of being a mixture of ettringite and Friedel's salt, which is shown in Figure 4.3.24. In the highlighted areas in this SEM image, the features that have been associated with ettringite from Phase I are seen. In EDS analysis A), both sulfur and chlorine present along with calcium and aluminium, while in EDS analysis B) very similar peaks are seen, except with sulfur being much lower. For all of the previously stated reasons, it is thought that the sulfoaluminates were able to react, although perhaps only partially, with the chlorides in the bleach and form Friedel's salt, as discussed earlier. Also in Figure 4.3.24, an iron deposit was found in a coarse aggregate particle, seen as the white area in the bottom middle of the image. Another area of the same sample that showed possible Friedel's salt is shown in Figure 4.3.25. The features highlighted by analysis B) here are very similar to what was seen in Figure 4.3.24 analysis A). The EDS peaks of the 2 are nearly identical, and thus, Friedel's salt is again suspected here. In EDS analysis A) of Figure 4.3.25, the peaks associated with gypsum are seen along with several other elements. Analysis C) shows all of the important elements present, but no conclusions can be drawn about the actual compound due to the relative amounts of all elements; this was likely a mixture of compounds. In Figure 4.3.26 a less magnified view of the same area is seen, the rectangle shows the area that was shown in Figure 4.3.25. The proximity to a coarse aggregate particle is seen, and large salt deposits were found in the air voids. Another interesting feature here is that the ITZ of the coarse aggregate was completely dissolved and filled with NaCl salts. Figure 4.3.27 shows an aggregate particle that was severely cracked, this particle is about 4mm long, and therefore cannot be definitely identified as a coarse or fine aggregate particle; although it is most likely a fine aggregate particle. In the same image other large cracks are seen extending across the image and more air voids were found packed full of NaCl salt.

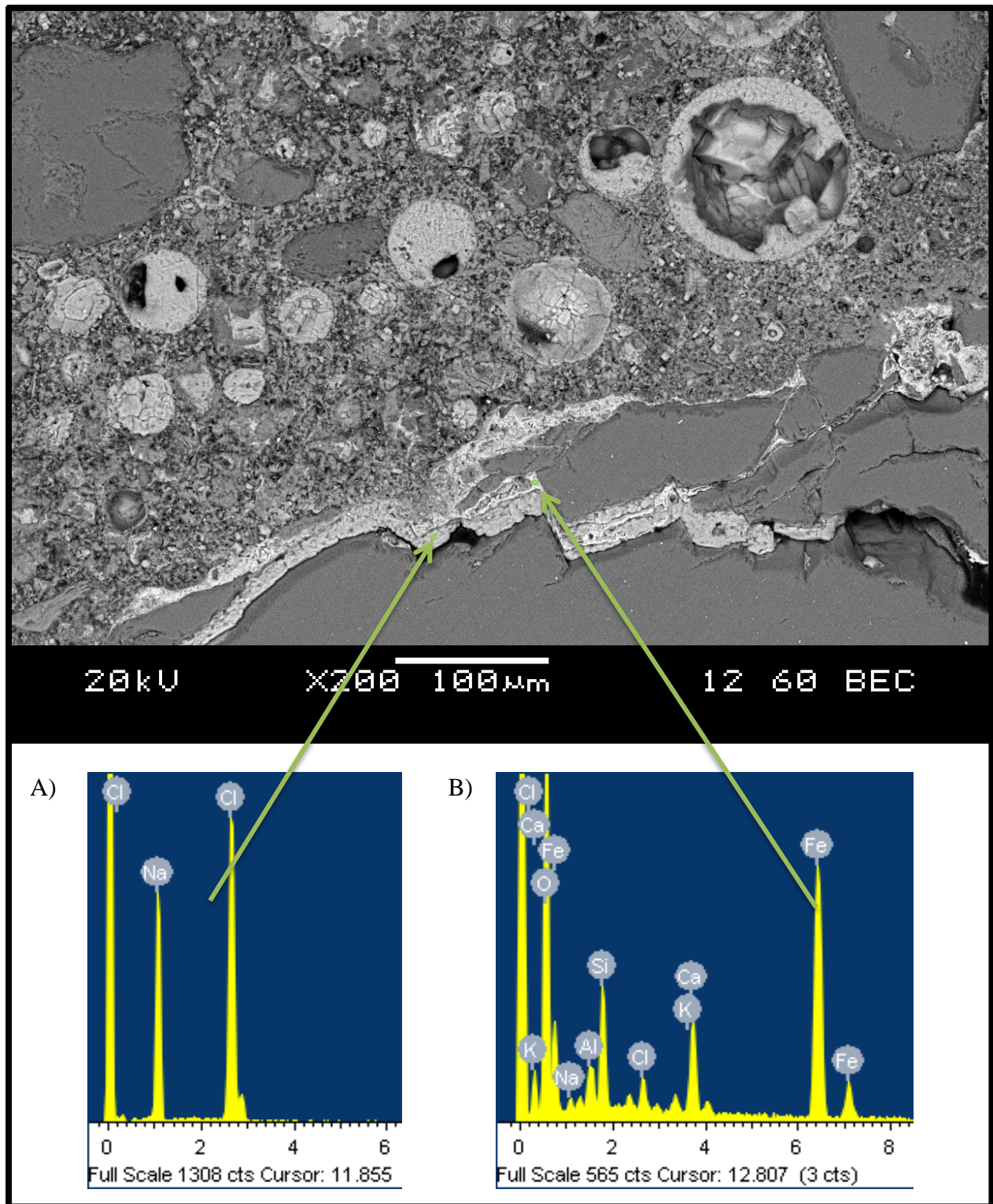


Figure 4.3.20: SEM image and EDS analysis for II-S60B showing NaCl salts in crack; made with Sulfide coarse aggregate, w/c of 0.65, and tested with drying at 60°C and 2-hours soaking in bleach at 23°C twice a week

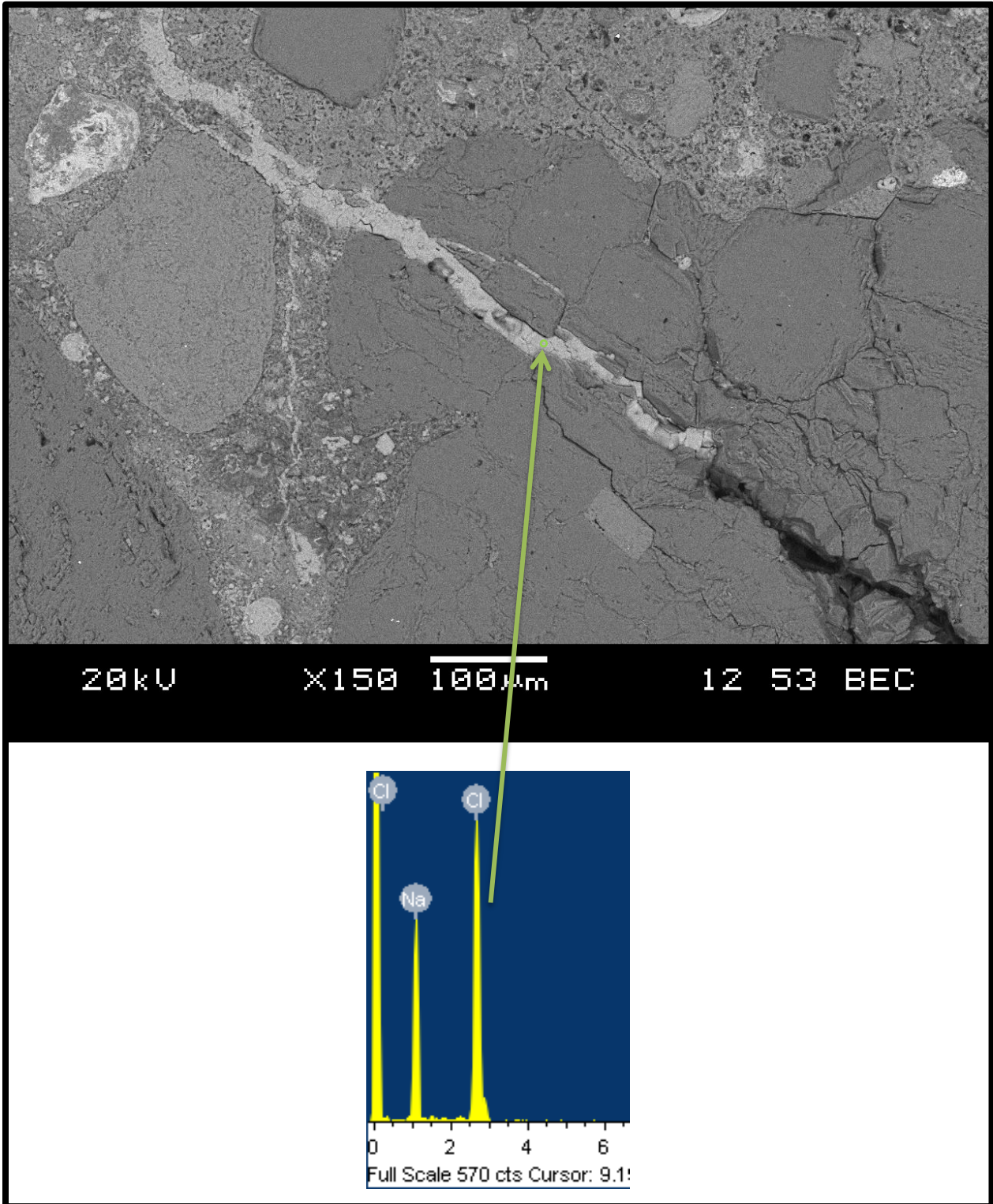


Figure 4.3.21: SEM image and EDS analysis for II-S60B showing NaCl salts in crack; made with Sulfide coarse aggregate, w/c of 0.65, and tested with drying at 60°C and 2-hours soaking in bleach at 23°C twice a week

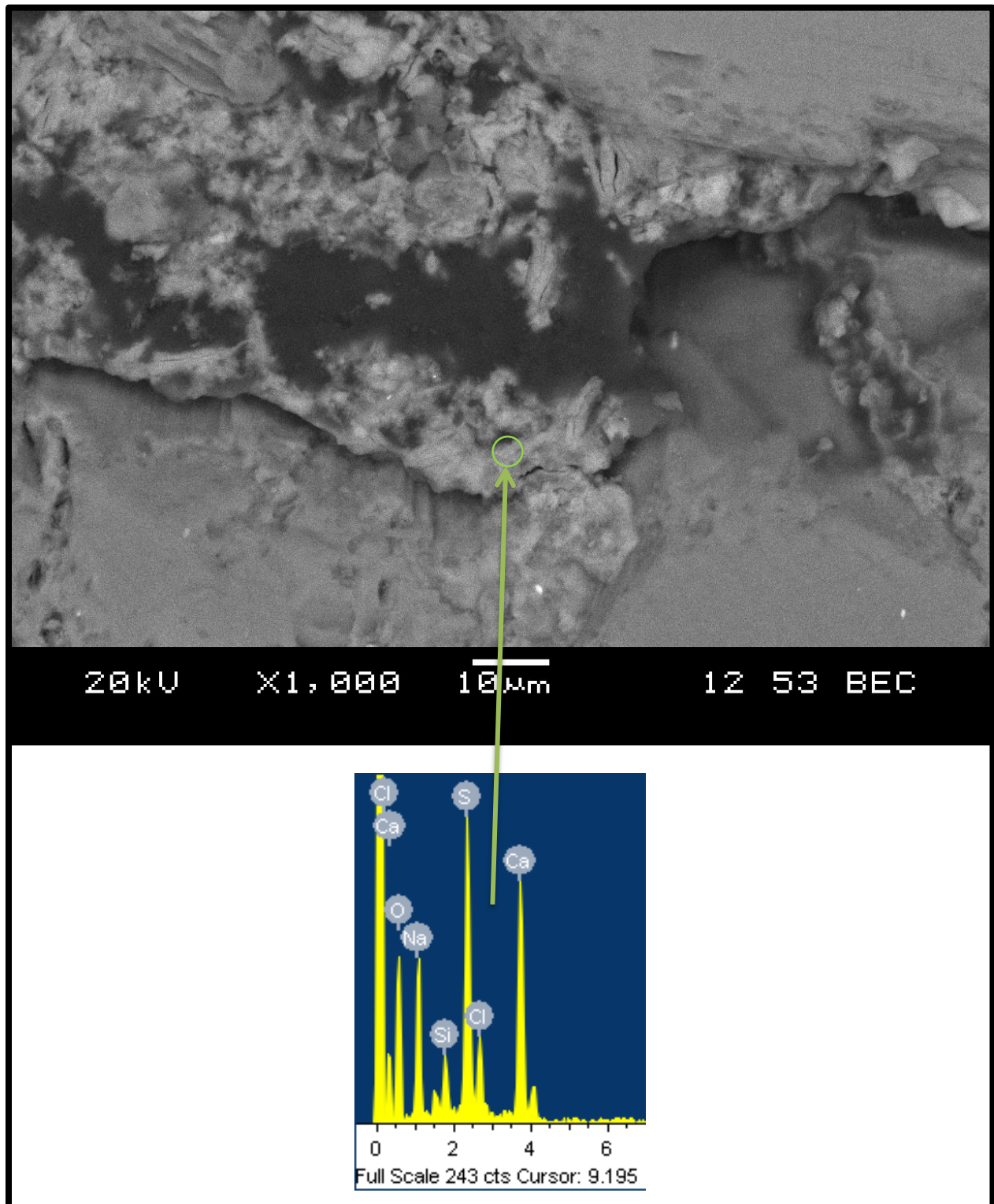


Figure 4.3.22: SEM image and EDS analysis for II-S60B showing gypsum in ITZ; made with Sulfide coarse aggregate, w/c of 0.65, and tested with drying at 60°C and 2-hours soaking in bleach at 23°C twice a week

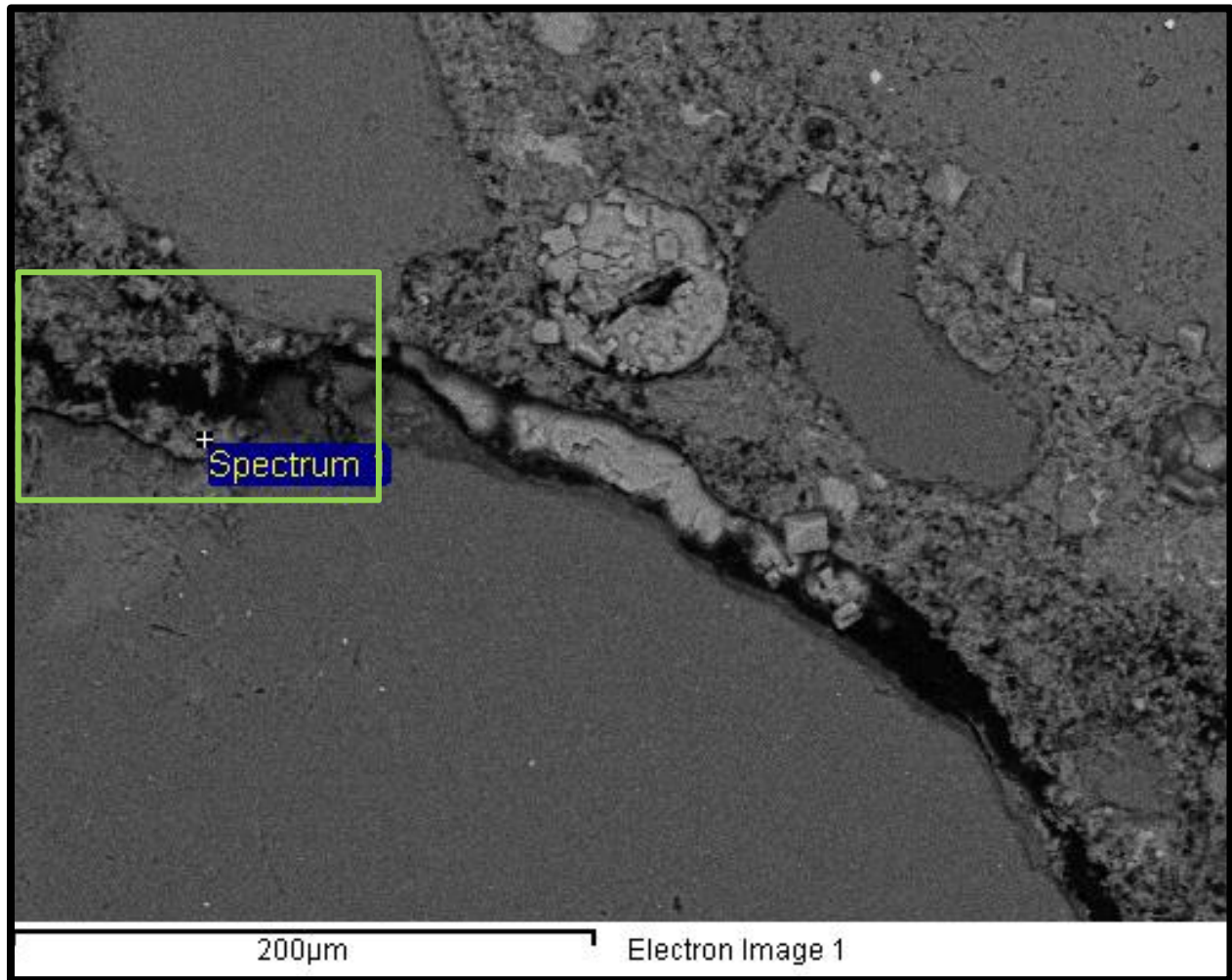


Figure 4.3.23: SEM image for II-S60B showing NaCl salts in crack; made with Sulfide coarse aggregate, w/c of 0.65, and tested with drying at 60°C and 2-hours soaking in bleach at 23°C twice a week

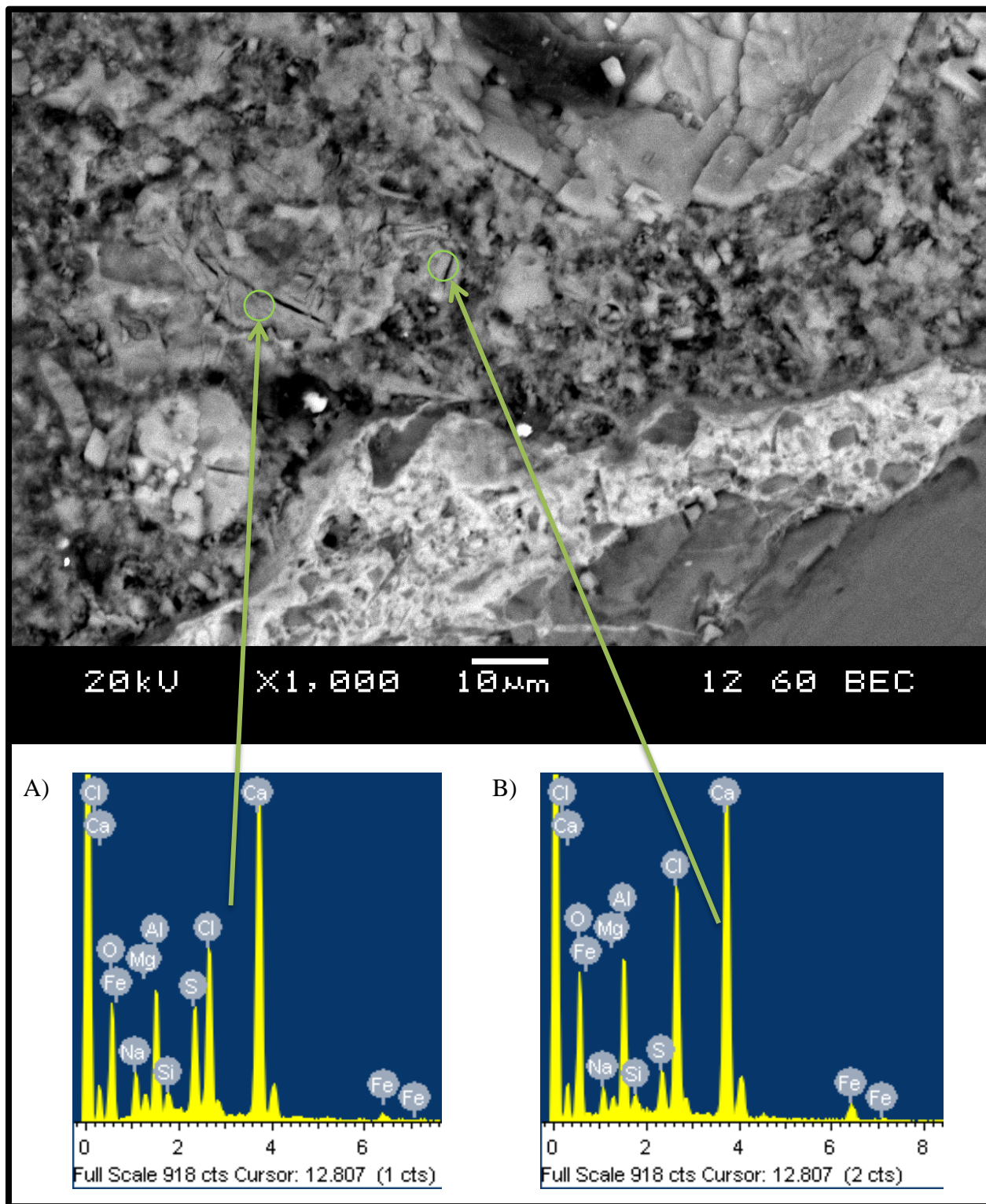


Figure 4.3.24: SEM image and EDS analysis for II-S60B showing Friedel's salt; made with Sulfide coarse aggregate, w/c of 0.65, and tested with drying at 60°C and 2-hours soaking in bleach at 23°C twice a week

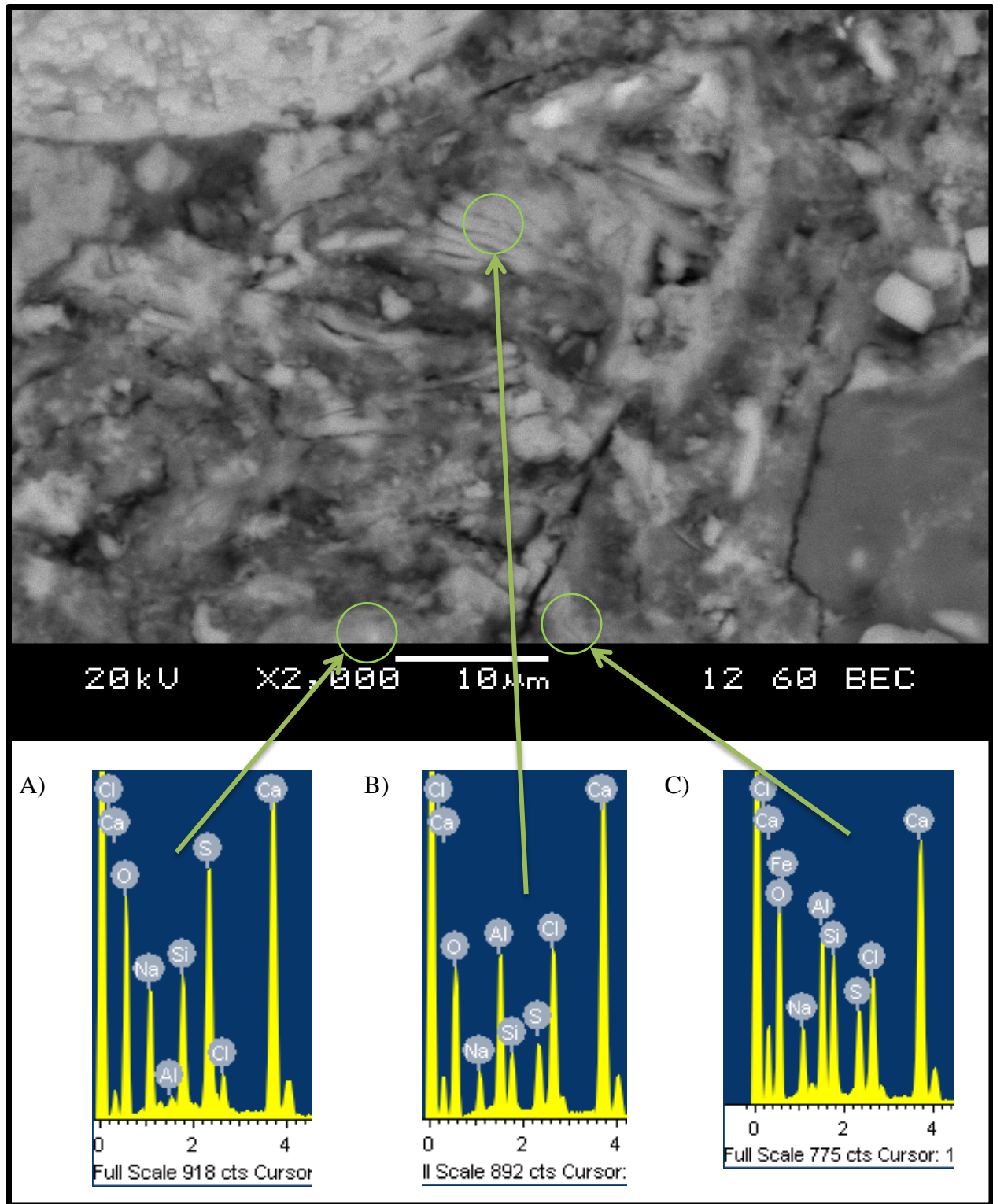


Figure 4.3.25: SEM image and EDS analysis for II-S60B showing a mixture of important elements and possible crystal formations; made with Sulfide coarse aggregate, w/c of 0.65, and tested with drying at 60°C and 2-hours soaking in bleach at 23°C twice a week

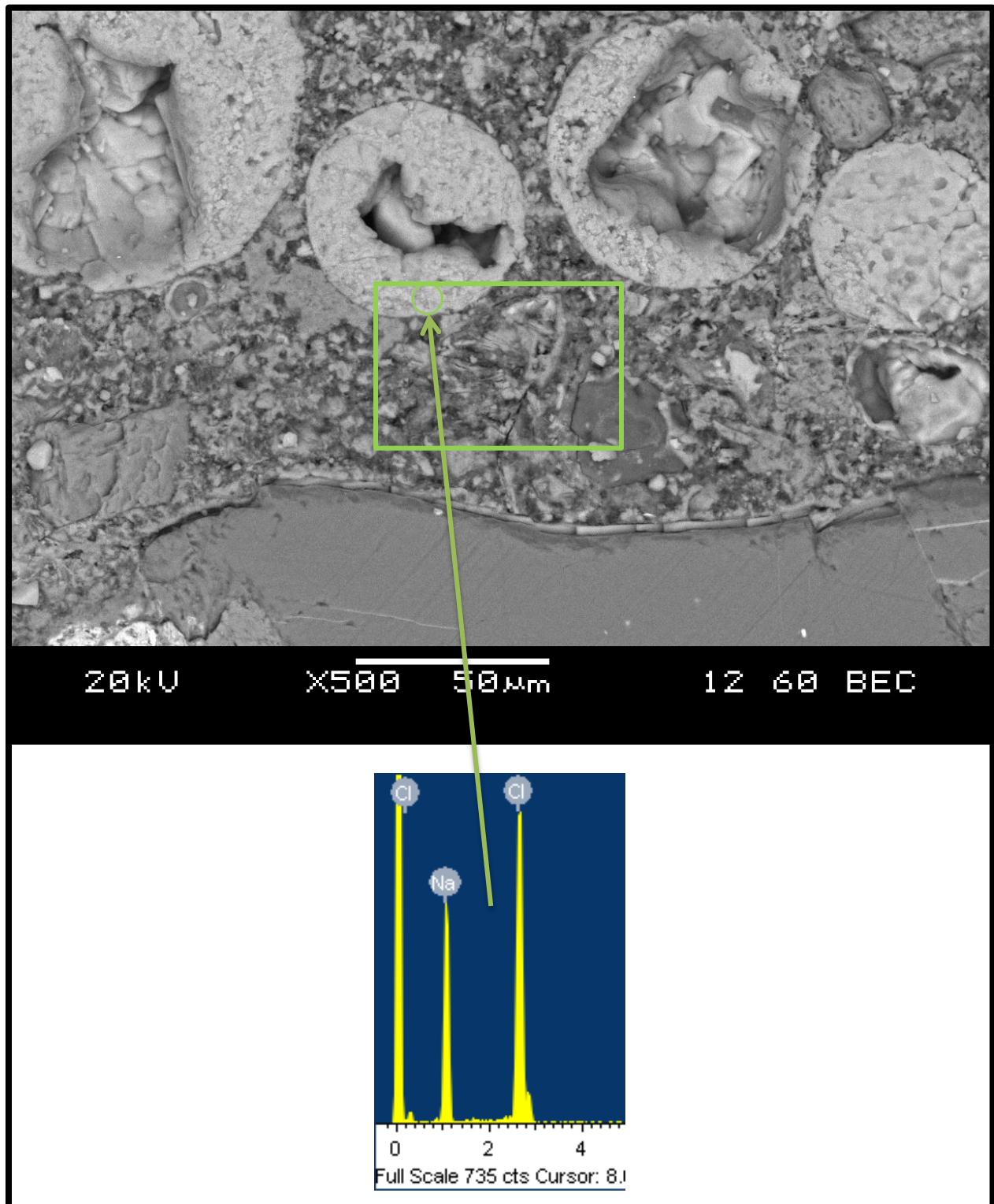


Figure 4.3.26: SEM image and EDS analysis for II-S60B showing NaCl salt; made with Sulfide coarse aggregate, w/c of 0.65, and tested with drying at 60°C and 2-hours soaking in bleach at 23°C twice a week

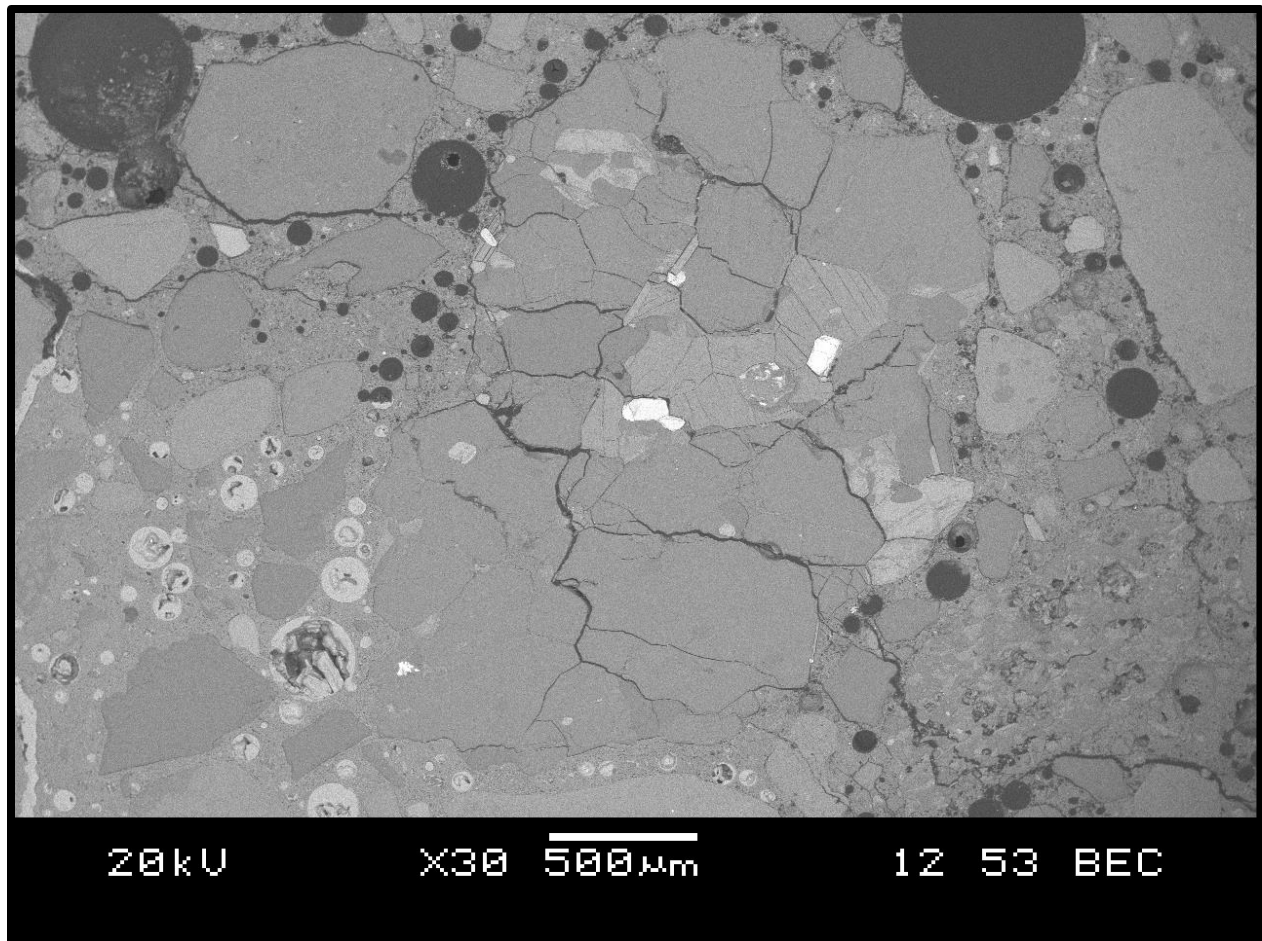


Figure 4.3.27: SEM image of II-S60B showing severe cracking in an aggregate particle; made with Sulfide coarse aggregate, w/c of 0.65, and tested with drying at 60°C and 2-hours soaking in bleach at 23°C twice a week

II-D60A

Since the Dolostone-0.65 sample followed a very similar expansion trend as the Sulfide-0.65 sample, scanning electron microscopy was again employed to investigate the reason for the Dolostone samples to expand. This sample was taken at a testing age of 22-weeks, and had an expansion of 0.078% at that time. In Figure 4.3.28 a low magnification SEM image of a Dolostone coarse aggregate particle is seen. What is immediately apparent is the relatively very high porosity of the aggregate compared to the Sulfide aggregate. The rectangle shown in Figure 4.3.28 was magnified to in Figure 4.3.29, where in EDS analysis A) indicates pure NaCl salts filling the crack. Analysis B) confirms the composition of the Dolostone aggregate. Figure 4.3.30 shows a cubic NaCl salt crystal that formed in an air void. Once again, when crystals are free to grow in an open space they will do so in their natural form, because they encounter no outside stresses. Friedel's salts are also found here in Figure 4.3.31, neither analysis shows any sulfur so one can only say that Friedel's salt was produced here. This may have occurred directly from the bleach reacting with monosulfate or ettringite that formed from the components of the cement. While Friedel's salt was found here, it was much less abundant than what was observed in the Sulfide samples discussed previously. The gold present in these analyses was from a gold coating used to provide a conductive thin layer at the sample, and can be ignored. A low magnification SEM image of the mortar of this sample is shown in Figure 4.3.32, where severe cracking of the cement matrix and some of the aggregate particles was experienced. The black halos are seen around some of the aggregates here again, as before. Some salt can be observed in the cracks and voids, but cannot be associated with the cause of the cracks, due to their relative sizes. The image in Figure 4.3.32 shows signs of severe deterioration, with a very little amount of salt present, suggesting that the salt is not the cause of the deterioration seen here. Instead, the wet/dry cycles are suspected of causing this cracking, but it is uncertain as to whether this cracking contributes to expansion. Therefore, it appears that the expansion of this sample was caused by the NaCl salt crystals formation inside the coarse aggregate particles, and in the cement paste, which put pressure on the concrete.

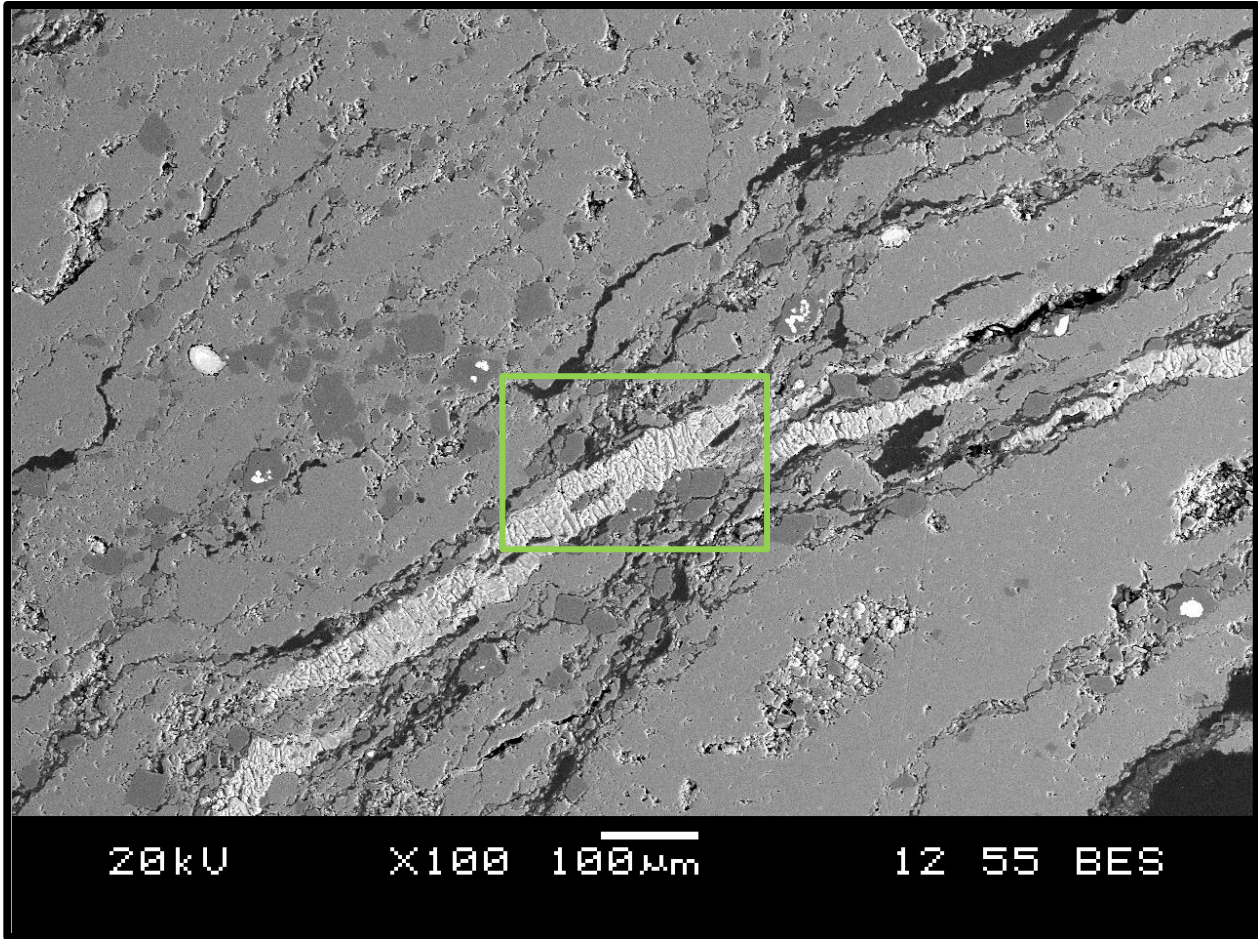


Figure 4.3.28 SEM image and EDS analysis for II-D60A showing NaCl salt in coarse aggregate; made with Dolostone coarse aggregate, w/c of 0.65, and tested with drying at 60°C and 2-hours soaking in bleach at 23°C twice a week

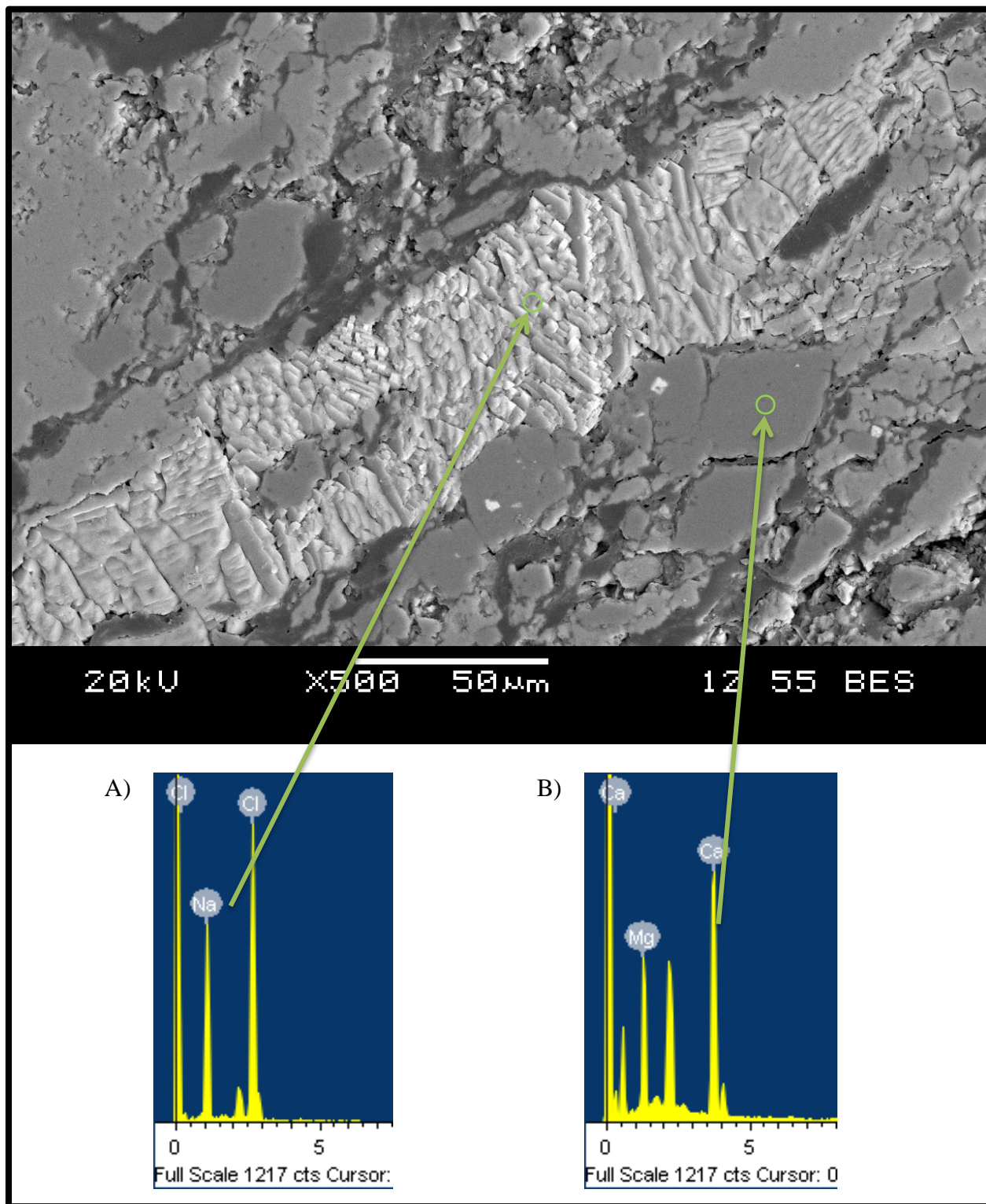


Figure 4.3.29: SEM image and EDS analysis for II-D60A showing NaCl salt in coarse aggregate; made with Dolostone coarse aggregate, w/c of 0.65, and tested with drying at 60°C and 2-hours soaking in bleach at 23°C twice a week

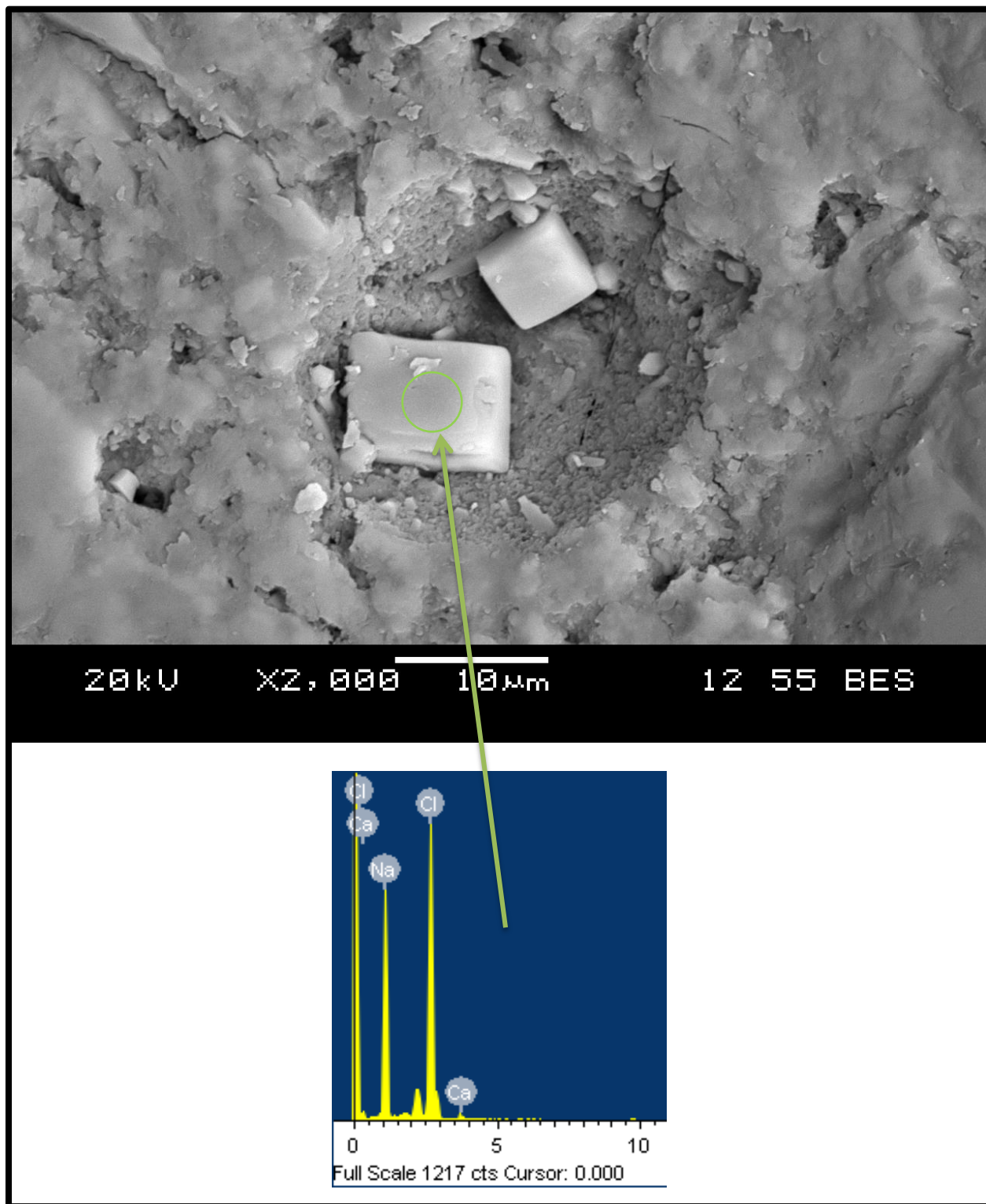


Figure 4.3.30: SEM image and EDS analysis for II-D60A showing cubic NaCl salt crystal in air void; made with Dolostone coarse aggregate, w/c of 0.65, and tested with drying at 60°C and 2-hours soaking in bleach at 23°C twice a week

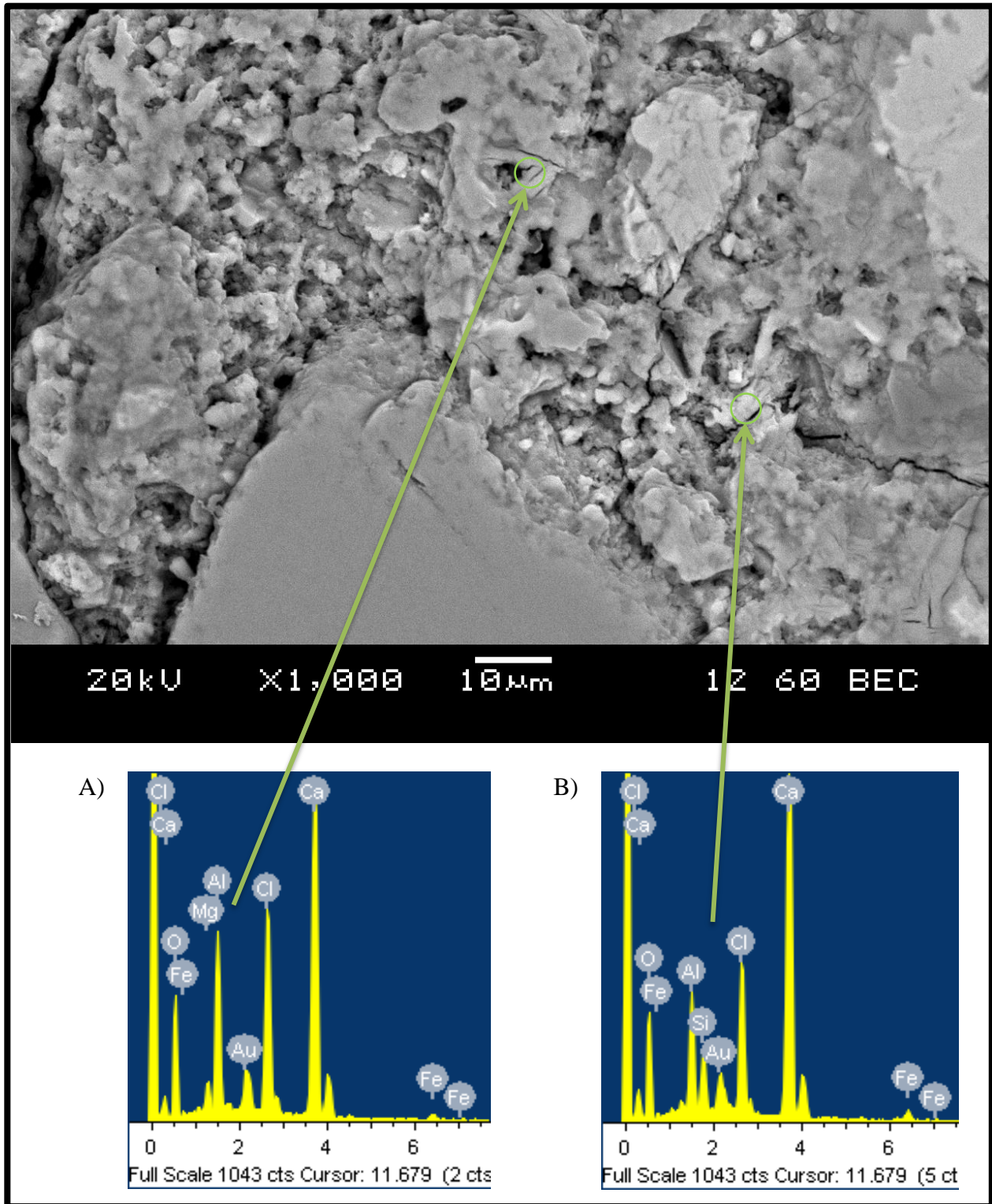


Figure 4.3.31: SEM image and EDS analysis for II-D60A showing Friedel's salt; made with Dolostone coarse aggregate, w/c of 0.65, and tested with drying at 60°C and 2-hours soaking in bleach at 23°C twice a week

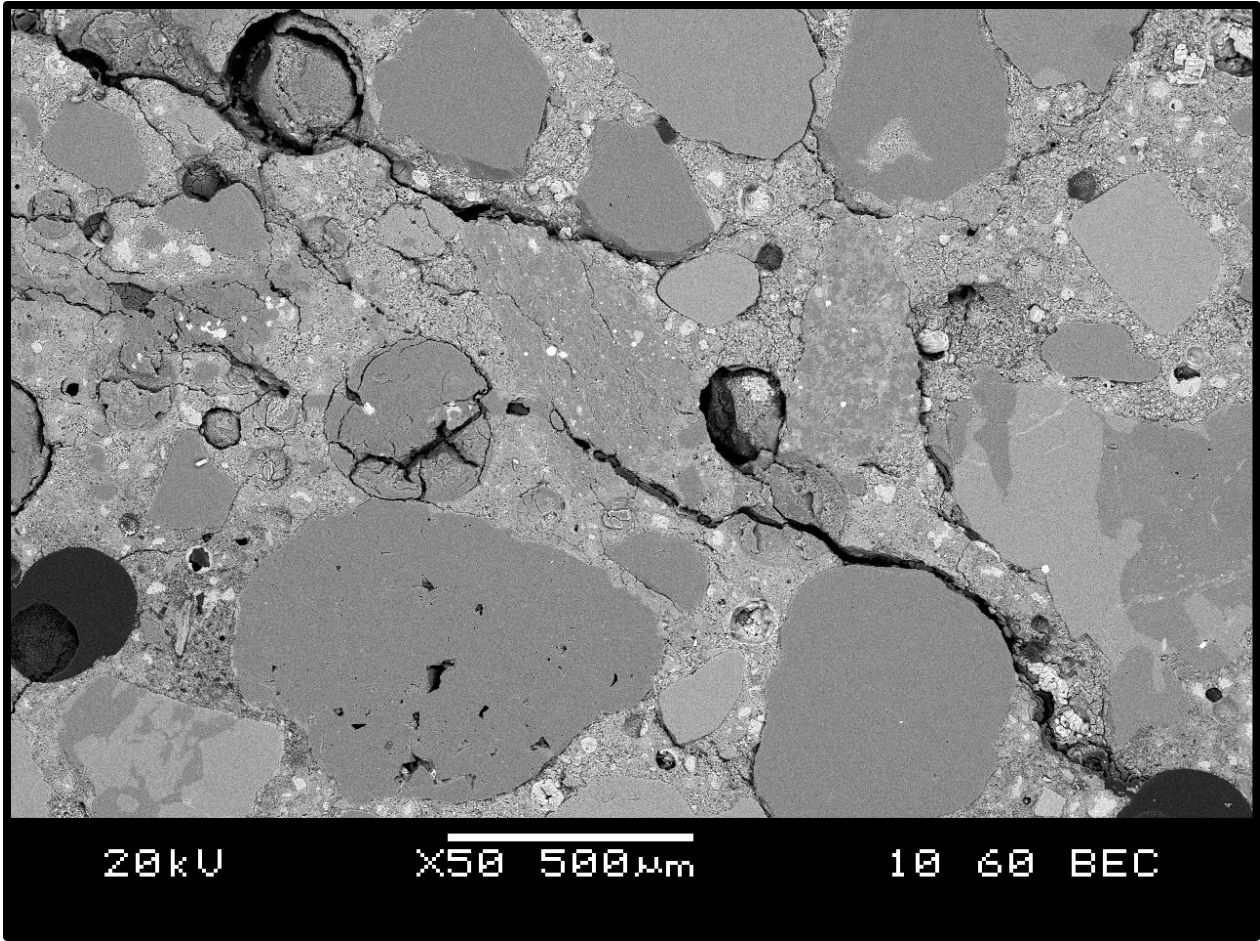


Figure 4.3.32: SEM image of II-D60A showing severe cracking; made with Dolostone coarse aggregate, w/c of 0.65, and tested with drying at 60°C and 2-hours soaking in bleach at 23°C twice a week

II-D60B

Another Dolostone sample was attained for SEM examination at a testing age of 26-weeks, only 4-weeks (8-cycles) after the previous sample (II-D60A) was taken. Some very similar features can be found here as before, although the degree to which the NaCl salt has infiltrated the concrete was much more here than in II-D60A. In Figure 4.3.33 another crack filled with NaCl salt was observed, which extends for a large distance across the sample; seen in Figure 4.3.34. A very large amount of NaCl salts was found in most of the voids in this sample. In Figure 4.3.35 salts crystals are seen to have filled a crack in the ITZ of a fine aggregate particle, this crack also continues for a large distance across the sample. It seems apparent that the NaCl salts were responsible for extending the cracks to the size seen here. It should be noted that this sample was re-examined to look specifically for ettringite, gypsum, and Friedel's salts, but none were found.

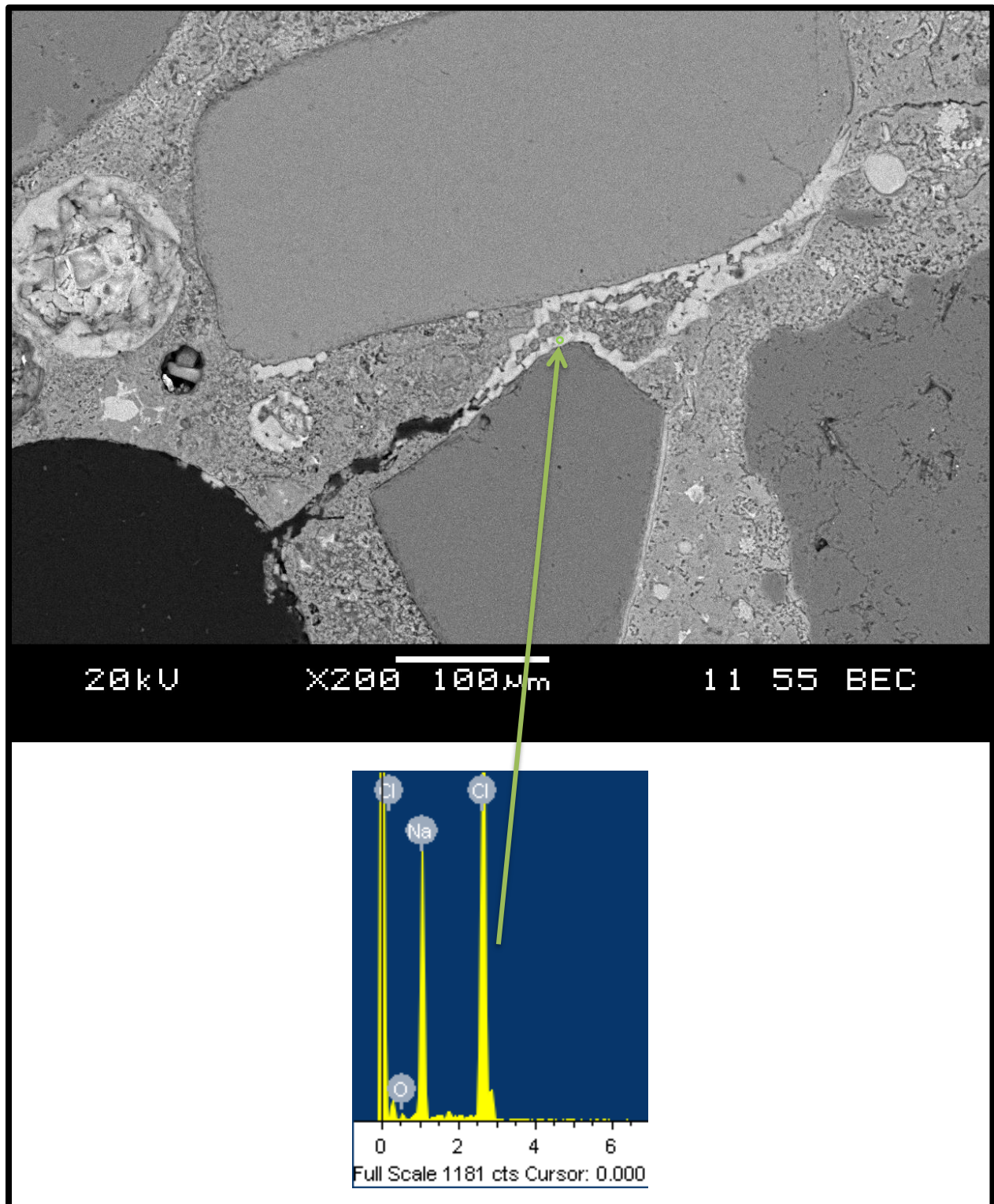


Figure 4.3.33: SEM image and EDS for II-D60B showing NaCl salt; made with Dolostone coarse aggregate, w/c of 0.65, and tested with drying at 60°C and 2-hours soaking in bleach at 23°C twice a week

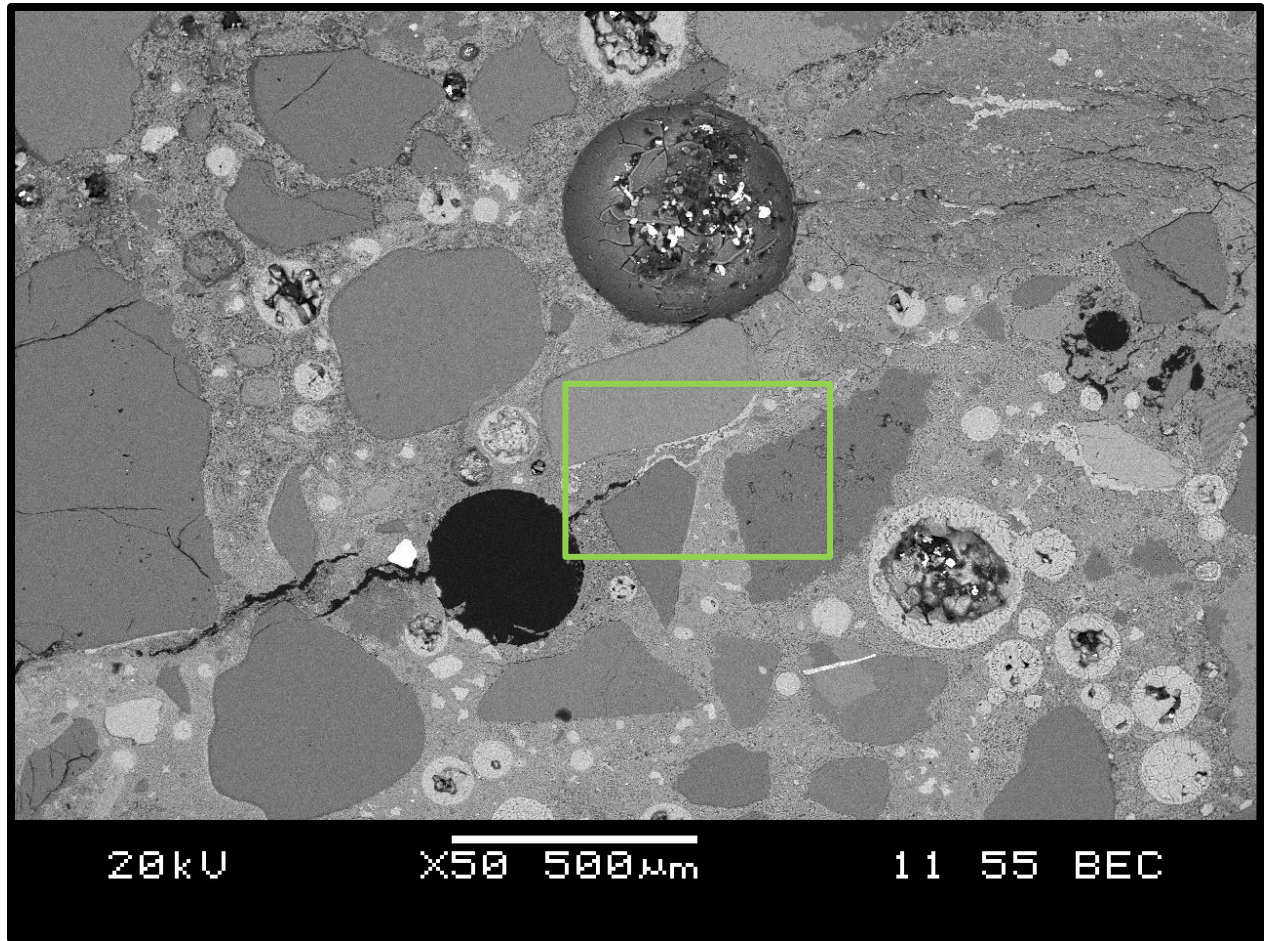


Figure 4.3.34: SEM image of II-D60B showing large cracks filled with NaCl salt; made with Dolostone coarse aggregate, w/c of 0.65, and tested with drying at 60°C and 2-hours soaking in bleach at 23°C twice a week

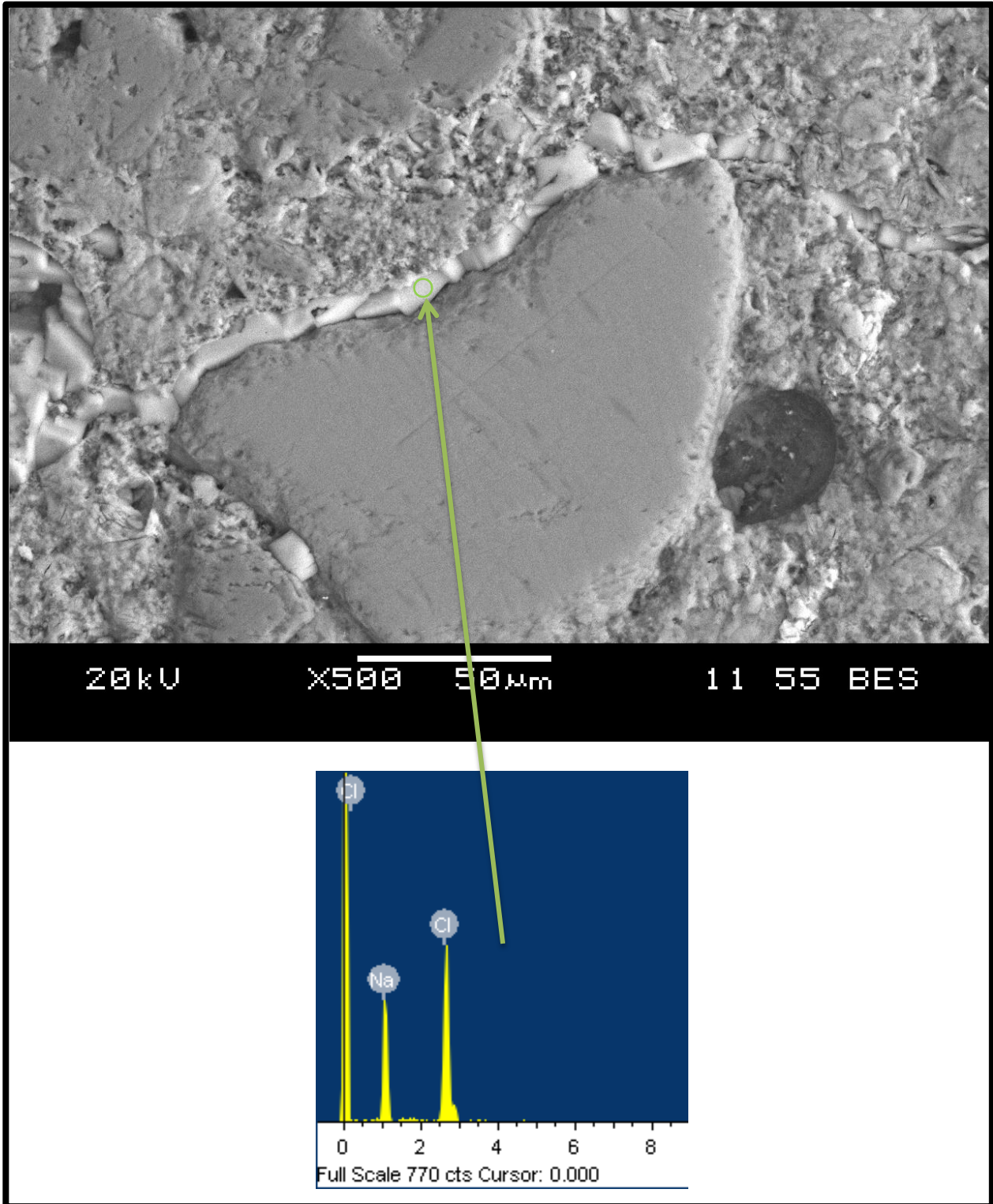


Figure 4.3.35: SEM image of II-D60B showing large crack in ITZ filled with NaCl salt; made with Dolostone coarse aggregate, w/c of 0.65, and tested with drying at 60°C and 2-hours soaking in bleach at 23°C twice a week

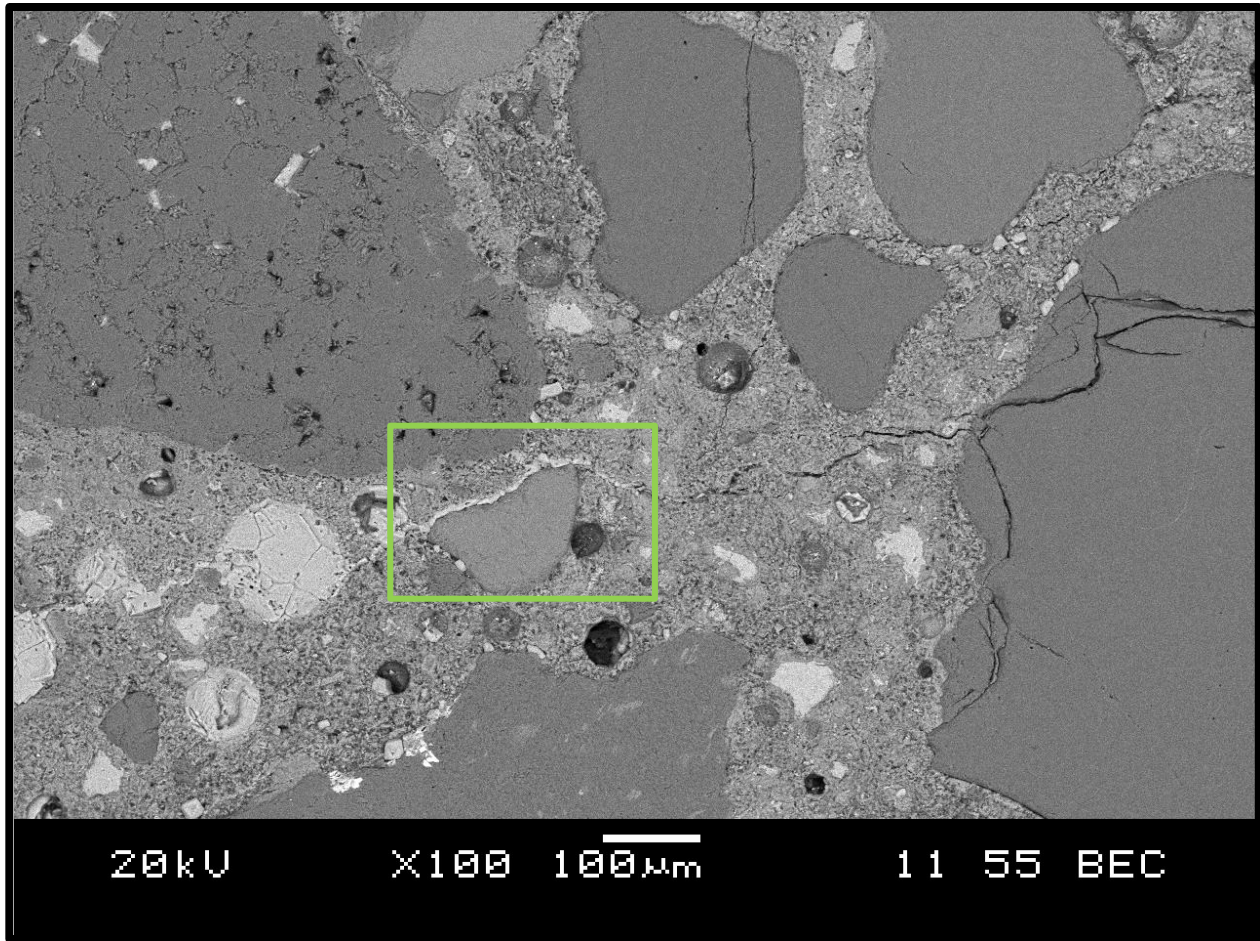


Figure 4.3.36: SEM image of II-D60B showing large cracks filled with NaCl salt; made with Dolostone coarse aggregate, w/c of 0.65, and tested with drying at 60°C and 2-hours soaking in bleach at 23°C twice a week

Comparison

The 31-week old Sulfide SEM sample (II-S60A) did not show any significant sign of NaCl salt, while the Dolostone samples showed a large amount of NaCl salt at both ages (22 and 26-weeks). It is possible that the small sample size required by the SEM may have caused the sample to be taken from an area that contained no salt crystals in the II-S60A sample. It is also possible that the sulfuric acid produced from iron sulfide oxidation reacted with the bleach, and produced sodium sulfate solution, which prevented the formation of NaCl salts for a period of time. The sodium sulfate would then be expected to continue to react with calcium hydroxide in the cement to form gypsum. Thus, the oxidation reaction may have prevented the formation of the NaCl salts, until the sulfuric acid become either depleted or overcome and the NaCl, and salt

formation took over. Sulfoaluminates are known have the capability to react with chlorides; Friedel's salt is formed where chlorine replaces sulfur. This is known to happen only at high concentrations of NaCl (>2M) (Zibara, 2001), which likely occurred during the super-saturation process caused by the bleach evaporation. Since the samples tested at 40°C with bleach did not expand, it seems that the micro-cracking provided by the more intense wet/dry cycles of the 60°C testing may have contributed to the expansion. The Dolostone aggregate had a high porosity and appeared relatively weak, this would have provided easier penetration of the bleach into the sample, and made the Dolostone aggregates more susceptible to salt weathering. Wet/dry cycles would have also been expected to cause more damage with the Dolostone samples for the same reason. With the Sulfide sample, the combination of heating to 60°C and bleach exposure appeared to cause the occurrence of the sulfate attack reaction of interest. This reaction appeared to proceed as expected in the early stages of testing, but then seemed to become neutralized, or affected by the bleach. Cracking caused by the oxidation reaction may have provided an area for the formation of the NaCl salts, which took over and controlled expansion by extending the cracks to the size seen here. Bleach is known to decompose upon heating above 40°C (ERCO, 2012), so it cannot be determined if initial cracking is necessary for the NaCl salts to form.

4.3.2.2 *Lime Soaking*

There were several samples tested that experienced the same cycles as in the previous sections, but with soaking in lime solution instead of bleach, the results of which are shown in Figure 4.3.37. There was no expansion in any of the samples; they all remained less than 0.03% through 26-weeks of testing. This amount of expansion could be expected from the repeated wet/dry cycles to 60°C. To aid in a comparison between the 0.45 w/c samples here with that of Phase I in Figure 4.2.12, their expansion values and number of cycles per month are shown in Table 4.3.2. Phase II cycles produced less expansion compared to Phase I, when soaked in lime solution to provide moisture. When the Dolostone-0.45 samples are compared directly, the Phase I sample is seen to have expanded slightly more. This expansion was likely caused by the wet/dry cycles, damaging the relatively weaker aggregate.

Table 4.3.2: Phase I and Phase II comparison of lime soaked samples

	Max 26-week expansion (%)		Wet/Dry cycles per 28-days (#)	
	Phase I	Phase II	Phase I	Phase II
Sulfide-0.45	0.049	0.009	2	8
Dolostone-0.45	0.028	0.023		

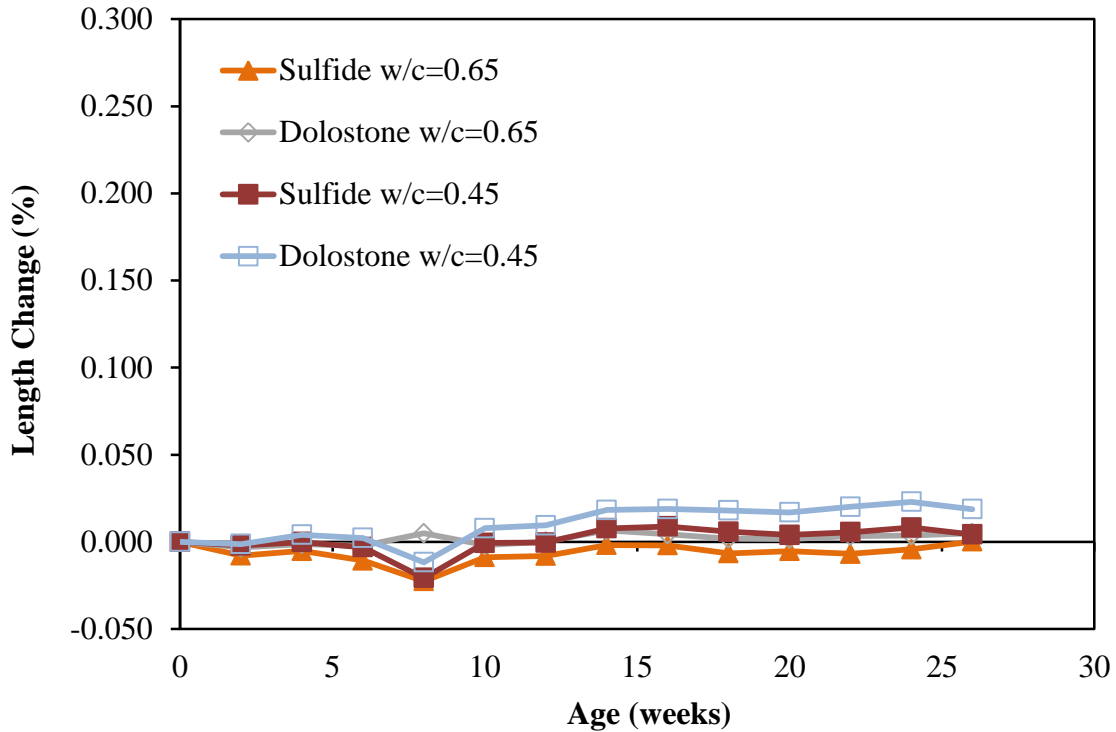


Figure 4.3.37: Phase II Series 2 Results; all samples were soaked in lime solution for 2-hours at 23°C twice a week, with drying at 60°C

Also, it was found in Section 4.1 that Phase I experienced more extreme drying when in the oven, which may have been responsible for greater micro-cracking. When looking at the Sulfide-0.45 samples, a very large difference is seen; Phase I expanded much more. This shows that a reaction with the Sulfide aggregate was produced in Phase I with lime solution, which was not produced in Phase II. The number of cycles per month was included to show that Phase II had a more harsh exposure testing regime, and would have likely caused more wet/dry damage. Since the Sulfide-0.45 samples from Phase II did not expand, it shows that the aggregate was sound, and would not typically suffer from this type of distress. It should be noted again that Phase I was made with a higher cement content, thus, it was higher strength and better quality concrete.

This will likely provide a better particle arrangement for retaining moisture inside the concrete while in the oven. The increased humidity of these samples, along with a lower amount of void space to accommodate for reaction products, could have caused worse damage.

4.3.3 Series 3

Testing here took place after some samples from Series 2 were tested, until the age when the Sulfide-0.65 sample reached an expansion level of 0.7%. At the point they were moved to Series 3, where they were saturated in lime solution at 5°C. The Series 2 and Series 3 results are shown in Figure 4.3.38 to illustrate the life of these samples.

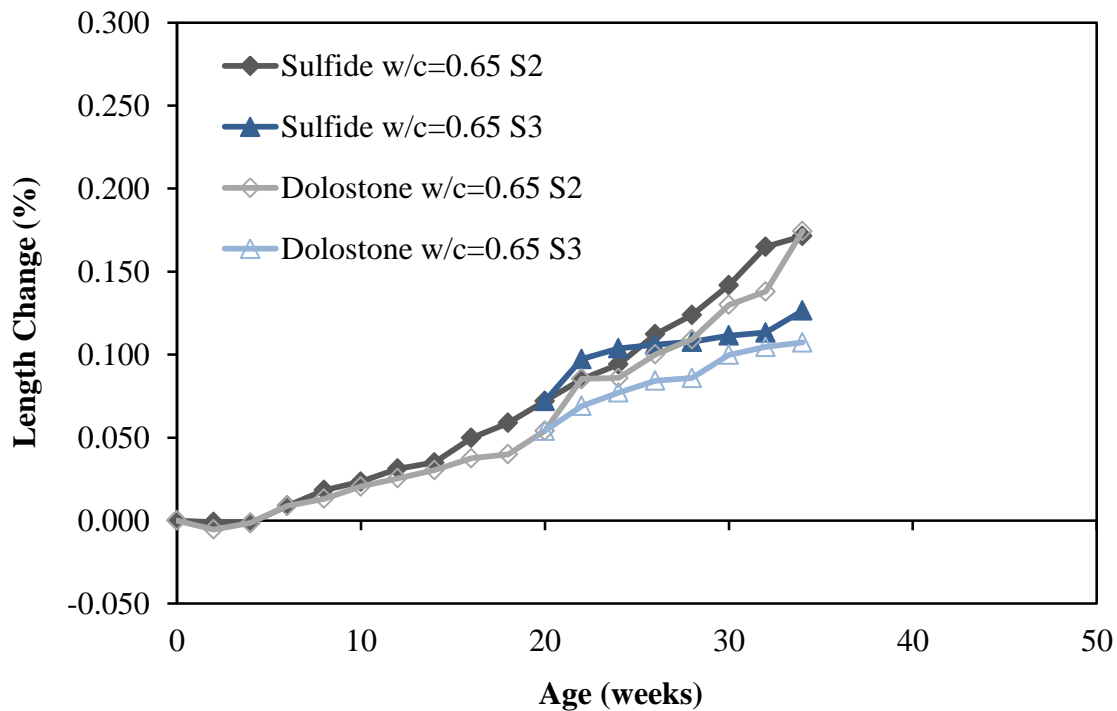


Figure 4.3.38: Phase II Series 3 results; after Series 2 exposure, samples soaked in lime solution at 5°C for 7-days, with hot/cold cycles to 23°C/5°C

When looking at the Series 3 results in Figure 4.3.38 the now familiar lines of the Series 2 samples are seen, the Series 3 samples started at an age of 20-weeks. Since Series 2 was measured dry and Series 3 was measured wet, it was expected to see a rise in the expansion reading caused by the sample becoming swollen in a saturated condition. This jump is observed in Figure 4.3.38 as the 22-weeks readings, after which the expansion of the Series 3 samples slowed down significantly. If there was excess sulfuric acid within the concrete, these conditions

would have been optimal to promote thaumasite attack within the concrete. Since there were no signs of this reaction taking place, it could be concluded that there was not a significant amount of sulfuric acid available to react at the time the samples were moved to Series 3.

4.3.4 Series 4

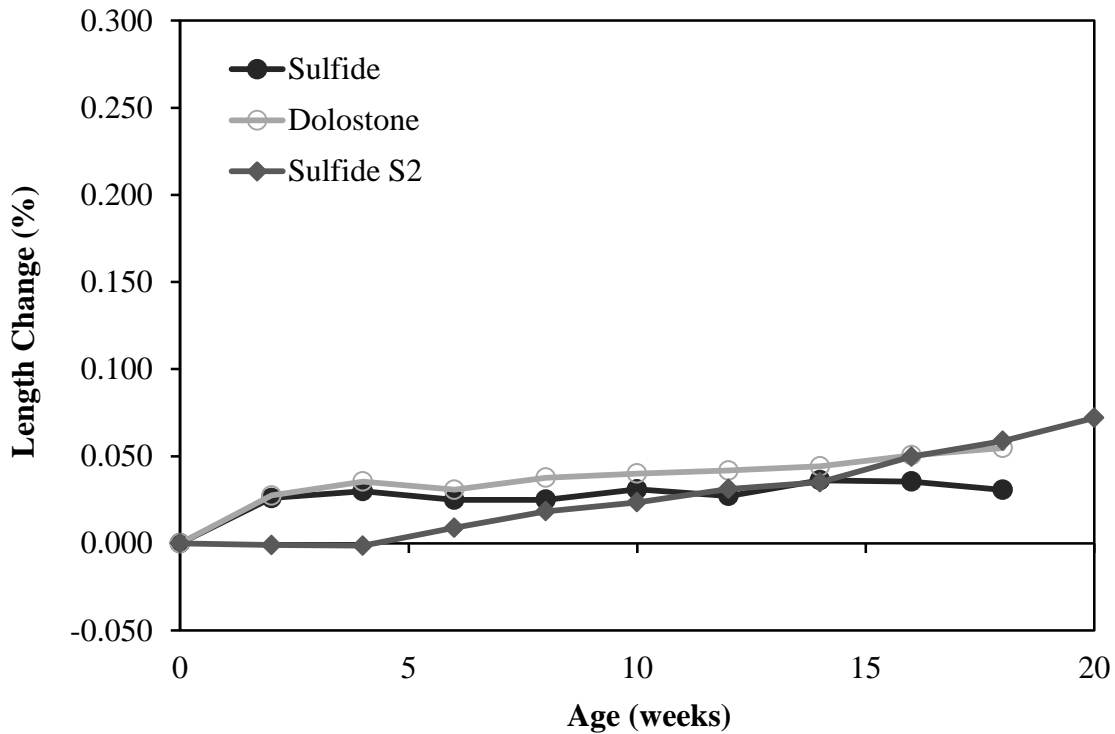


Figure 4.3.39: Phase II Series 4 results; all samples tested with humidity maintained at 100% at all times, all samples had w/c of 0.65, heating to 60°C with 2-hour bleach soaking at 23°C twice a week

The Series 4 samples were tested with their relative humidity (RH) maintained at 100% throughout testing. This was done to prevent the evaporation of the bleach, which may have been forming damaging NaCl salts inside the concrete. The results of these samples, plus that of Sulfide-0.65 from Series 2, are shown in Figure 4.3.39 for comparison. Only a single Sulfide-0.65 sample and a single Dolostone-0.65 sample were tested to test this hypothesis. After 18-weeks of testing, the samples were at nearly the same level of expansion, although this could be misleading. The initial swelling of the 100% RH samples was caused by the absorption of water and subsequent swelling of the sample resulting from the exposure to the 100% RH environment. Since these samples experienced the same 14-day drying period prior to their testing, this

swelling was expected. Therefore, 2 sets of wet measurements (Series 4) are being compared with a set of dry measurements (Series 2) in this graph. If the 100% RH results were adjusted for this swelling, the 100% RH samples would likely show expansion around 0.00%. A longer testing period is needed here to determine if these samples will remain at this level or begin to expand.

4.4 Phase III

The results from Phase III testing can be seen in Figure 4.4.1. Testing of this phase was carried out for only 12-weeks. These samples were tested with 24-hour soaking at 23°C twice a week, and 24-hours heating/drying to 60°C twice a week. The Sulfide-0.65 sample from Phase II was included in Figure 4.4.1 for scale and comparison.

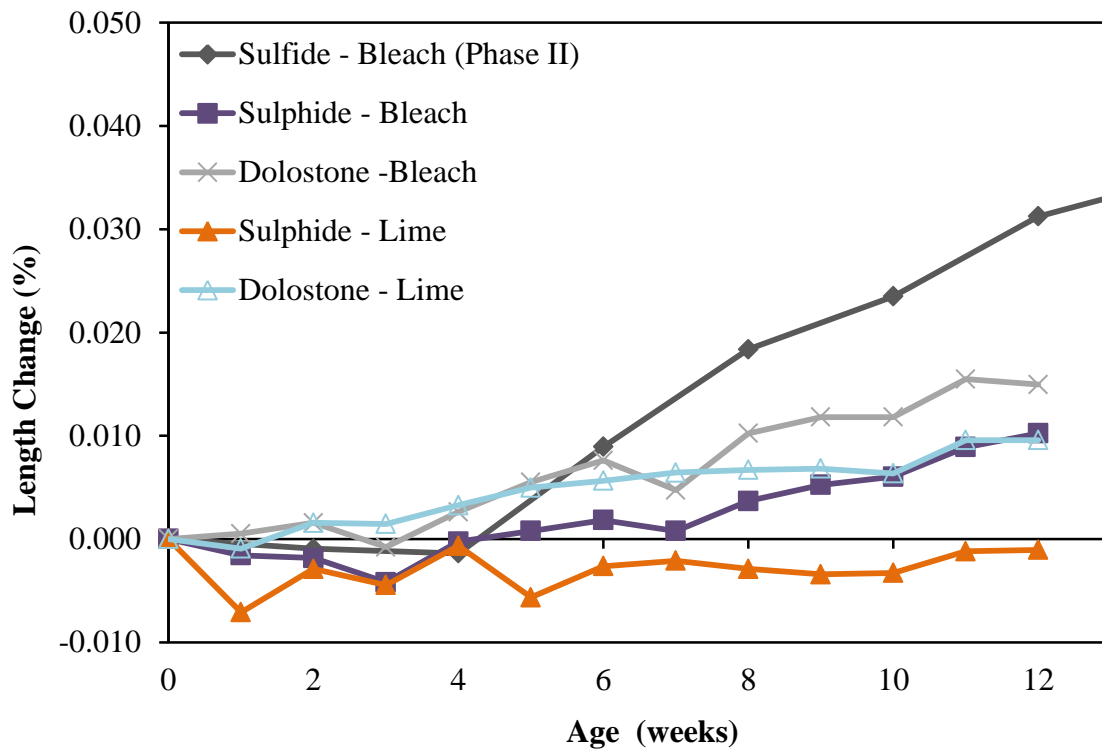


Figure 4.4.1: Phase 3 results; all samples have w/c=0.65, were tested with 24-hour soaking at 23°C twice a week, and 24-hours heating/drying to 60°C twice a week

The Phase II samples are seen to have expanded faster than all of the Phase III samples. Within Phase III, the Dolostone samples clearly expanded more than the Sulfide sample in each case, at this age. It does seem that the Sulfide-0.65 bleach soaked sample could have been beginning an

expansion trend, but the gauge studs had begun to rust severely, and measurements were no longer able to be taken accurately. At that point it was decided that Phase III was not to be continued because the Phase II samples had produced more promising results. The Phase III samples that were tested in lime solution were then recycled and used in Phase IV, as they were still in good condition.

4.5 Phase IV

The samples used for Phase IV were recycled from Phase III lime solution testing after 12-weeks of exposure. These samples were tested with 24-hour soaking at 23°C once a week, and 5-days heating/drying to 60°C. Since Phase IV cycles include more time in the oven, a drying shrinkage was expected, and observed in Figure 4.5.1 during the first couple weeks of testing. After this time, all of the samples seemed to level off, and none showed any definite signs of expansion. Testing was continued for 14-weeks, after which it was once again determined that Phase I and Phase II were more promising, and Phase IV was discontinued.

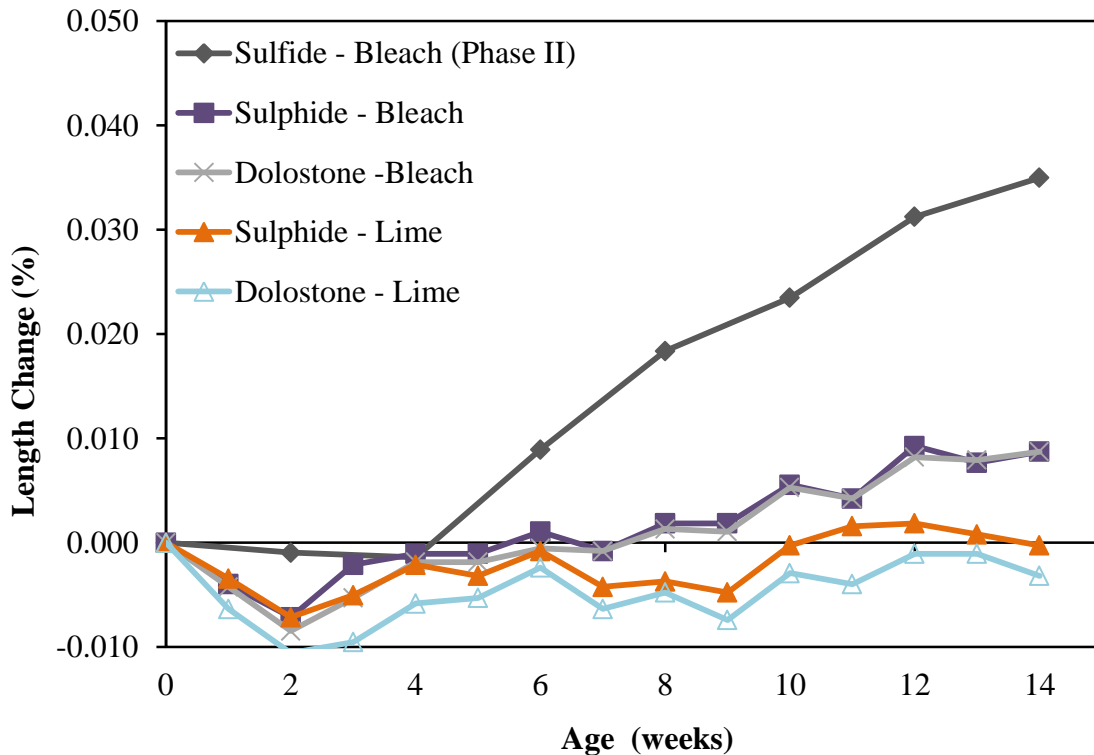


Figure 4.5.1: Phase IV results; all samples have w/c=0.65, were tested with 24-hour soaking at 23°C once a week, and 5-days heating/drying to 60°C

4.6 Additional Testing

4.6.1 Phase III Cylinders

It was suspected that that the bleach affected the concrete in other ways than providing oxygen to the aggregates. This was apparent by the yellowish staining of the concrete that was observed, an example of which is shown in Figure 4.6.1. Both sets of cylinders were tested under Phase III exposure cycles. The sample on the left had soaking in bleach, while the sample on the right had soaking in lime solution, in Figure 4.6.1.



Figure 4.6.1: Cylinders tested under Phase III conditions, bleach soaked on left, lime solution soaked on the right; all samples have $w/c=0.65$, were tested with 24-hour soaking at 23°C twice a week, and 24-hours heating/drying to 60°C twice a week

When inspecting this figure carefully, scratches can be seen on the bleach cylinder shown; this was done with a key, to see how deep the staining penetrated. It was observed that the staining

was only superficial, and did not penetrate much into the sample. Strength testing was conducted on these samples after 16-weeks of Phase III exposure, the results of which are shown in Table 4.6.1. Indirect tension and compressive strength results are shown for 2 different ages here; 28-days is considered as the zero reading, taken before any testing-cycles. Since there were 2 wet/dry cycles per week, over 16-weeks of testing the samples experienced 32-cycles, which is the age for the second set of values in Table 4.6.1. The compressive strength shows there was an increase in strength after the testing cycles. This trend was expected in the lime soaked sample, as the extra moisture would provide additional curing of the concrete. The compressive strength values of the bleach soaked samples were expected to decrease slightly, but the strength values seen here were very similar. There was no initial tensile strength testing conducted, but the second value is in the expected range when comparing it to the compressive strength. Since the bleach samples showed nearly identical strength results, it is concluded that the bleach cycles did not affect the strength of the concrete, when it was tested under Phase III cycles for 16-weeks.

Table 4.6.1: Strength results for Phase III cylinder testing; all samples have w/c=0.65, were tested with 24-hour soaking at 23°C twice a week, and 24-hours heating/drying to 60°C twice a week

Solution	Tensile Strength (MPa)		Compressive Strength (MPa)	
	28-days	32-cycles	28-days	32-cycles
Lime	-	1.93	17	21
Bleach	-	1.74	17	20

4.6.2 Raw Aggregates

Some “Raw” aggregates were examined under the SEM microscope; these samples were taken from the aggregate stockpile, and were not tested in concrete. This testing was done to examine the level of oxidation of the iron sulfides inside the sulfide aggregate, prior to testing. A large aggregate particle was cut open and polished. The cross-section of the Sulfide coarse aggregate particle is shown in Figure 4.6.2 through Figure 4.6.4. When looking at the SEM image in Figure 4.6.2, a large pyrrhotite intrusion can be seen as the white area in the image. EDS analyses are included to confirm the composition of the pyrrhotite. The rectangle in Figure 4.6.2 highlights

the area that was magnified to in Figure 4.6.3, where the oxidized pyrrhotite was highlighted by the EDS analyses. There was only a slight amount of oxidation found around the edges of the pyrrhotite on the right side of the image, seen in analysis B), and in the most exposed particles on the left side of the image, seen in analysis A). Again here, the oxidized area was suspected by the lack of sulfur and presence of iron, found at the edge of a pyrrhotite inclusion. Another area of the same sample shows an intrusion that has possibly experienced oxidation that penetrated deeper into the aggregate, shown in Figure 4.6.4. Here a pyrrhotite stream that extended into the core of the sample is seen, and when EDS analysis B) and C) were compared, it seemed to indicate that oxidation could be found well past the surface of the aggregate. Oxidation was also seen at the exterior surface of the aggregate in analysis A), in Figure 4.6.4. All pyrrhotite found during this testing showed oxidation at its exterior surface, if it was exposed at the exterior of the aggregate particle. Some intrusions within the interior of the aggregate also showed signs of oxidation. When examining the samples, some intrusions found showed oxidation penetration, while others did not. It seems that oxidation of the surface of the raw aggregate could be expected before testing, and varying levels of oxidation could be seen penetrating into the interior of the aggregate at this time also. It is not confirmed that iron sulfide oxidation was occurring and the interior of the sample, or if the mineral formed in such a way.

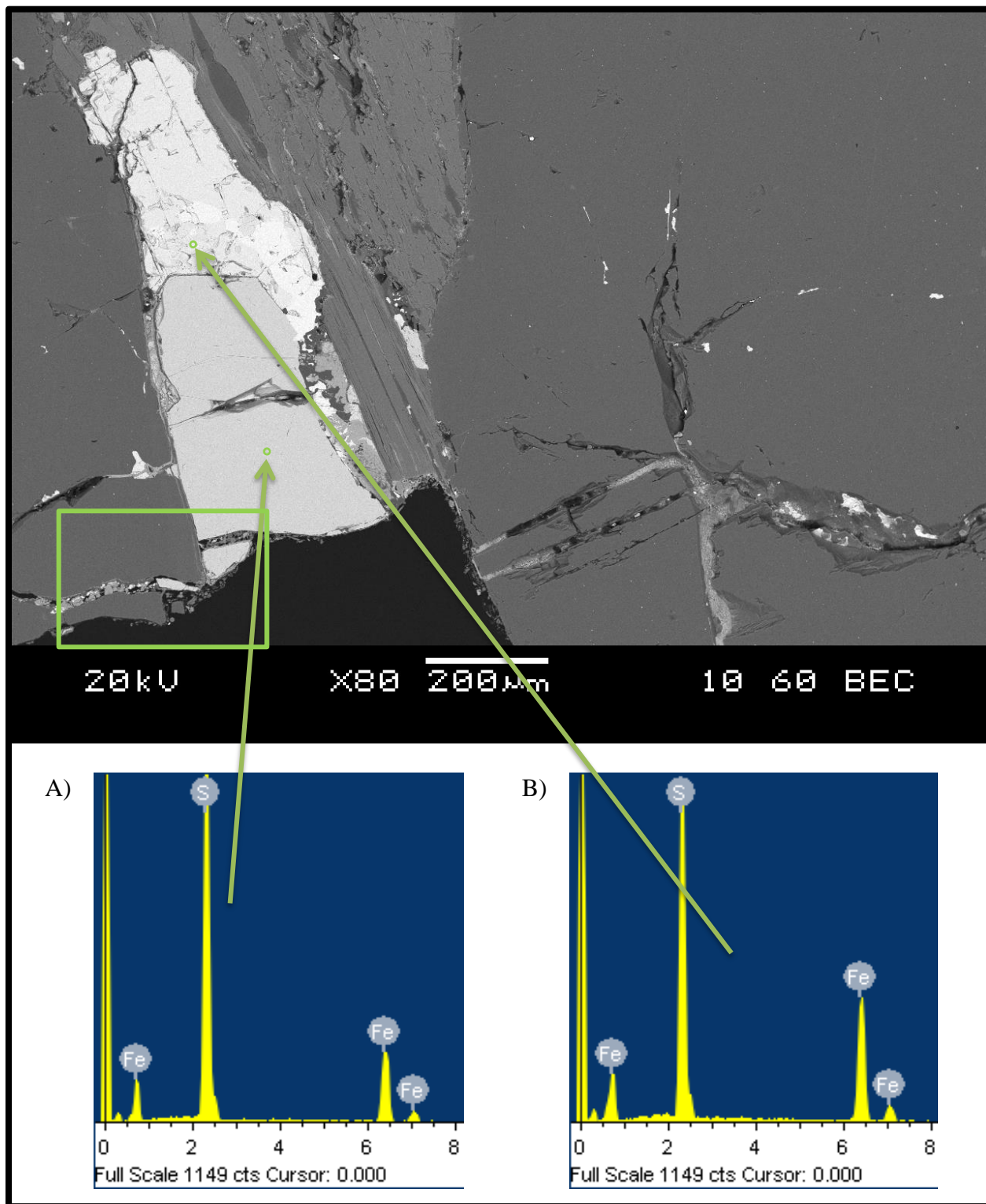


Figure 4.6.2: SEM image and EDS analysis for Sulfide aggregate showing pyrrhotite; exposed only to environmental conditions

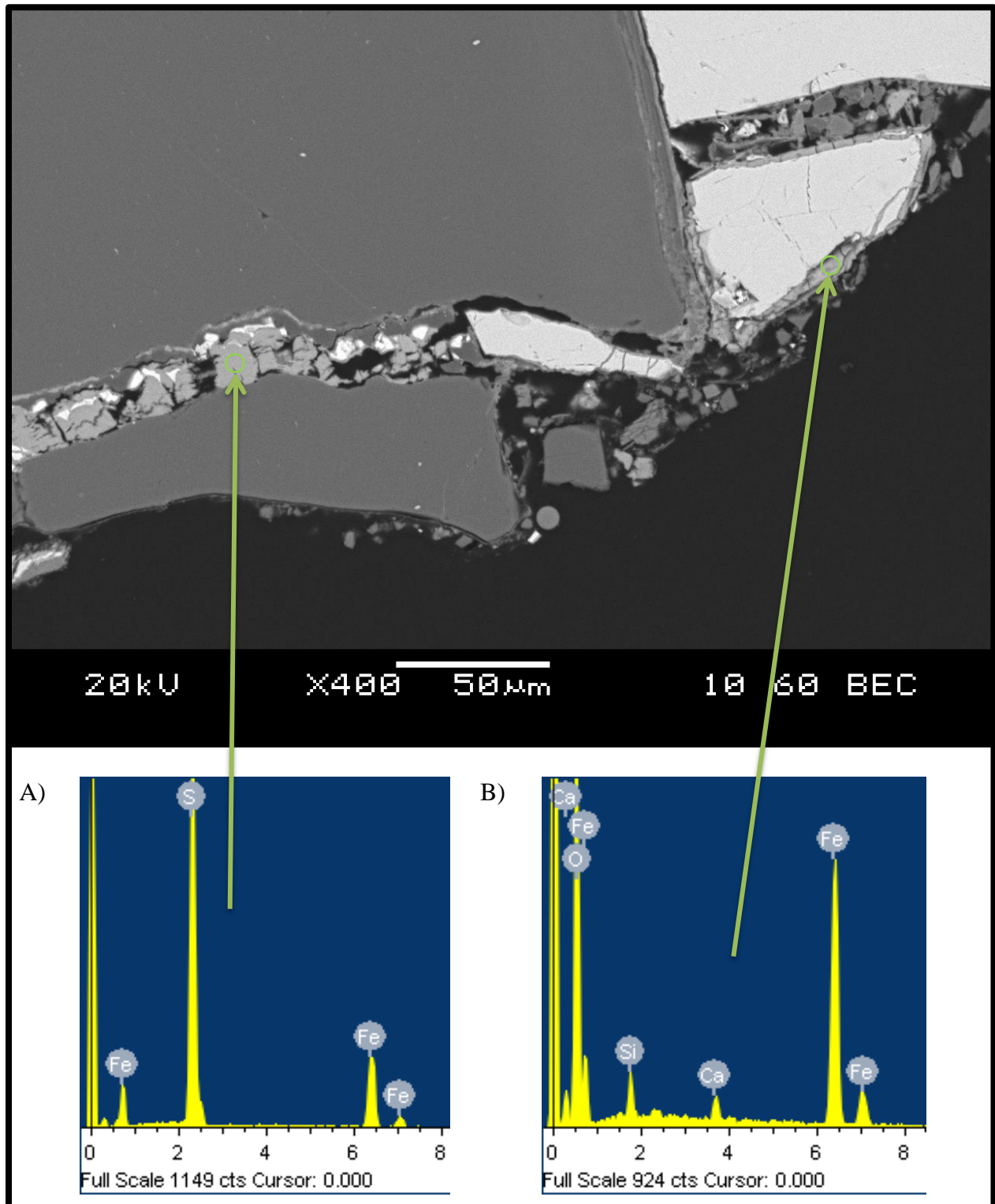


Figure 4.6.3: SEM image and EDS analysis for Sulfide aggregate showing oxidized pyrrhotite; exposed only to environmental conditions

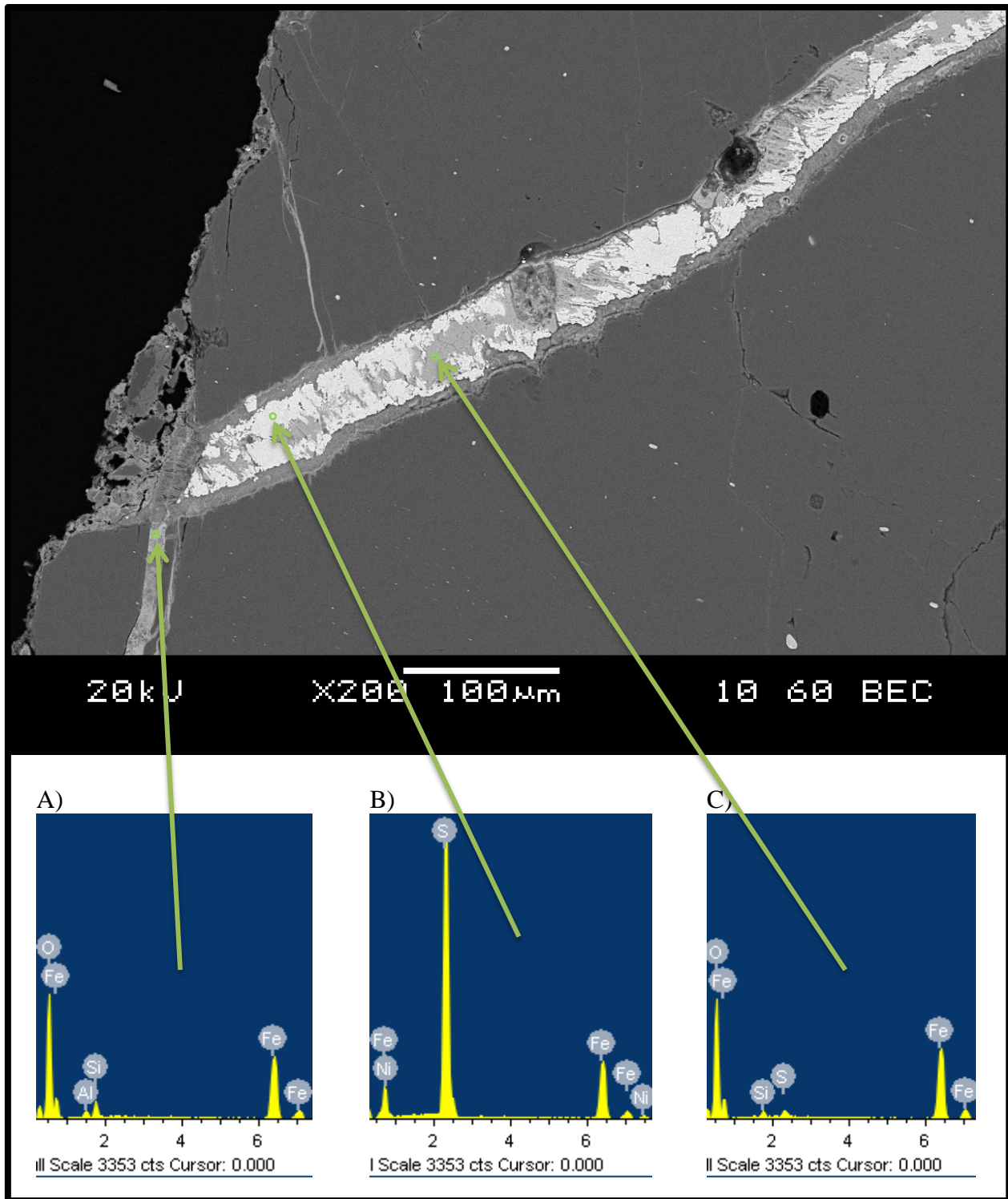


Figure 4.6.4: SEM image and EDS analysis for Sulfide aggregate showing potentially oxidized pyrrhotite; exposed only to environmental conditions

5 Discussion

5.1 Analysis of Reaction Mechanisms

5.1.1 Phase I

When heating the samples to 150°C for 7-days, individual coarse aggregate particles were seen to cause fracturing of the concrete, observed with both aggregate types. The stones were undergoing a physical alteration, which caused a volume change and fracturing of the concrete. Much more expansion was experienced when the samples were soaked for 7-days at 23°C as opposed to 5°C, or with dry testing. Therefore, it was suspected that this expansion was related to ettringite; all other types of expansion mechanisms were expected to produce more severe expansion upon the increase in temperature differential provided during 5°C testing. There was an unrelated and obvious reaction occurring with the Dolostone aggregate upon heating to 150°C in a saturated condition, which was not the reaction of interest and deemed to be and unrelated to this research topic. The 150°C testing made it hard to monitor any expansion caused by the iron sulfides, and was thus considered too harsh of conditions to sustain all concrete and aggregate types, and was therefore eliminated from future testing.

The Sulfide sample with w/c of 0.45 tested in Phase I with 7-day heating to 60°C and 7-day soaking in lime solution at 23°C, showed significantly more expansion than the other samples tested under the same conditions. There were signs of oxidation in this sample, and a large concentration of ettringite near the suspected oxidation. There was no gypsum found in this sample, even when it was re-examined after the discovery of gypsum in other samples. If ettringite had formed following pyrrhotite oxidation, one would have expected to see gypsum in the area. Therefore, some oxidation may have occurred in the Sulfide-0.45 sample, perhaps at a very slow rate or for only a limited amount; any gypsum that formed may have had sufficient time to transform into ettringite. The oxidation of iron sulfides did not cause the extent of damage that was expected and any contribution seen here by the iron sulfide was only minor.

A large amount of ettringite was found in the Phase I samples examined under the SEM, which had 7-day heating to 60°C and 7-day soaking in lime solution at 23°C. Since an important amount of ettringite was observed in both the Dolostone and the Sulfide samples with w/c of

0.45, it was suspected that a large portion of the ettringite found in the samples was likely not caused by iron sulfide oxidation. When these results were compared with the results from similar testing at 5°C they showed a comparable trend, including the Dolostone-0.45 sample. The culmination of these results suggests that the wet/dry cycles of Phase I promoted secondary ettringite to form in these samples, which caused some expansion. The sulfates were likely decomposed from either monosulfate or primary ettringite present in the cement. A similar phenomenon has been observed by others with heating to only 40°C with mortar (Batic et al., 2000); the reaction is likely slower with concrete, but similar trends are expected. The wet/dry cycles were expected to cause micro-cracking within the concrete, the amount of expansion was likely insignificant, but the micro-cracking is known to be a pre-cursor to SEF expansion (Colleparidi, 2003). A significant amount of ettringite was seen in the ITZ in both aggregate types, and cracking patterns were observed, both of which are known to be associated with SEF damage. Since the Sulfide-0.45 sample expanded more than Dolostone-0.45 sample, it is thought that the iron sulfide contributed to the formation of ettringite, the results of which were then amplified by subsequent dissolving and reformation of ettringite, caused by the heating cycles to 60°C with saturation in lime solution at 23°C. Therefore, heating cycles to 80°C would likely cause further amplification of the effects of ettringite formation caused by iron sulfides; since ettringite is known to be unstable at 80°C.

Considering the amount of cracking observed in the concrete foundations in Trois-Rivières, a large amount of expansion was expected in the lab after 1 year of testing. There was evidence of iron oxides found on the surface of the coarse aggregate particles before testing, suggesting that they had already undergone some oxidation prior to testing. Oxidized pyrrhotite was confirmed on the surface of untested coarse aggregate particles during SEM investigation. These findings raise a major question with the validity of all of the results shown here; were the aggregates used in the foundations oxidized prior to use at all, or to a similar level as what was received in the lab. The aggregates that were obtained for laboratory purposes were obtained several years after the quarry was deemed unfit for use in concrete, and closed. Over this time, the already crushed aggregate was allowed to oxidize naturally in the environment.

5.1.2 Phase II

There was expansion in several samples in Phase II, all of which followed a very similar trend. These samples were tested with heating to 60°C for either 48 or 72-hours per cycle, and had a 2-hour soaking in bleach twice a week. The long-term expansion of the Sulfide and Dolostone samples were found to be very similar and large amounts of NaCl salt crystals were found in both samples investigated under SEM. This expansion was likely not related to the iron sulfides in the coarse aggregate, and is therefore not the reaction that was desired. With both aggregate types, it could not be determined from the SEM images if the NaCl salt was a part of the initial crack formation, or if it formed in the cracks after initial cracking occurred from a different source. Either way, it seemed apparent that the NaCl salt was responsible for extending the cracks to the size observed. Since the samples tested similarly with bleach and heating to 40°C did not expand, it seems that heating cycles to 60°C is necessary to promote this expansion. Bleach is known to decompose upon heating above 40°C (ERCO, 2012); thus heating to 60°C is surely causing bleach decomposition and subsequent NaCl crystallization, while heating to 40°C may not.

The samples made with HSF cement showed no expansion, they were tested the same with heating to 60°C; the increased fineness of the blended cement likely prevented the ingress of the bleach into the paste. This showed that heating to 60°C alone is not causing any expansion related to differential thermal expansion. It seems that the combination of bleach penetration into the paste, with heating to 60°C, and uncontrolled (very low) relative humidity caused the crystallization of NaCl salts and related damage. The SEM investigation found that these Sulfide samples showed signs of iron sulfide oxidation while inside concrete, and also the formation of gypsum. These 2 observations are strong evidence for sulfuric acid attack being induced in the concrete. Therefore, the combination of heating to 60°C and bleach exposure appeared to cause the occurrence of the oxidation reaction that was desired. While these conditions are an extreme type of exposure, it is possible that the same reaction process may be promoted in accelerated fashion compared to what was observed in the foundations. A diagram of the proposed reaction series is presented in Figure 5.1.1 to show the course of reactions and aid in discussion. This reaction appeared to proceed as expected in the early stages of testing; sulfuric acid was thought to cause sulfate attack either directly or via the formation of sodium sulfate. Either way, gypsum

was formed, and once the sulfuric acid reacted the NaCl salts would have been allowed to form. Ettringite could not be confirmed in this sample, but Friedel's salt was. The ettringite formation and its associated expansion seemed to be hindered by the chlorides from the bleach. This would have been much more than that produced by gypsum formation. There were some features that showed signs of being ettringite, others that showed strong signs of being Friedel's salt, and some features appeared to be a mixture of both.

It seems that the bleach reacted with the sulfoaluminates and replaced the sulfur with chlorine. Ettringite is known to be unstable in the presence of high concentrations of chlorides, where the formation of Friedel's salt is favoured (Zibara, 2001). The ettringite production reaction was likely slower than the Friedel's salt production reaction. Therefore, ettringite may not have been allowed to form, and expansion from ettringite was not observed because it was hindered by the chlorides, and Friedel's salt formed instead. A diagram of this series of reactions is shown in Figure 5.1.1; a detailed description of each of these reactions is presented in Chapter 2.

The 31-week old Sulfide SEM sample (II-S60A) did not show any significant signs of NaCl salt, while the 59-week old sample did. The Dolostone samples showed a large amount of NaCl salt at both ages (22 and 26-weeks). It is possible that NaCl salts were not able to form because the sulfuric acid from the oxidation reacted with the bleach to produce sodium sulfate solution instead. The sodium sulfate would then have continued to react with calcium hydroxide in the cement and form gypsum. Thus, the oxidation reaction may have prevented the formation of the NaCl salts for a period of time, after which the sulfuric acid became either depleted or overcome and the NaCl salts took over. It is also possible that no salt was observed in the 31-week old sample because the small investigation area required by the SEM was taken from an area that did not contain NaCl salt, while other areas may have.

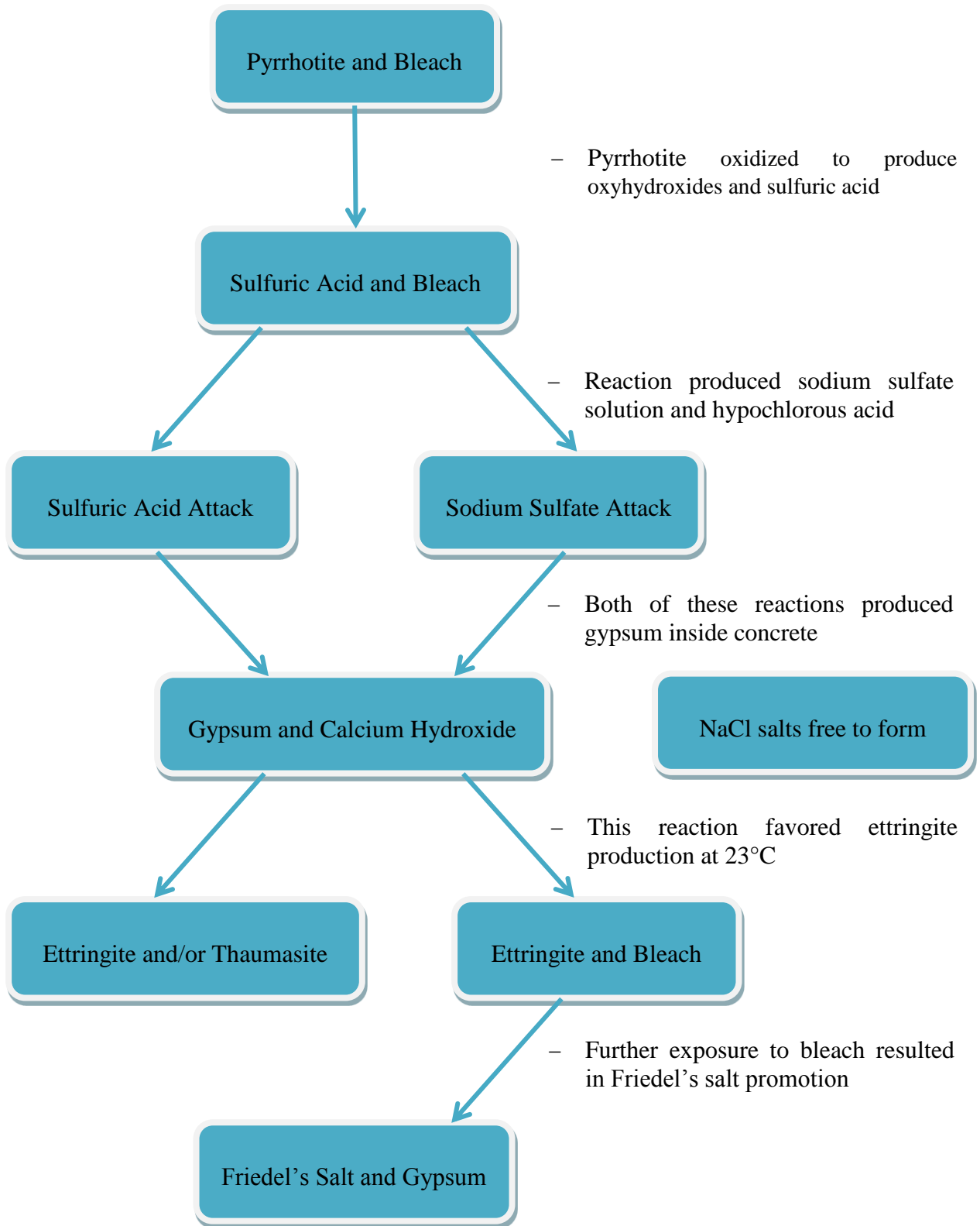


Figure 5.1.1: Proposed reaction series for Phase II Series 2 Sulfide sample; made with w/c of 0.65, and tested with drying at 60°C and 2-hours soaking in bleach at 23°C twice a week

5.2 Performance Test Development

From all of the previously discussed testing, there were 2 testing exposures that produced positive results with regards to a test development; Phase I with 7-day heating to 60°C and 7-day soaking in lime solution at 23°C, and Phase II Series 2, with 2-day or 3-day heating to 60°C and 2-hour soaking in bleach at 23°C twice a week. In Phase I there were signs of oxidation while using only lime solution for moisture. Also in Phase I, expansion was seen in the Sulfide-0.45 sample where it was not seen in the Dolostone-0.45 sample. In Phase II (with bleach) the expansion results of the Sulfide and Dolostone samples were nearly identical, although, there were definite signs of oxidation and sulfate attack found in the Sulfide sample upon SEM investigation. Testing in Phase II, Phase III, and Phase IV all included both bleach and lime solution in their testing, to test if either would promote oxidation. In light of these results, it would seem intuitive to separate the 2 solutions, and test them under different exposure conditions. Therefore, to aid in discussion, the 2 solutions will be discussed separately, with regards to test development and promoting oxidation, in the following sections. This could also be considered as testing with or without an oxidizing agent to be more general. Since heating to 60°C with no wet cycles produced no expansion in either Phase I or Phase II in many different samples, external moisture should be provided in all future testing.

5.2.1 Testing Without Oxidizing Agent

A reaction with the Sulfide aggregate was produced in Phase I with lime solution, and it occurred much more efficiently than in Phase II. With lime solution testing, the humidity level inside the concrete is very important for the oxidation reaction. Upon reviewing the moisture content results from Section 4.1, it would seem that the Phase I-0.45 samples were able to retain relative humidity within the core of the sample, even after 7-days in the oven. The center of these samples reached an equilibrium relative humidity level that they dried to each week, being about 40% for the 0.45 samples. Therefore, the 0.45 samples likely spent a significant amount of time at an effective humidity level for promoting oxidation. Therefore, higher strength and better quality concrete is better suited for this style of testing because it would retain moisture and humidity better. Since Phase I lime testing expanded more than Phase II lime testing, it seems that the longer time period for saturation produced better conditions for expansion. The SEF

expansion seen in Phase I was not observed in Phase II, therefore it was not the large number of cycles that caused the SEF, but rather the length of time spent at each temperature. For the SEF reaction to occur, it needed the time at an elevated temperature to dissolve the sulfates (60°C), and time at room temperature (23°C) with moisture to allow for the formation of ettringite. Thus, to avoid the SEF reaction, one of the testing temperatures needs to be eliminated. Therefore, it should be suggested that excessive hot/cold cycles above 40°C be avoided in future testing, or other techniques to mitigate or account for SEF expansion should be examined. If the hot/cold cycles were eliminated, SEF expansion would no longer be a factor, allowing for heating to 80°C to be tested. With lime testing, it may be more effective to eliminate the soaking of the samples, and instead, fluctuate the humidity levels between 60% and 90%, while maintaining heat. This would provide more time at an effective humidity level, and the heat provided would accelerate the oxidation reaction. Maintaining heat during testing would prevent the SEF damage, and would provide a consistent environment for the formation of reaction products. After some amount of expansion has been recorded, a shift in the testing may provide valuable insight. Similar to the procedure from Phase II Series 3, the samples could be cooled to 23°C or 5°C with the humidity maintained, provided the temperature change was done gradually and a length measurement was taken at 23°C before continuing to 5°C. This would provide optimal conditions for any excess sulfuric acid, which had accumulated inside the sample, to react with the cement and form ettringite and/or thaumasite. This type of 2-stage testing was proposed by Rodrigues et al. (Rodrigues et al., 2012). For this reason, samples should be made with 6 specimens to allow for simultaneous testing of the same sample, as was done in Phase II Series 2 and Series 3 of this work. Phase IV testing cycles appear to be sufficient to expect oxidation, although, SEF expansion would be expected as in Phase I. Since Phase IV samples were recycled, there was not a Sulfide-0.45 sample tested in lime solution in Phase IV.

5.2.2 Testing With Oxidizing Agent

It was seen that expansion in Phase II only occurred upon heating to 60°C, and thus, heating to 60°C is necessary to accelerate the type of expansion. In Phase II, the wet/dry cycles appeared to cause damage in the Dolostone samples. It seems that 2 problems are associated with the low moisture condition in the oven. The micro-cracking of the samples was thought to be caused by the wet/dry cycles, and the NaCl salt are thought to be associated with the evaporation of the

bleach upon drying. Therefore, it seems apparent that a certain level of humidity needs to be maintained during heating. When comparing Phase II with Phase III, it is seen that Phase III was soaked in bleach for much longer each week; thus, more bleach may not produce more accelerated expansion. Therefore, soaking in bleach should be carried out for 2-hours, twice a week. When comparing Phase II with Phase IV, it is seen that Phase IV spent more time in the oven than Phase II did; thus, more heat may not give more expansion either. Therefore, to further develop this style of testing, heat and/or humidity must be maintained throughout testing. If both soaking and measuring were completed at 60°C or 80°C, the samples would not be exposed to the hot/cold cycles. If a certain level of humidity was maintained during all testing, the wet/dry cycles would be avoided, and the bleach would not be allowed to evaporate. Since NaCl is known to crystallize at a RH of about 75-80% (Langlet et al., 2011), the relative humidity level should be maintained to a minimum of 80% throughout testing with bleach. It seems that adding Silica Fume was effective to prevent the expansion caused in Phase II. This suggests that the damage observed was a result of the bleach penetrating inside the concrete, and reacting. Therefore, a mitigation technique for this test could involve blocking the voids of the concrete, to prevent the bleach from penetrating into the concrete. This also indicates that lower quality concrete would be more suitable for this style of testing.

6 Conclusions

The goal of this research was to reproduce the concrete degradation experienced in Trois-Rivières under accelerated laboratory conditions. Information gained from this will provide insight towards a performance test development, and eventually mitigation. A summary of the findings of this work are presented below.

1. Heating to 150°C was too harsh for this type of concrete testing; it provoked unwanted reactions or processes to occur. Individual particles in both aggregate types were detrimentally affected by the heating cycles, which caused some concrete prisms to fracture.
2. The iron sulfide likely contributed to the expansion in Phase I Sulfide sample with w/c of 0.45, tested at with 7-day heating to 60°C, and 7-day soaking at 23°C. Oxidation may have occurred, however, it is believed factors other than oxidation and sulphate attack could have been significant contributors to the expansion.
3. The Prolonged hot/cold, and extreme wet/dry cycles of Phase I samples tested to 60°C with soaking in lime solution, caused the decomposition of sulphotoaluminate phases in the cement paste. This caused the occurrence of a phenomenon known as secondary ettringite formation (SEF), which resulted in a concentration of ettringite around the aggregate particles. This reaction is unrelated to iron sulfide oxidation, and occurred with both aggregate types. There was also evidence of aggregate particle weathering within both aggregate types, this seemed unrelated to the SEF.
4. The NaCl salt controlled the long term expansion in Phase II samples heated to 60°C with bleach soaking for 2-hours twice a week. The NaCl salt crystallization appears to require heating to 60°C, the penetration of bleach into the paste, and low relative humidity levels (<50%).
5. The Phase II Series 2 Sulfide sample that was heated to 60°C with bleach soaking for 2-hours twice a week, experienced pyrrhotite oxidation. The resulting sulfuric acid was thought to react with the bleach to produce sodium sulfate, which continued to

react and produce gypsum. The ettringite formation seemed to be hindered by the presence of chlorides in the bleach, which promoted Friedel's salt instead.

6. Upon evaporation of the bleach, supersaturation was thought to occur within the concrete, this provided the high concentrations of NaCl necessary to promote the reaction first with monosulfate, and then with any ettringite. Friedel's salt and gypsum were formed as a result of these reactions.
7. It could not be concluded that gypsum or Friedel's salt caused expansion of the sample; any effects that their formation may have had were masked by the expansion caused by the NaCl salt.
8. The Sulfide coarse aggregate received in the lab was suspected of being less reactive than what was used in the foundations. It may have suffered some oxidation from environmental exposure prior to being placed in the concrete samples.

7 Recommendations for Future Research

- The Sulfide coarse aggregates received in the lab seemed to have been partially oxidized prior to testing in concrete, this likely occurred from environmental exposure. Therefore, freshly crushed, and un-oxidized Sulfide coarse aggregate should be obtained and tested for comparison. Alternatively, crushed aggregates could be used in mortar bars or microbars, although the smaller sample sizes and different mixture proportions would not be truly representative of concrete used in the field.
- Oxidation can be promoted with an oxidizing agent or without, however the reactions occur at different rates, and their mechanisms have different requirements. Optimizing a test protocol involving an oxidizing agent should be carried out separately from that which does not involve an oxidizing agent. Therefore, these different styles of testing should be carried out separately with different exposure conditions.
- In light of the results of this work, detailed testing regimes were recommended in Section 5.2. The separate exposure conditions suggested are tailored to promote oxidation with, and without the incorporation of an oxidizing agent; a summary of each is shown below. Once an accelerated test is established a comparative field trial will need to be carried out to correlate the expansion with actual service life.
 - For testing with an oxidizing agent such as bleach, relative humidity needs to be maintained at a minimum of 80% during all testing, to prevent drying of the samples and NaCl formation. Soaking in bleach should be carried out for 2-hours, twice a week, at a temperature of 60°C or 80°C. Measurements should be taken while the samples are hot, thus, the samples should not be cooled, to avoid temperature fluctuations. After a certain age of testing (once oxidation causes expansion greater than 0.01%), samples should be cooled to 23°C and 5°C with relative humidity maintained at 80% to promote ettringite and/or thaumasite formation.
 - Testing without an oxidizing agent should also be carried out at a temperature of 60°C or 80°C to avoid temperature fluctuations. Soaking of the samples should be

eliminated; instead, relative humidity levels should be fluctuated between 60% and 90%. This will prevent drying of the samples and provide oxygen and moisture inside the concrete. Also here, after a certain amount of testing the samples should be cooled to 23°C and 5°C with relative humidity maintained at 80% to promote ettringite and/or thaumasite formation. This type of 2-stage testing was proposed by Rodrigues et al. (Rodrigues et al., 2012).

- Since chlorine seems to be affecting the stability of ettringite, using an oxidizing agent that does not contain chlorine would prevent complications arising from chlorides reacting with the different phases inside concrete. A non-chloride oxidizing agent was used in this study but was found ineffective, and more research should focus on finding a more suitable oxidizing agent.
- Some stainless steel gauge studs cast into the concrete were seen to experience some oxidation during testing. Therefore, titanium gauge studs should be used when testing involves an oxidizing agent, to prevent oxidation of studs in the future. This had already been adopted in this study.

Appendices

Appendix A

Sunday	Monday	Tuesday	Wednesday	Thursday	Friday	Saturday
1	2 • CAST	3 • DEMOLD	4	5	6	7
8 • MOVE TO OVEN	9	10 • REMOVE FROM OVEN	11 • ZERO READING / MOVE TO OVEN	12	13	14
15	16	17 • REMOVE FROM OVEN	18 • SUBSEQUENT READING / MOVE TO OVEN	19	20	21
22	23	24 • REMOVE FROM OVEN	25 • SUBSEQUENT READING / MOVE TO OVEN	26	27	28
29	30	31 • REMOVE FROM OVEN	1 • SUBSEQUENT READING / MOVE TO OVEN	2	3	4

Figure A.5.2.1: Typical month of Phase I dry testing

Sunday	Monday	Tuesday	Wednesday	Thursday	Friday	Saturday
1	2 • CAST	3 • DEMOLD	4	5	6	7
8 • MOVE TO OVEN	9	10 • REMOVE FROM OVEN	11 • ZERO DRY READING / MOVE TO OVEN	12	13	14
15	16	17 • REMOVE FROM OVEN	18 • SUBSEQUENT DRY READING / MOVE TO WATER	19	20	21
22	23	24 • REMOVE FROM WATER	25 • ZERO WET READING / MOVE TO OVEN	26	27	28
29	30	31 • REMOVE FROM OVEN	1 • SUBSEQUENT READING / MOVE TO WATER	2	3	4

Figure A.5.2.2: Typical month of Phase I wet/dry testing

Sun 31	Mon 1	Tue 2	Wed 3	Thu 4	Fri 5	Sat 6
● CAST	● DEMOLD ● MOVE TO 100%RH					
7	8	9	10	11	12	13
● ZERO WET READING ● MOVE TO 50%RH						
14	15	16	17	18	19	20
21	22	23	24	25	26	27
● ZERO DRY READING ● MOVE TO 50%RH	● SUBSEQUENT READING ● 2 HOUR SOAK ● MOVE TO OVEN		● MOVE TO 50%RH	● SUBSEQUENT READING ● 2 HOUR SOAK ● MOVE TO OVEN		
28	29	30	1	2	3	4
● MOVE TO 50%RH	● SUBSEQUENT READING ● 2 HOUR SOAK ● MOVE TO OVEN		● MOVE TO 50%RH	● SUBSEQUENT READING ● 2 HOUR SOAK ● MOVE TO OVEN		

Figure A.5.2.3: Typical month of Phase II Series 2 testing

Sun 28	Mon 29	Tue 30	Wed 1	Thu 2	Fri 3	Sat 4
● MOVE TO 50%RH	● SUBSEQUENT READING ● 2 HOUR SOAK ● MOVE TO OVEN		● MOVE TO 50%RH	● SUBSEQUENT READING ● 2 HOUR SOAK ● MOVE TO OVEN		
5	6	7	8	9	10	11
● ZERO DRY READING ● MOVE TO 50%RH	● SUBSEQUENT READING ● 2 HOUR SOAK ● MOVE TO OVEN		● MOVE TO 50%RH	● SUBSEQUENT READING ● 2 HOUR SOAK ● MOVE TO OVEN		
12	13	14	15	16	17	18
● MOVE TO 50%RH	● SUBSEQUENT READING ● SATURATE SAMPLES ● MOVE TO FRIDGE					
19	20	21	22	23	24	25
● MOVE TO 50%RH	● SUBSEQUENT READING ● SATURATE SAMPLES ● MOVE TO FRIDGE					
26	27	28	29	30	31	1
● MOVE TO 50%RH	● SUBSEQUENT READING ● SATURATE SAMPLES ● MOVE TO FRIDGE					

Figure A.5.2.4: Transition from Phase II Series 2 to Series 3 testing

Appendix B

Table B.1: Phase I concrete mix proportions with w/c of 0.62 and Sulfide coarse aggregate

	Mass (kg/m ³)
Water	260
Cement	420
Coarse Aggregate	1012
Fine Aggregate	675

Table B.2: Phase I concrete mix proportions with w/c of 0.45 and Sulfide coarse aggregate

	Mass (kg/m ³)
Water	189
Cement	420
Coarse Aggregate	1131
Fine Aggregate	755

Table B.3: Phase II concrete mix proportions with w/c of 0.65 and Sulfide coarse aggregate

	Mass (kg/m ³)
Water	176
Cement	250
Coarse Aggregate	1078
Fine Aggregate	819

Table B.4: Phase II concrete mix proportions with w/c of 0.45 and Sulfide coarse aggregate

	Mass (kg/m ³)
Water	157.5
Cement	350
Coarse Aggregate	1078
Fine Aggregate	749

List of References

ACI Committee 211, -. (1991). *Standard practice for selecting proportions for normal, heavyweight and mass concrete (reapproved 2009)*. (No. ACI 211.1-91). Farmington Hills, Michigan: American Concrete Institute.

Barnett, S. J., Adam, C. D., & Jackson, A. R. W. (2000). Solid solutions between ettringite, $\text{Ca}_6\text{Al}_2(\text{SO}_4)_3(\text{OH})_{12}\cdot 26\text{H}_2\text{O}$, and thaumasite, $\text{Ca}_3\text{SiSO}_4\text{CO}_3(\text{OH})_6\cdot 12\text{H}_2\text{O}$. *Journal of Materials Science*, 35(16), 4109-4114. doi: 10.1023/A:1004898623884

Batic, O. R., Milanese, C. A., Maiza, P. J., & Marfil, S. A. (2000). Secondary ettringite formation in concrete subjected to different curing conditions. *Cement and Concrete Research*, 30(9), 1407-1412. doi: 10.1016/S0008-8846(00)00343-4

Beddoe, R. E., & Dorner, H. W. (2005). Modelling acid attack on concrete: Part I. the essential mechanisms. *Cement and Concrete Research*, 35(12), 2333-9. doi: 10.1016/j.cemconres.2005.04.002

Belzile, N., Chen, Y., Cai, M., & Li, Y. (2004). A review on pyrrhotite oxidation. *Journal of Geochemical Exploration*, 84(2), 65-76. doi: 10.1016/j.gexplo.2004.03.003

Bouzabata, H., Multon, S., Sellier, A., & Houari, H. (2012). Swellings due to alkali-silica reaction and delayed ettringite formation: Characterisation of expansion isotropy and effect of moisture conditions. *Cement and Concrete Composites*, 34(3), 349-56. doi: 10.1016/j.cemconcomp.2011.10.006

Brown, P. W. (2002). Thaumasite formation and other forms of sulfate attack. *Cement & Concrete Composites*, , 301-303.

Chinchon-Paya, S., Aguado, A., & Chinchon, S. (2012). A comparative investigation of the degradation of pyrite and pyrrhotite under simulated laboratory conditions. *Engineering Geology*, 127, 75-80. doi: 10.1016/j.enggeo.2011.12.003

Clifton, J. R., & Pommersheim, J. M. (1994). *Sulfate attack of cementitious materials: Volumetric relations and expansions*. (No. NISTIR 5390). Gaithersburg, MD: U.S. Department of Commerce.

Collepardi, M. (2003). A state-of-the-art review on delayed ettringite attack on concrete. *Cement and Concrete Composites*, 25(4-5), 401-407. doi: 10.1016/S0958-9465(02)00080-X

Darwin, D., Browning, J., Gong, L., & Hughes, S. R. (2008). Effects of deicers on concrete deterioration. *ACI Materials Journal*, 105(6), 622-627.

Duchesne, J., & Fournier, B. (2011). Petrography of concrete deteriorated by weathering of sulphide minerals. *33rd International Conference on Cement Microscopy 2011, April 17, 2011 - April 20, 2011*, 242-261.

Ekolu, S. O., Thomas, M. D. A., & Hooton, R. D. (2006). Pessimism effect of externally applied chlorides on expansion due to delayed ettringite formation: Proposed mechanism. *Cement and Concrete Research*, 36(4), 688-96. doi: 10.1016/j.cemconres.2005.11.020

ERCO, W. (2012). *Sodium hypochlorite solution: Material safely data sheet*. (No. #3). Toronto: ERCO Worldwide.

Fu, Y., & Beaudoin, J. J. (1996). On the distinction between delayed and secondary ettringite formation in concrete. *Cement and Concrete Research*, 26(6), 979-980. doi: 10.1016/0008-8846(96)00080-4

Grabowski, E., Czarnecki, B., Gillott, J. E., Duggan, C. R., & Scott, J. F. (1992). Rapid test of concrete expansivity due to internal sulfate attack. *ACI Materials Journal*, 89(5), 469-480.

Haynes, H., O'Neill, R., Neff, M., & Kumar Mehta, P. (2010). Salt weathering of concrete by sodium carbonate and sodium chloride. *ACI Materials Journal*, 107(3), 258-266.

Hobbs, D. W., & Taylor, M. G. (2000). Nature of the thaumasite sulfate attack mechanism in field concrete. *Cement and Concrete Research*, 30(4), 529-533. doi: 10.1016/s0008-8846(99)00255-0

Hove, K. R. S. (2011). Investigation of the effect of high temperature exposure on the oxidizing power of sodium hypochlorite bleach.

Jacobson, E. (2013). Sulfuric acid and chlorine bleach reaction. Retrieved 07/30, 2013, from http://www.ehow.com/about_6521382_sulfuric-acid-chlorine-bleach-reaction.html

Jones, M. R., Macphee, D. E., Chudek, J. A., Hunter, G., Lannegrand, R., Talero, R., & Scrimgeour, S. N. (2003). Studies using ²⁷Al MAS NMR of AFm and AFt phases and the formation of friedel's salt. *Cement and Concrete Research*, 33(2), 177-182. doi: 10.1016/S0008-8846(02)00901-8

Kohler, S., Heinz, D., & Urbonas, L. (2006). Effect of ettringite on thaumasite formation. *Cement and Concrete Research*, 36(4), 697-706. doi: 10.1016/j.cemconres.2005.11.006

Kosmatka, S. H., Kerkhoff, B., Hooton, R. D., & McGrath, R. J. (2011). Design and control of concrete mixtures: The guide to application, methods, and materials (8th ed.). Ottawa, Canada: Cement Association of Canada.

Langlet, M., Nadaud, F., Benali, M., Pezron, I., Saleh, K., Guigon, P., & Metlas-Komunjer, L. (2011). Kinetics of dissolution and recrystallization of sodium chloride at controlled relative humidity. *KONA Powder and Particle Journal*, 29, 168-179.

Leklou, N., Aubert, J. -, & Escadeillas, G. (2012). Effect of wetting-drying cycles on mortar samples affected by DEF. *European Journal of Environmental and Civil Engineering*, 16(5), 582-588. doi: 10.1080/19648189.2012.668017

- Lubelli, B., van Hees, R. P. J., & Groot, C. J. W. P. (2006). Sodium chloride crystallization in a "salt transporting" restoration plaster. *Cement and Concrete Research*, 36(8), 1467-1474. doi: 10.1016/j.cemconres.2006.03.027
- Monteny, J., Vincke, E., Beeldens, A., De Belie, N., Taerwe, L., & Van Gemert, D. (2000). Chemical, microbiological, and in situ test methods for biogenic sulfuric acid corrosion of concrete. *Cement and Concrete Research*, 30, 623-634.
- Neville, A. M. (2011). *Properties of concrete* (5th ed.). Edinburgh Gate, England: Pearson.
- Neville, A. (2004). The confused world of sulfate attack on concrete. *Cement and Concrete Research*, , 1275-1296.
- O'Connell, M., McNally, C., & Richardson, M. G. (2010). Biochemical attack on concrete in wastewater applications: A state of the art review. *Cement and Concrete Composites*, 32(7), 479-485. doi: 10.1016/j.cemconcomp.2010.05.001
- Rodrigues, A., Duchesne, J., Fournier, B., Durand, B., Rivard, P., & Shehata, M. (2012). Mineralogical and chemical assessment of concrete damaged by the oxidation of sulfide-bearing aggregates: Importance of thaumasite formation on reaction mechanisms. *Cement and Concrete Research*, 42(10), 1336-47. doi: 10.1016/j.cemconres.2012.06.008
- Schmidt, T., Leemann, A., Gallucci, E., & Scrivener, K. (2011). Physical and microstructural aspects of iron sulfide degradation in concrete. *Cement and Concrete Research*, 41(3), 263-269. doi: 10.1016/j.cemconres.2010.11.011
- Shi, C., Wang, D., & Behnood, A. (2012). Review of thaumasite sulfate attack on cement mortar and concrete. *Journal of Materials in Civil Engineering*, , 1450-1460.
- Taylor, H. F. W., Famy, C., & Scrivener, K. L. (2001). Delayed ettringite formation. *Cement and Concrete Research*, 31(5), 683-693. doi: 10.1016/S0008-8846(01)00466-5
- Yee-Ching, G. (2012). *The effect of low temperature on the binding of external chlorides*. (M.A.Sc., University of Toronto).
- Zibara, H. (2001). *Binding of external chlorides by cement pastes*. University of Toronto).